

Building, Energy and Environment Research Group

Department of Architecture and Built Environment

Faculty of Engineering

Dynamic thermal simulation of slinky-loop heat exchangers for ground source heat pump systems in the UK

Thesis by

Man Luo, BEng, MSc.

30th December 2023

Thesis submitted to the University of Nottingham

For the Degree of Doctor of Philosophy in Building Technology

Table of contents

Table of contents i

Abstract vi

Acknowledgements vii

List of Figures viii

List of Tables xv

Nomenclature xviii

Chapter 1: Introduction 1

1.1 Background 1

1.2 Statement of problems 6

1.3 Aim and objectives 7

1.4 Novelty of the research 8

1.5 Thesis structure 11

Chapter 2: Literature Review 13

2.1 Classification of GSHP systems 13

2.1.1 Open-loop ground heat exchangers 13

2.1.2 Closed-loop ground heat exchangers 14

2.2 Analytical models 20

2.2.1 Kelvin's line source model 21

2.2.2 Cylindrical source model 23

2.2.3 Eskilson's model 24
2.2.4 Finite line source model 25
2.2.5 Ring heat source models 26
2.2.5.1 Spiral GHE 26
2.2.5.2 Slinky-loop ground heat exchanger 30
2.3 Numerical model 32
2.3.1 Vertical ground heat exchanger model 32
2.3.2 Linear ground heat exchanger model 35
2.3.3 Spiral ground heat exchanger model 40
2.3.4 Slinky-loop ground heat exchanger model 43
2.4 Comparison between analytical and numerical models 55
2.5 Experimental methods on HGSHP 57
2.6 Summary 60
Chapter 3: Methodology of numerical slinky-loop ground heat exchanger model 64
3.1 Introduction 64
3.2 Governing equations 64
3.3 Description of the model 66
3.3.1 Slinky-loop ground heat exchanger model 68
3.3.2 Topsoil boundary condition 71
3.3.2.1 The effect of different topsoil surface boundary conditions 72
3.3.3 Initial soil temperature 75

3.3.3.1 The effect of initial soil temperature 78
3.3.4 Pipe boundary condition 84
3.3.4.1 The effect of the pipe temperature 86
3.3.5 Mesh independence study 92
3.3.6 Time step study 97
3.4 Simulation process 100
3.5 Validation of CFD model 102
3.6 Conclusion 105
Chapter 4: Investigation into the thermal interference of slinky-loop ground heat exchangers 107
4.1 Introduction 107
4.2 Description of the model 107
4.2.1 Parallel slinky-loop ground heat exchanger model 108
4.2.2 Soil properties used in simulation model 109
4.3 Results and discussion 110
4.3.1 The effect of the interference of different slinky-loop ground heat exchangers for a base case 110
4.3.2 The effect of the soil thermal conductivity on the interference of different slinky-loop ground heat exchangers 120
4.3.3 The effect of installation depth on the interference of different slinky-loop ground heat exchangers 128
4.4 Conclusion 135

Chapter 5: Analysis of slinky-loop ground heat exchanger models with intermittent operation and different layout 137

5.1 Introduction 137

5.2 Description of conditions for simulation 138

5.2.1 Slinky-loop ground heat exchanger geometric characteristics . 138

5.2.2 Validation of loop configuration with different pitch 144

5.3 Results and discussion 146

5.3.1 Intermittent 6 h,12 h and 18 h operation 147

5.3.2 Intermittent 12 h operation with different loop pitch 156

5.3.3 The effect of intermittent operation on the interference of different slinky-loop ground heat exchangers 160

5.3.4 Ground thermal recovery within one-year operation..... 165

5.4 Conclusions 176

Chapter 6: Analysis of heat demands-varying on-off period operation and installation sites for slinky-loop ground heat exchanger models..... 179

6.1 Introduction 179

6.2 Description of heating hours 180

6.2.1 Heating degree day heating hours..... 180

6.2.2 Domestic house heating hours 182

6.2.3 Three typical meteorological condition..... 183

6.3 Results and Discussion 185

6.3.1 Comparison for heating degree day heating hours and real house

heating hours 185

6.3.2 Comparison for heating degree day operation and intermittent 12 h operation modes 189

6.3.3 Comparison for three locations.....192

6.4 Conclusions.....196

Chapter 7: Design and application consideration of slinky-loop ground heat exchanger system for a building case 198

7.1 Design consideration.....198

7.2 Annual space heating demand.....202

7.3 Required length of slinky-loop ground heat exchanger 205

7.4 Calculation for circulating pump 208

7.5 Coefficient of Performance 209

7.6 Energy and environmental saving.....211

7.7 Economic considerations 214

7.8 Discounted payback period.....217

7.9 Comparison for different heat pump system.....220

Chapter 8: Conclusion and future work.....227

8.1 Main conclusion.....227

8.2 Recommendation for future work 232

Reference list 234

Appendix.....245

Abstract

Horizontal slinky-loop ground heat exchanger systems provide a cost-effective alternative to vertical ground source heat pump systems. These shallow-depth systems are increasingly gaining popularity. Hence, it is crucial to optimise these designs in order to ensure maximum efficiency and minimise the use of land space and piping materials. This study aims to examine the effect of various operating conditions, thermal interference, installation configurations, intermittent operation mode, ground thermal recovery, and annual operation on the thermal performance of slinky-loop ground heat exchanger. This study develops three-dimensional computational fluid dynamics (CFD) simulations to analyse the thermal performance of GHE models throughout the heating season. This transient 3D model is also validated by previous literature. The regression equations between energy output ratio/total heat extraction and various factors, such as spacing distances, pipe temperatures, loop pitches, and daily operation hours, are obtained for prediction in future designs. Soil thermal conductivity of the installation site is found to have a significant impact on thermal performance. The heating degree day prediction method for evaluating the thermal performance of a horizontal ground source heat pump system was feasible for a real-life prediction. The work finally provided the design considerations for a slinky-loop ground heat exchanger system. The predicted discounted payback period is 7 years for the HGSHP system, mainly determined by the local soil properties. This HGSHP system would be able to decrease annual CO2 emissions by about 71.4% and 71.9% compared to gas and electricity heating systems, respectively.

Acknowledgements

At the culmination of this incredible journey, I am filled with deep gratitude and appreciation for those who have been instrumental in my academic and personal growth.

Foremost, I extend my heartfelt thanks to my supervisor, Dr. Guohui Gan. His expertise, invaluable advice, continuous support, and patience have not only shaped my research but have also profoundly influenced my professional development. His guidance has been a cornerstone of my doctoral experience.

I am immensely grateful to my colleagues and friends: Ke Qu, Shaofan Wang, Yingrui Li, Tianhong Zheng, Ziwei Chen, and Wanfang Zhao. Their camaraderie, intellectual exchanges, and encouragement have been invaluable. Their perspectives and support have greatly contributed to both the challenges and joys of my research journey.

My deepest appreciation goes to my parents, Wei Luo and Ling Xu. Their love, sacrifice, and unflagging belief in me have been my constant source of strength and inspiration. They have instilled in me the values and resilience that have guided me through this journey.

Finally, my thanks to my dearest boyfriend, Lingze Lin. I find it difficult to express my appreciation because it is so boundless. He is my most enthusiastic cheerleader; he is my best friend. His presence has been a source of joy and comfort throughout the highs and lows of this academic pursuit.

To all, I owe a debt of gratitude that words can scarcely express. This accomplishment is not just my own, but also a reflection of the collective support and faith of everyone who has been a part of my life during this journey.

List of Figures

Figure 1.1 Carbon Dioxide Emissions from global energy sources, 1990-2021 [1].....1

Figure 1.2 Monthly average gas price in UK from October 2015 to October 2022 [4].....2

Figure 2.1 Open-loop geothermal heat pump system [39]. 13

Figure 2.2 Fundamental concept of closed loop GSHP systems [41]. 16

Figure 2.3 Cross-section of various borehole heat exchangers [45].....16

Figure 2.4 The percentages of various BHE pipe types from 2010 to 2018 [46]. 17

Figure 2.5 Horizontal closed GHE: (a) linear-loop; (b) slinky-loop; (c) spiral-coil [53].....20

Figure 2.6 Schematic view of spiral coil source [68]. 28

Figure 2.7 Schematic representation of signal ring-coil in a semi-infinite medium [72].....29

Figure 2.8 (a) Schematic view of different configurations of spiral GHEs and (b) mesh structure of different configurations in COMSOL with d = 6 m (top view) [79].....41

Figure 2.9 Schematic diagram of (a) model domain of GHE, (b) linear GHE, (c) slinky-loop ground heat exchanger, and (d) spiral GHE [101].....46

Figure 3.1 Computational domain for soil with slinky-loop ground heat exchanger. 69

Figure 3.2 Computational domain for soil with symmetrical slinky-loop ground heat exchanger. 70

Figure 3.3 Heat transfer rate of different top surface boundary conditions at the

end of each month under continuous operation. 74
Figure 3.4 Monthly heat extraction under different top surface boundary conditions.....75
Figure 3.5 Initial ground temperature profile. 77
Figure 3.6 Isotherm generated from prediction for different initial soil temperature in vertical section view. 82
Figure 3.7 Effect of initial soil temperature on the predicted heat extraction through the heat exchanger. 83
Figure 3.8 Effect of initial soil temperature on the predicted variation of soil temperature at various times. 84
Figure 3.9 Variation of monthly heat extraction for different pipe temperature. 89
Figure 3.10 Isotherm generated from prediction for different pipe temperature at the end of September in vertical section view. 90
Figure 3.11 Total heat extraction amount of slinky-loop heat exchangers with different heat exchanger pipe temperature. 91
Figure 3.12 Predicted variation of soil temperature with depth, for different pipe temperature at the end of September. 91
Figure 3.13 The vertical cross-section of the generated mesh for different mesh sizes.....94
Figure 3.14 Mesh independence study.....96
Figure 3.15 The details of mesh generated near the slinky-loop ground heat exchanger surface. 96
Figure 3.16 Heat transfer rate for various time step size on the first day. 97
Figure 3.17 The difference between time step size 60s and 3600s at selected time.

.....99
Figure 3.18 Heat transfer amount for various time step size during different period. 99
Figure 3.19 Comparison of the soil temperature between the present numerical model and the experimental results of Wu et al. at different time. [23]. 105
Figure 4.1 Schematic of slinky-loop ground heat exchanger system. 108
Figure 4.2 Computational domain for soil with slinky-loop ground heat exchanger. 109
Figure 4.3 Soil temperature distribution (K) on a vertical section located at the centre of the slinky loops at the end of March for different spacing distances. 113
Figure 4.4 Effect of spacing distance on variations in soil temperature through the slinky-loop ground heat exchanger. 114
Figure 4.5 Monthly heat extraction under different spacing distances. 114
Figure 4.6 Effect of spacing distance between adjacent trenches on heat extraction through the slinky-loop ground heat exchanger (Base case). 116
Figure 4.7 The regression line from polynomial. 119
Figure 4.8 The regression line with quadratic and cubic polynomial within 5 meters spacing distance. 119
Figure 4.9 Temperature distribution on vertical section with three soil types for the separation distance of 1.5 m slinky-loop ground heat exchanger at the end of March. 122
Figure 4.10 Predicted variation of soil temperature with depth, at different times for different soil thermal conductivities. 123
Figure 4.11 Effect of soil type on variations in heat extraction through the slinky-

loop ground heat exchanger. 124
Figure 4.12 The regression line with quadratic polynomial for clayey soil. ..126
Figure 4.13 The regression line with quadratic polynomial for sandy soil. ...127
Figure 4.14 Effect of installation depth on variations in heat extraction through the slinky-loop ground heat exchanger (heating season). 130
Figure 4.15 Effect of installation depth on variations in heat extraction through the slinky-loop ground heat exchanger starting from in December. 131
Figure 4.16 Predicted variation of soil temperature with depth, at the end of Dec and Mar for different soil thermal conductivities. 133
Figure 4.17 The regression line with quadratic polynomial at depth of 0.9 m. 134
Figure 4.18 The regression line with quadratic polynomial at depth of 1.5 m. 134
Figure 5.1 Schematic diagram of different loop pitches of slinky-loop ground heat exchanger. 140
Figure 5.2 Computational domain for soil with slinky-loop ground heat exchanger. 142
Figure 5.3 The details of mesh generated for Case 4. 144
Figure 5.4 Variations in heat extraction rates of slinky-loop ground heat exchangers (loop diameter, D = 1 m, loop pitch, LP = 0.25 m, 0.5 m, 1 m and 2 m) with time. 145
Figure 5.5 Heat transfer rate at first week for continuous operation and intermittent operation. 149
Figure 5.6 Heat transfer rate at selected date for continuous operation and intermittent operation. 150

Figure 5.7 Heat transfer rate of intermittent and continuous operation on selected day. 151
Figure 5.8 The difference of daily mean heat transfer rate between continuous operation and intermittent operation on selected date. 153
Figure 5.9 The difference of daily heat extraction amount between continuous operation and intermittent operation on selected date. 154
Figure 5.10 Variation of monthly heat extraction at different operation mode. 155
Figure 5.11 Variations in monthly heat extraction amount of slinky-loop ground heat exchangers (loop pitch= 0.25 m, loop pitch= 0.5 m, loop pitch= 1 m and loop pitch= 2 m). 158
Figure 5.12 Regression line for total heat extraction amount of slinky-loop ground heat exchangers over seven months and varying loop pitch. 159
Figure 5.13 Variations in heat extraction by slinky-loop ground heat exchangers (in continuous and intermittent operation). 162
Figure 5.14 The regression line with quadratic polynomial under intermittent 12-h operation mode. 164
Figure 5.15 Annual operation method according to base case condition. 165
Figure 5.16 Comparision in heat extraction of the Ocotober in the second year for different operation mode. 167
Figure 5.17 Variations in ground temperature at the end of October (the second year) at the center of heat exchanger for different operation mode (top soil surface temperature = 10.6℃). 170
Figure 5.18 Isotherm generated for the effect of heating operation at the end of March in vertical section view. 172

Figure 5.19 Isotherm generated for the effect of heating operation at the end of first recovery month (April) in vertical section view.....173
Figure 5.20 Isotherm generated for the effect of heating operation at the end of second recovery month (May) in vertical section view. 174
Figure 5.21 Effect of heating operation on the predicted variation of soil temperature from April to July in recovery peroid. 174
Figure 5.22 Variations in ground temperature at the end of August at the center of heat exchanger for different operation mode. 176
Figure 6.1 Monthly heat extraction proportion of the heating season based on heating degree day method and real house operation mode. 188
Figure 6.2 Effect of HDD and real house operation modes on the predicted variation of soil temperature at the end of first four months. 188
Figure 6.3 Monthly heat extraction in three operation modes. 191
Figure 6.4 The monthly heat extraction per unit length of the trench for three installation locations using the same soil type (loamy). 194
Figure 6.5 The monthly heat extraction per unit length of the trench for three installation locations using the local soil type. 195
Figure 7.1 Proposed horizontal ground-source heat pump system. 199
Figure 7.2 Outlook of the case study building. 203
Figure 7.3 Floor plan layout of the semidetached house. 204
Figure 7.4 Case study 3D model geometric wireframe view. 204
Figure 7.5 Annual space heating demand. 205
Figure 7.6 Schematics of installation layout for slinky-loop ground heat exchanger system. 206
Figure 7.7 Comparison of annual energy consumed and $CO2$ emission of

different heating system. 213

Figure 7.8 Comparison of accumulated $CO2$ emission of different heating systems. 213

Figure 7.9 Breaking point for the discounted payback period of HGSHP & electric heating system in loamy soil. 219

Figure 7.10 Breaking point for the discounted payback period of HGSHP & electric heating system installed in sandy soil with higher thermal conductivity. 219

Figure 7.11 The daily average soil temperature at a depth of 1.2 m from Sept 1st to Mar 31st. 221

Figure 7.12 Comparison of accumulated $CO2$ emission of HGSHP, BGSHP, and ASHP heating systems. 223

Figure 7.13 Breaking point for the discounted payback period of BGSHP & electric heating system. 226

Figure 7.14 Breaking point for the discounted payback period of ASHP & electric heating system. 226

List of Tables

Table 2.1 Outline of studies related to slinky-loop ground heat exchangers. ...49

Table 3.1 Main properties of the materials used in the simulations [85, 119]. .66

Table 3.2 Monthly air temperature and wind speed in Coventry. 72

Table 3.3 Boundary condition of CFD simulation. 72

Table 3.4 Data for estimating ground temperature variation at the beginning of September. 77

Table 3.5 Boundary condition of CFD simulation. 78

Table 3.6 Boundary condition of CFD simulation. 86

Table 3.7 Mesh sizes for mesh independence study. 92

Table 3.8 Time step size study. 98

Table 4.1 Soil properties for simulation. 110

Table 4.2 Boundary condition of CFD simulation. 110

Table 4.3 Boundary condition of CFD simulation. 120

Table 4.4 Boundary condition of CFD simulation. 128

Table 5.1 Comparison of the heat exchange rate between the current work and the previous simulation results of Chong et al. [23]. 146

Table 5.2 Boundary condition of CFD simulation. 147

Table 5.3 Daily average heat transfer rate on selected date. 153

Table 5.4 Overall heat extraction and heat transfer rates under various modes. 156

Table 5.5 Boundary condition of CFD simulation. 156

Table 5.6 Boundary condition of CFD simulation. 160

Table 5.7 Boundary condition of CFD simulation. 165

Table 6.1 Daily operation hours calculation through heating degree day method.

.....181

Table 6.2 Predicted daily and monthly operation hours through heating degree day method.....181

Table 6.3 Daily operation hours calculation through energy consumption. ...182

Table 6.4 Predicted daily and monthly operation hours through energy consumption.....183

Table 6.5 Soil properties from three locations.....183

Table 6.6 Monthly average ambient temperature for three cities. 184

Table 6.7 Monthly average wind speed for three cities. 184

Table 6.8 Boundary condition of CFD simulation.....185

Table 6.9 Monthly heating time and heat extraction by two operation modes. 189

Table 6.10 Boundary condition of CFD simulation.....189

Table 6.11 Daily heating time in three operation modes. 191

Table 6.12 Monthly heat extraction in three operation modes. 191

Table 6.13 Boundary condition of CFD simulation.....192

Table 7.1 Specifications of heat pump.....206

Table 7.2 Specifications of water pump. 209

Table 7.3 Comparison of energy consumption and $CO2$ emission of various heating systems.....211

Table 7.4 Initial investment of horizontal ground source heat pump system and conventional heating system.....214

Table 7.5 Economic indicators and energy price increase rate.....216

Table 7.6 Estimated COP for BGSHP and ASHP system.....221

Table 7.7 Comparison of energy consumption and $CO2$ emission of various heat

pump systems 222
Table 7.8 Initial investment of borehole ground source heat pump system and air source heat pump system. 223

Nomenclature

A	surface area (m^2)
ASHP	air source heat pump
BGSHP	borehole ground source heat pump
BHE	borehole heat exchanger
C	roughness factor
COP	coefficient of performance
c_p	specific heat capacity (J/kgK)
D	diameter (m^2)
D_{damp}	annual fluctuation damping depth (m)
$D_{T,v}$	thermal vapour moisture diffusivity (m^2/sK)
$D_{\theta,v}$	isothermal vapour moisture diffusivity (m^2/s)
DPP	discounted payback period
EH	elevation head (m)
FH	friction head (m)
g	acceleration due to gravity (m/s^2)
GHE	ground heat exchanger
$GSHP$	ground source heat pump
h	convective heat transfer coefficient on pipe inner surface (W/m^2K)
h_c	convective heat transfer coefficient on soil surface (W/m^2K)
H	internal heat generation (W/ m^3)
HDD	heating degree day
$HDPE$	high density polyethylene
HF	heat flux rate per unit pipe surface area (W/m^2)

$HGSHP$	horizontal ground source heat pump
i	analysis period of year
k	thermal conductivity of soil (W/mK)
k_{pipe}	thermal conductivity of pipe (W/mK)
L	distance of trench separation (m)
L_c	trench length of the connecting pipe (m)
L_{index}	length of the index circuit
L_{pipe}	length of the heat exchanger pipe (m)
L_{slinky}	trench length of the slinky loop heat exchanger (m)
L_{trench}	total length of trench (m)
L_{water}	latent heat of water (J/kg)
n	current year
NPV	net present value
Nu	Nusselt number
ΔP	pressure drop (Pa)
PH	pressure head (m)
Pr	Prandtl number
PV	accumulated present value
PVC	present value cost
q	heat transfer rate per meter length trench (W/m)
$\dot{q}$	heat gain/loss (W)
Q	heat extraction (kWh)
Q_b	total heating load (kWh)
Q_{cp}	energy consumption of circulating water pump (kWh)

Q_d	heat extraction with thermal interference (kWh)
Q_{hp}	energy consumption of heat pump (kWh)
Q_s	heat extraction without thermal interference (kWh)
R_d	real discount rate (%)
R_i	inflation rate (%)
R_m	market interest (%)
R_n	net cash flow
Re	Reynolds number
S	loop pitch (m)
$SCOP$	seasonal coefficient of performance
t	time (s)
T	temperature (℃)
T_a	annual average temperature of soil (℃)
T_{amp}	annual amplitude temperature of soil surface (℃)
T_{pipe}	heat exchange pipe temperature (℃)
∇T	temperature gradient (℃)
TDH	total dynamic head (m)
u	viscosity (m^2/s)
v	fluid velocity (m/s)
v_{wind}	wind speed (m/s)
V	total volumetric flow rate (m^3/h)
V_s	slinky loop volumetric flow rate (m^3/h)
VGHE	vertical ground heat exchanger
VGSHP	vertical ground source heat pump

W_{pump}	pump power consumption (kW)
Z	soil depth (m)
Z_d	total depth of computational soil domain (m)
Z_1	installation depth (m)
Z_2	the distance between heat exchanger and soil domain bottom (m)

Greek letters

α	Soil diffusivity (m^2/day)
ρ	density (kg/m^3)
θ	volumetric moisture content (m^3/m^3)
η	energy output ratio (%)

Subscripts

l	liquid
max	maximum
min	minimum
$pipe$	pipe
$pump$	pump

Chapter 1: Introduction

1.1 Background

The burning of fossil fuels like petroleum, natural gas, and coal contributes to climate change on a worldwide scale, which is one of the most serious challenges that humanity will face in the 21st century. Carbon dioxide is the major cause of climate change that contributes to global warming. Fig. 1.1 depicts global carbon dioxide emissions over the last 21 years from the report of Global Energy Review [1]. In 2021, global CO_2 emissions from the burning of traditional energy sources and industrial activity reached their highest annual level ever recorded. Based on the IEA's detailed study, emissions climbed by 11.7% from 2010 to 36.3 gigatons (Gt).

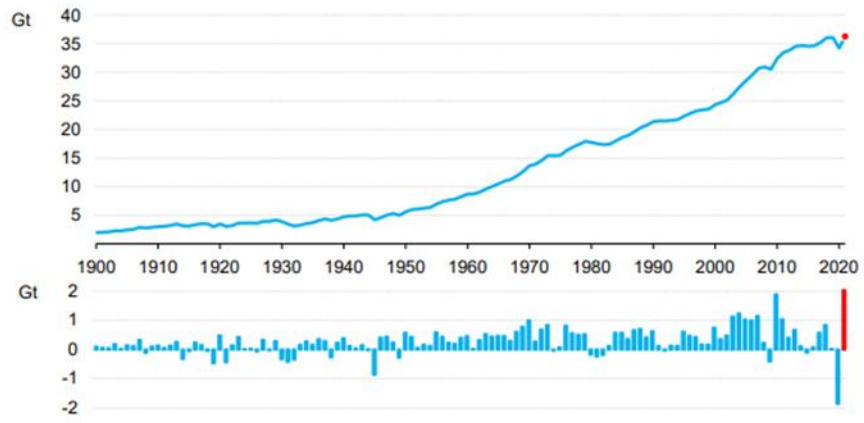


Figure 1.1 Carbon Dioxide Emissions from global energy sources, 1990-2021 [1].

Department for Energy Security and Net Zero pointed out that nearly a quarter of the United Kingdom's carbon emissions come from heating buildings, and

half of the fossil fuel gas consumed annually in the United Kingdom is used for heating [2]. Therefore, all heat generation in buildings must be decarbonized to achieve net zero targets. The electrification of heat is considered as a crucial move in decreasing emissions from homes, since the majority of emissions are connected with boilers now running on natural gas, as part of UK Government initiatives to reduce emissions from buildings over the coming decades. Global gas price increases have resulted in a considerable increase in the energy price cap (+96% or +£1223 yearly costs for the average household by October 2022, compared to October 2021) [3]. As shown in Fig. 1.2, electricity prices in the UK increased by 65%, while gas prices increased by 128.9% in the year of 2022 [4]. Affordability is a growing concern and a significant public policy challenge with the wider cost-of-living crisis.

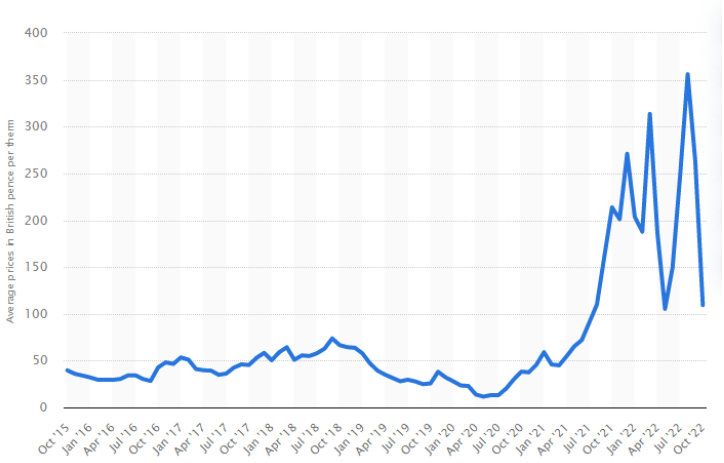


Figure 1.2 Monthly average gas price in UK from October 2015 to October 2022 [4].

Renewable and green energy sources such as solar, wind, geothermal, and wave energy are supposed to be utilized to decrease the dependence on petroleum and coal to meet ever-increasing energy consumption and the cost of living [5]. Ground source heat pumps (GSHP) use geothermal reservoir energy to provide

heating and cooling for a building. GSHP perform better than traditional air source heat pumps (ASHP) systems due to the relatively stable ground temperature. On the other hand, seasonal and temporal fluctuations of air temperature have an impact on the operation of ASHP systems. As a result of their good thermal performance and low emissions of greenhouse gases, ground source heat pumps have emerged among the most environmentally friendly and sustainable options for conditioning and heating both residential as well as business properties [6]. As stated in the European Heat Pump Association (EHPA) report of 2021, Norway topped the rankings with 49.77 installations per 1,000 households, while the UK installed the fewest heat pumps per household in all of Europe, with only 1.5 heat pumps installed for every 1,000 houses [7]. The independent Climate Change Committee pointed out that the UK must reach 15.3 installations per 1,000 households in order to achieve the nation's 2050 net-zero goal [8]. An ambition to lower heat pump expenses by 25-50% before 2025 will go a long way toward making heat pumps a compelling alternative [9]. The UK government launched the Boiler Upgrade Scheme to take the role of the Domestic Renewable Heat Incentive (RHI) and offer subsidies of £5,000 and £6,000, respectively, to encourage the use of air source and ground source heat pumps from 2022. According to government statistics, around 90,000 residences are anticipated to benefit from it [10]. Domestic heating accounts for 14% of the UK's carbon dioxide emissions, based on the report from the Committee on Climate Change (CCC) [8]. The Boiler Upgrade Scheme will play a significant role in guaranteeing that all new heating system installations are low carbon by 2035 [11]. By 2028, the government hopes to have installed 600,000 new homes annually [12].

Ground source heat pump systems have the ability to operate in either heating or cooling mode. This is achieved through the extraction of heat from the ground and transferring it to the building, or by absorbing heat from the building and transferring it to the ground via a ground heat exchanger (GHE). Shallow ground source heat pump systems are commonly regarded as semi-permanent energy sources, with an estimated lifespan of approximately 40 to 50 years [13].

GHE is one of the key components of a ground source heat pump system. GHE are classified as vertical or horizontal according to their placement orientation. Vertical ground heat exchanger (VGHE) pipes are installed vertically in deep boreholes with varying depths from 15.2 to 183 meters [14]. Deep vertical pipes give the heat exchanger greater energy extraction amount and need less land than horizontal ground heat exchangers. However, the widespread adoption of this technology is mainly limited by the high initial installation drilling cost, and local consent may be needed in most countries. Horizontal ground heat exchangers (HGHE) are placed underground, typically at a depth of one to two meters. Horizontal trenches require far less excavation costs than vertical boreholes and can be a cost-effective option for the installation of ground heat exchangers in situations where surrounding land space is available. The installation costs can be further reduced using horizontal slinky-loop ground heat exchanger [15], making HGHE an attractive technology for house and small office building applications [16]. Slinky-loop ground heat exchanger can obtain more heat transfer per unit soil length than straight pipe because of their longer pipe length per soil length [17]. Therefore, the use of slinky-loop ground heat exchanger can minimize the need for land area, making it possible to apply heat pump systems with HGHE even in situations where available land for

installation is not substantial.

Thus, horizontal ground heat exchangers have been the focus of numerous experimental and numerical investigations. However, in contrast to VGHE, HGHE are susceptible to significant impacts from meteorological factors. Empirical estimation is often used for the design of slinky-coil heat exchangers due to the lack of reliable prediction tools [18]. This can result in the inappropriate design of GSHP systems. In addition to experimental setups, dynamic modelling and simulation, which offer a practical and economical method for evaluating the performance of HGHE system, have gained the attention of design engineers for the purpose of evaluating the dynamic performance of HGHE. In numerical simulations, linear-type and spiral-type GHE are frequently investigated because their geometries can be constructed with less effort. However, in comparison to linear-type and spiral-type GHE, not a lot of research has been carried out on slinky-loop ground heat exchanger system due to the complicated geometry [19] and the limited amount of installations that have been made. In the design stage of horizontal slinky-loop ground heat exchanger system, it is useful to predict the HGHE's performance as accurately as possible, which can be achieved through numerical modelling, leading to significant reductions in investment costs.

Given that the UK government has committed to reducing CO_2 emissions by at least 100% of 1990 levels (net zero) by 2050, the project is highly relevant. The GSHP industry in the UK has recently grown rapidly. In addition to offering a great chance to grow the market for heating and cooling systems, the suggested slinky-loop ground heat exchanger system would also bring about benefits for both the economy and the environment.

1.2 Statement of problems

- Most previous evaluations studied on modelling methodologies, system design, configuration optimisation, and techno-economic analysis for GSHP systems, with the focus being on VGHE rather than HGHE. The effect of different operating conditions on HGSHP system is a lack of analysis.
- There is a lack of published information and optimal design data related to their heat extraction amount about the installation of commercial horizontal slinky-loop ground heat exchangers in the United Kingdom, particularly when it comes to the thermal performance of such systems in the context of intermittent and annual operation.
- Little attention has been paid so far to the performance of pipe groups, while thermal interference between parallel pipes cannot be neglected. When pipes are connected in parallel, it is necessary to investigate the effects of different center-to-center trench spacing.
- Increasing numbers of these slinky-loop ground heat exchangers are being installed in the UK, but no scientific design procedure has been developed in order to size the slinky-loop ground heat exchangers accurately for typical regions with local climate conditions and soil properties in the UK.
- Currently, one of the main obstacles to adopting GSHP systems is the high initial costs, although the potential savings from the operating costs will enable the systems to be cost-effective in long-term operation. The payback period for these installations needs to be predicted.

1.3 Aim and objectives

Ground source heat pump systems have advantages in terms of offering a highly efficient solution for space heating and cooling, while also mitigating the environmental impact. It is important that further work be done to shorten the payback period for these installations. This study aims to optimise a key component of GSHP systems – slinky-loop ground heat exchanger – in order to reduce the system costs and attract more potential owners especially homeowners, small and medium enterprises. The primary objective of this study is to optimise slinky-loop ground heat exchangers in terms of their sizing and efficiency. In an attempt to fill the aforementioned gaps, the thermal performance of slinky-loop ground heat exchanger system including various pipe arrangements under different operating conditions will be assessed and compared. GSHP systems for typical UK climate regions will then be analysed to provide a better understanding of the economic and environmental benefits of using slinky-loop ground heat exchanger systems within the UK. This will be achieved within the scope of work that covers the underlying objectives outlined below:

1. To review the start-of-the-art of the analytical models, numerical models and experimental methods for GHE design and analysis.
2. To develop a numerical model for simulation of slinky-loop ground heat exchanger in different configurations and layouts.
3. To validate the numerical model based on previous literature.
4. To investigate the effects of the interaction between atmosphere and ground surface, initial soil temperature and the thermal interference of neighbouring pipes on the performance of slinky-loop ground heat exchanger.

5. To perform simulations of the slinky-loop ground heat exchanger thermal performance using the developed model for different operating modes (continuous and intermittent) and boundary conditions.
6. To analyse the ground thermal behaviour and temperature distribution and their effects on the slinky-loop ground heat exchanger thermal performance for one-year operation.
7. To investigate the effects of the installation depth of slinky-loop ground heat exchanger, the soil properties in different major UK climate regions, and the pipe temperature in different working conditions to provide more accurate data for the design of HGSHP systems within the UK.
8. To analyse the economic and environmental impacts of representative slinky-loop ground heat exchanger installations for the UK conditions.

1.4 Novelty of the research

Previous studies found some factors that affect the thermal performance of slinky-loop ground heat exchangers. For example, the effect of operating conditions (ambient and inlet temperatures), and thermal properties (conductivity, density and specific heat) of the soil. These findings were based on the simulation during cooling season or a short period in heating season[20-23]. Few studies have been performed to deeply investigate the effects of various factors in the whole heating season. Specifically, the influence mechanism of different factors on the total heat extraction amount/energy output ratio was still less understood. Considering the operation of slinky-loop ground heat exchanger in UK is mainly for heating system, the parametric study is performed to identify the important factors affecting the thermal performance of the slinky-loop

ground heat exchanger over a seven-month heating season. This PhD thesis presented a simulation study of dynamic thermal performance of a slinky-loop ground heat exchanger to analyse the thermal performance of slinky-loop ground heat exchanger, including various pipe arrangements, under different inlet temperature, and initial soil temperature were assessed during the whole heating season.

According to earlier studies, the ground surface boundary condition was generally simplified and taken to be a (seasonal mean) constant-temperature because the CFD simulations were conducted over a short time period (6 days or 2 months) [22-24]. The effect of monthly varying ambient conditions was investigated in this research work.

While it is well understood that, in general, the ground heat exchanger efficiency decreases with decreasing spacing distance between parallel pipes[20, 25], it is not well understood how the energy output ratio changes with different levels of spacing distance between the slinky-loop ground heat exchangers[26], even though it is an important consideration for sizing and designing the slinky-loop ground heat exchanger. This study investigated that the thermal performance of slinky-loop ground heat exchangers and thermal interference between parallel heat exchanger pipes vary with trench separation, installation depth, soil properties and daily operation duration. The obtained equation for energy output ratio prediction were based on the typical UK climatic conditions over a seven-month heating season.

Although some previous studies have investigated the effects of intermittent operation mode on thermal performance of ground source heat pump system, most simulation results were focused on vertical ground heat exchangers[27-30].

Very few of them investigated the intermittent operation for the slinky-loop ground heat exchanger systems. It also lacks of considering heat demands-varying on-off period operation[31]. This work created a novel intermittent operating strategy that takes into account the degree-day method as a potential solution for accurately predicting the daily operation hours. The impact of monthly variations of thermal load on the intermittent operation method in real-life situation was discussed.

Little attention has been paid about the annual performance of slinky-loop ground heat exchanger systems[32-34]. This study considered the single heating season operation and the double cooling and heating season operation. The variation of ground temperature can be used as the indicator to compare the long-term performance under the assumption that the building heating/cooling demand is fully met with the GSHP system.

The slinky-loop ground heat exchanger systems in UK climatic regions lack of evaluation to provide a better understanding of the economic (financial) and environmental benefits of using this heat pump system[35]. It is important to know the heating load of a building, the electricity consumed, the local electricity price, the subsidy from the government and the predicted payback period time. Accurately predicting the performance of slinky-loop ground heat exchanger systems during the design stage is beneficial as it leads to significant cost savings on investments. Based on the simulation results, design of a slinky-loop ground heat exchanger for application of ground source heat pump in an example building is discussed. The coefficient of performance of slinky-loop ground heat exchanger systems for typical UK climate regions were calculated by the predicted heat transfer rate from simulation results. The economic and

environmental benefits of promoting the use of slinky-loop ground heat exchanger systems were analysed. The comparison between air source heat pump, borehole ground source heat pump and slinky-loop ground heat exchanger systems were also conducted.

1.5 Thesis structure

Chapter 2 is a literature review covering horizontal heat exchanger of GSHP systems, including various types of heat exchanger design, thermal performance analysis, design and simulation tools of these heat exchangers in both analytical and numerical methods. This study also compared the analytical models and numerical models. Chapter 3 describes numerical methodology for the dynamic thermal simulation of slinky-loop ground heat exchanger. This includes the description of a three-dimension CFD model, assumption, boundary condition, and validation. It also presents analysis of topsoil surface boundary condition, the initial soil temperature condition and the effect of different pipe temperature. Chapter 4 focus on the thermal performance prediction of slinky-loop ground heat exchanger for different trench separations. The installation depths and soil properties with emphasis on the thermal interference between parallel heat exchanger pipes are also studied. Chapter 5 covers the study of intermittent operation method. Results obtained from the simulation for the effect of different daily operation hours, loop pitch, thermal interference from parallel pipe and annual operation mode on slinky-loop ground heat exchanger thermal performance.

Chapter 6 creates a novel intermittent operating strategy that takes into account of the heating degree day method for predicting accurately the daily operation

hours and study the effects of the intermittent operation method in real situation. The impact of installation sites is also investigated.

In Chapter 7, design considerations for a HGSHP system are outlined. These considerations consist of the building heating load, estimated ground temperature, selection of working fluids, soil thermal properties, method of system control strategies etc. The chapter concludes with an economic analysis, energy savings, and environmental savings implemented for the slinky-loop ground heat exchanger system. In the comparison, ASHP and borehole GSHP are also included. Chapter 8 summarises conclusions derived from this research and provides the recommendation for future work.

Chapter 2: Literature Review

2.1 Classification of GSHP systems

GSHP systems are categorised as either closed-loop or open-loop depending on the working fluid's connection between the ground heat exchanger and the heat pump unit [36].

2.1.1 Open-loop ground heat exchangers

A typical open-loop ground heat exchanger system consists of two boreholes: one for water extraction, which pumps groundwater, and the other for injection, which uses the same aquifer to inject either cold or warm water with the identical velocity but at a various temperature [37]. In addition, it can be used for other things like consumption and irrigation. The boreholes are only 50 meters deep [38]. There are many ways to connect open-loop heat exchanger systems, one of which is shown in Fig. 2.1.

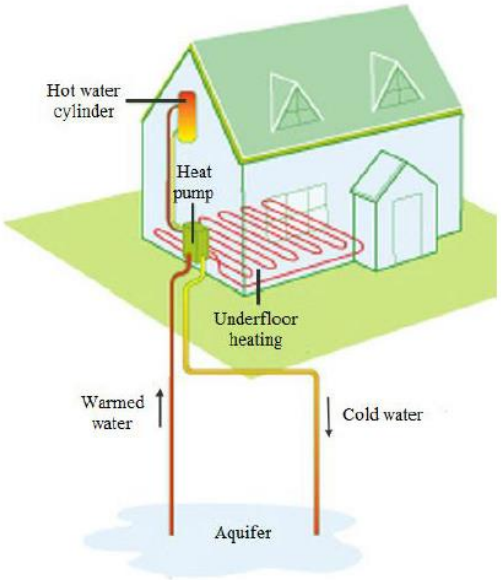


Figure 2.1 Open-loop geothermal heat pump system [39].

These systems work extremely effectively for facilities with high power requirements, such as hospitals, airports, or data centres. However, some risk factors, such as groundwater chemical properties and ground subsidence, must be considered in addition to extracting wells. Before use, chemical characteristics should be assessed because blockage and corrosion problems could occur. To avoid potential effects on the quality of groundwater and aquatic ecology, the material of the pipes should be carefully chosen for environmental protection. Investigation of the local lithological sequence, heat flow, stress regime, and hydrogeological conditions is essential [40]. Because the heat carrier fluid is in direct contact with the heat source/sink, open systems operate better overall in the subsurface. However, the system is not available in areas where there is a shortage of water, and its environmental issue has increased because of contaminated water.

2.1.2 Closed-loop ground heat exchangers

In contrast to open-loop ground heat exchanger systems, an aquifer is not necessary for closed-loop systems. Hence, it causes minimal negative environmental impacts. They are the most widely used ground heat exchangers [37]. Fig. 2.2 depicts the fundamental concept of GSHP systems that operate in heating mode with a closed loop. They are made up of three main components: a ground-heat exchange loop, a heat pump unit, and a heat distribution system. Closed-loop systems can be divided into either horizontal or vertical. The U-tube, concentric tube, and pile heat exchangers are the three major forms of the vertical GHE, which necessitates holes in the soil roughly 50-150m deep. The horizontal GHE, on the other hand, typically takes the form of linear-loop, panel, spiral-coil, or slinky-coil heat exchangers, and can be put in horizontal trenches

as shallow as 1 to 2 meters deep [38].

For vertical closed-loop system, a heat exchanger is inserted into a vertically drilled borehole. To maintain thermal contact, the space between the heat exchanger and the borehole wall is backfilled. Sand, bentonite, or reinforced cement are the three most common materials used to fill boreholes. The heat carrier fluid is circulated in the heat exchangers, which allows for the transfer of heat from the earth to the heat pump and vice versa. Borehole spacing is typically between 5 and 6 meters to reduce the potential for thermal interference from neighbouring boreholes. The thermal efficiency of a Borehole heat exchanger (BHE) is determined by a variety of elements, including the kind of heat exchanger, the material used for grouting, the length, and the diameter of the BHE. The thermal properties, hydraulic properties, and ground starting temperature of the ground also play an important role in ground heat exchanger system [32]. As can be seen in Fig. 2.3, there are primarily two distinct types of heat exchangers that can be used in a vertical GSHP system: U-pipes and Coaxial heat exchanger.

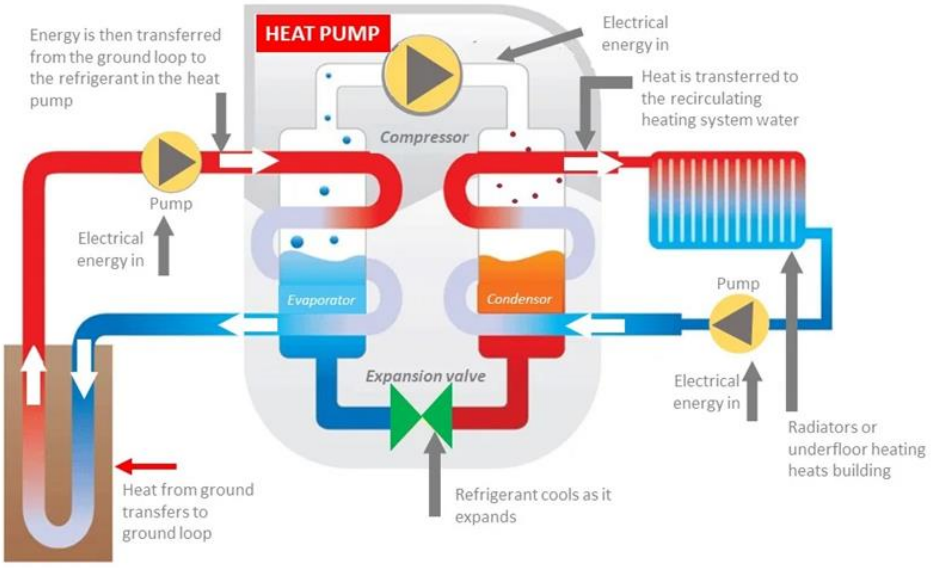


Figure 2.2 Fundamental concept of closed loop GSHP systems [41].

There are primarily two kinds of U-pipes used in practice: single-U and double-U. A number of previous studies found that heat exchangers with double-U pipes had a higher thermal efficiency than those with single-U pipes [42, 43]. Nonetheless, when considering the building's capital expenses and energy consumption, the single-U may also be an appropriate option [44].

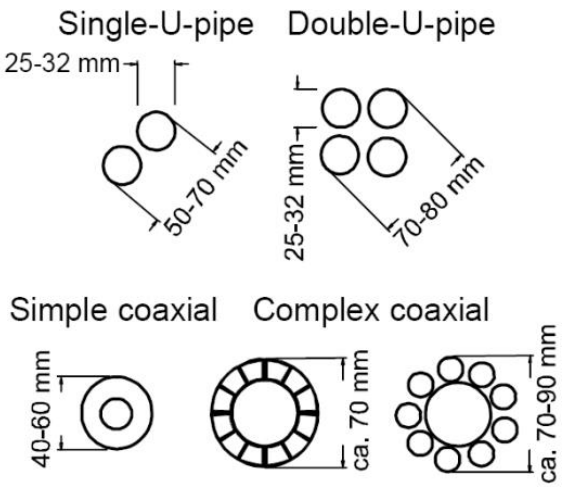


Figure 2.3 Cross-section of various borehole heat exchangers [45].

On the other hand, coaxial heat exchangers can also be divided into two categories: simple and complex coaxial. In most cases, simple coaxial heat exchangers are utilized for boreholes measuring between 40 and 60 millimetres in diameter. Complex coaxial heat exchangers are typically utilized for boreholes with diameters more than sixty millimetres. The percentage of various pipe layouts is displayed in Fig. 2.4, which may be seen here.

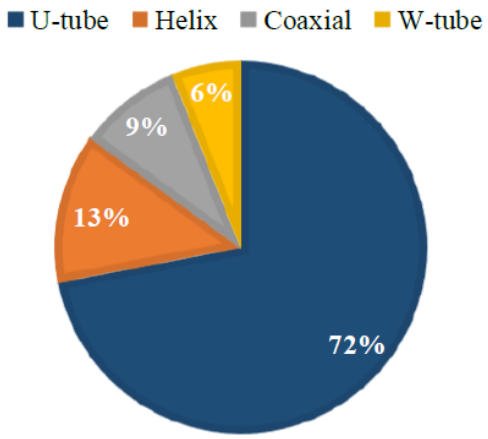


Figure 2.4 The percentages of various BHE pipe types from 2010 to 2018 [46].

According to the data, the U-pipe form of BHE is by far the most common, accounting for 72% of all BHE. This is followed by the helix configuration (13%) and the coaxial and W-tube configurations (9% and 6%, respectively). According to Javadi et al. [46], polyethylene (PE) pipe is the most commonly used material for heat exchanger. The "energy pile" is another key application in GSHP systems. Heat exchangers can be connected into the building's foundation piles for both space heating and cooling. Since they are required for structural support, the initial drilling expense is avoided [5]. According to research by Cui et al. [35] and You et al. [47], concrete is an excellent heat transfer medium because of its high thermal energy storage capacity and high thermal

conductivity. The length-to-diameter ratios for BHE range from 200 to 1500, which can be used with many different shapes (W shape, single-U shape, double-U shape, spiral). In contrast, energy piles are usually shorter and wider than boreholes, and their length-to-diameter ratios (aspect ratios) are usually below 50 [48]. Since energy piles are typically built beneath structures, it is necessary to estimate the cooling and heating load correctly in the design process to ensure there won't be any unforeseen mechanical issues. Traditional methods of installing energy piles in building foundations put the structure at risk due to thermally induced extra settlement or load. To keep structural integrity, prevent soil from freezing, and prevent any loss of bearing capacity, fluid temperatures in energy piles must be maintained above 0 (to 2) °C [48].

A variety of additional uses for GSHP systems are being developed, such as tunnel water and hot water from waste oil wells. Furthermore, GSHP systems only take up a minimal amount of space inside of buildings and operate quietly, and they are more effective than HGHE due to the fact that they are located deeper below the ground surface. The system's high and consistent performance can be attributed to its position deep in the earth, which also reduces the amount of piping needed. However, the initial cost of the BHE is significantly greater when compared to the cost of traditional heating and cooling systems. This is mostly due to the costly borehole drilling work that is required to install the BHE. As a result of the many benefits described above [49], GSHP systems have become increasingly popular in recent years and have been installed in a variety of business and residential buildings. There are a few things that need to be taken into consideration before selecting the appropriate system for a particular installation. These include the geological conditions, the area limitation, the

capital costs, the construction works, and the system management. When sizing a GSHP system, it is vital to consider all relevant elements in order to achieve optimal performance at the lowest possible cost.

Depending on the terrain and other local factors, the drilling cost of vertical GHE was estimated to be between 50% and 70% of the total initial cost of the entire GSHP system [50]. Horizontal ground heat exchangers (HGHE) are placed underground, typically at a depth of one to two metres. Horizontal trenches require far less excavation costs than vertical boreholes and can be a cost-effective option for the installation of ground heat exchangers (GHE) in situations where surrounding land space is available. Although HGHE has been widely used in the GSHP system in several regions of the world, particularly in North America [51], less research has been conducted on HGHE compared to VGHE in Europe and other regions [52] due to the smaller number of installations.

As indicated in Fig. 2.5, horizontal ground heat exchanger is categorised into three types: linear, slinky-loop, and spiral-coil arrangements. The slinky-loop and spiral-coil layouts both have greater heat exchange rates per trench unit length than the linear pipe.

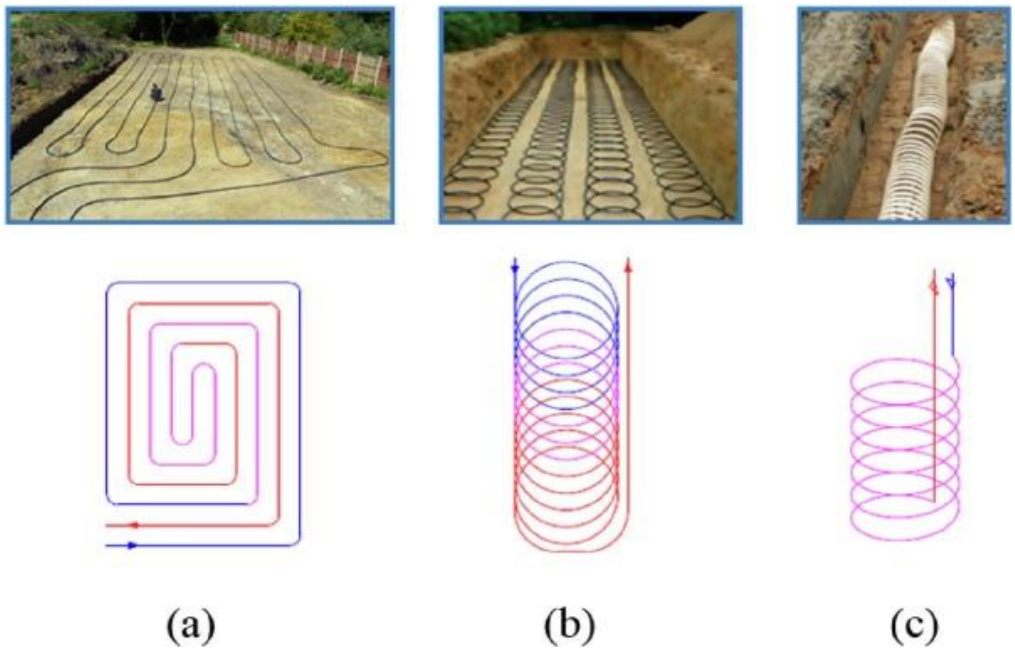


Figure 2.5 Horizontal closed GHE: (a) linear-loop; (b) slinky-loop; (c) spiral-coil [53].

2.2 Analytical models

Both analytic and numerical methods are available for GHE thermal analysis. They have many applications, including the prediction of borehole thermal interferences, conductive heat transfer from a borehole, and the mechanism of borehole thermal transfer itself. Analytical models are founded on the principle of the superposition of several independent elementary heat transfer processes. These models often use long time steps to simulate the heat transfer from a GHE in a steady state [54].

According to Yang, Cui, and Fang [55], the process of heat transfer may typically be divided into two distinct zones for the purpose of analysis. This is due to the complexity of the problem as well as the long-time scale involved. The first is the solid soil or rock that is outside the borehole or trench. This is the part of the

system where heat conduction needs to be considered as a transient process. Once the temperature response in the ground has been determined, the temperature on the borehole wall can be calculated for any given time under a given set of operational conditions.

The region inside the borehole, which includes the grout, the GHE pipes, and the circulating fluid in the pipes, is another part of the system that is frequently separated for the purpose of research. Depending on the context, this region may be analysed as a transient, steady, or quasi-steady state. On the wall of the borehole, the analyses of the two different spatial zones are connected to one another. Recently, a variety of analytical models for heat transfer outside the borehole have been published, the majority of which were conducted based on either analytical or numerical analysis.

2.2.1 Kelvin’s line source model

The first method used to predict the thermal transfer all around a heat exchanger in the ground was Kelvin's line source theory, also recognized as the infinite line source theory. According to Sarbu and Sebarchievici [56], the infinite line source method takes the borehole as a line heat source that constantly creates and rejects heat through pure conduction heat transfer. An abstract concept is an instantaneous point source (analogous to the mass point in mechanics). Taking this solution as a fundamental solution (Green's function for an infinite medium) allows one to obtain the solution for a continuous point source by integrating the fundamental solution over time, providing a clear and simple physical meaning for this model. The temperature response in the ground due to a constant heat rate, according to Kelvin's line source hypothesis, is given by:

$$T(r,t) - T_0 = \frac{q_1}{4\pi k} \int_{\frac{r^2}{4at}}^{\infty} \frac{e^{-u}}{u} du \quad (2.1)$$

Where r represents the distance from the line source and τ is the amount of time that has passed since the operation began; T is the temperature of the ground at distance r and time t; T_0 is the initial temperature of the ground; q_l is the heating rate per length of the line source; k and a are the thermal conductivity and diffusivity of the ground.

This method has been utilized to simulate the thermal performance of BHE and be used in the thermal response test (TRT) in order to evaluate the thermophysical properties of the soil. When modelling U-tube boreholes, the infinite line source method positions the line source at the centre of the borehole and calculates the average wall temperature of the borehole as a result. Based on the assumptions made by Morgensen [57], the temperature of the fluid can be calculated by taking into account that the heat transfer occurring within the borehole is in a quasi-steady state. According to Spitler and Gehlin [58], making this assumption enables all the internal heat transfer in the borehole to be modelled as a straightforward borehole thermal resistance. Because it is based on the assumption of an infinite line source, this model can only be used for tiny pipes within a limited time period of several hours to a few months [59]. Even though it is distinguished by its simplicity and the fact that it requires less time to calculate. The problem with this model is that it takes the borehole as an infinite line, and as a result, it does not take end effects into consideration.

A variety of optimizations for this methodology have been proposed in order to solve certain complex elements and achieve accuracy comparable to numerical methods. Among these various approaches that utilise Kelvin's line source

theory, the Hart and Couvillion method is considered to be more precise than the others [60].

2.2.2 Cylindrical source model

The finite diameter of the borehole is considered rather than modelling the borehole as a line. Carslaw and Jaeger [61] were the first to create the cylindrical source solution for a constant heat transfer rate; Ingersoll et al. [62] further improved upon it, and it has since been utilised in a variety of research investigations [63]. Under the boundary conditions of either a constant pipe surface temperature or a constant heat exchange rate between the buried pipe and the ground, it is assumed that the borehole is made up of a cylindrical volume with an infinite length.

In addition, it is assumed that there is perfect contact between the borehole and the soil, resulting in 100% conduction of heat. The temperature distribution on the ground can be represented in cylindrical coordinates by using the Laplace transformation and the Bessel function when combined with the specified boundary and beginning conditions:

$$\begin{aligned} &\frac{\partial^2 T}{\partial r^2}+\frac{1}{r}\frac{\partial T}{\partial r}+\frac{1}{a}\frac{\partial T}{\partial r} && r_b < r < \infty \\ &-2\pi r_b k\frac{\partial T}{\partial r}=q_1 && r=r_b, t>0 \\ &T-T_0=0 && \tau=0, r>r_b \end{aligned} \tag{2.2}$$

The cylindrical source solution is given as follows.

$$T-T_0=\frac{q_1}{k}G(z,p) \tag{2.3}$$

Where $z=\frac{at}{r_b}, p=\frac{r}{r_b}$

According to Carlaw and Jaeger's definition, the expression $G\ (z,\ p)$ is only a

function of time and borehole centre distance. The temperature on the borehole wall, where $r = r_b$, $p = 1$, is of relevance because it is the representative temperature for the design of geothermal heat exchangers. However, the expression $G(z,p)$ is relatively complicated, requiring integration from zero to infinity of a complicated function that involves Bessel functions.

2.2.3 Eskilson's model

The axial heat flow down the borehole depth is ignored by both the one-dimensional Kelvin's theory model and the cylindrical source model. Eskilson [64] made a significant step forward in taking into account the finite length of the borehole. The heat conduction equation in cylindrical dimensions governs the fundamental formulation of the ground temperature:

$$\frac{\partial^2 T}{\partial r^2} + \frac{1}{r}\frac{\partial T}{\partial r} + \frac{1}{a}\frac{\partial T}{\partial t}$$

$$T\,(r, 0, t) = T_0$$

$$T\,(r, z, 0) = T_0$$

$$q_l(t) = \frac{1}{H}\int_D^{D+H} 2\pi k \frac{\partial T}{\partial r}\,|r = r_b\; dz \tag{2.4}$$

where H is the length of the borehole and D is the top of the borehole, which can be thermally disregarded in engineering practice.

The final mathematical description of the temperature response at the borehole wall to a unit-step heat pulse is only a function of t/t_s and r_b/H:

$$T_b - T_0 = -\frac{q_l}{2\pi k} g\left(\frac{t}{t_s}, \frac{r_b}{H}\right) \tag{2.5}$$

where t_s=$H^2/9a$ means the steady-state time. The g-function is essentially the dimensionless temperature response at the borehole wall, which was computed numerically.

2.2.4 Finite line source model

The infinite line source model is used as a foundation for the finite line source model, which extends it by modelling the ground surface with end effects and a boundary condition. Modelling the ground surface involves reflecting the borehole line source as a line sink along the boundary of the modelling area. This method of image simulates the surface of the ground with a constant temperature boundary condition. According to Spitler and Bernier [65], this is of utmost significance for GHE modelling when the design time is larger than one year, as this is the point at which the importance of the model's accuracy increases. When the integral of the point source model is assessed numerically, it resolves into a sequence of point sources. This is due to the fact that the finite line source model is based on the integral of the point source model. An analytical solution to the problem of the finite line source has been established by Zeng et al. [66] on the basis of Eskilson's model. This solution takes into account the effects of the finite length of the borehole as well as the ground surface as a boundary. The formula for the temperature excess is as follows:

$$T(r,z,t)-T_0=\frac{q_1}{4\pi k}\int_0^H\left\{\frac{erfc(\frac{\sqrt{r^2+(z-h)^2}}{2\sqrt{at}})}{\sqrt{r^2+(z-h)^2}}+\frac{erfc(\frac{\sqrt{r^2+(z+h)^2}}{2\sqrt{at}})}{\sqrt{r^2+(z+h)^2}}\right\}dh \tag{2.6}$$

Eq. (2.6) shows that the temperature on the borehole wall, where r=rb, varies with time and borehole length. The temperature in the borehole's centre ($z = H/2$) is typically used as its representative temperature. The numerical integration of this equation can also be used to calculate the integral mean temperature along the borehole length.

2.2.5 Ring heat source models

Previous models that are based on line and cylindrical sources are not sufficient for coil-type heat exchangers [67]. This is due to the limitations of simplifying assumptions regarding the heat source. In the line source model, the heat source is in the centre of the borehole. Thus, the line source model may estimate a slightly lower rise in soil temperature than the others.

In contrast, the heat source in the cylindrical source model is situated close to the wall of the borehole, which has a cylindrical face. Therefore, it is possible that the cylindrical source model will predict a somewhat greater rise in soil temperature in comparison to the other models [68].

2.2.5.1 Spiral GHE

Researchers have presented unique analytical models to better understand and predict the heat transport of buried spiral pipes. In general, these solutions are based on the continuous point source solution and Green's function theory. Man et al. [69] and Cui et al. [70] performed specified analytical investigations on an energy pile containing a spiral coil heat exchanger as solid cylindrical (SC) and ring-coil (RC) heat sources generating a constant heat flux. Then, using a governing equation of transient heat conduction in radial-axial coordinates and Green's function theory, the temperature distributions inside and outside of the energy pile are solved analytically. Specifically, the analytical solutions of the RC model can also take into consideration the effect of coil pitch on the behaviour of heat transfer by positioning discrete heat sources in depth, also known as ring-coil It was discovered that the ring-coil source model with a finite length may more properly describe the heat performance in pile geothermal heat exchangers (PGHEs) with spiral coils than the infinite ring-coil model and the

cylindrical source model. However, the analytical models are dependent on ideal simplifications such as the calculation domain having homogenous thermal characteristics, the coil pipe having zero volume, and the vertical return pipe being neglected. Consequently, for better design of the helical heat exchanger, Park et al. [71] proposed simple modifications of the *SC* and *RC* models by assuming the coil heat exchanger as a combination of solid cylinder or ring-coil heat sources for the coil part and a finite-length line heat source (*FL*) for the return pipe. It was discovered that by including a finite-length line source solution to consider the vertical return pipe of a coil heat exchanger, the axisymmetric finite element analysis, analytical solutions of solid cylindrical and ring-coil heat source models can more precisely estimate soil temperature rises at the exterior of the heat exchanger. Even if this research evaluates the reliable heat transfer performance of a helical heat exchanger buried in a homogeneous ground, they suggest that the estimation of effective thermal properties should be appropriately considered when applying the heat source models for energy pile.

An efficient spiral coil source model is also presented by Park et al. [68]. This model takes into account the three-dimensional shape effects as well as the radial dimension effects of a spiral coil-type ground heat exchanger, and it is based on Green's function approach. Fig. 2.6 displays this model：

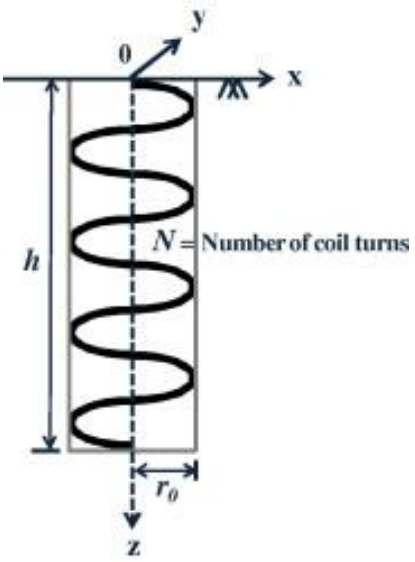


Figure 2.6 Schematic view of spiral coil source [68].

By using an error function to avoid singular integrals, it was possible to avoid computational limitations. Moreover, they compared the model's prediction results implemented in ABAQUS/Standard with test measurements obtained from a thermal response test conducted in a model. Both methods produce reliable results that agree well with one another. In conclusion, it was determined that the newly developed analytical model offered an effective prediction tool for the spiral coil GHE.

Wang et al. [72] recently utilized Green's function theory to construct a mathematical vertical ring-coil model for describing the heat transfer process of HGHE with vertical spiral coils. This new model simplifies the spiral heat exchanger to a series of ring coils that exchange heat with a semi-infinite medium. Then a single ring model in an infinite medium has been presented. In a semi-infinite medium, the image approach is used to determine the single ring source. The same virtual ring source is applied symmetrically over the boundary surface, as seen in Fig. 2.7. The heat exchange rate of the virtual ring source is

thought to be the inverse of the original. A multiple-ring-coils analytical solution was obtained from the method of images and superposition.

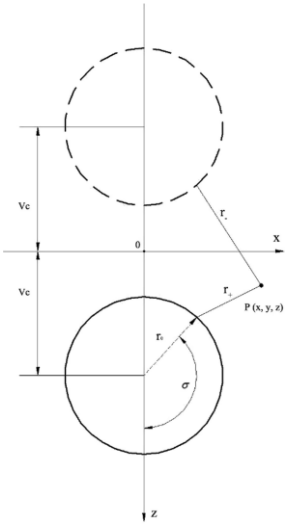


Figure 2.7 Schematic representation of signal ring-coil in a semi-infinite medium [72].

Using the Laplace approach, Wang, Lu, and Cui [73] also created a unique analytical model that reveals the heat transfer process of pile geothermal heat exchangers with spiral coils. Because of this new model's simplification of the spiral pipe as a series of ring coils, it is possible to draw the conclusion that the difference in temperature between the pile and the soil has an important effect on the processes of heat transfer. According to the findings, the newly established analytical model provides a more accurate description of the pile geothermal heat exchangers with spiral coils heat transfer mechanism, particularly the temperature responses of the pile foundation. It is a more accurate tool that may be used for estimating performance and serving as a guideline for design.

Jeon, Lee, and Kim [74] developed a mathematical model for spiral coil-type HGHE by using the mirror image approach and superposition to research the

effect of a semi-infinite medium and ground temperature distribution. It was built on Park et al.'s [68] spiral coil source mathematical model, which was originally designed for energy piles and VGHE, utilizing the mirror image approach and superposition. On-site experiments and numerical analysis findings developed in COMSOL Multiphysics were also used for validation. Furthermore, the proposed mathematical model was compared to Wang et al.'s [72] multiple ring-coil source model. It was demonstrated that this new mathematical model can accurately capture the structure of the spiral coil. Furthermore, it improves the multiple ring-source model in terms of ground temperature prediction as elapsing time progresses.

2.2.5.2 Slinky-loop ground heat exchanger

Heat source solutions have also been applied in the modelling of slinky loop ground heat exchanger. Mukerji et al. [75] created a line source approximation (LSA) model for coiled tube GHE. The spiral or Slinky coiled tube is regarded as a spiral or Slinky™ heat source in this model, with the heat source coiled in the same manner as the tube. This research produced an analytical answer for a performance factor (PF). The PF is the heat transfer rate per unit tube length of coiled tubing divided by that of straight tubing. The authors present the PF as a simple approach for incorporating Slinky™ GHE design into existing HGHE design tools. The resulting solutions, however, are limited to the steady-state heat transfer case. Li et al. [76] proposed a "spiral heat exchangers" ring source concept for Slinky™ GHE. Slinky™ GHE are represented mathematically with multiple ring sources in a semi-infinite homogeneous medium. The ground surface is believed to be either isothermal in warm regions or adiabatic in cold parts. The study develops solutions for the ground temperature response and the

mean tube wall temperature response to the heat transfer rate per tube length. An experiment validated the solution of multiple ring sources. Another study that used an analytical solution to investigate the temperature response of a slinky GHE with groundwater flow was presented by Li et al. [77]. They created a moving ring source model using the moving point source theory of Green's function to describe the heat transfer of the heat exchanger and the calculated results show good agreement with the experimental results. It was found that the impact of the groundwater flow on the heat transfer process may be prominent at different positions of the tube surface. Furthermore, the approximation algorithms were introduced to reduce the calculation time. The approximation approach has been proven to run thousands of times faster than the initial method, and the calculation results are in 97% agreement with those of the initial method. A response function method was used by Xiong, Fisher, and Spitler [15] to compute the exiting fluid temperature and heat transfer rate of Slinky™ GHE by superimposing ring sources. This was done with knowledge of the time-varying entering fluid temperature. To ensure that the results were as accurate as possible, the diameter of the tube was taken account into the calculation of the thermal interactions between the rings. In addition to this, it was validated using the experimental data that was published by Fujii et al. [78]. As a result, it is appropriate for use in programmes that simulate the energy use of the entire building. According to the findings of this simulation, a divergence of 1% in the temperature response factor might cause an error of up to 0.2 degrees Celsius in the temperature that is projected to be present in the heat pump's working fluid during annual simulations. It has been demonstrated that this analytical model is accurate and has a large increase in computing speed. Thus, the amount of time

required to calculate the temperature response factor for coupling to other components in a whole-system simulation has been significantly reduced.

2.3 Numerical model

Numerical models use the principle of solving the whole system in small cells or grids and then applying the governing equations to these discrete elements to find numerical solutions [79]. These numerical solutions can be calculated for things like pressure distribution, temperature gradients, and flow parameters. Transient heat transfer in GHE is the primary focus of models based on short time-step response. These models have a time step of an hour or less. GHE can be designed from scratch with the use of numerical models through simulation software, which can also be used for diagnosing or optimizing an existing system. In the same way as numerical simulation models for vertical ground heat exchanger has improved accuracy, numerical models for horizontal ground heat exchanger do as well since they are able to explore other aspects that are relevant to the real in-situ situation. There are many kinds of commercial computational fluid dynamics (CFD) tools for numerical modelling.

2.3.1 Vertical ground heat exchanger model

Li et al. [80] developed a three-dimensional dynamic simulation model to investigate the effect of soil thermal characteristics on the long-term performance of the GSHP system. Consequently, in the tenth year as compared to the first year, the coefficient of performance (COP) for heating in the actual conditions of dense clay and dry shale declined by 1.67% and 2.56%, respectively.

The study conducted by Choi et al. [34] investigated the effects of long operation

of GSHP systems on the thermal conditions of the subsurface in urban regions. After a decade of operation, the subsurface thermal state exhibited an overall increase of 7 °C in comparison to the initial temperature. Consequently, thermal interference occurred in the neighbouring building areas. The imbalance in soil thermal conditions is a significant factor contributing to the decline in performance and lifespan of GSHP systems, and it induces adverse environmental impacts in the surrounding soil. Soil thermal imbalance specifically leads to an imbalance in the heating and cooling energy demand of buildings in regions where a specific climate (hot or cold) is distinct. As a result of the long operational period of GSHP systems, the average annual soil temperature has continual fluctuations, leading to a reduction in system efficiency [81].

Yuan et al. [27]created a mixed numerical method to study the thermal performance and thermal interference of multiple vertical GHE. They found that increasing the intermittent ratio from 0.5 to 2 could enhance the heat exchange rate, while increasing the separation distance between adjacent pipe has a little improvement about overall heat flux. When compared to a continuous operation, an intermittent mode can reduce the thermal interference coefficient by roughly 1/3-1/2.

Man et al. [82] presented a novel hybrid ground coupled heat pump system in which nocturnal cooling radiators (NCR) works as alternative heat rejecters. Under ideal meteorological conditions, NCR is activated to reduce heat accumulation around GHE. From 10:00 pm to 6:00 am, the water circulation pump is activated to send the circulating water flow through the NCR installed on the roof for rejecting the accumulated heat around the GHE. The circulation

pump is turned off at 6:00 am. This hybrid ground coupled heat pump system is designed to produce domestic hot water via a desuperheater to reduce the amount of heat discharged into the ground and maximise the use of waste heat. In comparison to a traditional GSHP system, the innovative hybrid GSHP system for a Hong Kong sample building can reduce operating costs by 10.22% over a decade.

Jahangir et al. [29] investigated numerically the impact of altering the operation of a single U-shaped pipe on the performance of the system in emitting and extracting modes. The results presented that if the pump operated continuously, the heat increase would be less than which the pump switched off every 12 hours. Bae et al. [83] developed a numerical model to analyse the effects of the intermittent operation method on the efficiency of the GSHP system and the underground thermal environment. Hence, the heat exchange rate of the GSHP system employing intermittent operation was up to 15% greater than that of the system employing continuous operation. It was found that the difference in underground temperature increased with decreasing interval time in intermittent operating method. These findings demonstrate that the intermittent operation strategy is superior in terms of optimising the underground thermal environment and mitigating soil thermal imbalance compared to the continuous operation method. Hu et al. [28] conducted a series of experiments to investigate the thermal and energy performance of ground source heat pump system operating in various intermittent ratios, particularly in the condition of high-frequency start and stop of the pump. The greater heat transfer happens primarily during the first 4 hours of heating and recovery periods. As a result, the further experiment performed in the 4h-4h mode suggests that the temperature recovery and heat

transfer performance is superior to the 12h-12h mode.

Jalaluddin and Miyara [30, 84] evaluated the thermal performances of borehole GHE under various operating modes, including a discontinuous 2 h operation in cooling mode and an alternative operation mode combining cooling and heating processes to provide hot water supply. By reducing the amount of heat accumulation surrounding the borehole, intermittent and alternative operations help to increase the rate of heat exchange.

2.3.2 Linear ground heat exchanger model

Fontaine et al. [25] created an analytical model using a finite line source to extend the steady-state results for parallel horizontal pipes to the transient case. When there is no freezing or thawing, the solution for the transient case is achieved by supposing that the fluid temperatures inside a single pipe decline gradually from inlet to outlet. A three-dimensional finite element numerical model is used to verify the accuracy of this analytical model. According to the findings, increasing depth *D* helps to maintain the ground's frozen state at this level and favours the extraction of more heat. Increasing spacing between pipes or length of pipes, on the other hand, is excellent for the amount of heat removed; however, it also increases the risk of thawing near the pipes. Both the model and the case study can be used in colder places to provide helpful guidance for the design of ground heat exchangers, which serve both the objective of freezing the ground and extracting heat.

Platts, Cameron, and Ward [85] presented a novel concept called the HGCHE 'Membrane Conduction Augmentation System' (MCAS). This was done by analysing thermo-physical parameters taken directly from the exposed excavation site material. Using solid state heat transfer for the soil, pipe wall,

and membrane, as well as dynamic simulation of the water in the pipe, two numerical models were constructed in ANSYS CFX in order to enhance heat transfer in unsaturated soils. These models were created in order to improve the heat transfer in unsaturated soils. The good agreement between the model and field experiments demonstrates that the same numerical model may serve as the basis for predictive performance in the cooling of buildings (both commercial and domestic) located in a multi-layered soil stratum. The CFD model can also simulate greater flows, although this requires adjustments to the spatial and temporal discretization to account for flows that are in a transitional or turbulent domain.

Pu et al. [20] investigated the performance of five different types of HGHE with varying bending numbers through ANSYS Fluent 15.0. Clearly, the heat transfer rates of a single pipe have superior thermal performance. In the meantime, two buried tube layouts are being investigated: in-line and staggered. It was illustrated that the performance of HGHE in a staggered arrangement is better than that of an in-line arrangement; though, when the relative offset distance D/S $\leqslant$1/3, the in-line design outperforms the staggered setup. They also look into the effects of thermal interference between underground pipes. It is found that the critical pipe spacing of the first and second layers for double-layered HGHE is 40d and 100d, respectively.

Despite using commercial software (FEFLOW, ANASYS, COMSOL Multiphysics, etc.), some in-house numerical simulation models were developed. For example, Esen, Inalli and Esen [86] developed a numerical model to determine the temperature distribution in the vicinity of the pipe by using a finite difference approximation. It is assumed that the temperature field is a two-

dimensional non-steady heat conduction problem with no internal heat generation and moisture migration. Meanwhile, it is not modelled with time-periodic boundary conditions, and heat is transferred mainly by conduction. An analytical solution for the transient temperature response has been derived in a semi-infinite medium with a line source of finite length. In the experimental study, there are three main components: the HGHE, heat pump unit equipment and auxiliary equipment. Experimental data show good agreement with the numerical results. It proves the adequacy of the mathematical model and the correctness of the calculations. It was found that the average value of the SCOP of the GSHP system was found to be 3.2 in the 2002–2003 heating season. Demir, Koyun and Temir [87] developed a new model considering all the weather effects in real life to find three-dimensional temperature distributions in the soil, and the effects of solution parameters on the results were investigated through MATLAB environment. The heat conduction equation was based on the alternating direction implicit (ADI) finite difference formulation and the Thomas algorithm. An experimental study was carried out to test the validity of the model. It was found that both horizontal and vertical temperature profiles matched the experimental data well. The heat conduction equation was based on the alternating direction implicit (ADI) finite difference formulation and the Thomas algorithm. The results indicate that outlet temperatures can be predicted accurately through the developed software. It can be easily used for the evaluation and optimization of parallel pipe horizontal GHE for a certain location if meteorological data are given. It is observed that soil thermal conductivity is the most influential soil property on the results. The burial depth and distance between pipes should also be considered in the design of the

horizontal parallel pipe GHE.

Tarnawski, Leong, Momose and Hamada [88] conducted a computer simulation for horizontal ground heat exchanger operation on about 200 m^2 of living space, 5.5 kW of design heating load and 3.3 kW of design cooling load, located in Sapporo (Japan). For these conditions, a 5.5 kW GSHP unit installed with a 300 m single-layer GHE buried at 0.5 m depth in a land area of 150 m^2 is needed. A computer simulation package called Ground Heat Exchanger Analysis, Design, and Simulation was used as a tool to simulate the thermodynamic performance of GSHP units and also the dynamic temperature and moisture movement around the GHE. The input parameters are daily meteorological data, house heating and cooling loads. It can output lots of technical characteristics of GHE. It was validated that the GSHP system remains more beneficial for space heating than traditional heating. It also has a low impact on the thermal degradation of the ground environment. Thus, the application of horizontal loops for new and retrofit residential and commercial use in northern Japan has proven to be feasible.

Rezaei B., Kolahdouz, Dargush and Weber [89] developed a numerical model to verify the influence of an intermediate insulation layer obtained from tire recycling on the temperature distribution and heat flow in the ground. It is demonstrated that the application of Tire Derived Aggregate (TDA) can increase energy extraction rates from the ground to maximum values of about 17% for cold climates, and about 5–6% for moderate climate conditions. They evaluated the effectiveness of the TDA blanket for GSHP pipe performance by comparing it with experimental data. It was found that the verification results showed a positive influence of the ground coverage. The developed model was then used

to conduct the parametric study with the TDA layer, including the optimum configuration for the TDA blanket, thickness and placement of the TDA layer, and potential energy savings for GSHP operation on an annual basis.

Gan [32] developed an in-house modelling programme to forecast the HGHE performance while taking the soil moisture transfer into account. For a horizontal heat exchanger, the seasonal heat transfer rate rises with the increase of installation depth. The heat exchanger placed at two meters depth can extract 19% more heat compared to the one installed one meter below the surface. The sand soil is able to have 17% more heat transfer compared to loamy sand soil, which is also 14.5% higher than clay loam soil. Gan [90] also found that while the daily and monthly heat extraction could be higher for shallow ground in March and later as the soil temperature can be increased, seasonal heat extraction can be increased with the increase of installation depth of ground heat exchanger. Drier soil and/or air contribute to a reduced rate of heat transfer. Seasonal heat transfer would be reduced by 5%, 11%, and 12%, respectively, if precipitation, vapour pressure, and both were reduced by half.

Kupiec et al.[91] developed a one-dimensional transient heat transfer model for the horizontal linear ground heat exchanger. After the model has been verified, the heat transfer rate in linear heat exchanger is assessed. It can also be used to examine the impact of different process parameters on the efficiency of the GHE. In the meantime, the simulation results have indicated that ground temperature reaches steady-state after around ten years of operation.

The study conducted by Benazza et al. [92] examined the implementation of concentrically arranged horizontal ground heat exchanger for the purpose of cooling. The researchers utilised a simple harmonic function to simulate the

variations in air and ground temperature during both continuous and cyclic running modes. According to the report, the implementation of a cyclic operation enables a specific thermal discharge to occur during the shut-up time, resulting in an enhanced heat exchange rate in comparison to continuous operation.

2.3.3 Spiral ground heat exchanger model

Go, Lee, N.V., and Yoon [93] provide a new algorithm for evaluating the performance of horizontal ground-coupled heat pump systems in terms of rainfall infiltration. The output data are then used as input boundary conditions for the numerical analysis model to determine how rainwater infiltration influences the HGHE's performance. The model was created with dimensions of 30 × 15 × 5 m (width × height × depth) to address three-dimensional heat exchange issues and determine the heat extraction of the HGHE. As the temperature difference between the inlet and outlet of the working fluid widened during the rainfall period, the efficiency of working fluid increased. In the meantime, groundwater movement increases the heat transfer between the heat source and the ground, and the advection effect is dependent on local ground conditions such as hydraulic conductivity and void ratios. If the ground has a high permeability coefficient and the trenches are shallow, a phenomenon known as free convection will occur when the cooling mode is activated. Thus, it is demonstrated that this algorithm has the potential to be utilised for the optimal operation.

Go, Lee, Yoon, and Kim [94] presented an optimal design for a horizontal ground-coupled heat pump system with a spiral-coil-loop heat exchanger. The prediction of the numerical simulation model was in good match with the indoor thermal response test results for both fluid temperature and soil medium

temperature. For the parametric studies, a finite element model was developed. It turned out that the amount of CO2 emissions can be reduced by up to 1.169 tonnes annually by using this model as a replacement for the HVAC system. It demonstrates that it is possible to earn carbon credits while simultaneously causing a significant increase in annual net profit. Accordingly, the payback period was 0.15 years shorter under ideal design circumstances.

Dehghan B. [95] used COMSOL software to compare different types of spiral GHE. Fig. 2.9 depicts various spiral GHE layouts (similar to the experimental application area configuration). According to the findings of this study, the average heat transfer rate value for nine spiral GHE is 6800 W after 3 months of non-stop operation under the most critical working conditions. Furthermore, the spacing between spiral GHE should be at least 6 m, because a large distance between GHE reduces thermal interactions between them. These studies also offer some important design recommendations for GSHP systems.

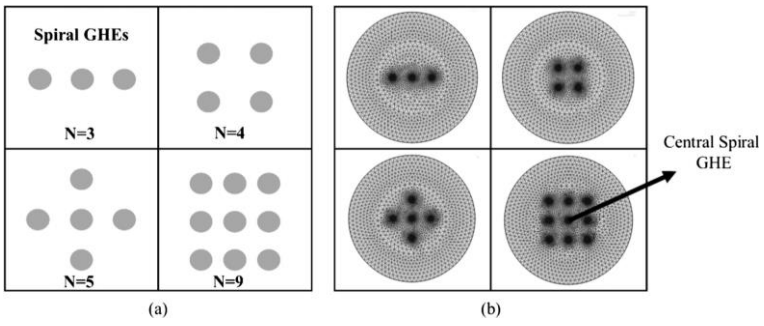


Figure 2.8 (a) Schematic view of different configurations of spiral GHEs and (b) mesh structure of different configurations in COMSOL with d = 6 m (top view) [79].

Kim, Lee, Yoon, and Jeon [96] proposed a design guideline for horizontal spiral-coil GHEs by altering the boundary conditions of a vertical GHE equation to

obtain the trench length calculation solution of the horizontal GHE. The design method was validated using a finite element method (FEM) simulation that was verified by laboratory TRT data acquired under the same conditions. The validated numerical model was then used for the simulation, which was a case study involving a general office. Using the design equation used on the GHE, the required trench lengths of a horizontal spiral-coil GHE under heating and cooling circumstances were found to be 131.9 m and 109.6 m, respectively. The simulation was run in July, which is typically the peak period for air conditioning. The fluid temperature at the output reached 32.09°C, which is below the expected working temperature (EWT) of 32.2°C. This demonstrates that the trench length of a horizontal spiral-coil GHE is adequate to cover the building load, and that the heat-exchange rate from the GHE through full-time operation for a month is greater than the needed peak and monthly load of the building.

Li et al. [97] proposed a numerical model to study the operating characteristics of the horizontal spiral-coil GSHP system. Both the variation of ambient air temperature and the geothermal gradient have been taken into consideration. Moreover, a heat pump model has also been developed to consider the effect of varying loads caused by certain COP features. It has been discovered that in heating and cooling models, the average inlet fluid temperatures could differ by 11.5% and 4.1%, respectively, depending on whether the heat pump was taken into account. Thus, the heat pump COP is crucial when examining the operation of GSHP system. The two primary factors affecting the performance of a horizontal spiral-coil ground source heat pump system are the pipe spacing distance and the soil thermal conductivity. For a horizontal spiral-coil GSHP system, it would be ideal if the soil thermal conductivity was higher than 1.0

$W \cdot m^{-1}$°C^{-1} and the pipe spacing was larger than 1.2m. Daily changes in load can be disregarded when assessing the horizontal GSHP's annual or average operation characteristics. The average performance of intermittent operation is lower than that of continuous operation, and day-high and night-low operation modes when the total loads are the same. Additionally, continuous operation mode has been proved to have the best performance.

2.3.4 Slinky-loop ground heat exchanger model

Wu et al. [23] investigated the thermal performance of a slinky-loop ground heat exchanger system in a UK climate using both experimental and numerical methods. The experimental measurements revealed that the system's average COP was 2.5 with a falling trend over the two-month period. The CFD modelling revealed that changing the diameter of the slinky coils had no significant effect on the total amount of heat transfer, whereas the heat extraction per metre length of trench increased as the loop diameter increased. However, the simulation of the system operation lasted for less than one week without considering the thermal equilibrium. Simulation of a longer operation time would provide more useful thermal performance for a slinky-loop ground heat exchanger. Congedo et al. [98] investigated the effect of different configurations of horizontal GHE over a year, both in summer and winter for typical climate conditions in the south of Italy. It was demonstrated that soil type and the carrying fluid velocity were critical factors influencing the energy behaviour of the GHE. However, the sizes of loop diameter and pitch in their simulation were much smaller than those for real design. And the numerical models built by Wu et al. [23] or by Congedo et al. [98] could handle only small-scale models and were not applicable for the

modelling of field-scale HGHE system.

Fujii et al. [78] then used numerical software, FEFLOW, to create a full-field numerical simulation model of single-layer slinky-loop ground heat exchanger with a simplified shape of Slinky-coils and then validated the model using data from a series of short-term and long-term heat-exchange experiments. Fujii et al. [99] also examined the heat exchange performance of horizontal and vertical settings of slinky-loop ground heat exchanger with varied loop angles and pitches in thermal response tests and long-term cooling and heating tests. The findings of the field tests indicate that the energy efficiency of slinky-loop is significantly higher when installed horizontally compared to vertical installation. This can be attributed to the greater distance between the loop and the land surface. Based on the findings presented above, Fujii et al. [100] created a full-field numerical simulation model of double-layer slinky-loop ground heat exchanger in Fukuoka, Japan, from December 2010 to February 2011. Through this computational model, sensitivity experiments were carried out in order to optimise the design of the double-layer slinky-loop ground heat exchanger. The optimal depth of the upper layer was found to be 1.5 m when the depth of the lower layer was set at 2.0 m. The most effective path for heat-medium circulation was then identified, and it was found that circulation from the upper layer to the bottom layer is more efficient. Furthermore, they revealed that lower albedo is recommended in heating operations, while higher albedo is preferable in cooling operations.

Chong et al. [22] investigated the influence of soil type, loop pitch and diameter on the thermal behaviour of a slinky-loop ground heat exchanger using CFD Fluent Software. The simulations included five loop pitch configurations and

three loop diameters. The effect of loop pitch was found to be greater than that of diameter. The heat exchange rate of intermittent operation was higher than that of continuous operation. In addition, it was found that local soil conditions were essential for an accurate prediction of the GHE thermal performance. To assess the impact of the needed amount of pipe material and excavation expenses on thermal performance, a cost-benefit analysis was also provided. However, these findings were based on 60-day simulation time with uniform initial soil temperature conditions, which might deviate from real operation conditions.

Dasare and Saha [21] built and validated the thermal performance of a variety of ground heat exchangers based on a three-dimensional FEM model utilizing CFD Fluent 14 to solve the governing equations. When compared to the linear horizontal GHE and slinky-loop ground heat exchanger, the spiral coil-type GHE is observed to have significantly better performance in terms of the extraction of heat energy. The thermal conductivity of the soil is crucial factor in the process of heat transfer. The volume of heat transfer fluid that was flowing through the system was a significant factor in determining the results. Additionally, the impact of trench depth on the thermal performance of ground heat exchangers is minimal. Next, an innovative and optimal design was presented to achieve high energy transfer with the double-layer ground heat exchanger. The best distance between two layers is 1.2 metres.

Asgari et al. [101] developed a 3D numerical model to evaluate the thermal performance of different GHE arrangements. The three various configurations are depicted in Fig. 2.8. The thermal performance of the double-layer linear GHE was approximately 21% higher than that of the single-layer arrangement, with the staggered double-layer slinky ground heat exchanger having the

maximum performance of 22% higher than the single-layer configuration. Unlike other varieties, single-layer and double-layer helical-coil HGHE have roughly equal thermal performance. Heat exchange rate per unit land area is 38% lower and 38% higher in soils with thermal conductivities of 0.75 and 1.75 (W/m/K) than in soils with a thermal conductivity of 1.24 (W/m/K).

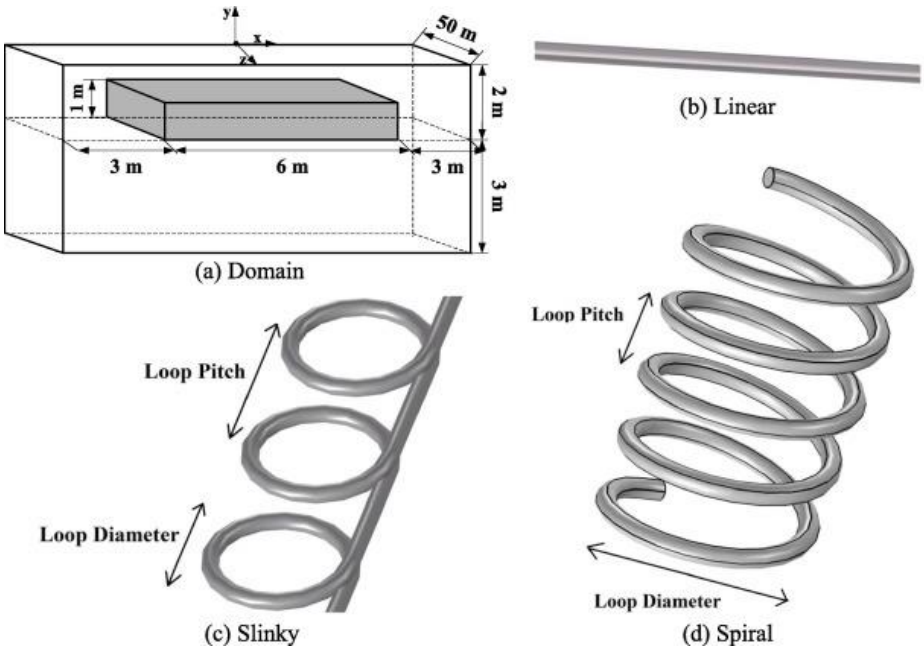


Figure 2.9 Schematic diagram of (a) model domain of GHE, (b) linear GHE, (c) slinky-loop ground heat exchanger, and (d) spiral GHE [101].

Selamat, Miyara, and Kariya [31] developed a three-dimensional model of slinky-loop ground heat exchanger in a variety of orientations and operation modes in order to explore thermal performance using the commercial CFD software FLUENT. It was presumed that there was no underground water flow in the ground and no rain infiltration. The top surface boundary condition is the variation of ground heat flux. The subsurface temperature profile was derived from the recorded experimental data at a site in Saga University, Japan.

Due to the minimal impact on thermal behavior, it was found that the effects of

loop orientation is negligible. While the data demonstrate that the heat exchange rate is profoundly limited by the thermal conductivity of the ground, the mean heat exchange rate of the copper loop increases by 48% when compared to the HDPE loop. In parallel loop operations, the mean heat exchange rate increases by 83% - 162% under identical conditions. Giving distance between adjacent loops can further boost performance in these situations by 10% - 14%. It was determined that the spacing helps to optimize thermal performance by reducing heat flow interference.

Kim, Lee, Yoon, and Go [102] used experiments and numerical simulation to investigate the performance of slinky-loop ground heat exchanger and spiral-coil GHE. Three-dimensional numerical models were generated with the support of Midas NFX. This model included the surrounding soil in the steel box and was based on the finite element method and computational fluid dynamics (CFD). It was found that the soil thermal conductivity is an important aspect in determining the heat exchange rate of a GHE. As a result, when developing a horizontal GHE, it is critical to select the appropriate type of horizontal GHE and take into account the surrounding soil thermal conductivity. The results of this study indicated that the numerical model produced might be applied to future research into the effects of various parameters on horizontal GHE.

Zhang et al. [103] developed a 2-D mathematical model of slinky-loop ground heat exchanger to investigate the effects of different parameters on the thermal behaviour of slinky-loop ground heat exchanger. The results revealed that an increase in inlet temperature can lead to an increase in soil excess temperature and the heat release rate of the slinky coil. It is demonstrated that the heat transfer rate in sandstone is the largest, followed by sand, and the lowest for clay.

Meanwhile, the influence of buried depth change on thermal performance is reduced with an increase of the buried depth. Reducing the coil central interval distance can also improve the heat transfer rate of the slinky-loop ground heat exchanger, but it should be selected with the heat exchanger rate per meter length of coil, pipe cost and available land area. In addition, the ground surface wind velocity can also affect the thermal performance of slinky-loop ground heat exchanger. It was found that the soil temperature operated in intermittent mode can get a recovery, and this helps to improve the heat release rate of the coil.

Tang and Nowamooz [19] created a slinky-loop ground heat exchanger model that included atmosphere-soil-HGHE interaction. To improve the proposed model's accuracy, the atmosphere-soil interaction was validated using a local instrumental temperature probe [104], and the soil-HGHE interaction was input using an experimental measurement result [105]. The results demonstrated that when the heat exchanger site was altered from 0.5 m to 2 m, the working fluid output temperature increased. Nonetheless, the increase was insignificant when the installation depth was increased from 0.5 m to 1 m. It was established that in a numerical modelling setting, consideration of the atmosphere-soil-HGHE was required for accurate prediction.

Zhou et al. [26] conducted a 3D numerical model for horizontal GHE and compared with the experiment in the countryside conditions in NSW, Australia. The results showed that as the distance of trench separation decreased, the carrier fluid temperature increased slightly (0.5°C). In terms of configuration, the dense slinky loop averaged 1.5ºC lower than the horizontal straight and slinky loop.

Numerical models are more time-consuming and complicated for the computing process; 2) it is very difficult to setup a normal mesh production program for

different arrangements; 3) the majority of the numerical methods are performed by the CFD, MATLAB, COMSOL and FEFLOW software. Table 2.1 demonstrates the summary of the numerical models for the slinky-loop ground heat exchanger.

Table 2.1 Outline of studies related to slinky-loop ground heat exchangers.

Year	**Author(s)**	**Studied parameters**	**Type of study**	**Highlighted results/findings**
2010	Wu et al. [23]	Coil diameter, coil central interval distance	Experimental test and numerical modelling (FLUENT)	The heat extraction rate of soil for slinky type was higher that straight type, the effect of coil diameter was limited while specific heat extraction can be improved with the increase of coil central interval.
2012	Fujii et al. [78]	Loop pitch	Experimental test and numerical modelling (FEFLOW)	Thermal conductivity can be decreased with the increase of loop pitch, by applying the surface energy balance, good agreement has been obtained between simulation results and measured data.
2012	Congedo et al. [98]	The pitch, depth of installation, thermal conductivity of ground, heat transfer fluid	Numerical modelling (FLUENT)	The thermal conductivity has the most important influence on thermal performance, the fluid velocity is also critical important, while the impact of installation depth on the system performance was

		velocity		limited.
2013	Fujii et al. [100]	Depth, direction of heat medium circulation, albedo	Experimental test and numerical modelling (FEFLOW)	The optimal depth of upper layer is 1.5m while the lower layer is 2.0m, the circulation from upper layer to lower layer is the best arrangement, lower albedo is more suitable for winter heating season while higher albedo is better for summer cooling season.
2013	Chong et al. [22]	Loop pitch, loop diameter, soil properties, intermittent operation.	Numerical modelling (FLUENT)	The system performance can be improved by decreasing the loop pitch, the effect of loop diameter is less significant while the soil thermal properties is the most important parameter, it is also recommended that the system can be running under intermittent operation for better performance.
2015	Dasare and Saha [21]	Depth of heat exchanger, velocity of heat transfer fluid, soil thermal conductivity	Numerical modelling (FLUENT)	The soil thermal conductivity have the most influence on the heat transfer process, the thermal performance can be improve with the increase of mass flow rate, the double-layer ground heat exchanger was presented to achieve higher energy transfer. The

				best distance between two layers is 1.2 metres.
2015	Selamat, Miyara and Kariya [17, 31]	Continuous operation, intermittent operation, parallel loops operation, orientation of HGHE installation	Numerical modelling (FLUENT)	For 2h discontinuous operation, the heat exchange rate is 16% higher than continuous operation, while the heat exchange rate can be increased by 33% and 21% for 9h operation and 12h operation, respectively. The thermal performance of double and triple loops system was 83% and 162% higher than single loop system.
2016	Selamat, Miyara and Kariya [17]	different layouts, operation mode and pipe materials	Numerical modelling (FLUENT)	HDPE pipe is 16% less effective than copper. When properly installed, vertical slinky-loop ground heat exchangers have a 14% longer effective heat exchange rate than horizontal ones. GHE cycles or alternate cooling-heating modes are best for domestic hot water supply.
2016	Kim et al. [102]	Type of heat exchanger, soil thermal	Experimental test and numerical	The horizontal coil type ground heat exchanger has presented a 10% higher heat

		conductivity, pipe diameter	modelling (Midas NFX)	exchange rate compared with slinky loop ground heat exchanger, the soil thermal conductivity is the most important parameter while the effect of pipe diameter is less significant.
2017	Zhang et al. [103]	Operation mode, groundwater advection velocity, soil type, buried depth	Experimental test and numerical modelling	The heat release rate increases with the increase of inlet fluid temperature, it can also be improved by using intermittent operation mode. The sandstone type soil is considered to have the best thermal performance, while the influence of buried depth is limited.
2017	Han et al. [106]	Design configurations, soil thermal properties, and incorporating with field monitored subsurface temperature	Numerical modelling (COMSOL)	The slinky-loop ground heat exchanger system can reach a 25% to 60% higher performance with accurate soil temperature, the impact of soil thermal properties on system performance is less significant, the usage of local geological data can improve the annual performance.
2018	Sangi and Muller [18]	Height of the soil cell, number of X-	Experimental test and numerical	The discretization of the mesh is the most important parameter for the numerical

		direction discretization, the flexible grid in marginal areas	modelling (Modelica)	model accuracy, good agreement was found between the proposed numerical models and published experimental results.
2020	Asgari, Habibi and Hakkaki-Fard [101]	Types of horizontal GHEs, pipe arrangement, soil thermal conductivity	Numerical modelling (FDM)	For linear GHE, the pipe arrangement with four layers can improve the thermal performance by 36% compared with conventional single-layer arrangement. Similar trend was found for slinky-loop ground heat exchanger, the thermal performance can be increased by 22% compared to conventional single-layer arrangement. No significant difference was found between single and double pipe arrangement for spiral GHE.
2020	Tang and Nowamooz [19]	Installation depth, the atmosphere soil interaction	Numerical modelling (FVM)	Good agreement was found between numerical results and existing data from literature, the ground heat flux can be affected by the soil surface temperature, with the increase of installation

				depth, the outlet fluid temperature can be increased. The atmosphere soil interaction plays a critical role for the accuracy of numerical modelling.
2020	DiCarlo, Videchak and Caldwell Jr. [107]	Comparison between winter heating season and summer cooling season, homogeneous and optimized	Numerical modelling (ANSYS CFX)	For winter heating season, the optimized heterogeneous soil configuration will lead to a significant increase of the thermal performance, while the performance for summer cooling season can be improved by soil with high thermal conductivity. The optimization method carried out in this study can be further adapted for better performance.
2021	Zhou et al. [26]	Industrial loading conditions, GHE configurations and trench separations, effective thermal conductivity	Numerical modelling (COMSOL)	The trench distance has less influence on slinky-loop ground heat exchanger performance compared with the change form slinky loop to dense loop. The effect of the GHE configurations and trench separations are more significant than the impact of effective thermal conductivity.

2.4 Comparison between analytical and numerical models

To solve the underlying physical mechanisms, numerical modelling methods including finite-difference, control-volume and finite-element methods have been well developed. Still, these methods seem to be impractical for engineering projects base on several reasons [108]:

1) For some large applications, sometimes the time and space scales are critical and have to be tackled, thus the simulation progress could be year-around and/or even life cycle.
2) The model of GHE simulation is complicated since the general grid generation program for different configurations of ground channels is difficult to develop for in-house programming.
3) According to previous studies, commercial software such as FLUENT and FEFLOW have been used for most of the numerical models.

Compared with analytical methods, numerical modelling methods can provide a high level of accuracy and flexibility particularly for short-term scales. However, with the utilization of cylindrical grids, most of the numerical models are computationally inefficient since there are a huge number of complex grids [55]. In reality, to participate directly with design or energy evaluation projects, the simulation data can be used if it was pre-computed or collected from a massive database.

Analytical models are developed according to several reasonable simplifications and assumptions to solve the mathematical models. As a result, it decreases the accuracy of final result based on the assumption of the line source at the centre

of the borehole, which ignore the physical size of the U-tube in the borehole [109]. However, less simulation time is required for analytical methods compared with running numerical models. Another advantage is that the straightforward algorithm derived from the analytical models can be easily combined into a design/simulation program.

The simplifications of heat and mass transfer model results have neglected some important issue including moisture transport in the ground, ground freezing and the ground surface effect since the line source theory has been broadly utilized for GHE modelling procedures. During the past decade, for GHE thermal analysis, the analytical models neglect the short-time response of GHE through either ignoring it completely or using oversimplified assumptions. However, the short-term variations have been proved to have magnificent impact on the performance of the heat pump and the entire system in real engineering applications [54].

Meanwhile, another important factor needs to be considered is the short-term response of the ground during heat flux build up stages. Research related to sub-hourly thermal energy use and the electrical demands of the ground coupled heat pump system also needs to analyze the effect of short-term response of the ground. Thus, more strict assumptions are needed for short-term response of GHE, and more complex models are required since a line or a cylindrical source are not enough. The actual geometry of the GHE is retained when determining its short-term response by solving the mathematical equation using numerical analysis (such as CFD software). When compared to the typical line and cylindrical source models, numerical models can provide more precise estimations of the ground heat and mass transfer process.

Overall, numerical models are more reliable for high accuracy of the simulation results or in parametric analysis. Thus, numerical models for GHE contribute to a more comprehensive analysis of GSHP systems. Based on previous studies, CFD has been proved to be more suitable for GHE thermal analyzation during the design and optimization process [110].

2.5 Experimental methods on HGSHP

There are two categories of experimental approaches for HGHEs: full-scale experiments and small-scale experiments. As the expense of excavating HGHE ditches is comparatively lower than that of drilling deep boreholes, conducting in-situ experiments on HGHE appears to be more feasible in comparison to shallow BHE.

Wu et al. [23] have studied the thermal behaviour of a slinky-loop ground heat exchanger built at Talbot Cottage, Drayton St Leonard site, Oxfordshire UK. In a paddock area with 80m length and 20 m width, 4 parallel slinky-loop heat exchangers were placed at a depth of approximately 1.2m below the ground surface. A mixture of water and ethylene glycol (30% by weight) has been used as antifreeze fluid. The ground surface above it was covered by grass. They have also employed soft sand in their experiment, both on top of and underneath the slinky heat exchanger.

Fujii et al. [78] tested a number of slinky-loop ground heat exchanger in a field at Kyushu University with a groundwater level of 18 meters. The polyethylene pipe’s inner and outer are 0.034 and 0.024 meters, respectively, while the loop diameter is 0.8 meters. The trench length and depth are 72.0 and 1.5 meters, respectively.

Adamovsky et al. [111] have investigated the thermal performance of slinky-loop and linear HGHE, which are utilized to heat a manufacturing halls and administration building of a company in Prague. For three loops with one meter span, the linear HGHE was installed 1.8m below the ground surface and has a total length of 330 metres ($41.473m^2$). Another 200 m ($20.107m^2$) long slinky-loop ground heat exchanger has been place in 53 circular loops with a 0.38m span at a depth of 1.5m. During these experiments, the antifreeze solution that had 33% ethanol and 67% water has been used for both HGHEs. In order to assess the temperature changes through the experiment procedure, thermal probes have also been placed underground.

Ali et al. [112] have carried out an in-situ experiment for slinky-loop ground heat exchanger of two orientations: standing (perpendicular to ground surface) and reclining (parallel to ground surface) in Sage University. These two different HGHE were placed 2m away from each other. To improve the efficiency of the HGHE, copper pipe with an exterior layer that coated in low density polyethylene (LDPE) has been used for the heat exchanger. For both standing and reclining HGHE, they both have 7 loops and the trench length and loop diameters were 7m and 1m respectively. The centre of the standing GHE was placed 1.5m under the ground surface in a trench that is 1.5m wide, while the reclining GHE was placed 1.5 below the ground surface with a trench width of 1.0m.

Small-scale experimental tests have also been conducted by many researchers. Yoon et al. [105] carried out two field tests in a sandy box with pipes that were 24m and 66m long, respectively. The indoor air temperature has been kept consistent by using a far-infrared radiation heater. During the experimental tests,

the polybutylene pipe with inner and outer diameter of 16mm and 20mm has been placed at 0.5m below the ground surface in a dry sand box with dimensions of 5m × 1m × 1m. The test period is 30 hours and water has been chose as carrying fluid.

Another small-scale experimental test has been developed and conducted by Al-Ameen et al. [16] in Nottingham Trent University to study and assess the thermal performance of a HGHE system, which is operating under charging and discharging modes with various backfill soil and carrying fluid flow rates. The sink tank model has internal dimensions of 1m × 0.5m × 0.125m. Copper pipe has been used with 5m length, and the carrying fluid is water.

Yang et al. [113] conducted a study on the thermal efficiency of helical-coil horizontal ground heat exchangers using a small-scale experimental setup. They examined various factors including inlet temperatures, pitch, surface wind speed, and soil types. The primary findings of this study can be summarised as follows: altering the working fluid inlet temperature during the cooling and heating seasons helps optimise the heat exchange rate of the HGSHP system; It indicate that decreasing the helical pitch can enhance the overall heat exchange rate, although it may reduce the heat exchange rate per unit length; By raising the speed of the surface wind, it is possible to boost the convective heat transfer that occurs between the ground surface and the atmosphere; the convective performance is increased when the buried depth is reduced; When compared to continuous operation, intermittent operation makes it possible to keep the soil temperature at a set level; Increasing the coil diameter can result in a minor improvement in the overall heat exchange rate, but it also results in a reduction in the heat exchange rate per unit length. An experimental investigation into the

thermal performance of Al2O3/ethylene glycol-water nano-fluid with different concentration ratios (0.1% and 0.2%) was carried out by Kapicioglu and Esen [114]. Research and analysis were conducted on both linear-loop and helical-coil types of GHE. According to the findings of the experiments, the linear-loop GHE with a concentration of 0.1% nano-fluid had a performance that was 19% higher than that of ethylene glycol-water, and 17.7% better than nano-fluid with 0.2% concentration. The values for helical-coil GHE were 21% and 37%, respectively.

Du et al. [115] conducted an experimental study to examine the effects of using nanofluid (CuO-water) as a heat transfer fluid on the performance of HGHE. It turned out that the use of nano fluid resulted in an increase of 16.6% in the pumping power consumption, 39.84% in the rate of heat exchanged, and 20.2% in the ratio of heat load to pumping power. Additionally, in order to achieve the objective of enhancing the influence of nano fluid, the length of the straight tube portion ought to be limited, and the number of bends ought to be increased.

2.6 Summary

This chapter begins with an introduction to the GSHP classification. Typically, applicable ground heat exchangers are classified as open and closed ground heat exchangers. This chapter presents a review of analytical, numerical, and experimental studies on the thermal performance of vertical and horizontal ground heat exchangers. Most previous evaluations relied on modelling methodologies, system design, configuration optimisation, and techno-economic analysis for GSHP systems, with the focus being on VGHE rather than HGHE. As a result, this chapter demonstrated and discussed the majority of the

most current notable research works on optimal thermodynamic analysis of HGHE, including the different configurations: linear-loops, slinky-loop, and helical-coils. Analytical and numerical models are the most commonly utilised methodologies for evaluating the performance of ground heat exchangers. Thus, comparisons of analytical and numerical models were summarised. This chapter also concludes several aspects impacting the performance of horizontal ground heat exchangers. Previous investigations have revealed the following research gaps between the previous research and current study:

- Few studies have been performed to deeply investigate the effects of various factors such as inlet temperature, ambient air temperature, ground surface wind velocity, soil type and buried depth on thermal performance of slinky-loop ground heat exchanger system in the whole heating season. Specifically, the influence mechanism of different factors on the total heat extraction amount/energy output ratio was still less understood. The key factors selected for this study will include installation depth and pipe configuration, operating conditions (ambient and fluid temperatures), and thermal properties (conductivity, density and specific heat) of the ground which are known factors that affect the performance of horizontal-type GHE from previous studies.
- HGHE are also influenced by the initial ground temperature profile, which should be taken into account. The heat recovery ability of the soil will also be assessed when the heat exchangers are not in operation. The effect of the ground surface is generally simplified and taken to be a (annual mean) constant-temperature boundary condition in previous researches. The effect of varying ambient conditions will be investigated.

- A HGSHP system model also lack of considering heat demands-varying on-off period operation. The impact of monthly variations of thermal load on the operation of HGSHP system need to be examined. For example, performances of three daily operation modes (continuous operation, intermittent operation and monthly changed intermittent operation) can be compared.
- Lack of estimating the economic behavior of a GSHP system, it is important to know the heating load of a building, the electricity consumed, the local electricity price, the subsidy from the local government and the predicted payback period time. The GSHP systems in UK climatic regions lack of evaluation to provide a better understanding of the economic (financial) and environmental benefits of using slinky-loop ground heat exchanger within the UK.
- Little attention has been paid so far to the performance of pipe groups while thermal interference between parallel pipes cannot be neglected. When pipes are connected in parallel, it is necessary to investigate the effects of different center-to-center trench spacing. The thermal interference between adjacent buried pipes is the significant factor affecting the thermal efficiency of HGHE, unless the pipe spacing reaches the critical pipe spacing. The critical pipe spacing is also affected by buried depth, soil properties, operation mode, etc. Although some research investigated the multiple layer arrangements, comparison between different arrangements and parallel pipe spacing has not yet been conducted.
- The annual performance of slinky-loop ground heat exchanger needs to

be evaluated by considering single heating season operation and double cooling and heating season operation. The variation of ground temperature can be used as the indicator to compare the long-term performance under the assumption that the building heating/cooling demand is fully met with the GSHP system.

- There is a lack of estimation methods for accurately calculating the required trench/pipe length for slinky-loop ground heat exchanger installation.

Chapter 3: Methodology of numerical slinky-loop ground heat exchanger model

3.1 Introduction

The majority of the literatures in GSHP system indicates that accurate results can be predicted by a numerical model that is appropriately established and simulated using proper parameters. The total cost of installation will increase if the design of the ground heat exchanger is not optimised for a specific application, and the land generally comes at a premium. Hence, the key objective of this research is to establish a numerical methodology for the dynamic thermal simulation of slinky-loop ground heat exchanger To achieve these objectives, a 3D numerical model is developed considering different initial and boundary conditions. There are several unidentified elements involved in the heat transfer process in a ground heat exchanger. The study will start with fundamental preparation: defining a method to develop a numerical model, verifying the simulation model, and simulating a validated model under different conditions. The effect of topsoil boundary condition, initial soil temperature and heat exchanger pipe temperature on thermal performance will be discussed in continuous or intermittent operation mode. Further significant factors that impact the thermal performance of slinky-loop ground heat exchanger have been identified.

3.2 Governing equations

Philip and de Vries [116] created the general equations for heat and moisture

flow in porous materials like soil under combined temperature and moisture gradients, and these equations serve as the basis for the governing equation here. First, take into account the heat transfer through the control volume. Heat gain and loss through soil in a control volume are the consequences of sensible heat transfer via conduction due to the temperature gradient and latent heat transfer by vapour movement due to the moisture gradient:

$$\dot{q} = -\left(k + L_{water}\rho_l D_{T,v}\right)\nabla T - L_{water}\rho_l D_{\theta,v}\nabla\theta \qquad (3.1)$$

where k is the thermal conductivity of soil (W/mK), the product $L\rho_l D_{T,v}$ is the contribution to the apparent thermal conductivity by latent heat transfer from vapour movement due to the temperature gradient and L_{water} is the latent heat (for evaporation/condensation) or fusion of water (for freezing/thawing) (J/kg). According to the principle of energy balance, it is necessary for the rate at which heat is gained or lost in a control volume to be equal to the total of net rate of heat flow into the volume and the rate of heat generation or dissipation occurring in the volume. For this study, the heat transfer equation in soil containing a slinky-loop ground heat exchanger is derived below with the following assumptions:

- Thermal properties（heat capacity, density and thermal conductivity）of soil were constant and uniform [22, 24, 98].
- The moisture transfer，the movement of solutes in the soil and rain infiltration during heating season was ignored [22, 23].

As a result, heat is transferred between the ground surface and the subsurface via sensible heat conduction. The subsurface temperature profile would be governed by heat conduction in the ground. The heat transfer in soil surrounding

a heat exchanger is determined by the following conduction equation:

$$\rho c_p \frac{\partial T}{\partial t} = H + \nabla(k \nabla T) \tag{3.2}$$

where ρ is the density of the soil (kg/m^3), c_p is the specific heat (J/kg K), T is the temperature (K), t is the time (s) and H is the heat generation or extraction (W/m^3).

In present study, commercial CFD software package ANSYS FLUENT [117] is used to solve the governing equations for transient 3D model.

3.3 Description of the model

In order to avoid potential freezing problems, a water-ethylene glycol (30% by weight) mixture is a typical antifreeze solution [23]. For several reasons, High-Density Polyethylene (HDPE) is by far the best material to use for geothermal piping [118], such as, high chemical resistance, high pressure rating, no mechanical fittings, and good thermal conductivity. The pipe temperature was fixed at 1 °C for operation in heating mode and 30°C for operation in cooling mode[85]. The thermal properties of the HDPE and water-ethylene glycol (30% by weight) mixture are shown in Table 3.1.

Table 3.1 Main properties of the materials used in the simulations [98, 119].

Symbol (unit)	Pipe (HDPE)	water-ethylene glycol (30% by weight) mixture at 1°C	water-ethylene glycol (30% by weight) mixture at 30°C
$\rho\ (kg/m^3)$	946	1047	1032

$k\ (W/mK)$	0.35	0.469	0.490
$c_p\ (J/kgK)$	1920	3652	3745
$u\ (\ m^2/s\ )$		4.13E-06	1.57E-06

For given operating conditions of a water-ethylene glycol (30% by weight) mixture in the HDHE pipe, the surface heat flux (W/m^2) and heat transfer rate (W/m) between the pipe and the surrounding soil can be obtained from simulation. The heat flux per unit pipe surface area was obtained from CFD software. The surface heat flux is the ratio of the heat transfer rate to the total pipe surface area. Since the horizontal ground heat exchanger was evaluated based on the heat transfer rate occurring at the interface between the surface of the pipe and the surrounding ground. The heat transfer rate expressed per unit trench length, q, is calculated using Eq. (3.3) for a single loop.

$$q = \frac{HF \cdot A}{L_{trench}} \tag{3.3}$$

where HF is the heat flux per unit pipe surface area, A is the surface area along the pipe, L_{trench} is the length of trench in the slinky-loop ground heat exchanger model.

These together with the total heat transfer for a period of operation (kWh) were used to evaluate the performance of slinky-loop ground heat exchanger. The simulations were conducted for the heating season in the UK from 1st September to 31st March. The simulation results are presented in terms of monthly or seasonal total heat transfer in kWh. The daily operating time for the simulations is 24-hour continuous operation.

3.3.1 Slinky-loop ground heat exchanger model

The arrangement of slinky-loop ground heat exchangers utilized in commercial installations for ground source heat pump (GSHP) systems varies across different countries. In the UK and Europe, the commonly used pipe diameters are OD25 (i.e., 25 mm), OD32 (i.e., 32 mm) and OD40 (i.e., 40 mm). OD40 is the most frequently utilized pipe diameter in the United Kingdom [120]. In Ireland, OD32 is most commonly used [121].

Slinky-loop ground heat exchangers installed in the UK and Europe have standard loop diameters of 0.8 m, 1.0 m, and 1.2 m. The most typical loop diameter is 1.0 m [122-124]. The loop pitch used in the UK and Europe is usually equal to the slinky-loop diameter [122-124].

The thermal performance of the slinky-loop ground heat exchanger was analysed using a transient 3-dimensional model. The main part of the horizontal heat exchanger consisted of a circular HDPE pipe with a 40 mm diameter. The ground heat exchanger loop with 1 m loop diameter and 1 m loop pitch was positioned horizontally at Z_1 =1.2 m below the ground surface. The CFD solution domain is shown in Fig. 3.1. The total depth Z_d (= Z_1+Z_2) of the computational domain was 10m.

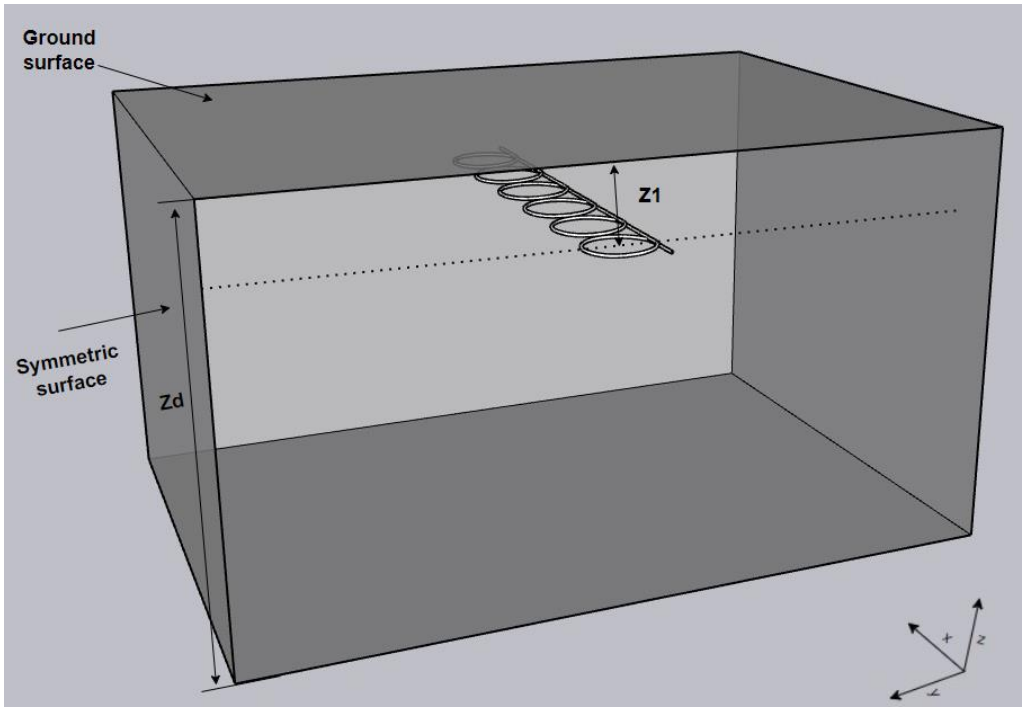


Figure 3.1 Computational domain for soil with slinky-loop ground heat exchanger.

Typically, the slinky-loop ground heat exchanger experiences a decrease in heat transfer along the flow direction as a result of an increase in the temperature of the fluid and a decrease in the temperature difference along the flow passage. This implies that an increase in the length of the heat exchanger results in a decrease in the mean heat transfer, which is averaged over the length. However, the temperature rise in the HDPE pipe is low considering the high mass flow rate. Specifically, it is less than 0.2 °C and 1 °C through 10 m and 40 m long heat exchangers, respectively, after flow has reached a state of fully established [125]. This means the temperature difference in a one-meter heat exchanger is less than 0.02°C. Hence, the heat transfer rate per meter length of trench for a slinky-loop ground heat exchanger can be considered almost independent of the length of the ground heat exchanger. The surface temperature of the slinky-loop

ground heat exchanger in one-meter length of trench can be considered as a fixed value. Therefore, for the purpose of reducing the amount of computing power that was required, a symmetrical slinky-loop ground heat exchanger was taken into consideration, and one half of the slinky-loop ground heat exchanger was modelled, as can be seen in Figure 3.2. The vertical boundary was defined as symmetrical surfaces, assuming the domain was part of a larger volume of soil buried with the same configuration of HE loops. A symmetric boundary condition was applied at the planes of symmetry, which indicated zero heat flux through the symmetric plane. The temperature of the bottom boundary was set as constant 10°C – the annual mean temperature of the deep soil in the UK [22].

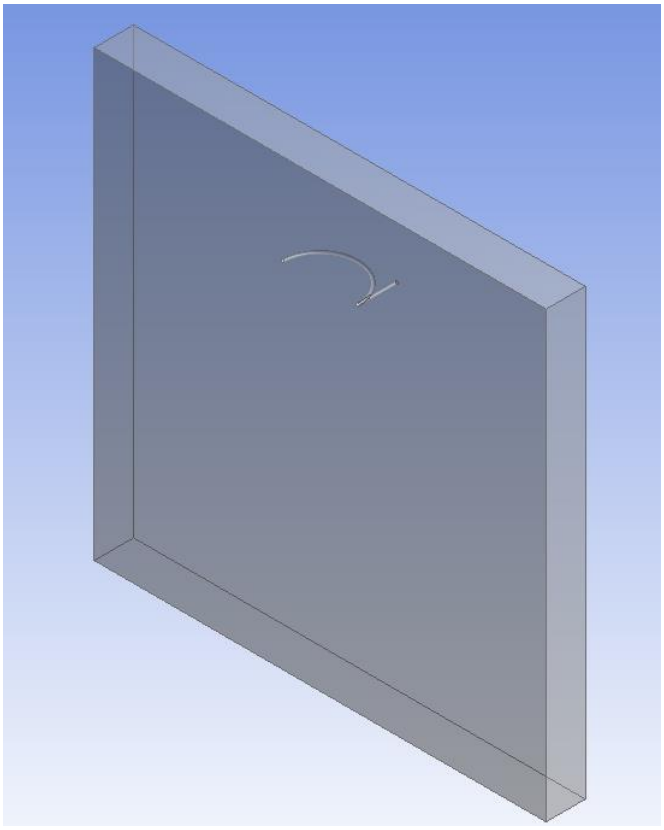


Figure 3.2 Computational domain for soil with symmetrical slinky-loop ground heat exchanger.

3.3.2 Topsoil boundary condition

Soil temperature varies in response to changes in the radiant, thermal, and latent energy exchange processes that take place primarily through the soil surface. The influence of the aggregated above ground phenomena within a short distance inside the solid domain of the formation and fill forms a thermal front descending through the solid domain by thermal conduction [126]. The thermal front is subdued further by the thermal damping of the formation mass.

Since the ambient temperature continuously varies, and is influenced by a degree of solar radiation, this study is not focused on the diurnal variation. The top surface of the model was assumed to vary monthly with a monthly average ambient air temperature and a monthly average wind speed to avoid short-term temperature perturbations resulting from day and night irr/radiation, precipitation condensation, and evaporation heat transfer under vegetation in heating seasons.

The outdoor ambient air temperature is stated as the soil surface temperature. The convection heat transfer coefficient between the topsoil and ambient air varies with wind speed as follows [78]:

$$h_c = 5.8 + 3.9 v_{wind} \quad (v_{wind} < 5 m/s) \tag{3.4}$$

$$h_c = 7.1 v_{wind}^{0.78} \quad (v_{wind} > 5 m/s) \tag{3.5}$$

Where h_c is the convective heat transfer coefficient at the topsoil surface (W/m^2K) and v_{wind} is the wind speed (m/s).

The monthly boundary conditions for Coventry as shown in Table 3.2 were used in the simulation [127].

Table 3.2 Monthly air temperature and wind speed in Coventry.

	Temperature (℃)	Wind speed (m/s)
September	13.83	4.68
October	10.63	5.08
November	7.33	5.20
December	4.75	5.52
January	4.5	5.78
February	4.67	5.60
March	6.13	5.31
Average	7.40	5.31

3.3.2.1 The effect of different topsoil surface boundary conditions

Table 3.3 Boundary condition of CFD simulation.

Installation depth	1.2 m
Soil type	Loamy soil
Operation mode	Continuous operation
The initial soil temperature	Varying temperature with the depth
Pipe temperature	1℃
Climate data	Coventry
Loop pitch	1.0 m

The boundary condition of the ground surface are generally taken to be constant-temperature (average for heating season) boundary condition [22]. In this project, the ground source heat pump was running for 7 months, thus it was critical to

evaluate the impact of realistic monthly changed soil surface boundary conditions. Monthly changed air temperature and wind speed of Coventry have been used for boundary conditions, which was compared using heating-season average air temperature and wind speed, as shown in Table 3.2. The results were obtained by assuming the initial soil temperature of varying temperature profile under the continuous heating operation. Table 3.3 shows the boundary conditions of the simulation.

Fig. 3.3 shows the comparison between the heat exchange rate per unit length of trench under monthly changed soil surface boundary condition and the heating-season average soil surface boundary condition. It is found that the slinky-loop ground heat exchanger exhibited a high heat transfer rate at the beginning because of the large temperature difference between the surrounding soil and working fluid. As the simulation continued, the heat transfer rate decreased gradually for using both monthly changed or heating-season average data. By the time the heating period reaches the 720^{th} hour (30 days), the difference between two different boundary conditions was 17.3 W/m, and it continued to reduce. The heat transfer rate of two different soil surface boundary conditions were almost the same around the 2348^{th} hour. Then, the heat transfer rate for using heating-season average conditions became slightly higher and almost stable. At the end of December, the heat transfer rate for this slinky-loop ground heat exchanger using a monthly changed boundary condition was 20.6 W/m and 23.3 W/m for using heating season average conditions, respectively. The heat transfer rate difference between the two boundary conditions reduced again in March. At the end of the heating period (5112^{th} hour), the heat transfer rate for this slinky-loop heat exchanger using the monthly changed boundary was 21.7

W/m and 22.0 W/m for using heating season average conditions, respectively.

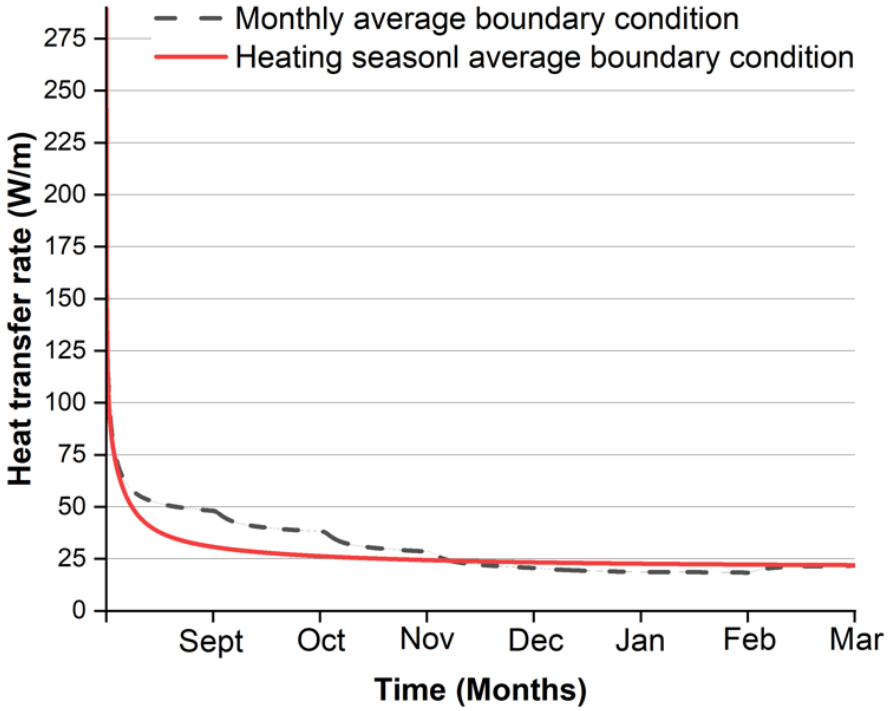


Figure 3.3 Heat transfer rate of different top surface boundary conditions at the end of each month under continuous operation.

Fig. 3.4 shows the variation of heat extracted amount from the surrounding soil in each month. Because of the decreasing heat transfer rate, the amount of monthly heat extraction decreases from September to February. From September to November, the heat extraction amount using the monthly changed boundary condition was higher than using the heating season average boundary condition. On the contrary, from December to March, using the average for the heating season was higher than monthly changed. This is because the monthly air temperature from September to November is higher than the average air temperature for the entire heating season, while the monthly air temperature for the rest of the months was lower than the average value. The total seven-month heat extracted amounts for average and monthly changed boundary conditions

are 138.9 kWh and 154.4 kWh, respectively, which is nearly the 10.01% difference. The heating-season average boundary conditions were adopted to simplify the simulation in some of previous research. This simulation result indicates that heating-season average boundary conditions could not be used to accurately estimate the total amount of heat extraction for the entire heating season. Especially, if hourly heat exchanger rate and monthly heat extraction amount prediction are required, using a monthly changed boundary condition is suggested for more accurate results.

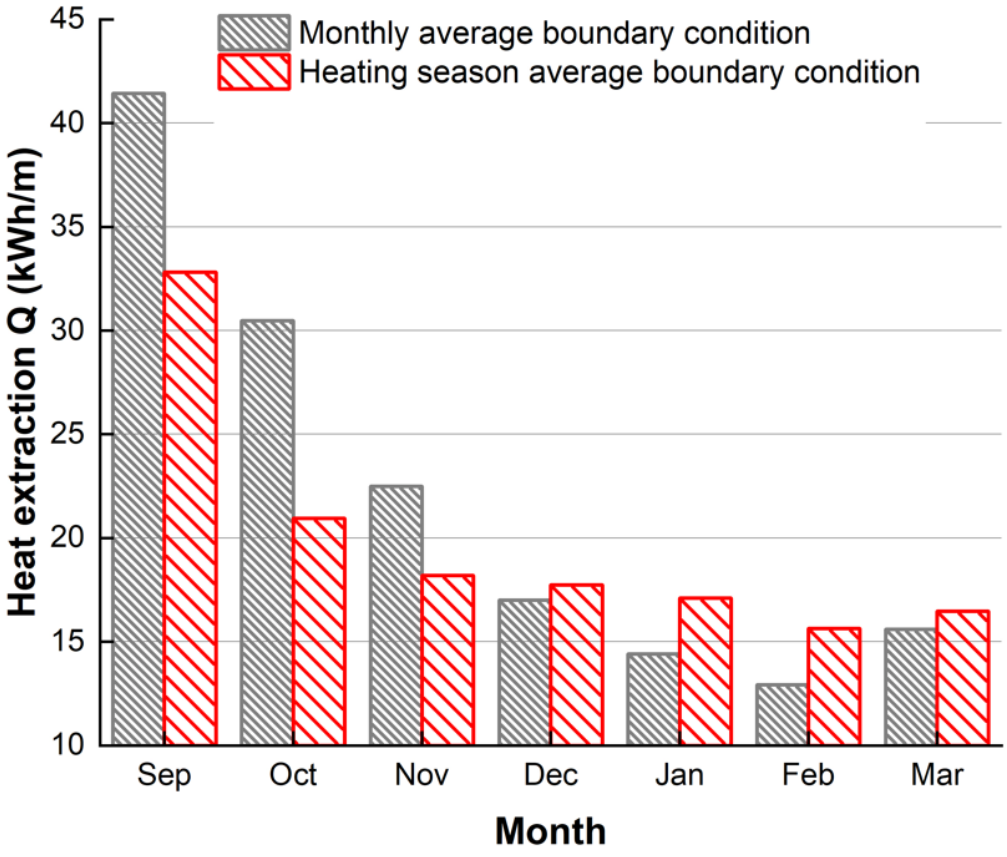


Figure 3.4 Monthly heat extraction under different top surface boundary conditions.

3.3.3 Initial soil temperature

The initial soil temperature is another essential set of data for the simulation and

design optimization of GSHPs. However, it is challenging to find published data for a specific microenvironment. Measuring locally unique data is also not always feasible due to time and budget constraints. In order to understand the variation, greater depth data must be collected and monitored for at least a year. Even if the situation permits data collection, there is no guarantee that the data will not fluctuate due to changing environmental events such as rainfall, water table movement, or the possible installation of energy systems in the surrounding area. The initial soil temperature depends on the time t (day) and lag t_0, which is from a beginning date to the day with the lowest temperature in a year (day). The initial soil temperature of different depths Z (m) for simulation at the start of the heating season was calculated with the following empirical equation for soil with homogeneous properties [32].

$$\mathrm{T} = T_a + T_{amp} e^{-\frac{Z}{D}} \sin\left((t - t_0)\frac{2\pi}{365} - \frac{Z}{D_{damping}} - \frac{\pi}{2}\right) \qquad (3.6)$$

Where T is the initial soil temperature (℃), T_a is the yearly average temperature of soil (℃), T_{amp} represents the yearly amplitude of surface temperature (℃) and $D_{damping}$ is the annual fluctuation damping depth (m).

This equation requires yearly data of ambient temperature and the thermal properties of soil. The climatic data utilized for the simulation were from a weather station in the Midlands (city of Coventry) UK in the year 2020, at the coordinates: Latitude 52°24′24″ North and Longitude -2 °29′16″ East. The values used for this estimation are listed in Table 3.4 [127].

Table 3.4 Data for estimating ground temperature variation at the beginning of September.

Mean ground temperature, T_a (℃)	10
Maximum average air temperature, T_{max}(℃)	17
Minimum average air temperature, T_{min} (℃)	4
Temperature amplitude of air, T_{amp} (℃)	6.5
Day of T_{min}, t_0	37
Soil diffusivity, α (m^2/day)	0.085 (for loam)

Fig. 3.5 depicts an example of the calculated soil temperature variation with depth for the site at the beginning of September. The variation of temperature at the time is close to linear up to 5 m deep. The calculated temperature data served as the initial conditions.

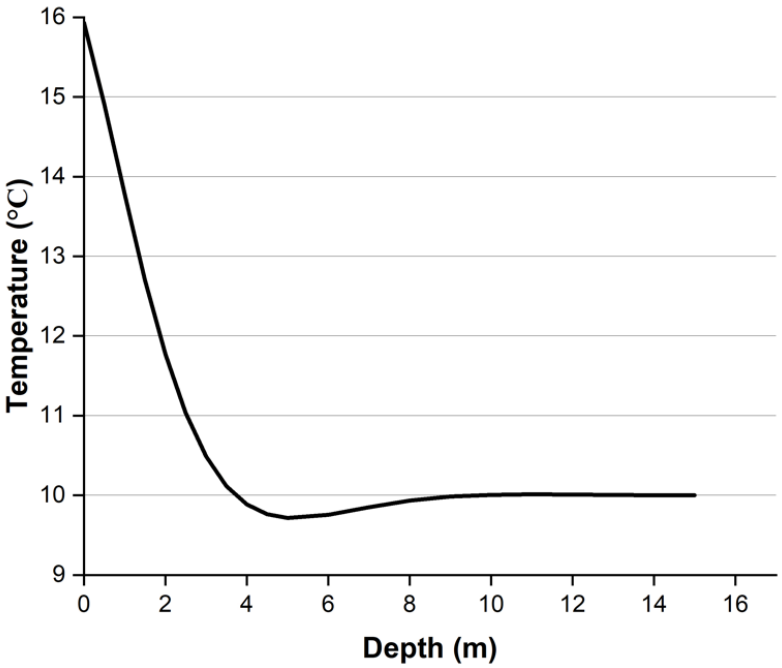


Figure 3.5 Initial ground temperature profile.

3.3.3.1 The effect of initial soil temperature

Table 3.5 Boundary condition of CFD simulation.

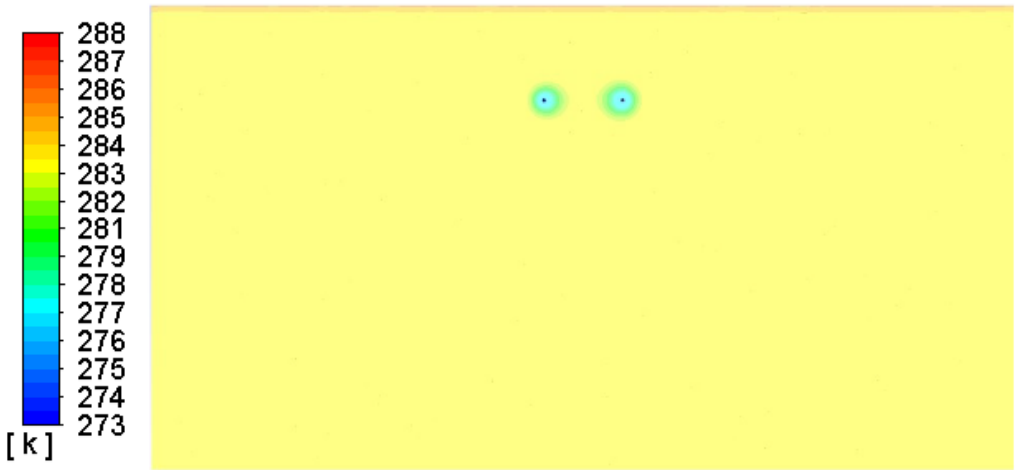
Installation depth	1.2 m
Soil type	Loamy soil
Operation mode	Continuous operation
Pipe temperature	1℃
Topsoil boundary condition	Monthly changed air temperature and wind speed
Climate data	Coventry
Loop pitch	1.0 m

The initial soil temperature are generally simplified and taken the same as the deep soil (283 K) [22]. Fig. 3.6 shows the temperature distributions for the slinky-loop ground heat exchanger at the depth of 1.2m in loamy soil, with two types of initial soil temperature - uniform soil temperature of 10℃ and varying temperature with the depth at the beginning of the heating season on a selected time. For more accurate prediction, the topsoil surface boundary condition was using monthly average ambient air temperature and monthly average wind speed. The simulation boundary conditions are displayed in Table 3.5. The temperature distribution of the slinky-loop ground heat exchanger with a uniform initial soil temperature has a significant difference with the varying initial soil temperature at the 10^{th} hour (see Fig. 3.6(a) -(b)); the low temperature region of 4°C near the heat exchanger's surface has formed, and it is larger with uniform initial soil temperature at the same time. From the 10^{th} day to the end of September, the low temperature region of both initial soil temperature

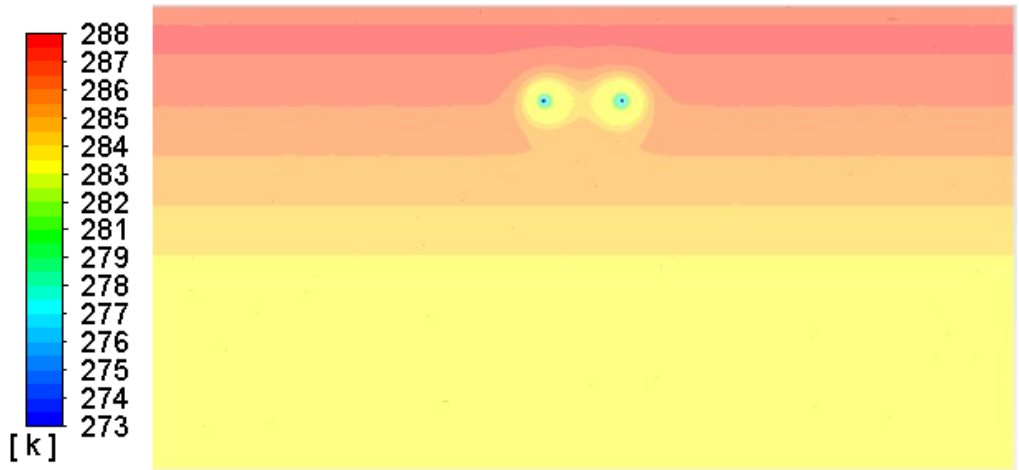
continues to spread up, and the soil near the top surface with a uniform initial soil temperature is warmed by the air temperature, as shown in Fig. 3.6(c)-(f). At the end of November, the temperature distribution became very close, as shown in Fig. 3.6(g)-(h). Soil with a maximum temperature of 4°C was still abundantly present around the heat exchanger, whereas soil with a temperature of 1°C was only found near its surface. It would therefore require more time to reach steady conditions.

Fig. 3.7 depicts the simulation results of the monthly heat transfer amount through slinky-loop ground heat exchanger. As mentioned in Chapter 3.3.3, the calculated initial temperature at 1.2 m deep, for instance, was 13.4 °C instead of the constant value of 10 °C and the resulting discrepancy in soil temperature would have a significant impact on the heat transfer rate in the first few heating months. The difference for the first month was 16%, and then decreased to 6% and 2% at the end of the second and third month, respectively. The effect of the initial soil temperature decreased further and became negligible at the end of the heating season. This difference reduction can be explained by Fig. 3.8(a), which illustrates the vertical soil temperature distribution at the centre of the slinky loop from the ground surface to 5 m below the surface. At the end of September, there are significant differences in the soil temperature from 1.2 m depth to 5 m depth between the two types of initial soil temperature. And the soil temperature difference between a uniform initial soil temperature and a varying initial soil temperature at 1.2 m below soil surface was approximately 0.28°C and decreased to around 1.23°C and 1.08 °C at a distance of 3 m and 4m below soil surface in vertical direction, respectively. It can be observed that this difference in the soil temperature decreased from 0.12 °C to 0.05°C (at 1.2 m depth),

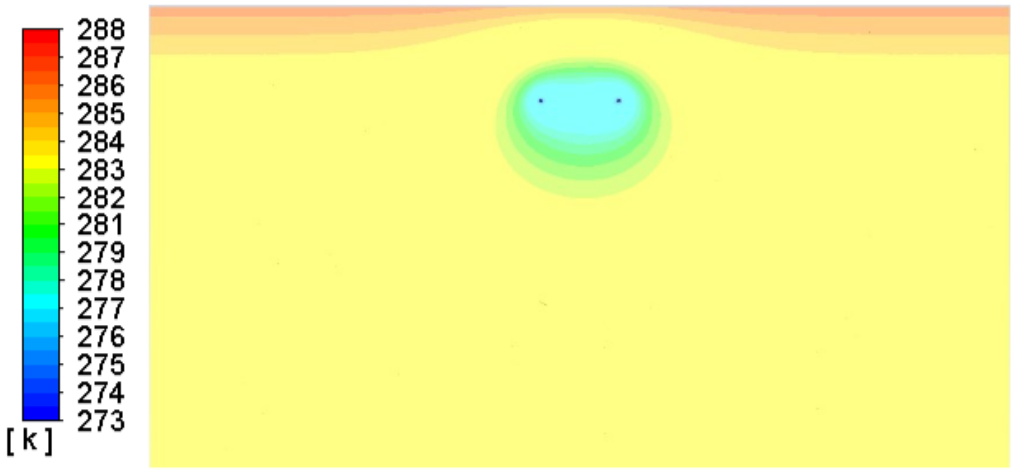
0.54°C to 0.25°C (at 3 m depth), for October and November. By the end of December, these two predicted soil temperature lines are nearly overlapped. The variation in soil temperature within 2 m depth of the first month has been compared. It can be observed from Fig. 3.8(b), the simulated soil temperature with an initial uniform profile from the ground surface to 1.2 m below the surface is lower than that calculated using Equation 3.8. The largest difference occurs at the first hour, and then the trend of two simulated lines becomes similar from the first day to the 10th day within two meters depth. It can be concluded that the initial soil temperature condition has a negligible impact on the soil temperature after three months of operation.



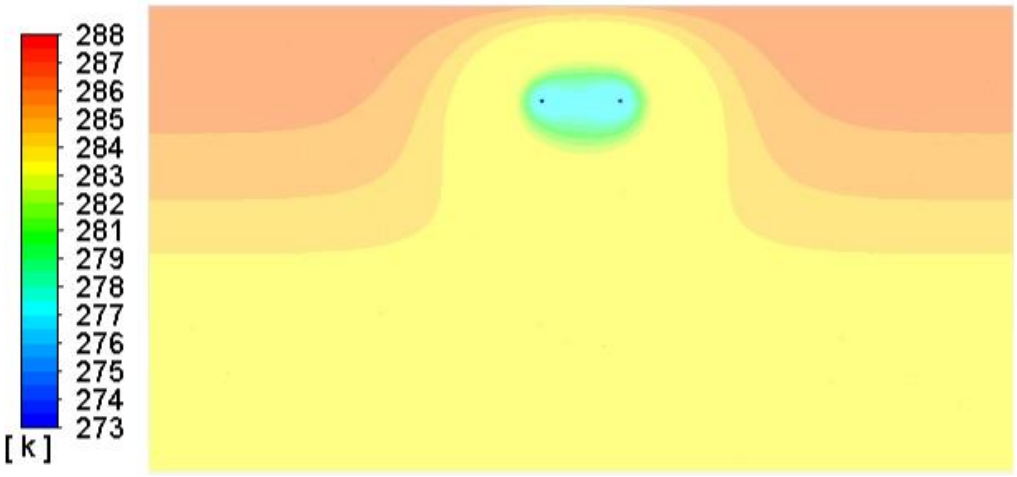
(a) The end of the 10th hour with uniform temperature



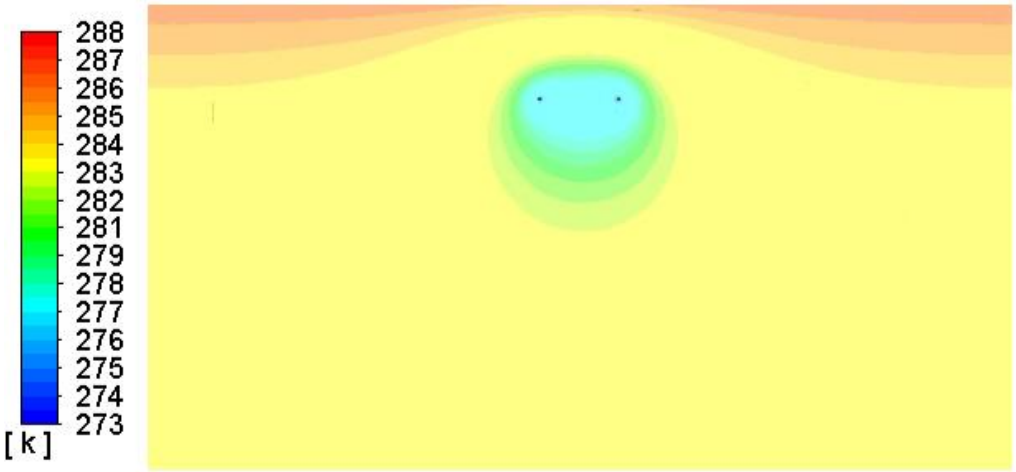
(b) The end of the 10th hour with varying temperature



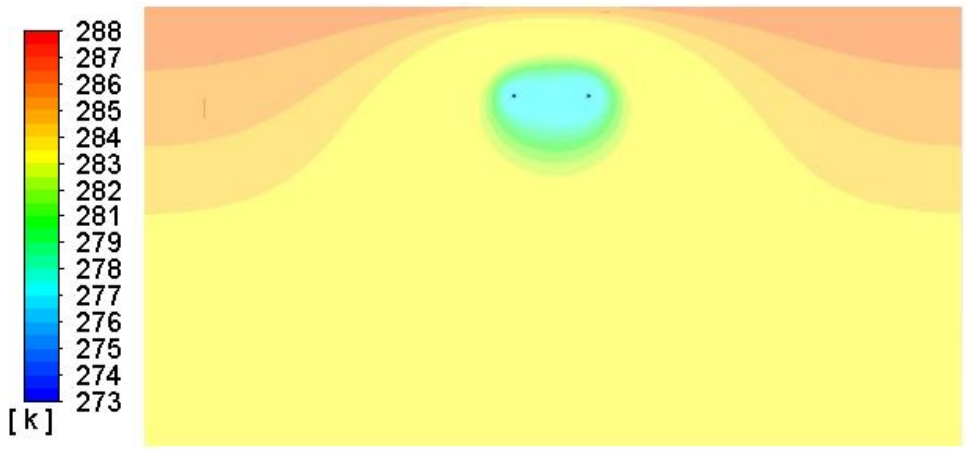
(c) The end of the 10th day with uniform temperature



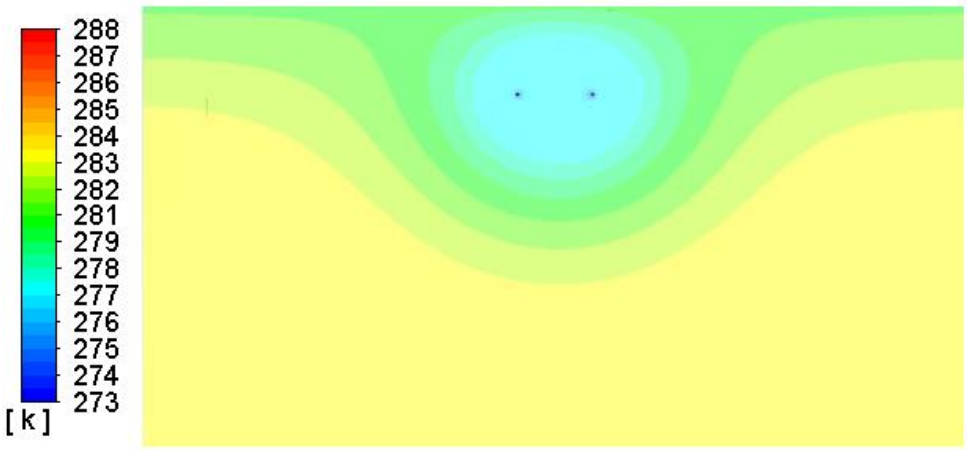
(d) The end of the 10th day with varying temperature



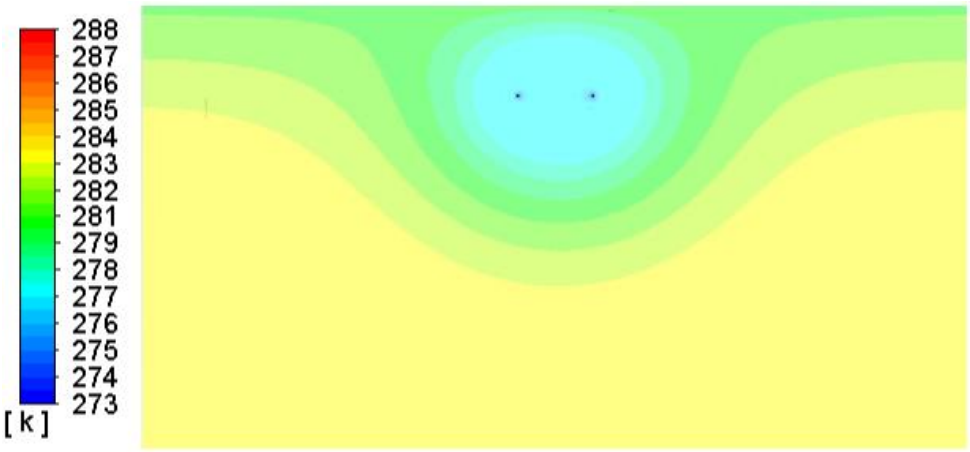
(e) The end of September with uniform temperature



(f) The end of September with varying temperature



(g) The end of November with uniform temperature



(h) The end of November with varying temperature

Figure 3.6 Isotherm generated from prediction for different initial soil temperature in vertical section view.

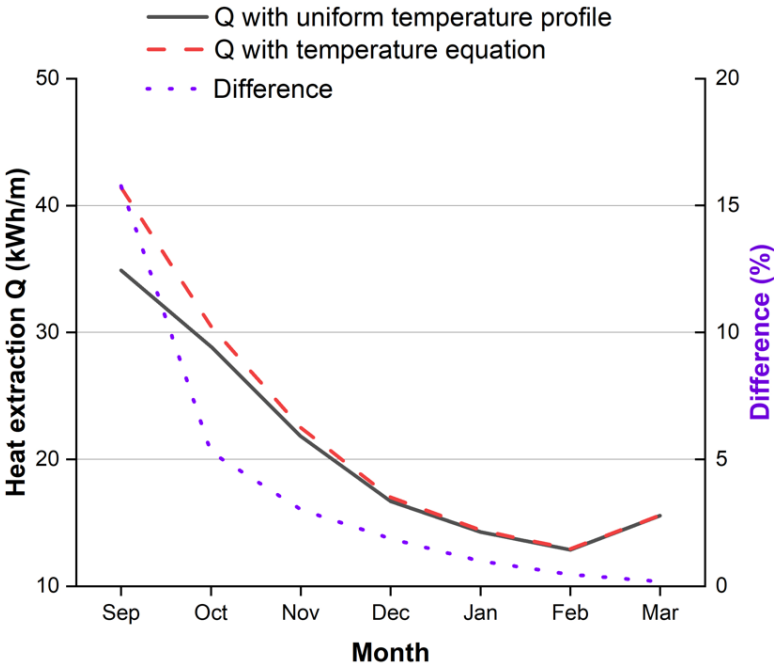
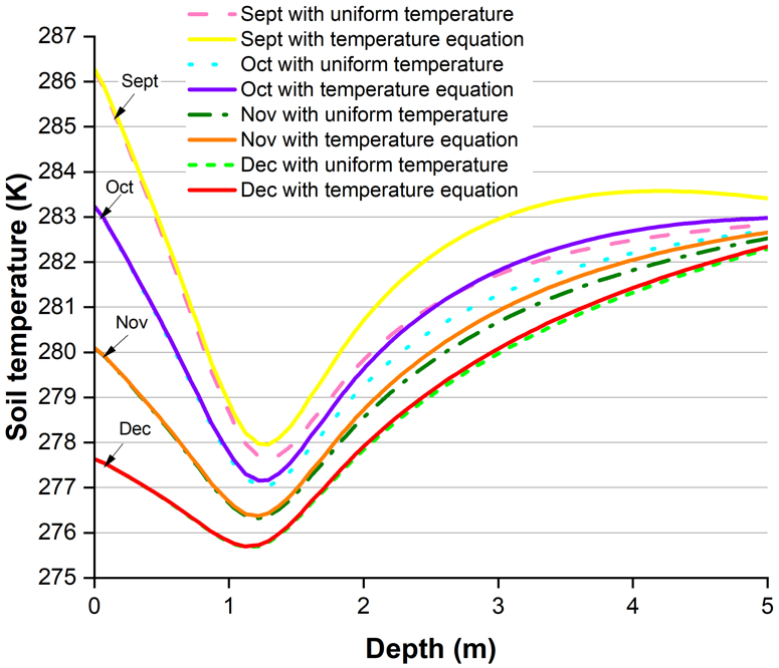
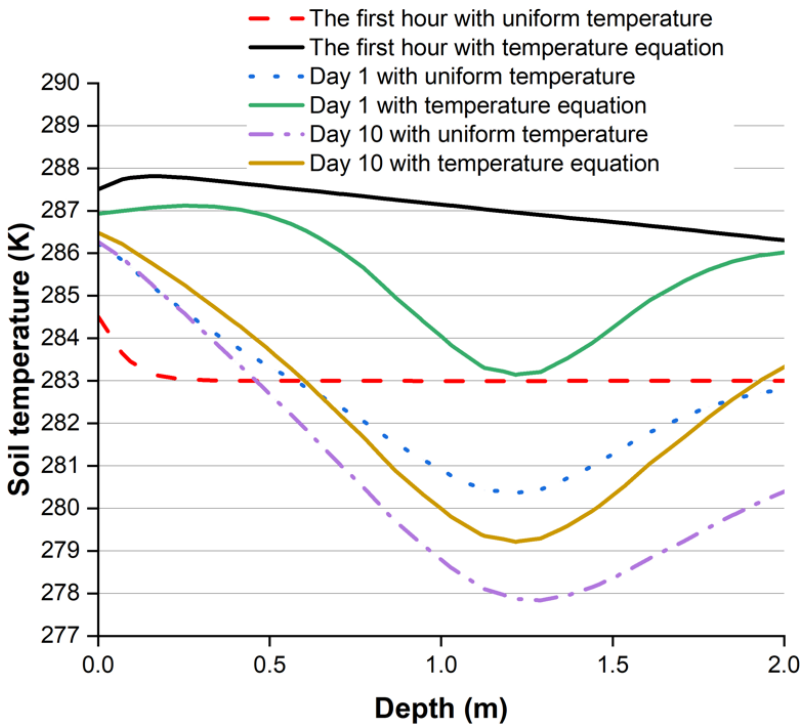


Figure 3.7 Effect of initial soil temperature on the predicted heat extraction through the heat exchanger.



(a) First 4 months



(b) First 10 days

Figure 3.8 Effect of initial soil temperature on the predicted variation of soil temperature at various times.

3.3.4 Pipe boundary condition

The lower temperature fluid flow from the evaporator will make the heat exchanger draw more heat and hence bring deep soil temperatures down more when air temperatures are low due to the increase in heat demand. Under UK environmental conditions, it is quite possible that if the soil temperatures near the slinky fall below the freezing point, it will affect their future performance because the earth will not be able to fully recharge for the following season during the summer [128]. Therefore, the fluid temperature should be maintained above 0°C in the UK.

In this study, the slinky-loop ground heat exchanger was maintained at a constant

inlet temperature 1℃, which was close to the published experimental results for fluid average temperature throughout the winter season in the UK when the GSHP was used for heating operation [24]. The average temperature can be substituted for a fluid temperature that fluctuates with the surrounding air or building demand in order to predict the heat transfer for the continuous operation of a ground source heat pump system with a maximum error of less than 10% [125].

During operation times, a water-ethylene glycol (30% by weight) mixture with a constant inlet temperature of 1℃ was assumed to circulate through the heat exchanger at a fluid velocity of $0.4m/s$. The selection of this velocity was based on the requirement of turbulent fluid flow in the pipes (Re = 4056) for efficient heat transfer but not too high to avoid excessive pressure loss. Based on these assumptions, the calculation process for pipe temperature is presented below.

For turbulent flow in smooth tubes, the Nusselt number can be expressed as [129]:

$$Nu = \frac{hd}{k} = 0.023Re^{0.8}Pr^{\frac{1}{3}} \tag{3.7}$$

Where the Prandtl number can be determined by:

$$Pr = \frac{c_p u}{k} \tag{3.8}$$

As mentioned in Table 3.1, the value of specific heat capacity c_p (kJ/kgK), kinematic viscosity u (m^2/s) and thermal conductivity k (W/mK) can be obtained. Thus, the value of convective heat transfer coefficient h (W/m^{2}K) can be calculated.

A single CFD simulation has been conducted to test the temperature of heat exchanger pipe surface under steady-state condition. The simulation results

illustrated the difference between pipe temperature and fluid temperature was 0.10 ℃. Thus, the fluid convection boundary condition could be replaced by the pipe temperature (= fluid temperature) in practical simulation without much loss of accuracy.

3.3.4.1 The effect of the pipe temperature

Table 3.6 Boundary condition of CFD simulation.

Installation depth	1.2 m
Soil type	Loamy soil
Operation mode	Intermittent 12 h operation
The initial soil temperature	Varying temperature with the depth
Pipe temperature	1, 2, 3, 4 and 5℃
Topsoil boundary condition	Monthly changed air temperature and wind speed
Climate data	Coventry
Loop pitch	1.0 m

The results were obtained by assuming the initial soil temperature of varying temperature profile under the intermittent heating operation (12 hours on and 12 hours off). The boundary conditions are displayed in Table 3.6. The slinky-loop ground heat exchanger was at the depth of 1.2m in loamy soil.

The effect of the water-ethylene glycol (30% by weight) mixture temperature was represented by the temperature of outer surface of the heat exchanger pipe. The difference between the pipe temperature and the surrounding soil temperature leads to heat transfer. The thermal characteristics of the slinky-loop ground heat exchanger and the soil were predicted for five heat exchanger outer

surface temperatures: 1, 2, 3, 4 and 5°C, with a monthly average ambient air temperature and a monthly average wind speed. The estimated monthly heat extraction for the slinky-loop ground heat exchanger at various pipe temperatures is shown in Fig. 3.9. Although the slinky-loop ground heat exchanger have different temperatures, the monthly heat extractions have similar characteristics. In the first month, the heat extraction was at 31.7, 29.1, 26.9, 24.0 and 21.7 kWh/m respectively, when the pipe temperature was at 1, 2, 3, 4 and 5°C. They decreased to 10.1, 8.0, 6.3, 3.8 and 2.1 kWh/m in February, and increased to 12.1, 9.9, 8.0, 5.4 and 3.6 kWh/m in March. They decreased significantly during the initial four months, and the decline slowed greatly from January to February. While the variation patterns remained consistent, it was observed that a higher monthly heat extraction rate was achieved at lower pipe temperatures. It can be seen from Fig. 3.10 that the region of soil temperature at 9°C around the heat exchanger covers a wider area in the lower pipe temperature. For the pipe temperature of 5°C, soil with a temperature less than 9°C was only found near the surface of the slinky-loop ground heat exchanger, whereas there was still plenty of soil surrounding the heat exchanger with a temperature as high as 10°C. This was because the lower temperature of the slinky-loop ground heat exchanger can extract more heat from the surrounding soil due to the higher temperature difference between the pipe surface and the surrounding soil.

The total heat extraction of heating season decreases with the increase of pipe surface temperature; it is 121.2, 105.3, 90.2, 74.9 and 60.4 kWh/m at the pipe temperature of 1, 2, 3, 4 and 5°C, respectively, as shown Fig. 3.11. From this figure, a nearly linear correlation can be obtained between total heat extraction and pipe temperature.

$$Q = -15.19T_{pipe} + 135.99\ (R - Square = 0.9973) \qquad (3.9)$$

Where Q is total heat extraction (kWh/m), T_{pipe} is the heat exchanger pipe temperature (°C). This correlation could be used to estimate the thermal performance of different slinky-loop ground heat exchanger pipe temperatures under intermittent 12-hour-on operation.

In terms of the rate per unit difference between pipe temperature and initial soil temperature (13.4℃ at 1.2m depth), the total heat extraction per unit temperature difference is 9,77, 9.23, 8.87, 7.82 and 7.16 kWh/m· ℃. This value decreases as the pipe temperature increases. Fig. 3.12 shows the predicted vertical soil temperature distributions along the centre of the heat exchanger loop at the end of September. The soil temperature difference between slinky-loop ground heat exchanger temperature of 1 °C and 5 °C at a 1.2 m installation depth was approximately 2.1 °C and decreased to around 1 °C and 0.4 °C for a distance of 1m below heat exchanger and 2m below the heat exchanger in vertical direction, respectively. At the same time and in the same position, the soil temperature decreased with the slinky-loop ground heat exchanger temperature.

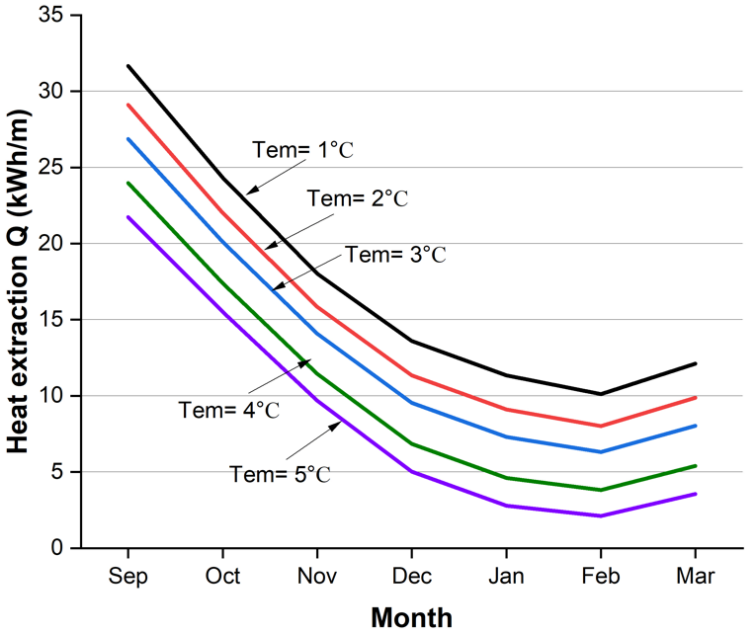
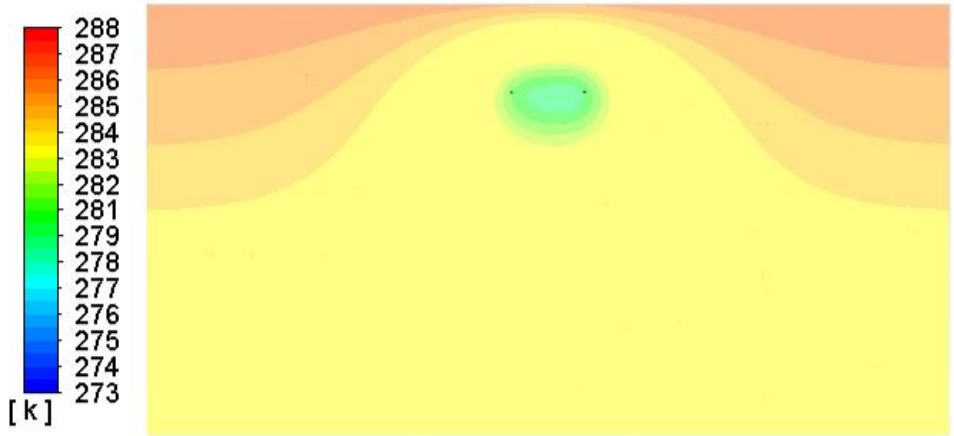
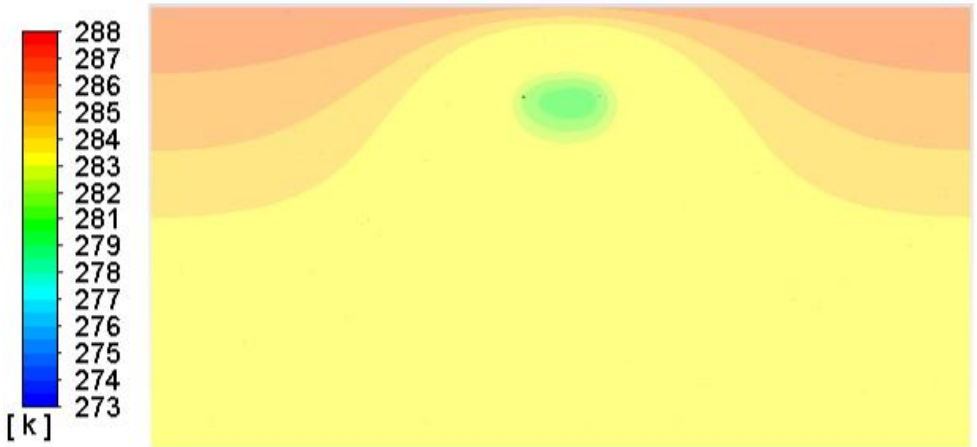


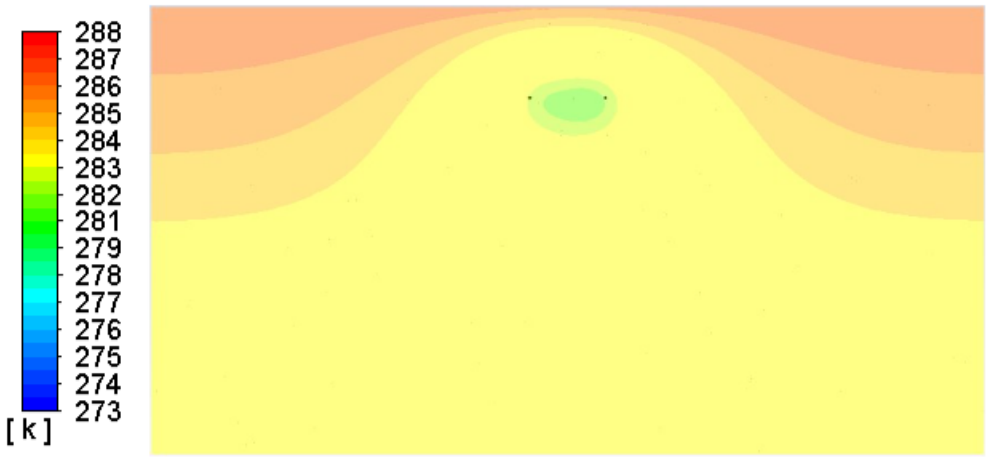
Figure 3.9 Variation of monthly heat extraction for different pipe temperature.



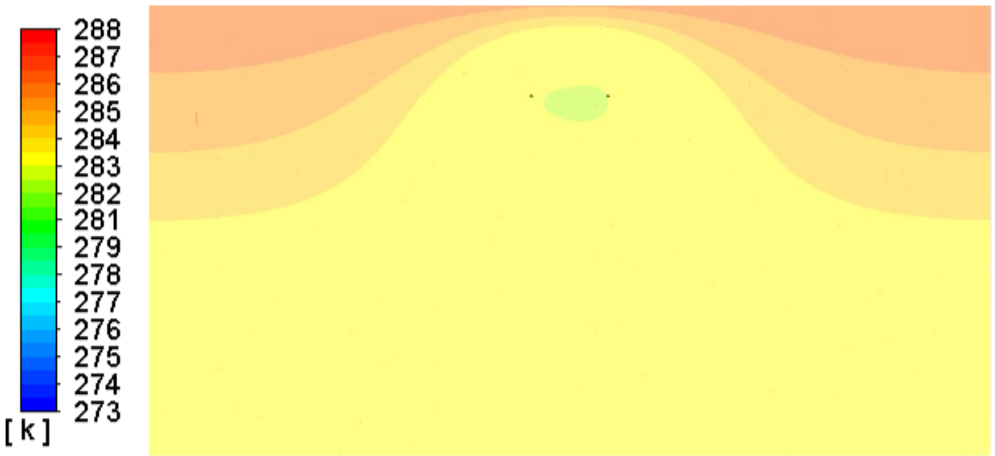
(a) Pipe temperature with 1 ℃



(b) Pipe temperature with 2 ℃



(c) Pipe temperature with 3 ℃



(d) Pipe temperature with 4 ℃



(e) Pipe temperature with 5 ℃

Figure 3.10 Isotherm generated from prediction for different pipe temperature at the end of September in vertical section view.

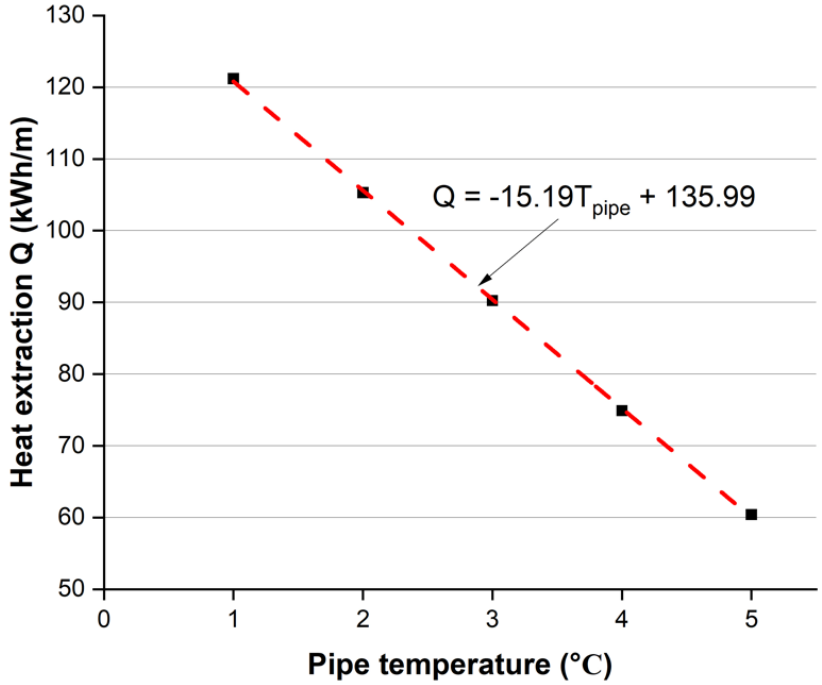


Figure 3.11 Total heat extraction amount of slinky-loop heat exchangers with different heat exchanger pipe temperature.

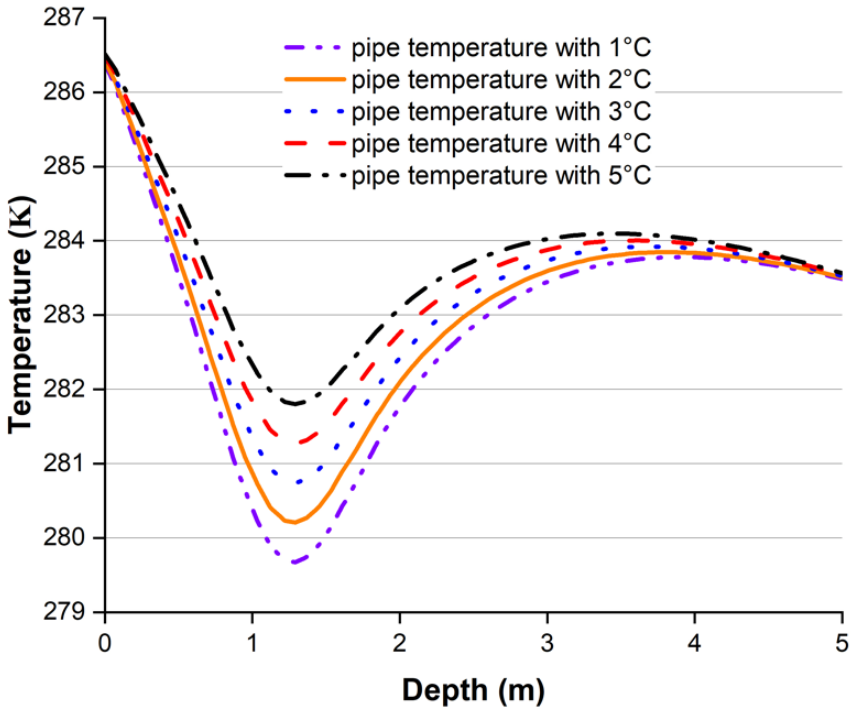


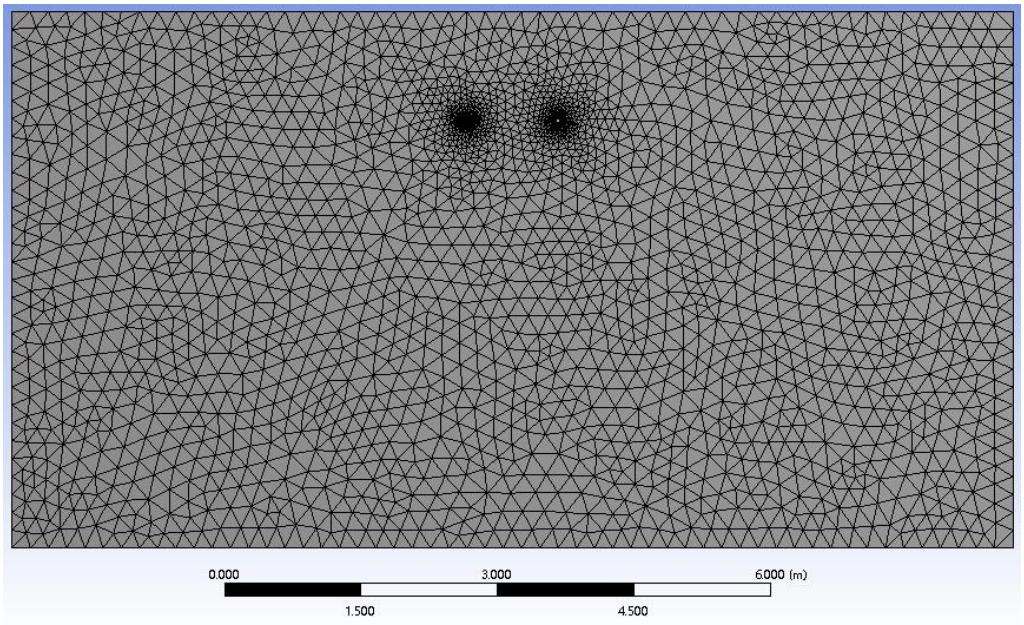
Figure 3.12 Predicted variation of soil temperature with depth, for different pipe temperature at the end of September.

3.3.5 Mesh independence study

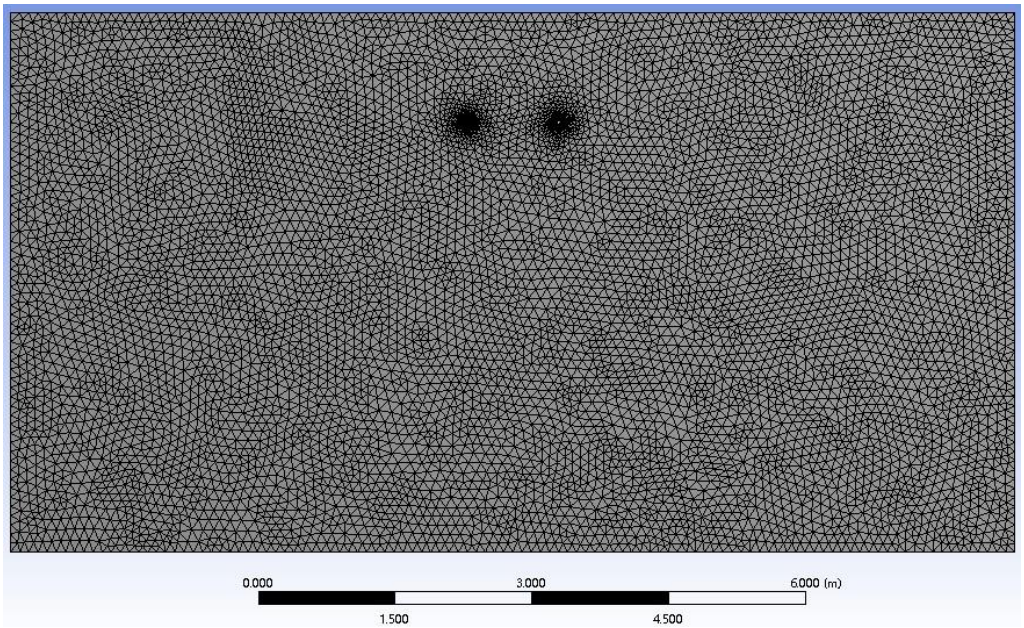
The accuracy of the numerical simulation could be significantly influenced by the mesh size. To obtain accurate simulation results, the grid independent independence study was explored by changing the mesh size until an appropriate one was found. Take a base case as an example, the time step was first set as 60 s for the first day. Four mesh sizes were considered as shown in Table 3.7. It can be seen from Fig. 3.13 that the computational mesh was denser in areas where the heat transfer would be highest, i.e., near the slinky-loop ground heat exchanger.

Table 3.7 Mesh sizes for mesh independence study.

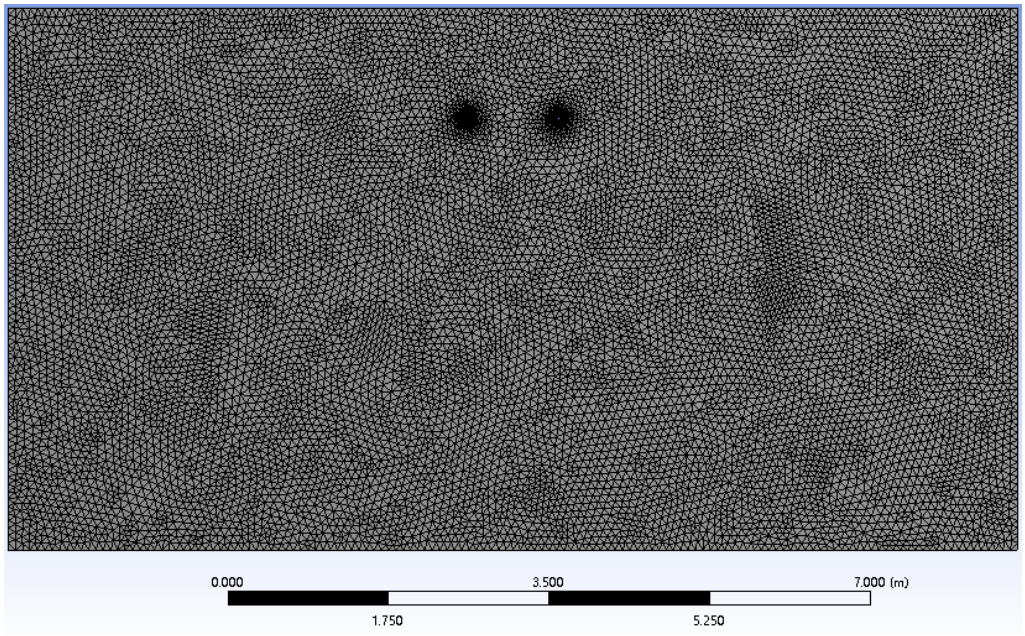
Mesh size number	Cell size near pipe	Cells away from pipe	Total cell number
i	0.02 m	0.2 m	240,168
ii	0.01 m	0.1 m	819,486
iii	0.006 m	0.08 m	1,478,186
iv	0.006 m	0.06 m	2,307,900



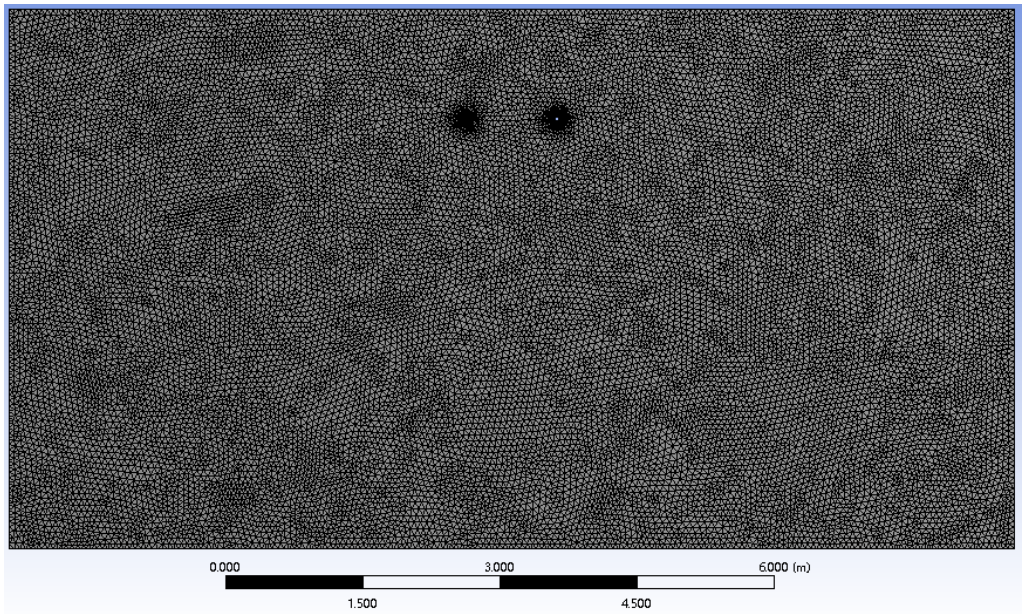
(i) Soil domain mesh size = 0.2, pipe mesh size = 0.02



(ii) Soil domain mesh size = 0.1, pipe mesh size = 0.01



(iii) Soil domain mesh size = 0.08, pipe mesh size = 0.006

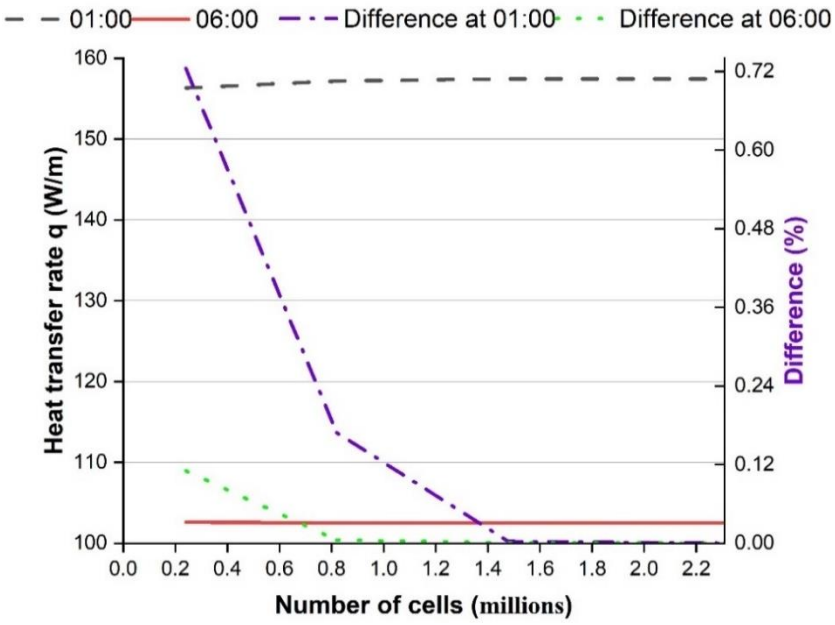


(iv) Soil domain mesh size = 0.06, pipe mesh size = 0.006

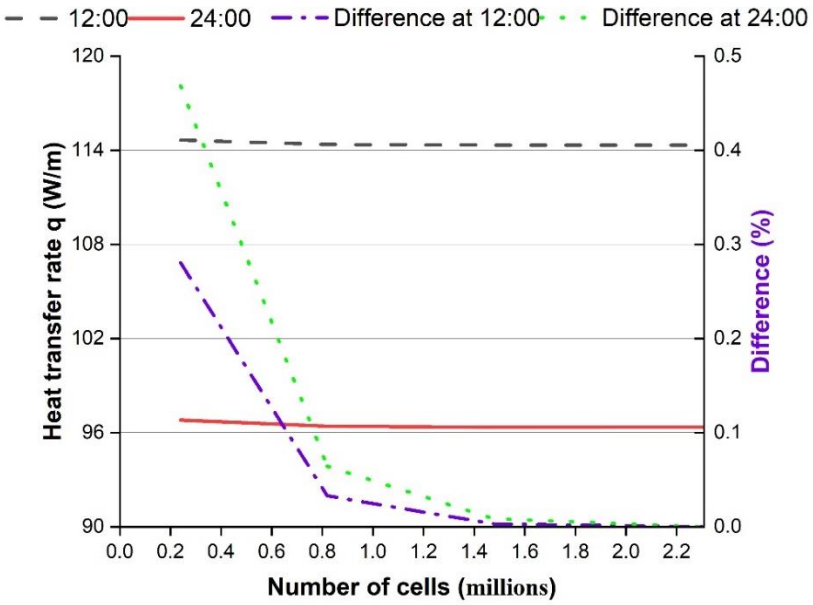
Figure 3.13 The vertical cross-section of the generated mesh for different mesh sizes.

The heat exchange rates for four mesh sizes in the 1st ,6th,12th hour and 24th hour

were selected for comparison. Fig. 3.14 depicts the heat transfer rates per unit trench length of the slinky-loop ground heat exchanger for various mesh sizes. It is noticeable that the difference in the predicted heat transfer decreases with the increase of the cell number. The relative difference between the two finest mesh sizes is lower than 0.1%; mesh size iii was therefore chosen for the CFD simulation. It is concluded that the soil domain element size can be set at 0.08 m, and the size near the pipe surface can be taken as 0.006 m. A total cells number of 1478186 shows a good balance between calculation time and accuracy. The details of the selected mesh size (iii) are illustrated in Fig. 3.15.



(a) The heat transfer rates per unit trench length of the slinky-loop ground heat exchanger for various mesh sizes at 01:00 and 06:00 during the first day



(b) The heat transfer rates per unit trench length of the slinky-loop ground heat exchanger for various mesh sizes at 12:00 and 24:00 during the first day

Figure 3.14 Mesh independence study.

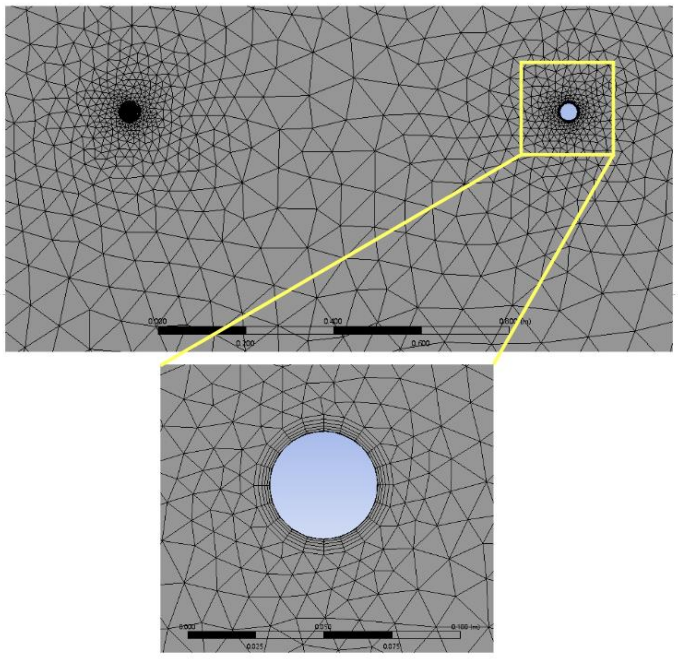


Figure 3.15 The details of mesh generated near the slinky-loop ground heat exchanger surface.

3.3.6 Time step study

To accurately model the transient heat flow in slinky-loop ground heat exchanger, it is necessary for the time step to be sufficiently small. This is crucial to capture the rapid temperature fluctuations that occur. The time step independence study was then performed with grid size iii. Different time step sizes were used ranging from 60s to 3600s. The simulation results in Fig. 3.16 show that for the first hour, the time step significantly affects calculation accuracy with a difference of about 30% in the heat transfer rate (q) with 600s and 3600s time steps. The difference decreased with time but was still 5% by the end of the third hour.

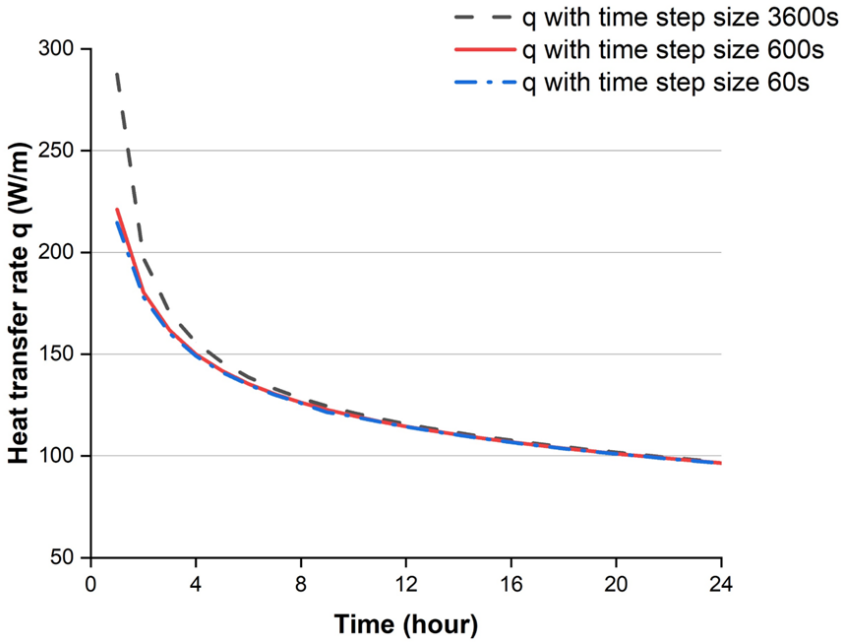


Figure 3.16 Heat transfer rate for various time step size on the first day.

Table 3.8 compares the simulation results for the heat transfer rate with three-time steps at different times. At the end of the first hour, the difference in the simulated heat transfer rate between 60s and 3600s time steps size was approximately 34%, while the difference between 60s and 600s time steps was

around 3%. The difference between the time steps size of 60s and 600s was less than 1% after the third hour. The difference in the simulated heat transfer rate at the end of first day was about 0.5% between the 600s and 3600s time steps, and the difference was negligible between the smaller time steps of 60s and 600s.

It can be seen from Fig. 3.17 that the difference in the simulated heat transfer rate between the larger time steps of 3600s and 60s was around 6% at the end of the third hour, and then decreased to 3% at the end of the sixth hour. The difference decreased with time, and at the end of the first day, it was less than 0.59%, and became lower than 0.07% after ten days of operation.

Table 3.8 Time step size study.

Time step size (s)	Heat transfer rate at the end of each hour/day (W/m)						
	1st hour	3rd hour	6th hour	Day 1	Day 2	Day 3	Day 10
60	214.64	160.30	134.93	96.47	80.37	72.04	54.89
600	221.11	161.68	135.47	96.55	80.41	72.06	54.89
3600	287.51	170.50	138.65	97.04	80.63	72.21	54.85

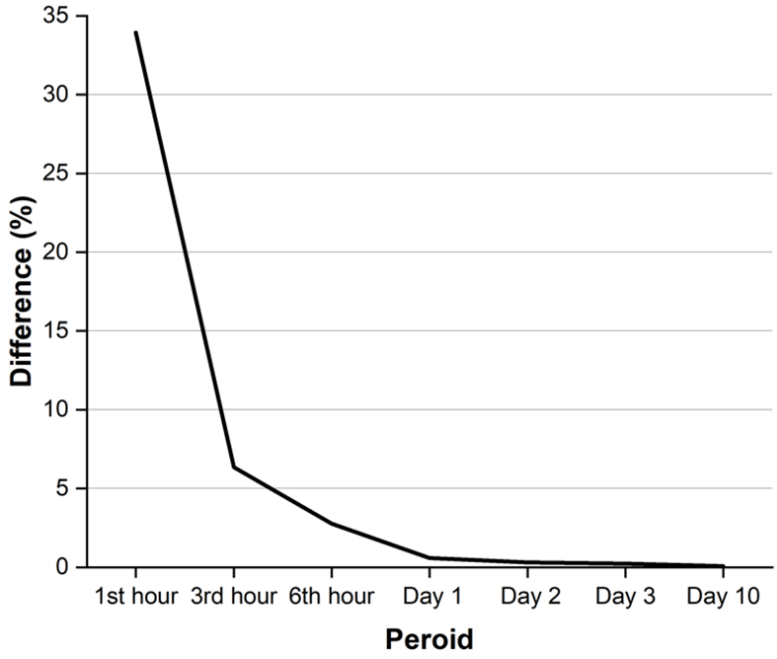


Figure 3.17 The difference between time step size 60s and 3600s at selected time.

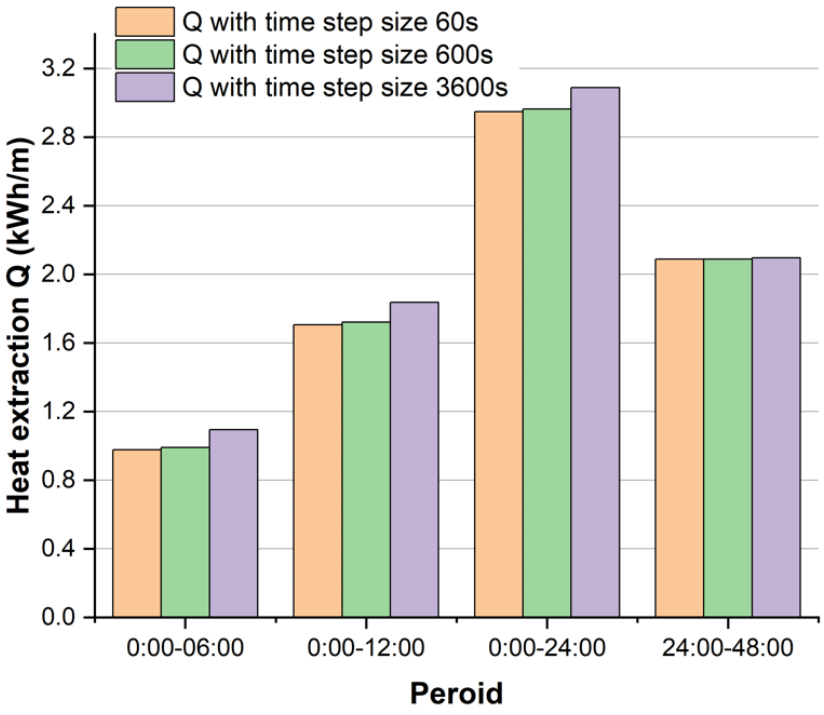


Figure 3.18 Heat transfer amount for various time step size during different period.

Fig. 3.18 shows the heat transfer amount for three-time step sizes during different periods. For the predicted amount of heat extraction on the first day, the difference between time step sizes of 60s and 3600s is approximately 9% and becomes negligible on the second day. Therefore, the time step was taken as 60s for the first day prediction, and a time step size of 3600s was used in the rest of the heating season simulation.

3.4 Simulation process

The geometry model and the mesh generation were built on the FLUENT workbench platform. The CFD simulations have been performed with the commercial software ANSYS Fluent. The initial values for the depth-varying soil temperature in the whole computational domain are determined based on the profiles corresponding to the time when the slinky-loop ground heat exchanger system starts working. A water-ethylene glycol (30% by weight) mixture with a constant inlet temperature of 1℃ was assumed to circulate through slinky-loop ground heat exchanger during the heating season. For a given site where the slinky-loop heat exchanger is installed, basic data for the properties of soil and atmospheric (boundary) conditions are obtained.

For the base case, the soil type used in simulation was loamy soil from Coventry. The thermal conductivity is 1.5 W/mK. The corresponding thermal diffusivity is about $0.9842 \times 10^{-6}\, m^2/s$, and the specific heat is 1.039 kJ/kgK. The amount of heat extraction from slinky-loop ground heat exchanger is influenced by the local air temperature and wind speed. The monthly boundary conditions for Coventry were used in the simulation. The installation depth of the base case is 1.2m, and the thermal interference from adjacent trench was ignored.

The centre-to-centre distances of adjacent pipe was set at 8 different levels (1.5m, 2.0m, 2.5m, 3.5m, 4.5m, 6.0m, 8.5m and 11.0m) in order to verify the thermal interference of adjacent pipe on heat transfer capabilities. All the geometry independent parameters were the same for all the layouts considered.

The slinky-loop ground heat exchanger is a long polyethylene pipe buried at a certain depth. Here three different depths (0.9 m, 1.2 m and 1.5 m) in the ground with an emphasis on the thermal interference between parallel slinky-loop ground heat exchanger pipes were taken into consideration. The three different depths were chosen as the most commonly used in commercial installations and sufficient to demonstrate performance trends with burying depth. In addition, the effect of trench spacing was tested using three soil types available in the UK: clayey soil (0.62 W/mK); loamy soil (1.5 W/mK); sandy soil (2.79 W/mK).

For intermittent operation, the base case had been simulated for 12-hour-on (heating) and 12-hour-off (recovery period) operation, 6-hour-on (heating) and 18-hour-off (recovery period) operation, 18-hour-on (heating) and 6-hour-off (recovery period) operation during a seven-month heating period. The analysis of this work also involved four main geometries of slinky-loop ground heat exchangers with various loop pitches (0.25 m, 0.5 m, 1.0 m, and 2.0 m). Dimensions were chosen to be consistent with the geometry of the ground modeled around the pipes in all the arrangements considered.

The cities of Edinburgh, Coventry, and Reading were selected to assess the impact of the installation location external environment and the local soil properties. The study also examined the thermal impact of a slinky-loop ground heat exchanger in the ground, taking into account various annual operation modes. Additionally, it compared the temperature of the soil with and without

the heat exchanger over the span of a year.

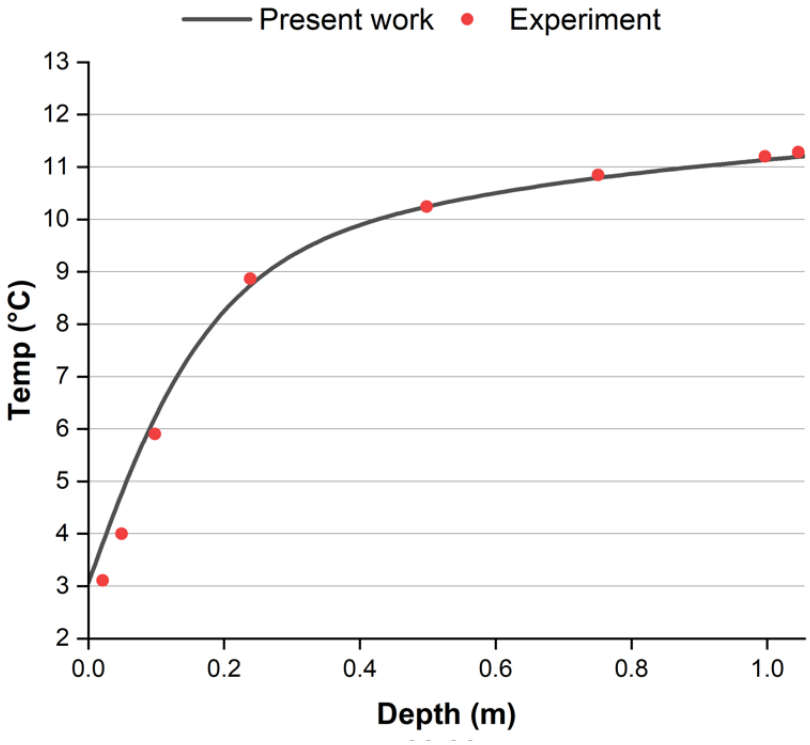
A novel intermittent operating strategy that takes into account of the heating degree day method for predicting accurately the daily operation hours was created and compared with the real situation and the intermittent 12-hour-on operation.

Different combinations of the parameters indicated above were utilised in the simulations to point out the most significant effects of the functional parameters Based on these findings, the coefficient of performance of slinky-loop ground heat exchanger systems for typical UK climate regions were calculated to analyze the economic and environmental benefits of the use of slinky-loop ground heat exchanger systems within the UK.

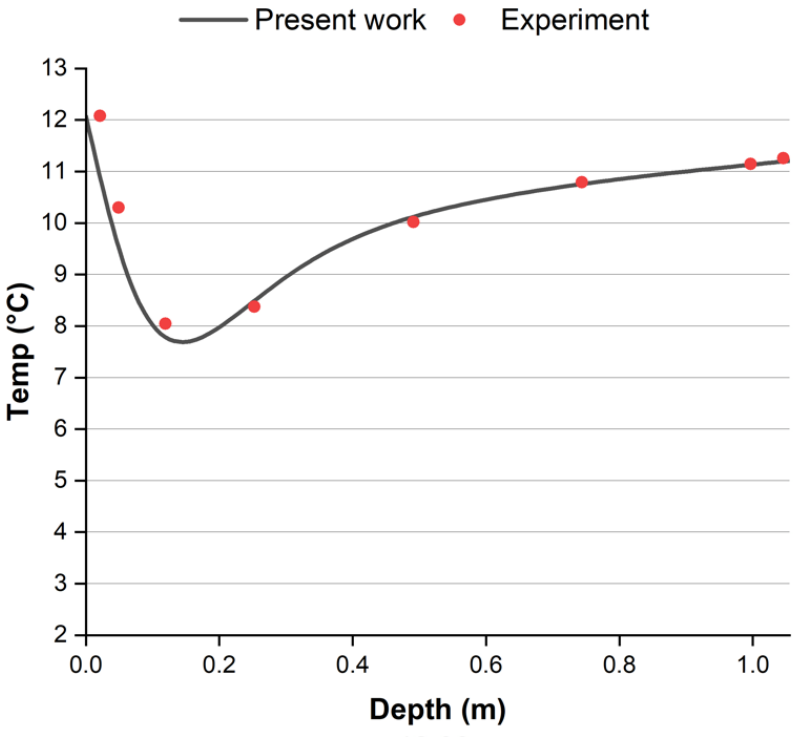
3.5 Validation of CFD model

The present simulation model was validated against the published experimental data measured by Wu et al [23]. They have investigated the performance of a slinky GHE by placing four parallel slinky-loop ground heat exchangers in an 80-meter-long by 20-meter-wide paddock area at a depth of approximately 1.2 meters beneath the ground surface. The soil temperature distribution at various times was recorded. For the validation, the measured average wind speed was around 1 m/s on 7th Nov. Also, the topsoil temperature at 00:00 on November 7, 2009 was set as the initial conditions. Fig. 3.19 shows that the predicted soil temperature profiles agree very well with the experimental results. The maximum difference between predicted and measured soil temperatures was 0.6°C at a depth of 0.02m in the middle of the day (12:00). This could be due to the model's assumption of constant and homogeneous soil thermophysical

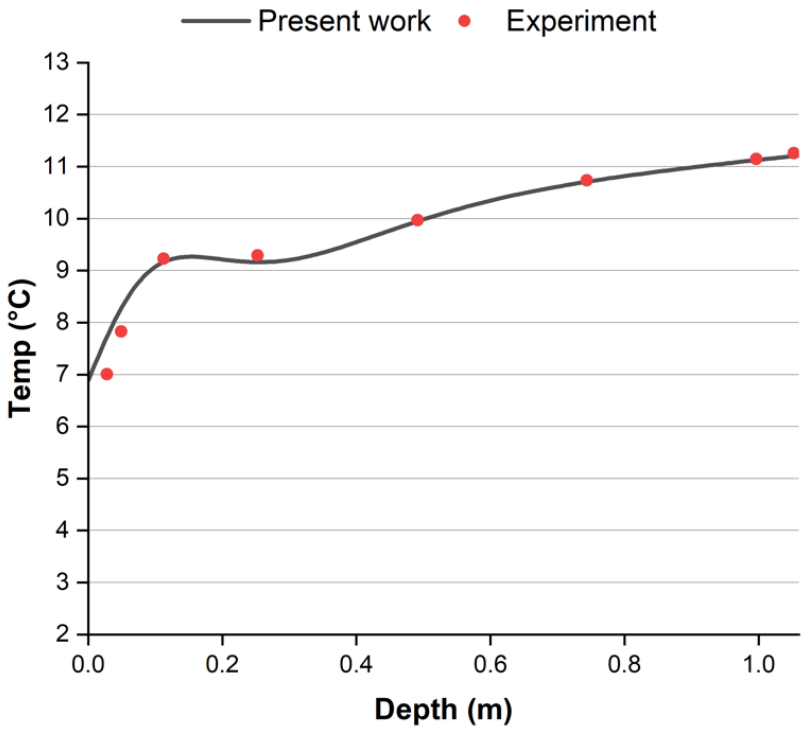
parameters; however, real soil properties might not be uniform, especially around the surface. For example, there was some vegetation, and the soil surface would not be as flat as assumed, with an unevenness likely to be 0.02m or more. When the depth is greater than 0.1m, the predicted temperature had the same trend as the measurement, indicating a good agreement between the current work and experimental measurements.



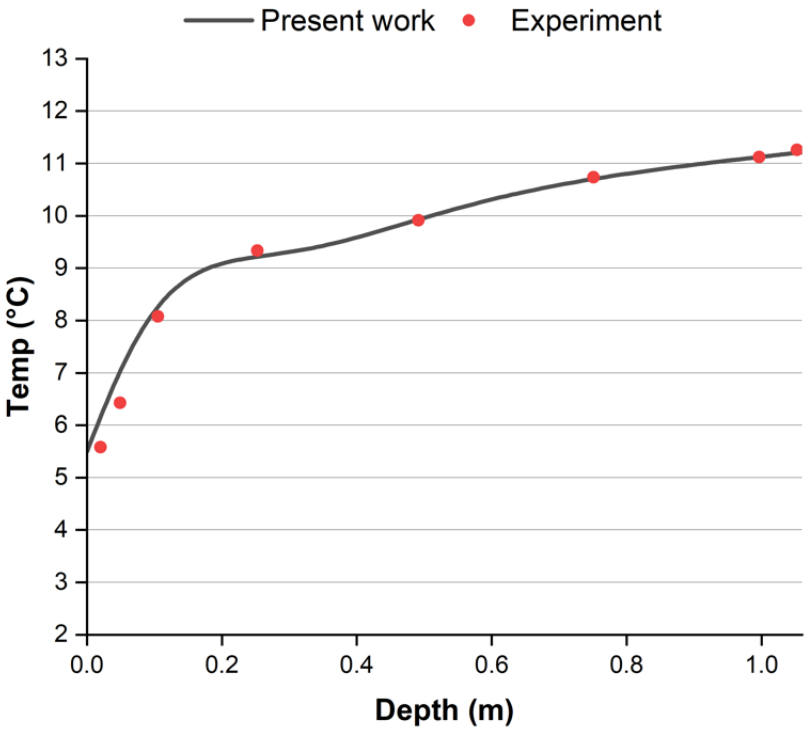
(a) 08:00


Present work
Experiment
Temp (°C)
Depth (m)
13
12
11
10
9
8
7
6
5
4
3
2
0.0
0.2
0.4
0.6
0.8
1.0

(b) 12:00


Present work
Experiment
Temp (°C)
Depth (m)
13
12
11
10
9
8
7
6
5
4
3
2
0.0
0.2
0.4
0.6
0.8
1.0

(c) 18:00



(d) 20:00

Figure 3.19 Comparison of the soil temperature between the present numerical model and the experimental results of Wu et al. at different time. [23].

3.6 Conclusion

This chapter describes numerical methodology for the dynamic thermal simulation of slinky-loop ground heat exchanger. This consists of the description of a three-dimension CFD model, assumption, governing equation, boundary condition, and validation. It also provided a brief description of the approaches used for simulation in Chapters 4 and 5, and design in Chapters 6 and 7. The effect of soil surface boundary condition, initial soil temperature and heat exchanger pipe temperature were investigated.

The monthly changed temperature and wind speed of Coventry have been used for boundary conditions, which was compared using average heating season

boundary condition. However, the difference of the total heat extraction amount between the two boundary conditions was around 10%. It is suggested to use monthly changed air temperature and wind speed for topsoil boundary conditions. It is more accurate for predicting the monthly heat exchanger rate and monthly heat extraction amount.

The thermal performance of a slinky-loop ground heat exchanger was predicted with two types of initial soil temperature – uniform and varying with depth. The discrepancy in predicted heat transfer through a 1.2 m deep heat exchanger in loamy soil using a constant temperature profile compared with that with varying temperature would be up to 16% at the end of the first month's operation, and then drop to 6% and 2% in the second and third months, respectively. The heat transfer difference for the first month would be far greater for a heat exchanger placed at shallower depths because of the larger temperature difference between the constant value and varying profile.

For different temperatures of the slinky-loop ground heat exchanger pipe, the lower the pipe temperature, the higher the monthly heat extraction rate was obtained. The quadratic polynomial equation could be used to estimate the thermal performance of different slinky-loop ground heat exchanger pipe temperatures.

Chapter 4: Investigation into the thermal interference of slinky-loop ground heat exchangers

4.1 Introduction

There is still a lack of comprehensive numerical investigation that would allow practical performance prediction and design of slinky-loop ground heat exchangers, particularly on the energy output ratio for the whole heating season. It has also been shown that the impacts of varied trench separations under diverse circumstances have not been investigated thoroughly, which makes it difficult to determine the size of slinky-loop ground heat exchanger and predict the system efficiency accurately. This chapter aims to evaluate the thermal performance of slinky-loop ground heat exchangers for different trench separations, installation depths, and soil properties using a numerical method with an emphasis on the thermal interference between parallel slinky-loop ground heat exchanger pipes.

4.2 Description of the model

The simulations were conducted for the heating season in the UK from 1st September to 31st March. The simulation results are presented in terms of monthly or seasonal total heat transfer in kWh and the variation of the surrounding soil temperature profile. The daily operating time for the simulations is 24-hour continuous operation.

4.2.1 Parallel slinky-loop ground heat exchanger model

The main part of the slinky-loop ground heat exchanger consisted of a OD40 (i.e., 40mm) circular HDPE pipe. The installation depth (Z_1) of 1.2 meters under the soil surface in loamy soil was selected as a base case. The impact of thermal interference was simulated for different distances (separations) between adjacent trenches (defined as the distance between centers of two trenches) ranging from 1.5 m to 11 m and for different soil types and installation depths. Fig. 4.1 shows the slinky-loop ground heat exchanger system. Fig. 4.2 shows the slinky-loop heat exchanger model and solution domain. The total depth Z_d (= Z_1+Z_2) of the computational domain was 10m.

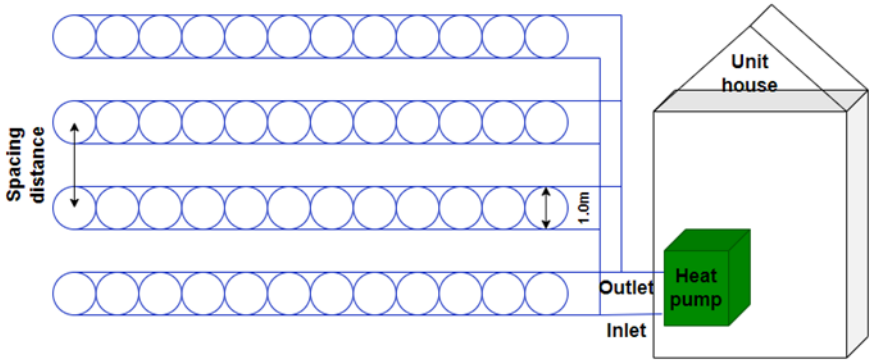


Figure 4.1 Schematic of slinky-loop ground heat exchanger system.

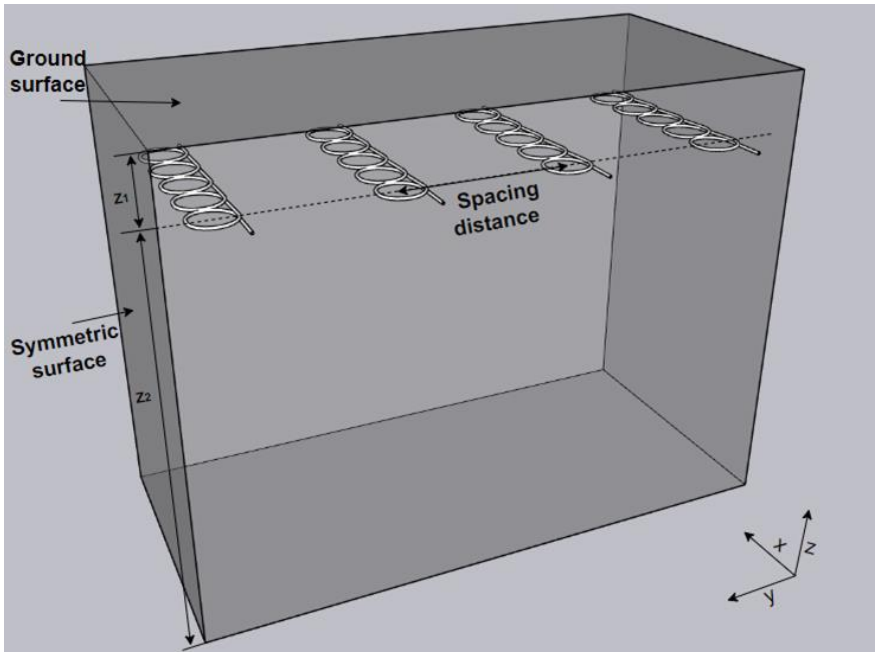


Figure 4.2 Computational domain for soil with slinky-loop ground heat exchanger.

4.2.2 Soil properties used in simulation model

The amount of heat extraction from slinky-loop ground heat exchanger is influenced by the local soil composition, soil moisture content and groundwater flow. Soil thermal diffusivities in the United Kingdom have been reported to range from 1.37×10^{-7} m^2/s to 4.33×10^{-6} m^2/s [22]. The thermal properties for three representative types of soil (loamy, clayey and sandy) as shown in Table 4.1 were used in the simulation based on the data recommended for the determination of thermal properties for horizontal ground collector loops [130]. The soil thermal diffusivities obtained are averaged over seasons by utilising data from seasonal temperature cycles that cover multiple years. The thermal conductivity is 1.5 W/mK for loamy soil, 0.62 W/mK for clayey soil and 2.79 W/mK for sandy soil. The corresponding thermal diffusivity is about

1.7971 and 0.4002 $10^{-6}m^2/s$ for sandy and clayey soils, respectively, compared with 0.9842 $10^{-6}m^2/s$ for loamy soil, and the specific heat is 1.014, 1.039 and 1.398 kJ/kgK for clayey, loamy and sandy soils, respectively.

Table 4.1 Soil properties for simulation.

Soil type	Name	Density (kg/m^3)	Specific Heat (kJ/kgK)	Thermal conductivity (W/mK)	Diffusivity ($10^{-6}m^2/s$)	Location
Loamy	A	1470	1.039	1.5	0.9842	Coventry
Clayey	B	1520	1.014	0.62	0.4002	Mylnefield
Sandy	C	1250	1.398	2.79	1.7971	Wellesbourne

4.3 Results and discussion

The numerical simulation of the slinky-loop ground heat exchanger performance was investigated for the effects of installation depth, soil thermal properties and loop trench spacing distance. The results are presented as temperature contours, soil temperature distribution and the amount of heat transfer per meter length of trench for a given period (in kWh/m).

4.3.1 The effect of the interference of different slinky-loop ground heat exchangers for a base case

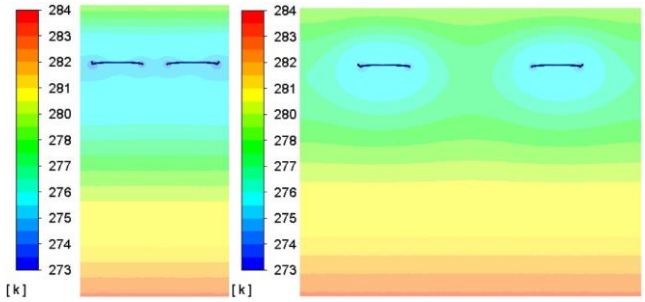
Table 4.2 Boundary condition of CFD simulation.

Installation depth	1.2 m
Soil type	Loamy soil

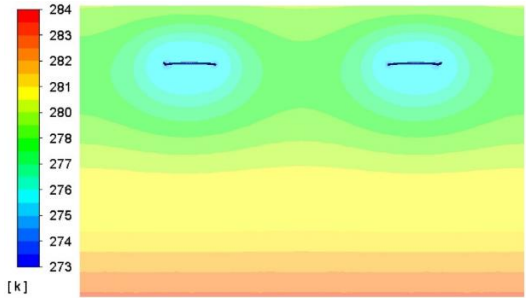
Operation mode	Continuous operation
The initial soil temperature	Varying temperature with the depth
Pipe temperature	1℃
Topsoil boundary condition	Monthly changed air temperature and wind speed
Climate data	Coventry
Loop pitch	1.0 m

To study the thermal interference in terms of the effect of spacing between adjacent loops on heat exchange, different cases have been simulated under the same boundary conditions with loamy soil. The centre-to-centre distances of 1.5m, 2.0m, 2.5m, 3.5m, 4.5m, 6.0m, 8.5m and 11.0m were considered. The base case was mentioned in the model description chapter with the heat exchanger 1.2 m deep from the top surface, as shown in Table 4.2. Fig. 4.3 presents typical temperature distributions from simulations for the slinky-loop ground heat exchanger and the surrounding soil domain. It can be seen that as the separation distance decreases, the area of low temperature surrounding each slinky-loop ground heat exchanger and between adjacent parallel heat exchangers increases. The soil temperature at the installation depth is close to the pipe surface temperature due to heat extraction from the surrounding soil. This indicates that thermal interference among short separation distances is more significant. However, this interaction impact becomes much less when the distance is over 6 m. This indicates that thermal interference between adjacent pipes decreases as the separation distance increases. Fig. 4.4 (a) illustrates the predicted soil temperature distribution in vertical direction at the slinky loop centre. The soil

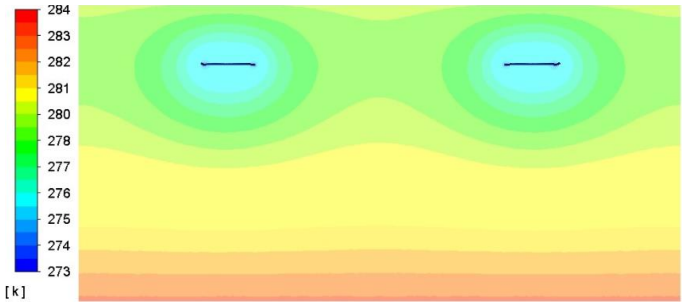
temperature lines are getting closer for distances over 6m. However, the difference between various separation distances at the centre of adjacent trenches in vertical direction is still large, as shown in Fig. 4.4 (b). This is another way to show the influence of spacing distance on the soil temperature or thermal interference between the adjacent trenches.



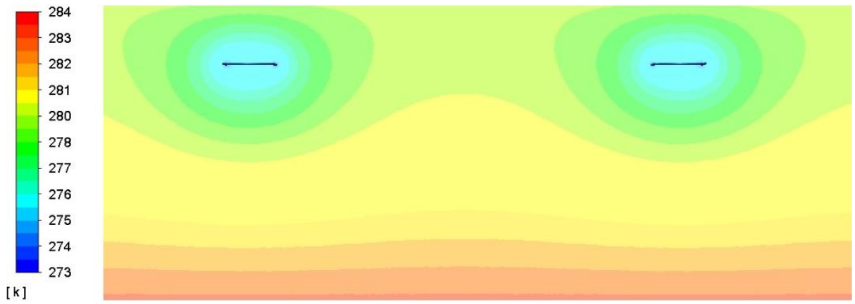
(a) Spacing distance of 1.5 m (b) Spacing distance of 3.5 m



(c) Spacing distance of 4.5 m

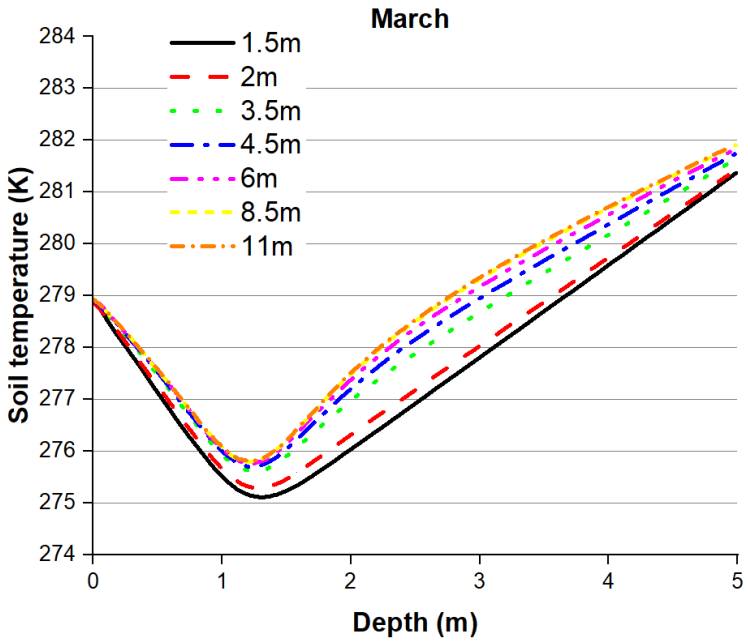


(d) Spacing distance of 6 m

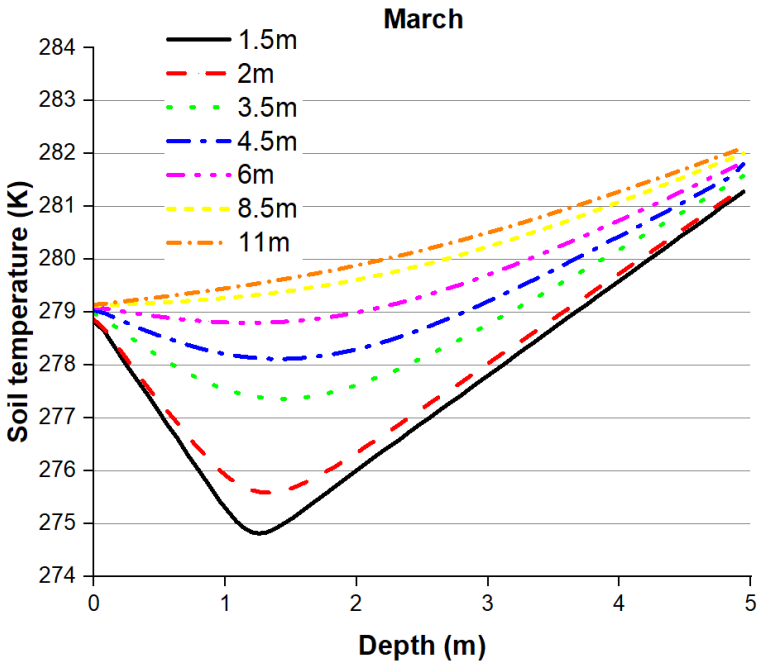


(e) Spacing distance of 8.5 m

Figure 4.3 Soil temperature distribution (K) on a vertical section located at the centre of the slinky loops at the end of March for different spacing distances.



(a) At the centre of slinky loop (at the end of March)



(b) At the centre of adjacent trench (at the end of March)

Figure 4.4 Effect of spacing distance on variations in soil temperature through the slinky-loop ground heat exchanger.

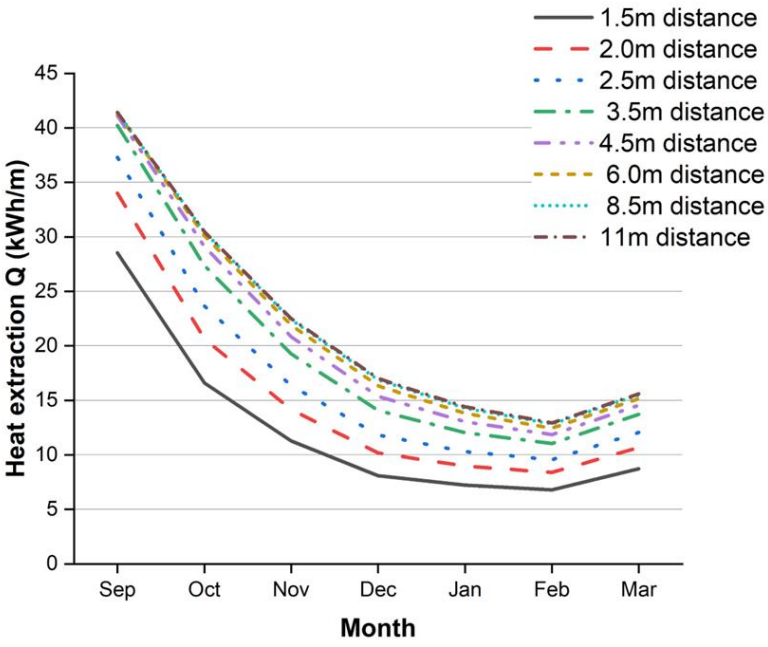
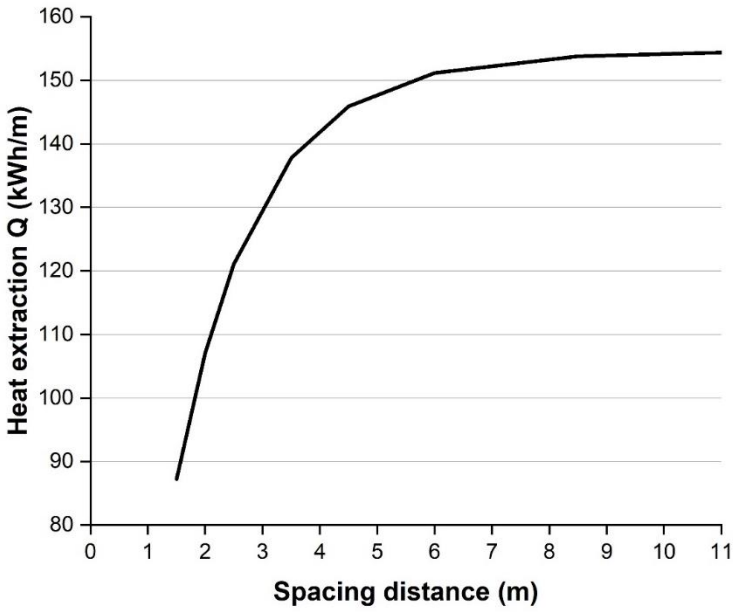


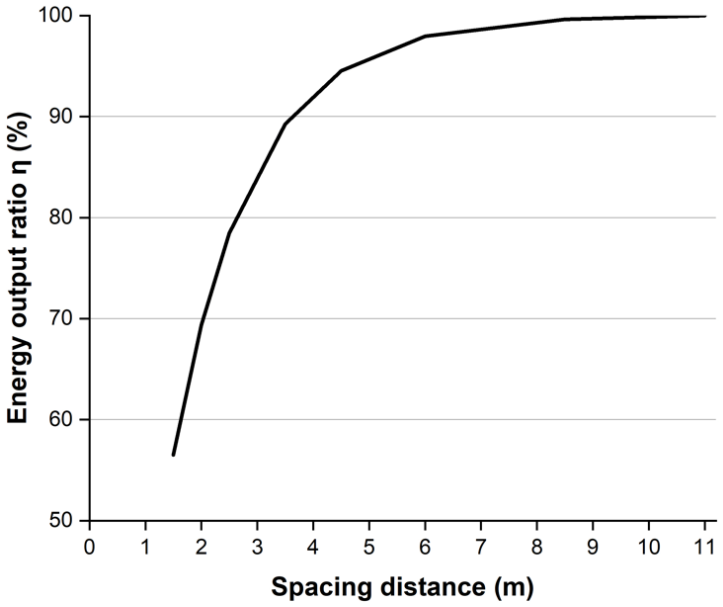
Figure 4.5 Monthly heat extraction under different spacing distances.

Fig. 4.5 shows the variation in monthly heat extraction per metre length of the trench occupied by heat exchangers at various loop spacing distances. The interference between parallel pipe loops decreased overall thermal performance. The monthly heat extraction amount decreased from September to February, and then increased during March. However, the monthly heat extraction amount decreased more slowly from December to February in shorter spacing distance. When the spacing distance between adjacent trenches is 2.0 m, the monthly heat extraction amount decreased by 17.56% from December to February, while 24.02% for the spacing distance of 8.5m.

When the spacing distance between slinky-loop ground heat exchanger is higher than 6 meters, the difference of the heat extraction amount is much less than in short distance cases. For example, in September, the heat extraction was 41.39 kWh/m, 41.42 kWh/m and 41.43 kWh/m, respectively, at 6.0m, 8.5m and 11m. By contrast, for spacing distances at 1.5m, 2.5m and 4.5m, the heat transfer amount in September is 28.54 kWh/m, 37.31 kWh/m and 41.12 kWh/m, respectively. The difference between the spacing distances of 1.5m and 6m was 31% in September, then increased to 51% in December and reduced to 42% in March. The results indicate that the thermal interference between adjacent slinky-loop ground heat exchangers is accumulated as operation time, especially when the ambient air is getting cold. In March, the soil in shallow depth was warmed up by the top surface air, which can help alleviate the influence of accumulated heat loss due to thermal interference from adjacent slinky-loop ground heat exchangers.



(a) Total heat extraction through the slinky-loop ground heat exchanger of different spacing distance between adjacent trenches



(b) Heating season energy output ratio through the slinky-loop ground heat exchanger of different spacing distance between adjacent trenches

Figure 4.6 Effect of spacing distance between adjacent trenches on heat extraction through the slinky-loop ground heat exchanger (Base case).

The total amount of heat extraction in the heating season from the slinky-loop ground heat exchanger is compared under different spacing distances in Fig. 4.6 (a). Fig. 4.6 (b) shows that by increasing the distance between slinky-loop ground heat exchangers, annual energy output approaches the single loop operation, i.e., no thermal interference. Energy output ratio η is calculated based on the 7-months heat extraction values for the slinky-loop ground heat exchanger using the following expression:

$$\eta = \frac{Q_d}{Q_s} \text{ x } 100\% \tag{4.1}$$

Where Q_S is the heat extraction of a single loop slinky-loop ground heat exchanger without considering multiple trench loop thermal interaction and Q_d is the heat extraction from one of the loops of slinky-loop ground heat exchanger under different trench separation distances.

From this figure, a nearly perfect polynomial correlation can be obtained between energy output ratio and spacing distance.

$$\eta = -0.03L^4 + 1.01L^3 - 11.17L^2 + 54.68L - 3.28 \tag{4.2}$$

Where η is energy output ratio (%), L is the distance of trench separation (m).

It can be seen from Fig. 4.7 that this quartic polynomial correlation fits very well with the simulated results. The value of R-Square is 0.9985. Hence, it could be used to accurately estimate the thermal performance of other different spacing distances. The thermal performance is greatly enhanced when the minimum is increased to 3.5 m. Further improvement is seen at 4.5m spacing, while the benefit of increasing spacing beyond 6 m becomes negligible. As a result, considering the practical construction of the slinky-loop ground heat exchangers,

the spacing distance between 5-6m is suggested compared with ideal (no interference) conditions, since further increasing the distance leads to less improvement of heat extraction rate and with a higher installation cost but with little gain in total energy output for a given land area. Considering the limit of the land area, if the spacing distance is less than 5m, the following simpler correlation can be used to predict the energy output ratio:

$$\eta = 0.82\, L^3 - 11.63L^2 + 58.36L - 7.56 \tag{4.3}$$

To further simplify the expression for the separation distance of not more than 5 m, a quadratic equation can be obtained:

$$\eta = -\, 3.69L^2 + 34.75L + 13.68 \tag{4.4}$$

As illustrated in Fig. 4.8, The regression line with quadratic and cubic polynomial has been compared within 5 meters spacing distance. The value of R-Square is 0.995 for quadratic polynomial and 0.9999 for cubic polynomial. It is found that the quadratic equation can be used to further simplify the prediction about the influence of different spacing distance between adjacent trenches with a loss of accuracy of less than 3%.

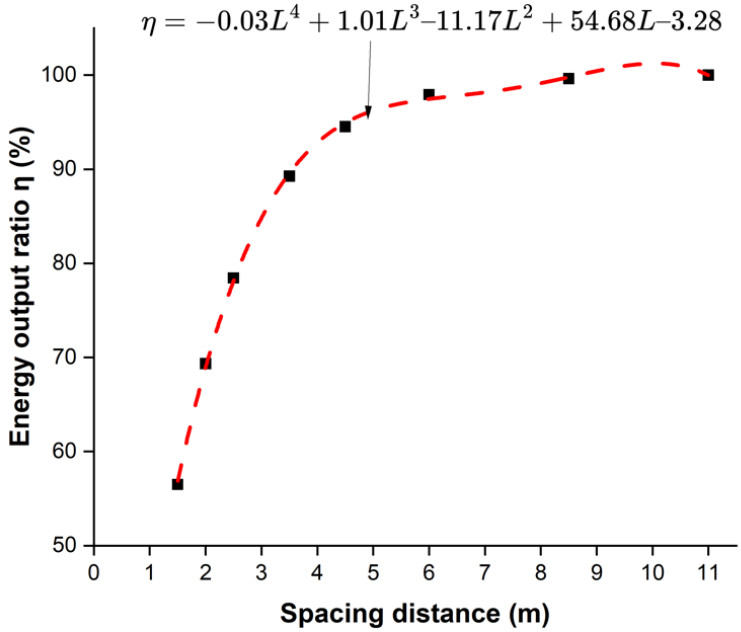


Figure 4.7 The regression line from polynomial.

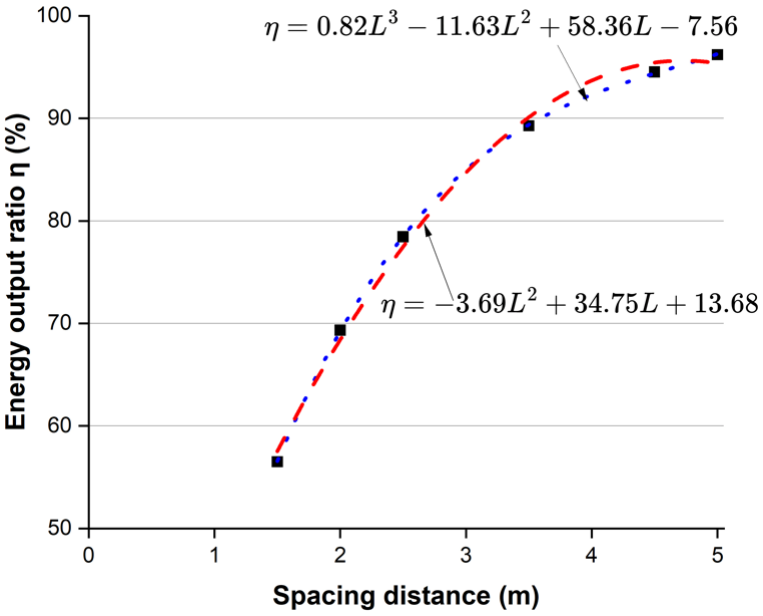


Figure 4.8 The regression line with quadratic and cubic polynomial within 5 meters spacing distance.

4.3.2 The effect of the soil thermal conductivity on the interference of different slinky-loop ground heat exchangers

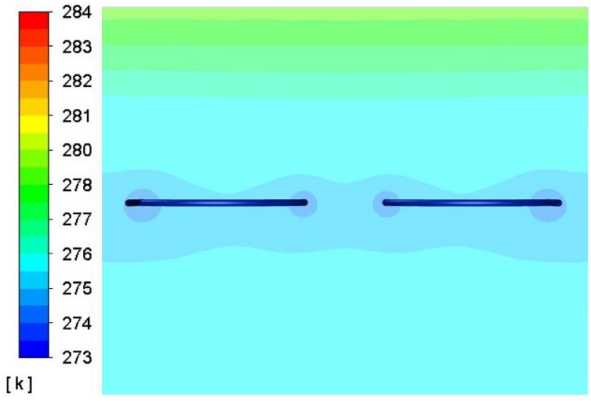
Table 4.3 Boundary condition of CFD simulation.

Installation depth	1.2 m
Soil type	Loamy soil, clayey soil, sandy soil
Operation mode	Continuous operation
The initial soil temperature	Varying temperature with the depth
Pipe temperature	1℃
Topsoil boundary condition	Monthly changed air temperature and wind speed
Climate data	Coventry
Loop pitch	1.0 m

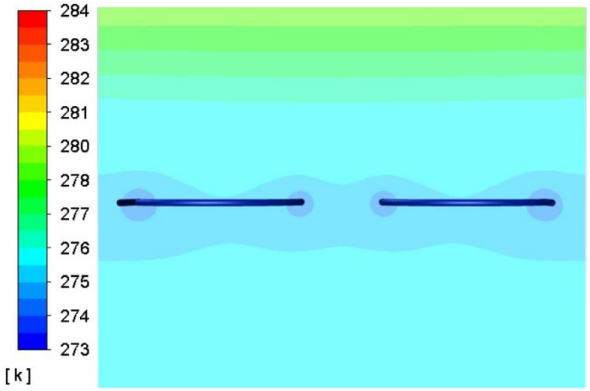
To investigate the impact of trench spacing distance and soil texture on the performance of the slinky-loop ground heat exchanger, further simulation was carried out using three types of soil, clayey soil with thermal conductivities of 0.62 W/mK, loamy soil (1.5 W/mK)and sandy soil (2.79 W/mK), as shown in Table 4.1. Table 4.3 displays the boundary conditions. The centre-to-centre distance of adjacent loops for simulation was from 1.5 m to 11m. The centre-to-centre distance of adjacent loops of 1.5m and at the installation depth of 1.2m for simulation is presented here as an example, as shown in Fig. 4.9. The soil temperature patterns of three types of soil are similar. The cooler soil temperature around the heat exchanger covers a wider area in the sandy soil shown in Fig. 4.9(a) than that in the clayey soil (lower thermal conductivity of

0.62 W/mK) shown in Figure 4.9(c).

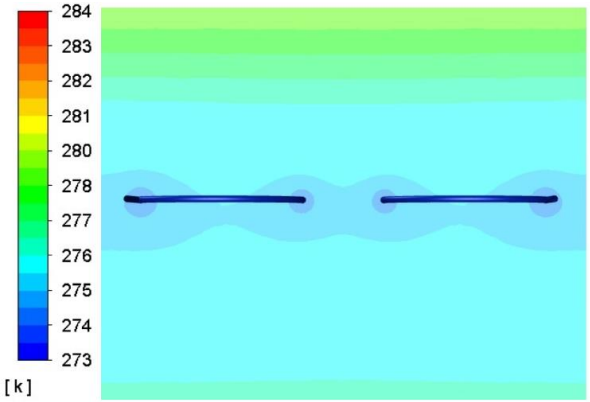
Fig. 4.10 shows the predicted vertical soil temperature distributions along the centre of the heat exchanger loop at three selected times. At the end of September, the soil temperature at a distance of 1m below the heat exchanger in vertical direction was approximately 281.02K for clayey soil (thermal conductivity = 0.62 W/mK, but decreased to around 278.74K and 277.80K for loamy soil (thermal conductivity = 1.5 W/mK) and sandy soil (thermal conductivity =2.79 W/mK), respectively. At the same time and same position, the soil temperature decreased with increasing thermal conductivity. The decrease in the predicted soil temperature is accelerated by heat extraction (relative to the initial temperature profile). The extent of temperature decrease increases with the increase of soil thermal conductivity at the beginning of the heating season. Thus, the heat exchanger installed in soil with a higher thermal conductivity had a higher heat transfer amount. However, the difference between the three types of soil deceased with the operation time. At the same position, the temperature of clayey soil and loamy soil is getting close in the end of December and almost becomes the same at the end of March. This is due to a lack of heat recovery in the short trench separation distance after a long period of continuous operation, and heat transfer rates in different soil types all drop to a low value, leading to a negligible difference in the surrounding soil temperature at the end of the heating season.



(a) Sandy soil, thermal conductivity = 2.79 W/mK

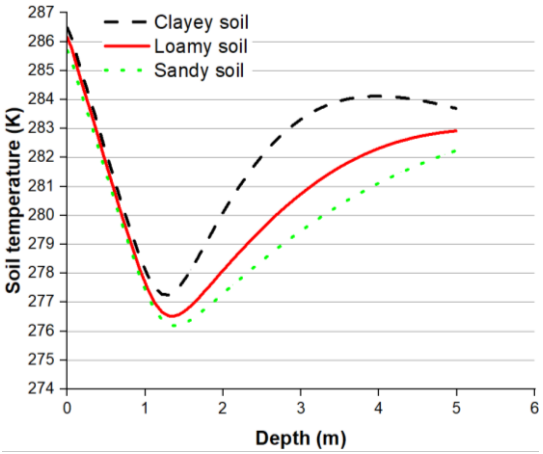


(b) Loamy soil, thermal conductivity = 1.5 W/mK

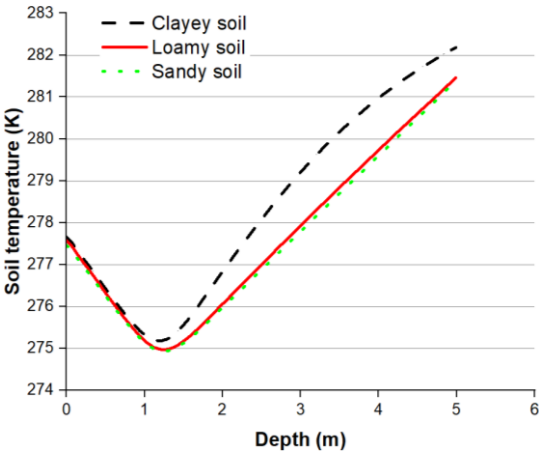


(c) Clayey soil, thermal conductivity = 0.62 W/mK

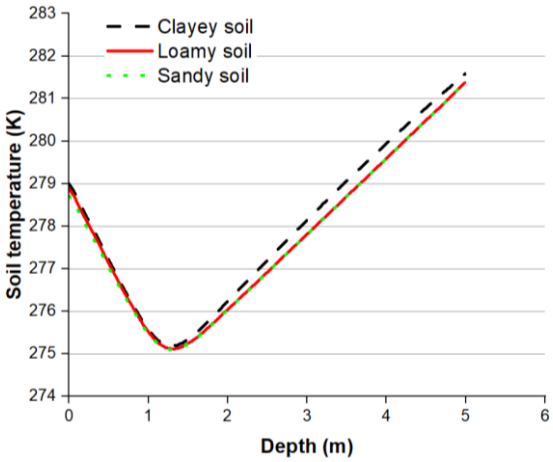
Figure 4.9 Temperature distribution on vertical section with three soil types for the separation distance of 1.5 m slinky-loop ground heat exchanger at the end of March.



(a) At the end of September

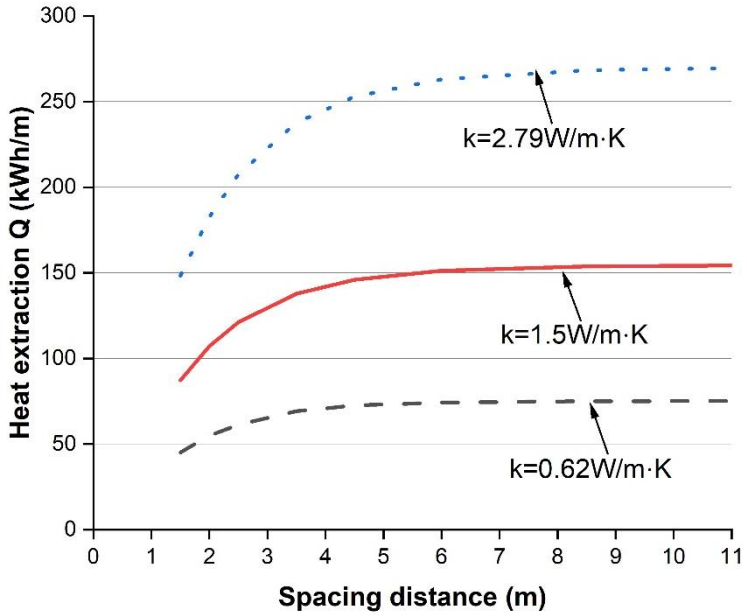


(b) At the end of December

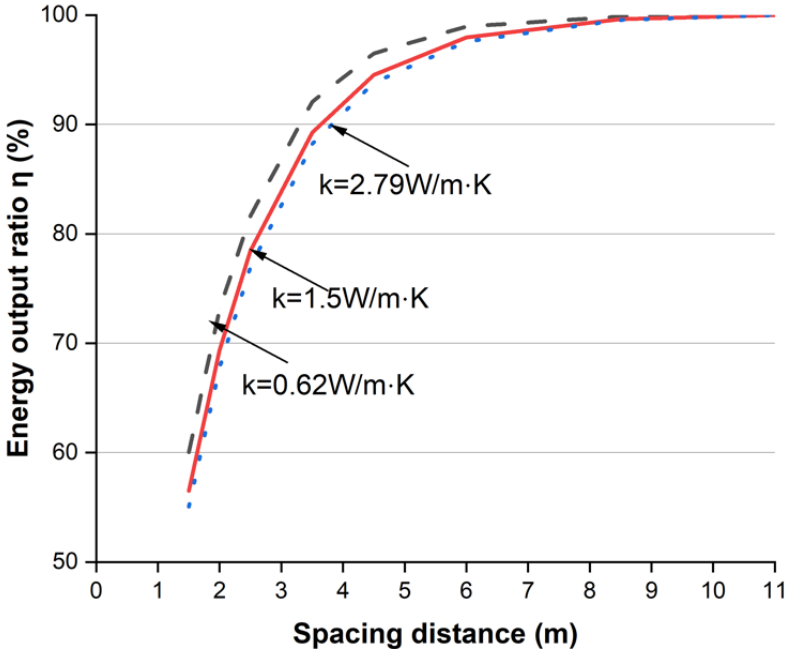


(c) At the end of March

Figure 4.10 Predicted variation of soil temperature with depth, at different times for different soil thermal conductivities.



(a) Total heat extraction through the slinky-loop ground heat exchanger of different spacing distance with various soil types from Sept to Mar.



(b) Heating season energy output ratio through the slinky-loop heat exchanger of different spacing distance with various soil types.

Figure 4.11 Effect of soil type on variations in heat extraction through the slinky-loop ground heat exchanger.

Fig. 4.11 (a) depicts that the amount of heat extraction for slinky-loop ground heat exchangers increases with the thermal conductivity of soil. The annual heat extraction was more than 2.5 times higher with sandy soil (thermal conductivity =2.79 W/mK) than that with clayey soil (thermal conductivity =0.62 W/mK). The total heat extraction from soil B (clayey) during the heating season increased from 45 kWh/m for the slinky-loop ground heat exchanger separated at 1.5 m distance to 75 kWh/m at 11 m distance. The total heat extraction from soil A (loamy) (87–154 kWh/m) and soil C (sandy) (148–267 kWh/m) was on average 123% and 297%, respectively, higher than that from soil B. Thus, higher thermal conductivity soil would allow more heat to be extracted from the surrounding soil, especially when the distance of trench separations increased. Therefore, the thermal conductivity of the soil surrounding the pipe is a very important parameter for the overall thermal performance of the slinky-loop ground heat exchanger.

The decrease in heat extraction was significant with a very small spacing distance of 1.5 m. This size of spacing would degrade overall thermal performance by 40-45%, as demonstrated in Fig. 4.11(b). The results show that thermal interactions between slinky-loop ground heat exchangers would have a larger impact with a smaller distance. At the end of seven months non-stop operation, compared with the loop without thermal interference (i.e., 100% ratio), the energy output ratio at spacing distance of 1.5m is 60%, 56.5%, and 55% for the soil thermal conductivity of 0.62 W/mK (clayey), 1.5 W/mK (loamy) and 2.79 W/mK (sandy) respectively. Moreover, the results indicate that by increasing the distance between slinky-loop ground heat exchanger, the variation of the ratio and the difference among the three types of soil decreased.

For clayey soil with a thermal conductivity of 0.62 W/mK and a maximum separation distance of 5 m, a simplified quadratic equation between energy output ratio and spacing distance can be derived:

$$\eta = -3.75L^2 + 34.62L + 17.7 \text{ (R-Square = 0.9946)} \quad (4.5)$$

For sandy soil with a thermal conductivity of 2.79 W/mK within a separation distance of 5 m, the relationship between energy output ratio and spacing distance can be expressed as a simplified quadratic equation:

$$\eta = -3.58L^2 + 34.40L + 12.45 \text{ (R-Square = 0.9965)} \quad (4.6)$$

As shown in Fig. 4.12-5.13, it shows good agreement for both regression lines.

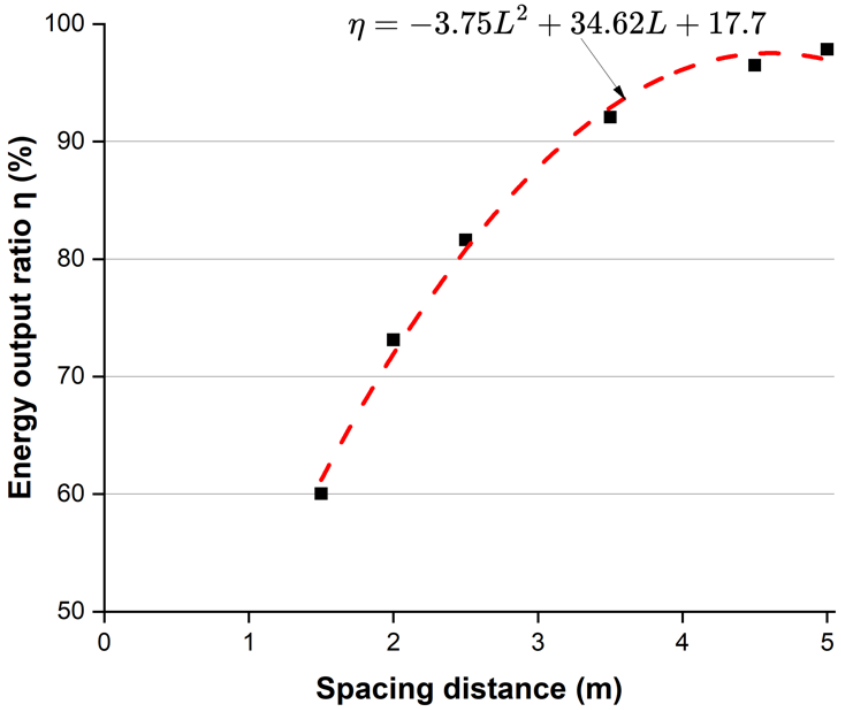


Figure 4.12 The regression line with quadratic polynomial for clayey soil.

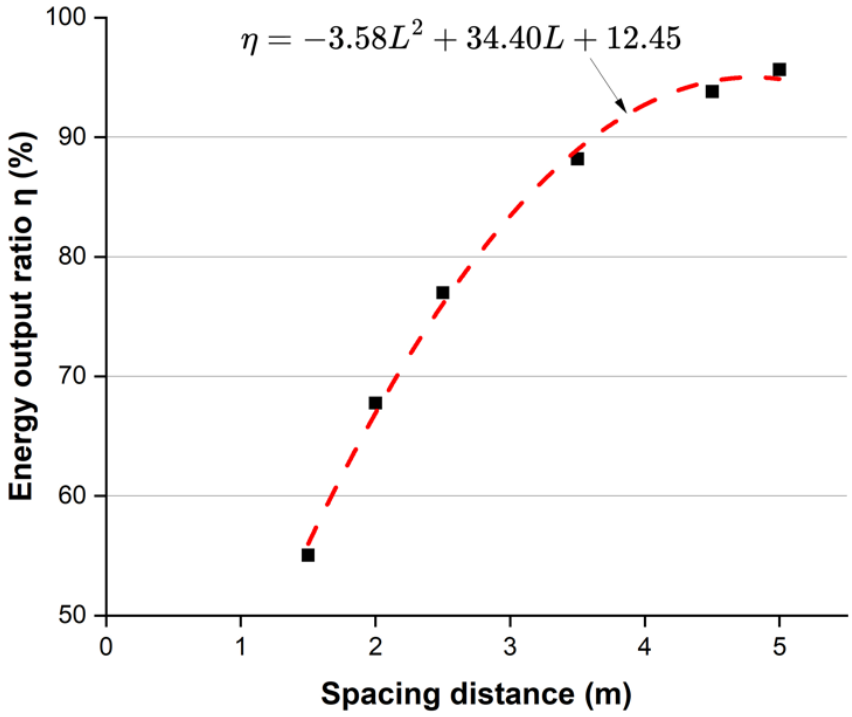


Figure 4.13 The regression line with quadratic polynomial for sandy soil.

It can be concluded that soil with high thermal conductivity would exacerbate the phenomenon of thermal interference between parallel pipes with a small separation distance. When installing slinky-loop ground heat exchanger in soil with high thermal conductivity, the spacing between pipes should be given consideration. However, in soil with low thermal conductivity, the impact of different spacing between pipes was relatively small compared to soil with high thermal conductivity.

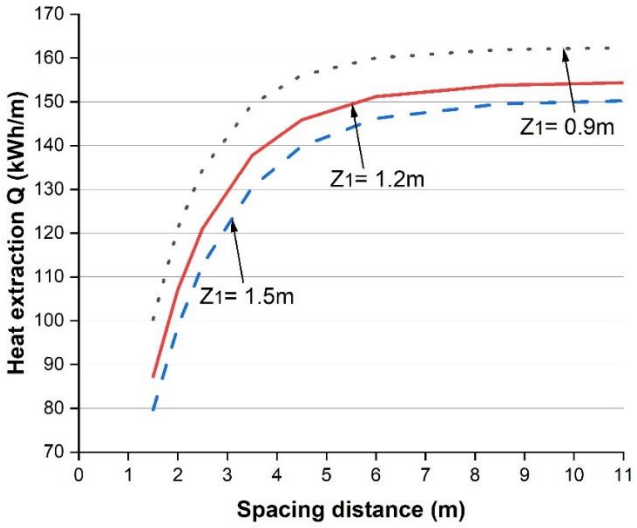
4.3.3 The effect of installation depth on the interference of different slinky-loop ground heat exchangers

Table 4.4 Boundary condition of CFD simulation.

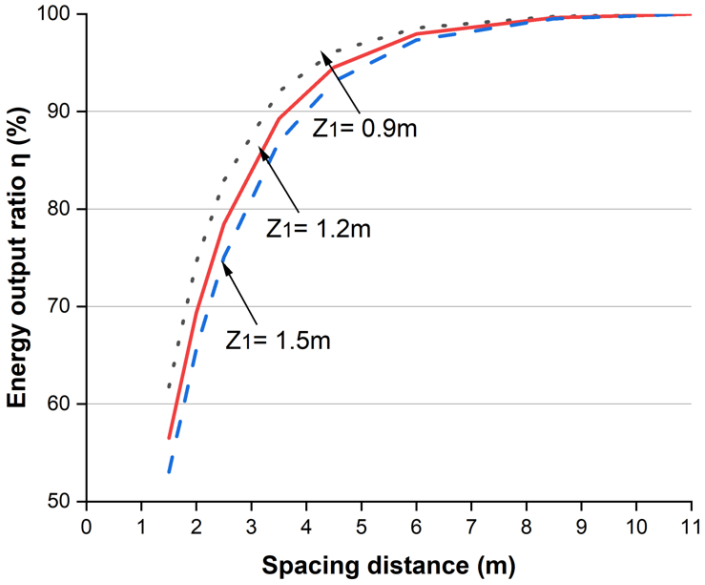
Installation depth	0.9 m, 1.2 m, 1.5 m
Soil type	Loamy soil
Operation mode	Continuous operation
The initial soil temperature	Varying temperature with the depth
Pipe temperature	1℃
Topsoil boundary condition	Monthly changed air temperature and wind speed
Climate data	Coventry
Loop pitch	1.0 m

Fig. 4.14 depicts the total heat extraction per unit length of trench for the heating season of seven months for three installation depths. The soil type for the simulation is loamy, as shown in Table 4.4. The energy extracted from the surrounding ground enhanced from 100 kWh/m to 162 kWh/m at a depth of 0.9m as the trench spacing distance increased from 1.5m to 11m. When the slinky-loop ground heat exchanger was installed at 1.2m and 1.5m, the heat extraction varied from 87 kWh/m to 154 kWh/m and 80 kWh/m to 150 kWh/m, respectively, under increasing trench separation distance. Contrary to conventional understanding (based on a constant and uniform initial soil temperature), the results indicated that the total heat extraction during seven months decreased with increasing installation depth of the slinky-loop ground

heat exchanger because of the higher initial soil temperature at shallower depth at the beginning of September. The topsoil was heated in the summer by solar radiation and warm air during the initial operating time, as shown in Fig. 3.5. In March, heat transfer amount through the heat exchanger in relatively shallow ground also increased due to the warming of the soil near the top surface by the surrounding air. However, the effect of depth depends on when the operation begins. If heating starts later from a cold month like December when the topsoil is cooler, the heat extraction for December would increase with the installation depth, as shown in Fig. 4.15. The heat extraction amount in December for the spacing distance of 6m was 18.5 kWh/m at 0.9 m depth, 18.9 kWh/m (1.2 m depth) and 19.5 kWh/m (1.5 m depth). The difference between varying depths is lower in the shorter spacing distance between adjacent trenches. For example, the heat extraction amount for 2 m spacing distance is 15.2kWh/m at 0.9m depth, 15.4kWh/m at 1.2m depth and 15.6 kWh/m at 1.5m depth. Because of this, the slinky-loop ground heat exchanger is designed to provide space heat during the winter months should be located at a deeper position in order to achieve maximum ratio. Installing the heat exchanger in a shallow trench, on the other hand, could be advantageous for a short period of operation in the autumn (or in the spring, if there is a requirement for heating, such as hot water).



(a) Total heat extraction through the slinky-loop ground heat exchanger of different spacing distance with various installation depths from Sept to Mar.



(b) Heating season energy output ratio through the slinky-loop ground heat exchanger of different spacing distance with various installation depths.

Figure 4.14 Effect of installation depth on variations in heat extraction through the slinky-loop ground heat exchanger (heating season).

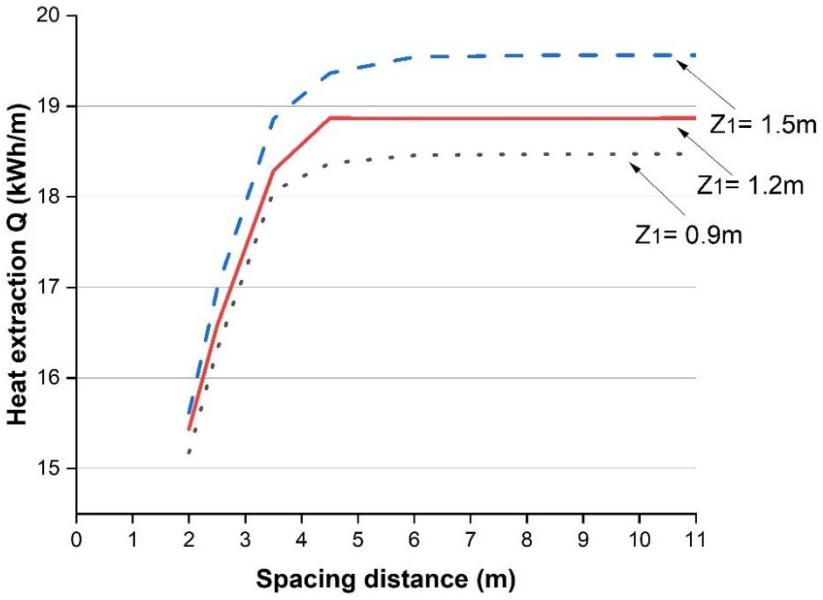
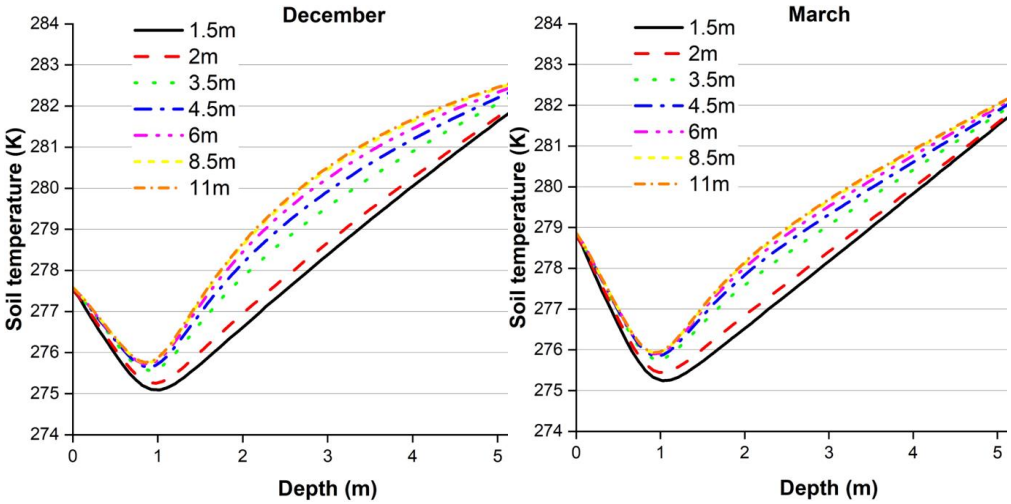


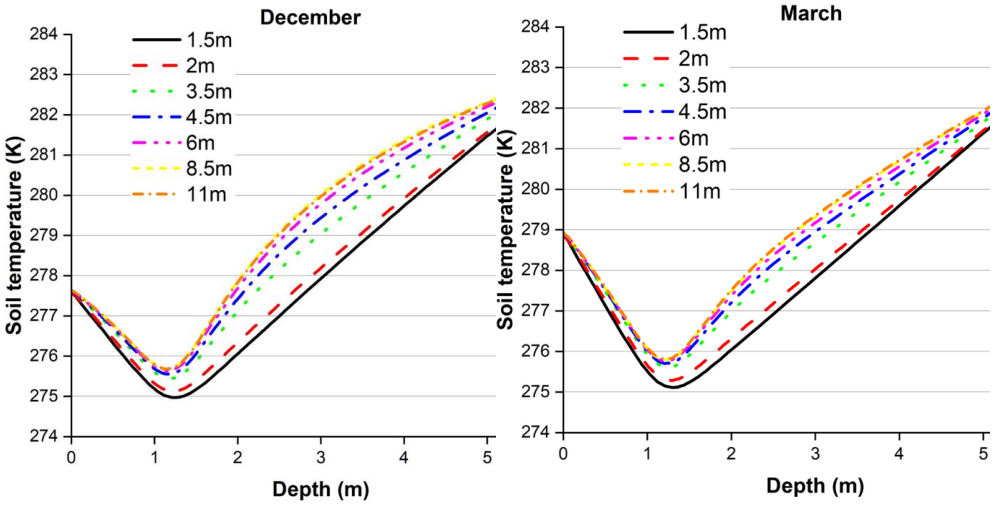
Figure 4.15 Effect of installation depth on variations in heat extraction through the slinky-loop ground heat exchanger starting from in December.

For trench spacing differences from 1.5m to 6m, the energy output compared to a single slinky-loop ground heat exchanger (without thermal interference in a parallel pipe) at 0.9m depth increased from 61.76% to 98.57%, while the energy output ratio for the depths of 1.2m and 1.5m changed from 56.51% to 97.94% and 53.02% to 97.33%, respectively. The changes of energy output at 0.9m depth was less than those of the heat exchanger buried deeper (1.2m and 1.5m). This can be explained by the fact that the performance of slinky-loop ground heat exchanger is affected by both climatic conditions and thermal interference, but the effect of the climatic conditions is greater in shallower soil. Fig. 4.16 shows the predicted vertical soil temperature distributions along the centre of the heat exchanger loop at two selected times. It can be seen that although the heat exchangers are installed at different depths, the soil temperature distribution have similar characteristics. At the end of December, the difference of soil

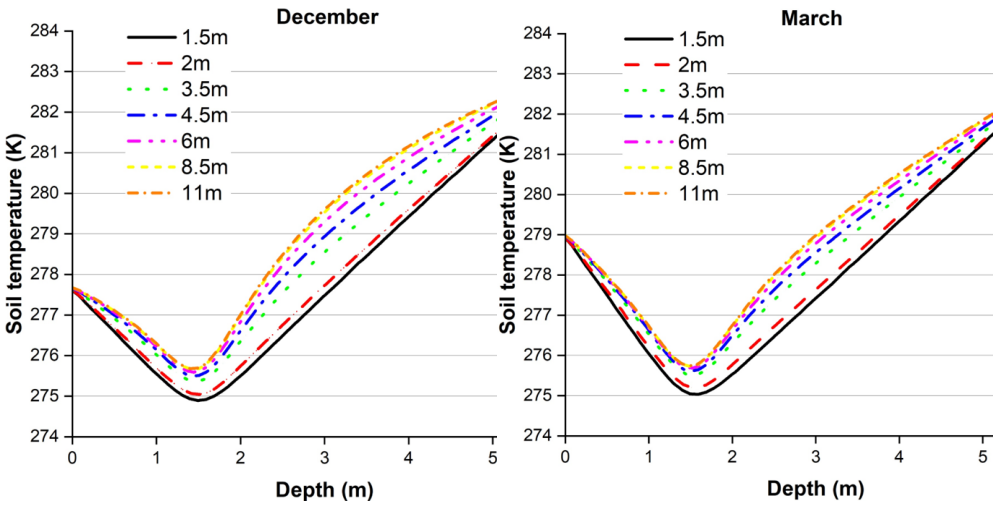
temperature between 1.5m and 11m spacing distances at a distance of 1m below the heat exchanger in vertical direction was approximately 1.48 K for a 0.9 m installation depth, but increased to around 1.52 K and 1.54 K for a 1.2 m depth and 1.5 m depth, respectively. These differences for three installation depths all decrease from December to March. As a result, the spacing distance between parallel pipes affects more for deeper installation.



(a) Installation depth of 0.9m



(b) Installation depth of 1.2m



(c) Installation depth of 1.5m

Figure 4.16 Predicted variation of soil temperature with depth, at the end of Dec and Mar for different soil thermal conductivities.

When the separation distance is less than 5 m and the installation depth is 0.9 m, a simplified quadratic equation between energy output ratio and spacing distance can be established:

$$\eta = -3.67L^2 + 33.37L + 21.24 \text{ (0.9 m depth)} \quad (4.7)$$

When the separation distance is no more than 5 m and the installation depth is 1.5 m, the relationship between energy output ratio and spacing distance can be described as:

$$\eta = -3.52\,L^2 + 34.46L + 10.07 \text{ (1.5 m depth)} \quad (4.8)$$

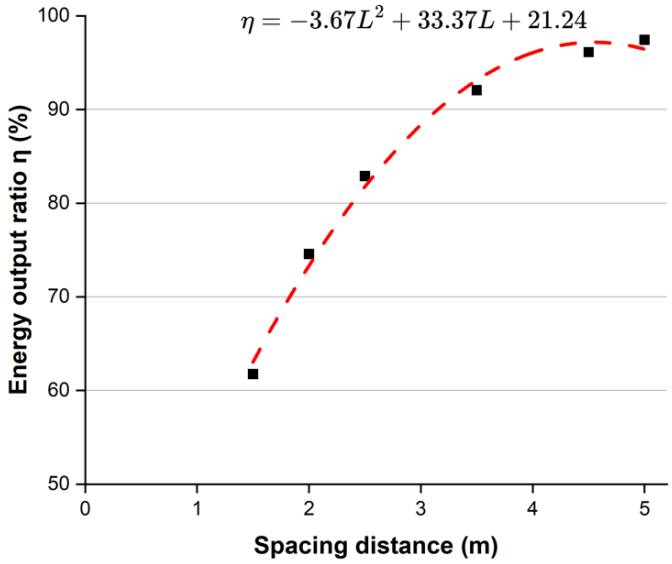


Figure 4.17 The regression line with quadratic polynomial at depth of 0.9 m.

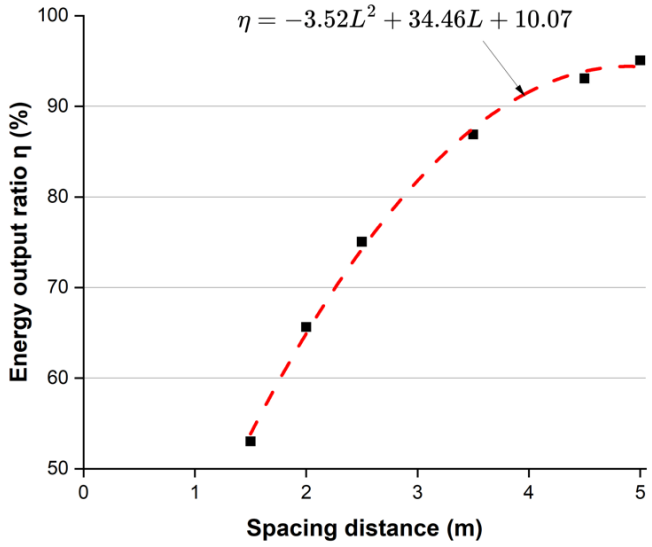


Figure 4.18 The regression line with quadratic polynomial at depth of 1.5 m.

As depicted in Fig. 4.17-4.18, the quadratic polynomial regression lines both fit the variation of energy output ratio for different spacing distance at various installation depths.

The results indicate that there was a similar variation trend with the separation distance for the three installation depths. Again, when the separation distance

was greater than 6 m, the variation in distance of pipe spacing had only a small change in energy output. By comparison, when the distance was much less than 6 m, the dependency of energy output on the pipe spacing distance would be considerable. Installation depth has less influence than trench separations on thermal performance.

4.4 Conclusion

A 3D CFD model has been developed for dynamic thermal performance simulation of the horizontal slinky-loop ground heat exchangers with different trench separations for different installation depths and soil properties. The effect of trench separation was analysed for separation distances from 1.5 to 11 m.

Heat transfer between parallel pipes would interfere with each other, resulting in a reduction in overall thermal performance if the separation distance is too small. Correlations have been developed from the numerical simulation to estimate the thermal performance of different spacing distances. It is suggested that the centre-to-centre trench separation distance should be between 5-6m to achieve good thermal performance while making use of the available land.

The heat transfer amount through slinky-loop ground heat exchanger is dependent on the depth of the installation and the texture of the soil. The predicted total heat extraction for a heating season would decrease with the increasing depth of installation. This is because the topsoil was heated in the summer by solar radiation and warm air in the early period of the heating season, while the rising air and soil temperatures in the later part of the heating season led to a higher temperature in the shallower soil. However, if heating starts later from a cold month like December, when the topsoil is cooler, the total heat

extraction would increase with the installation depth. The results of the simulation also indicated that the effect of the trench separation would increase with the installation depth. But installation depth has less influence than trench separations on thermal performance.

The simulation results showed that the increase in soil thermal conductivity would greatly improve the overall performance during a seven-month long heat extraction for slinky-loop ground heat exchanger installed at 1.2 m depth, with 297% and 123% higher in sandy and loam soil, respectively, than in clayey soil. Besides, soil with a higher thermal conductivity will exacerbate the phenomenon of thermal interference between parallel pipes with a shorter separation distance.

Chapter 5: Analysis of slinky-loop ground heat exchanger models with intermittent operation and different layout

5.1 Introduction

Ground source heat pump systems have the potential to perform better than traditional air source heat pump systems by using the stable soil temperature. Nevertheless, the continuous operation of the GSHP system may lead to an imbalance in soil thermal conditions. As a result, increasing the spacing and depth of trench, as well as combining GSHP systems with auxiliary heat sources, are employed to prevent soil thermal imbalance. However, these methods necessitate large areas and increases the initial investment cost. By modifying the GSHP system operation mode, this study suggests intermittent operation as an alternative to minimising the imbalance of soil thermal performance.

As mentioned in the above literature review, numerous research on the influence of the operation strategy of the vertical ground source heat pump through the numerical model with or without simple experimental validation have been published. However, the impact of various daily operating hours on the thermal performance of horizontal slinky-loop ground heat exchanger system was still less understood. During the operation of a ground source heat pump system, the COP of the unit can be enhanced through the adoption of reasonable intermittent control, which is dependent on the soil temperature recovery. This indicates the necessity of further investigation in the field. In order to accurately evaluate the effects of the intermittent operation method, the numerical modelling of slinky-

loop ground heat exchanger in various operation modes was simulated, which would provide a realistic condition. This study designed one continuous and three intermittent operating conditions. Seven-month simulation of these four operating conditions were conducted to determine the optimal intermittent operating condition to lay the foundation of the application of GSHP intermittent operation in practical engineering. The effect of different daily operation hours, loop pitch, thermal interference from parallel pipe, and annual operation mode on slinky-loop ground heat exchanger thermal performance are also discussed.

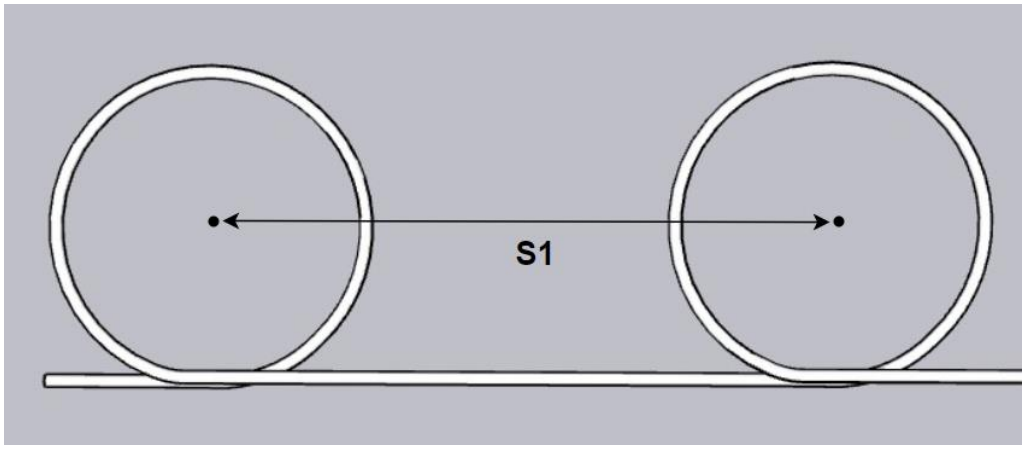
5.2 Description of conditions for simulation

The simulations were conducted for the heating season in the UK from 1st of September to 31st of March. The simulated GSHP system was operated intermittently, 6 h operation, 12 h operation and 18 h operation a day during a seven-month period without thermal interference from adjacent trenches. The present work adopts a similar approach with previous chapters in carrying out the modelling of slinky-loop ground heat exchanger. The soil properties and climatic data used were based on Coventry. During the switch-off (recovery) period of intermittent operation and the non-heating season, zero heat flux is specified as the boundary condition for the pipe surface.

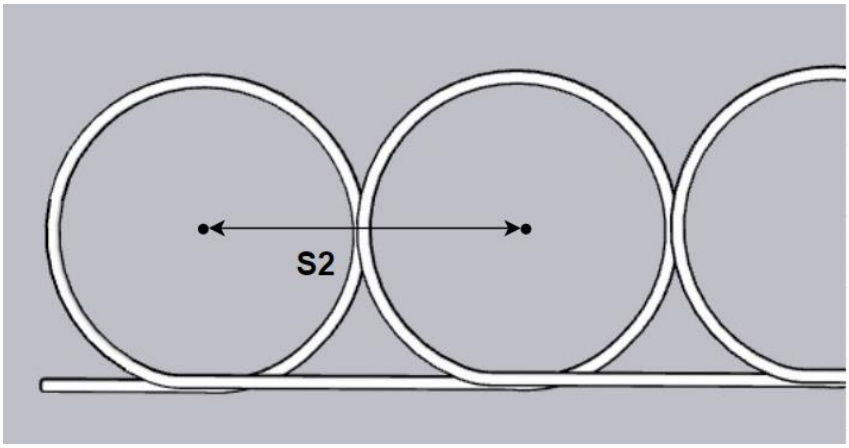
5.2.1 Slinky-loop ground heat exchanger geometric characteristics

The loop pitch of the slinky-loop ground heat exchanger is one of the geometric characteristics that has a direct impact on material cost and installation. The length of the trench and the number of pipe lengths needed to build the heat exchanger are both directly related to this feature. As a result, it is critical to

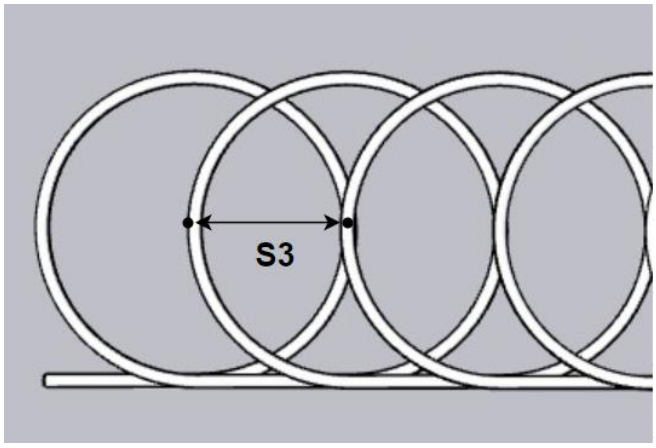
investigate the effect of loop pitch on the heat exchanger and the thermal performance of the HGSHP system. Shortening the distance between horizontal loops would increase the overall length of pipe needed for the system. Fig. 5.1(a)-(d) shows the schematic diagram of different loop pitches of slinky-loop ground heat exchanger. In the present analysis, four different loop pitches were considered, the spacing were S_1=2.0 m, S_2=1.0 m, S_3=0.5 m and S_4= 0.25 m (i.e., Cases 1, 2, 3, 4, respectively).



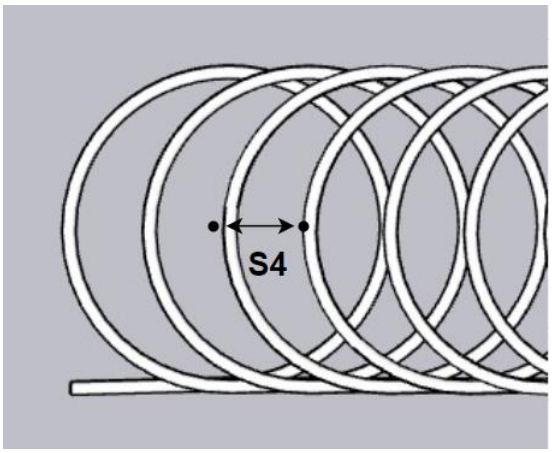
(a) Case 1, with loop pitch of 2 m



(b) Case 2, loop pitch of 1 m



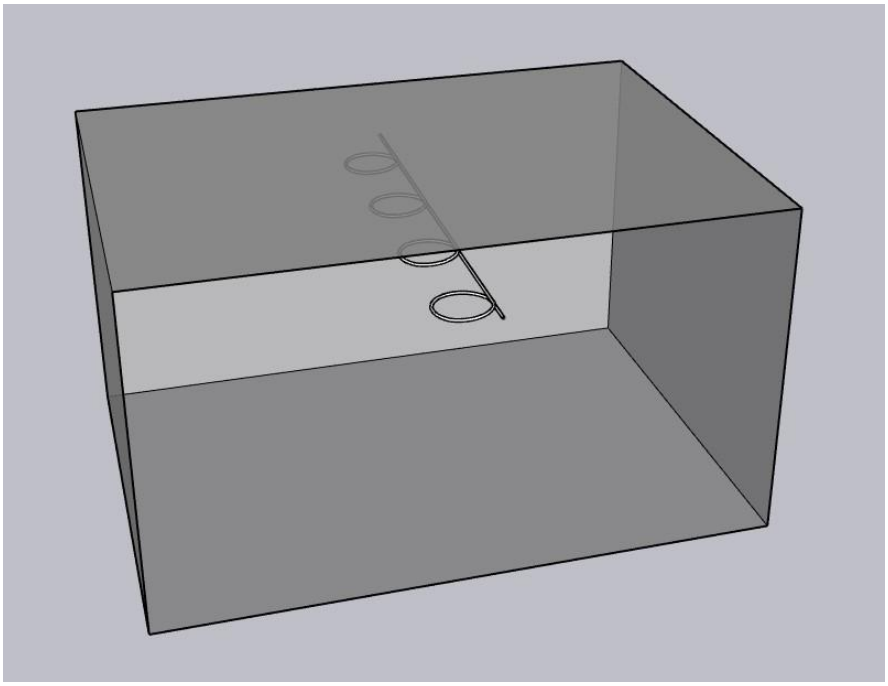
(c) Case 3, loop pitch of 0.5 m



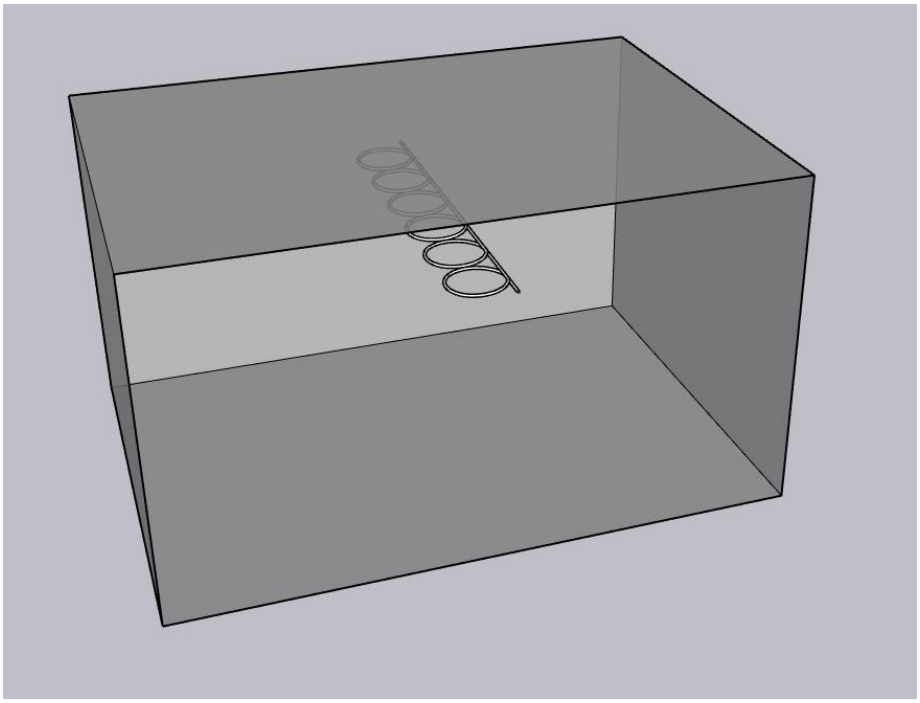
(d) Case 3, loop pitch of 0.25 m

Figure 5.1 Schematic diagram of different loop pitches of slinky-loop ground heat exchanger.

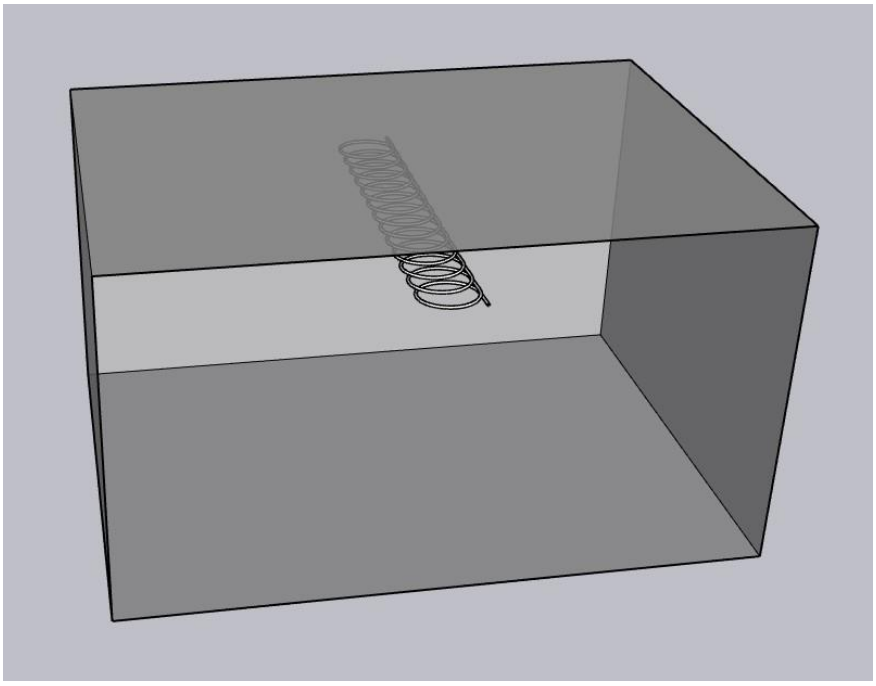
The main part of the slinky-loop ground heat exchanger consisted of a circular HDPE pipe with a 40 mm diameter. The slinky-loop ground heat exchanger with 1 m loop diameter and varying loop pitch were installed horizontally at 1.2 m below the ground surface. The total depth of the computational domain was 10m. The CFD solution domain is shown in Fig. 5.2.



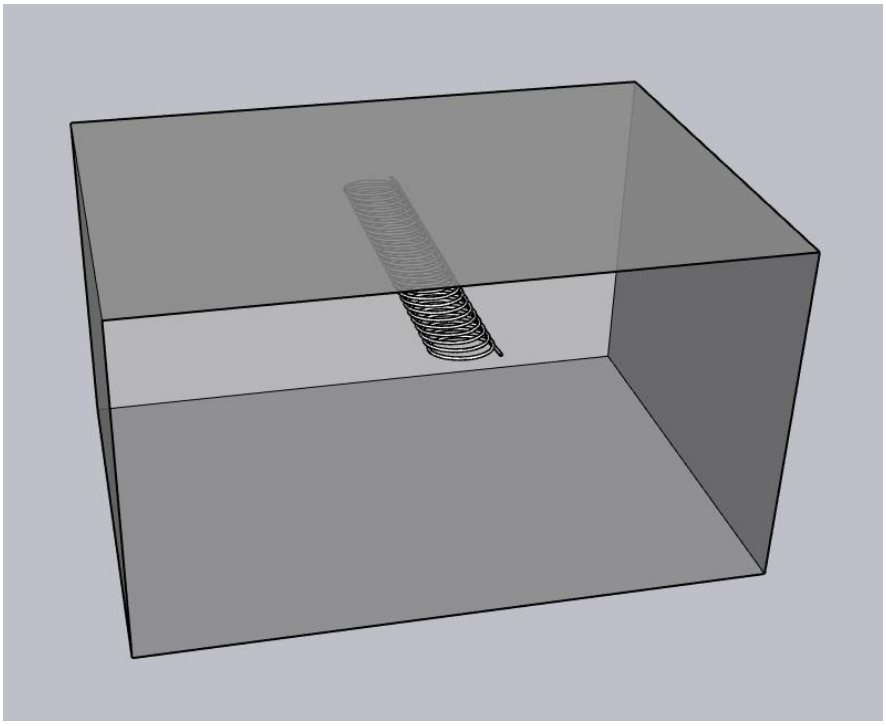
(a) Case 1, CFD solution domain with loop pitch of 2 m



(b) Case 2, CFD solution domain with loop pitch of 1 m



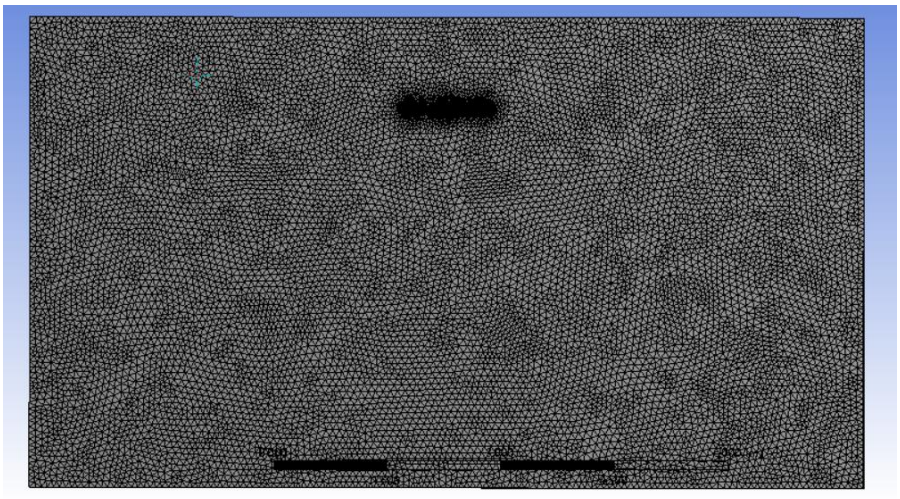
(c) Case 3, CFD solution domain with loop pitch of 0.5 m



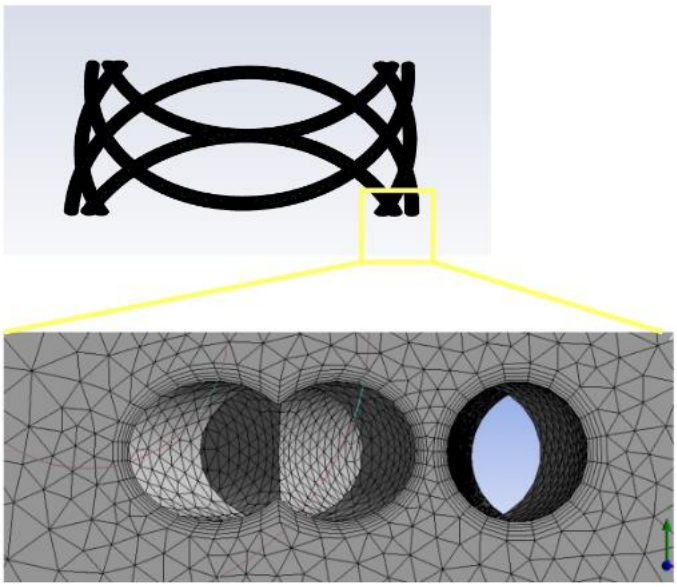
(d) Case 4, CFD solution domain with loop pitch of 0.25 m

Figure 5.2 Computational domain for soil with slinky-loop ground heat exchanger.

A symmetrical slinky-loop ground heat exchanger is proposed, since it would otherwise need significant computing processing time and data storage. To limit the amount of computing power required, only a portion of the slinky-loop ground heat exchanger is simulated. The details of the mesh generated for the slinky-loop ground heat exchanger model with a 0.25 m loop pitch is presented in Fig. 5.3 (a)–(b). The mesh was denser in close proximity to the pipework, where temperature gradients are greatest. The soil domain element size was set at 0.08 m, and the size near the pipe surface was taken as 0.006 m.



(a) The vertical cross-section of the generated mesh



(b) The denser mesh near the heat exchanger

Figure 5.3 The details of mesh generated for Case 4.

5.2.2 Validation of loop configuration with different pitch

The loop pitch of the slinky-loop ground heat exchanger is one of the geometric characteristics that has an important impact on the system's initial cost and installation. This parameter is also related with the amount of pipe lengths needed for the construction of the heat exchanger, as well as the length of excavation required. It is important to evaluate the various values of loop pitch on the heat exchanger and the thermal performance of the HGSHP system.

The validation of these slinky-loop ground heat exchanger models were assessed from the duration of heating under continuous operation with the same boundary condition as Chong et.al. [22]. The vertical far-field boundary was considered as adiabatic surfaces, whereas the bottom boundary was given a constant temperature of 10 °C, which is the yearly mean temperature of deep soil in the

United Kingdom. The boundary condition at the top soil surface was set to 5 °C ambient air temperature and a wind speed of 3 m/s. The pipe surface temperature was measured at 1 °C. The initial soil temperature was set to the same as the deep soil (10 °C).

Fig. 5.4 shows that all four cases exhibited a high heat extraction rate at the beginning and decreased gradually until the heat extraction of the soil surrounding the pipe achieved a nearly constant level of heat extraction rate.

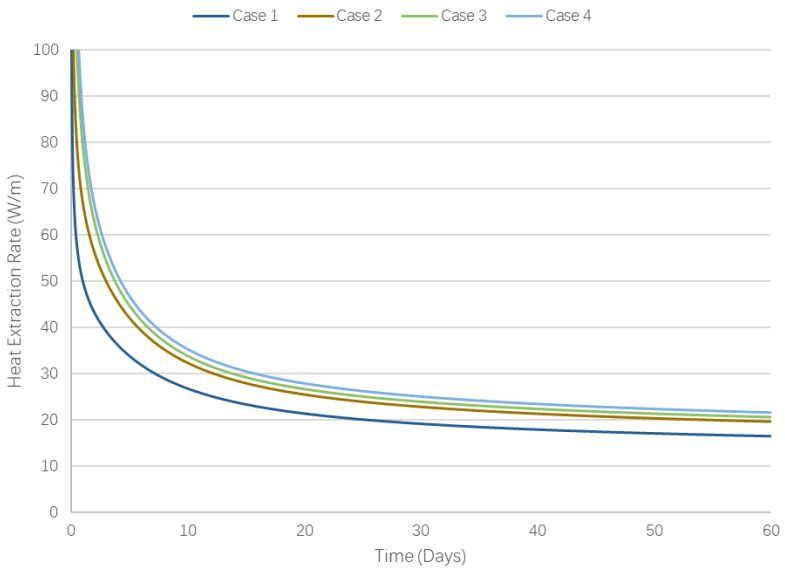


Figure 5.4 Variations in heat extraction rates of slinky-loop ground heat exchangers (loop diameter, D = 1 m, loop pitch, LP = 0.25 m, 0.5 m, 1 m and 2 m) with time.

For instance, the heat extraction rate after one day of operation for the slinky-loop ground heat exchanger with 0.25 m loop pitch (i.e., Case 4) was 85.61 W/m, 79.74 W/m for 0.5 m (i.e., Case 3), 65.10 W/m for 1.0 m (i.e., Case 2) and 50.16 W/m for 2.0 m (i.e., Case 1). The heat extraction rate gradually decreased during the continuous heating operation and stabilized after 45 days. The heat flow from the surrounding soil to the slinky-loop ground heat exchanger had

reached equilibrium, and a constant heat transfer rate had been established by the time the simulation reached 60 days; 22.57 W/m for the loop pitch of 0.25 m (i.e., Case 4), 21.25 W/m for 0.5 m (i.e., Case 3), 19.55 W/m for 1.0 m (i.e., Case 2) and 16.87 W/m for 2.0 m (i.e., Case 1). According to Table 5.1, it shows good agreement with the simulation result from Chong et.al.

Table 5.1 Comparison of the heat exchange rate between the current work and the previous simulation results of Chong et al. [23].

Case	Loop diameter(m)	Loop pitch (m)	Day 1 heat exchange rate (w/m)	Day 1 heat exchange rate (w/m) (Chong et al.)	Day 60 heat exchange rate (w/m)	Day 60 heat exchange rate (w/m) (Chong et al.)
1	1	2	50.16	50.17	16.87	16.87
2	1	1	65.10	65.09	19.55	19.55
3	1	0.5	79.74	79.76	21.25	21.24
4	1	0.25	85.61	85.63	22.57	22.58

5.3 Results and discussion

The effect of different daily operation hours, loop pitch, and annual operation mode are discussed. The simulation results are presented as temperature contours, soil temperature distribution, heat transfer rate (in W/m), and the amount of heat transfer per meter length of trench for a given period (in kWh/m).

5.3.1 Intermittent 6 h,12 h and 18 h operation

Table 5.2 Boundary condition of CFD simulation.

Installation depth	1.2 m
Soil type	Loamy soil
Operation mode	Intermittent 6 h, 12 h and 18 h operation
The initial soil temperature	Varying temperature with the depth
Pipe temperature	1℃
Topsoil boundary condition	Monthly changed air temperature and wind speed
Climate data	Coventry
Loop pitch	1.0 m

In this chapter, the daily operation time of the system was divided into 24, 18, 12, and 6 hours. The 24-hour system operation is defined as the full-load condition without soil temperature recovery time. For intermittent operation, the system had been simulated for 12-hour-on (heating) and 12-hour-off (recovery period) operation, 6-hour-on (heating) and 18-hour-off (recovery period) operation, 18-hour-on (heating) and 6-hour-off (recovery period) operation, which include the soil thermal recovery time every day during a seven-month heating period. As described previously, the same boundary conditions were applied with Coventry monthly average air temperature, wind speed and local loamy soil properties. The results were obtained by assuming the initial varying soil temperature. The slinky-loop ground heat exchanger temperature was fixed at 1 °C with a loop diameter of 1 m and loop pitch of 1 m buried at 1.2 m depth

without considering the thermal interference from adjacent trench, as shown in Table 5.2. Fig. 5.5 illustrates the predicted heat exchange rate in the first week for discontinuous 6 h, 12 h, 18 h and 24 h continuous operations in heating mode. The heat transfer rate decreased with time during the ON period or at the same time of different days. Initially, it was approximately 287W/m for the first hour of running the HGSHP on the first day; it decreased to approximately 60W/m for the first hour on the seventh day in continuous mode, 125W/m in discontinuous 18 h, 171W/m in discontinuous 12 h and 214W/m in discontinuous 6 h, respectively. Under continuous mode, heat transfer rate per unit length decreases quickly and gradually becomes stable after a few days of operation. Under intermittent mode, the overall trend also decreases gradually, but after each intermittence, the heat transfer rate recovers to some extent. For example, 6 hours operation a day has a soil temperature recovery time of 18 hours after continuous operation for 6 hours. The system operation time decreased and the soil temperature recovery time increased compared to that in 12 hours operation a day. Hence, the decrease in the heat transfer rate at the operation start point was smaller than that at the 12 hours operation time. It indicates that the extended period of off operation increases the heat transfer rate in the next flow cycle. This means that the intermittent operation method has a smaller effect on the soil temperature than the continuous operation method.

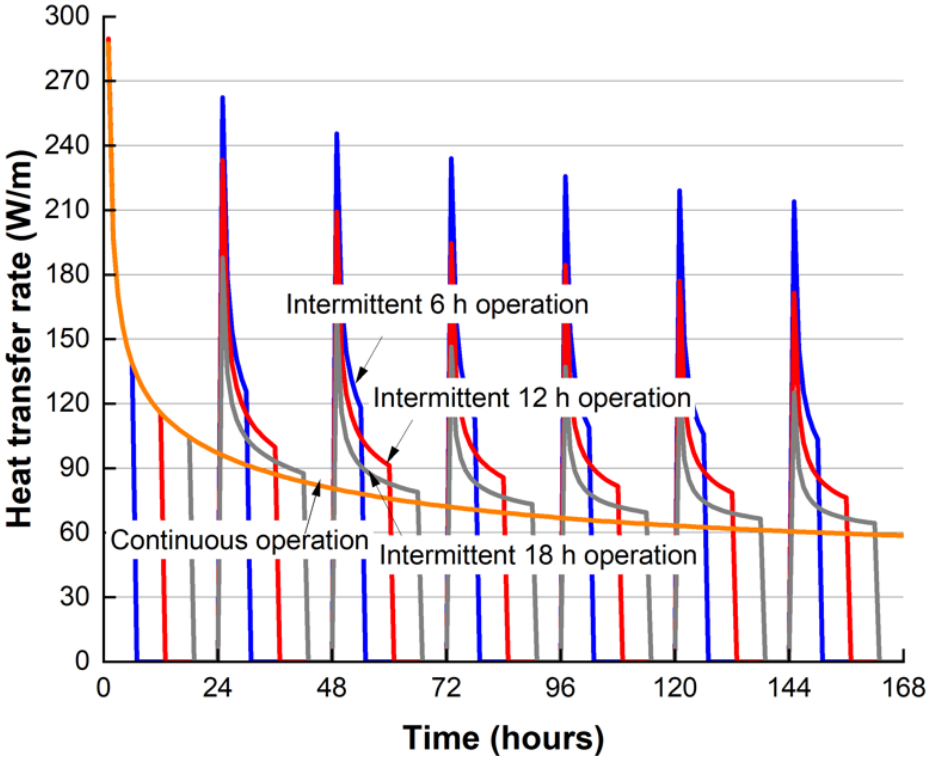


Figure 5.5 Heat transfer rate at first week for continuous operation and intermittent operation.

To investigate the effect of intermittent operation over a long period, the heat exchange rate of intermittent mode was compared against that of continuous operation, as given in Fig. 5.6. The daily minimum heat transfer rate was obtained at the end of the switch-on (operation) period. This value with three intermittent operating conditions of the heat exchanger during heating season were higher than that of the continuous operating condition. For example, the heat transfer rate for continuous operation drops from 22.35 W/m to 22.20 W/m on day 106 (15/12), while it is (47.40–24.60 W/m), (71.88–30.01 W/m), and (94.08–43.21 W/m) for intermittent 18-h operation, 12-h operation, and 6-h operation, as shown in Fig. 5.7 (c). The heat transfer rate for continuous operation decreases slower with time and seems to be near constant because of

the minimal difference between the first hour and the last hour of the same day. It can be obtained from Fig. 5.7 (a) and (b) that the heat transfer rate of continuous operation decreased by 15.38 W/m on the second day and by 5.02 W/m on the fourth day. As time goes on, there will be less of a difference in the heat transfer rate between the first hour and the last hour of the same day.

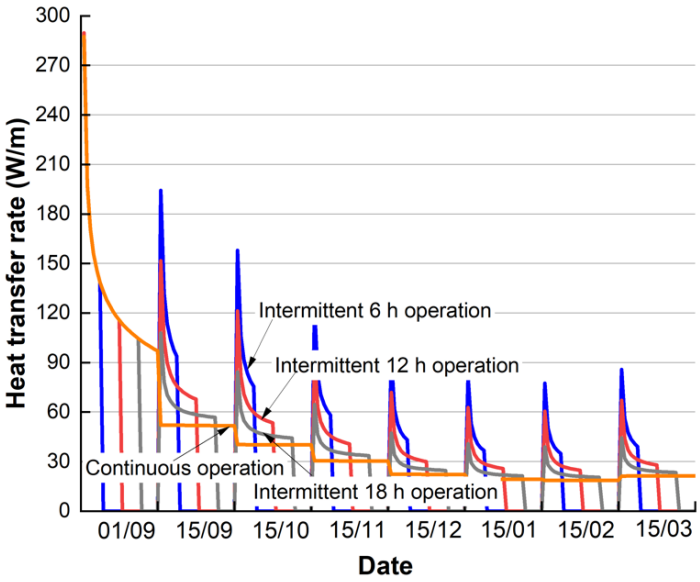
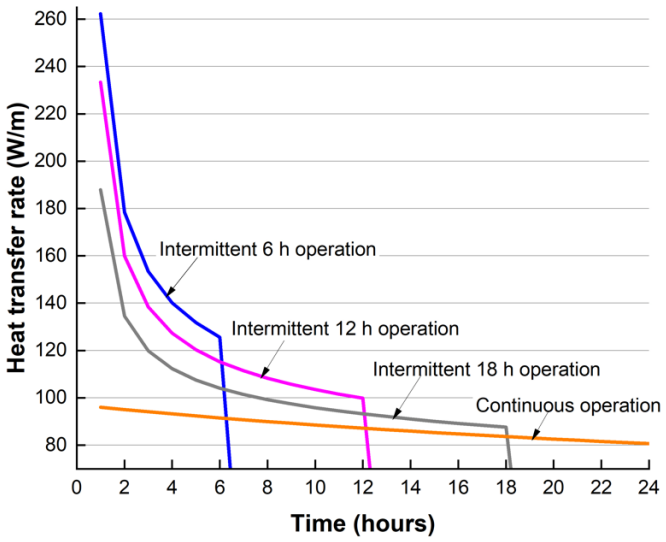
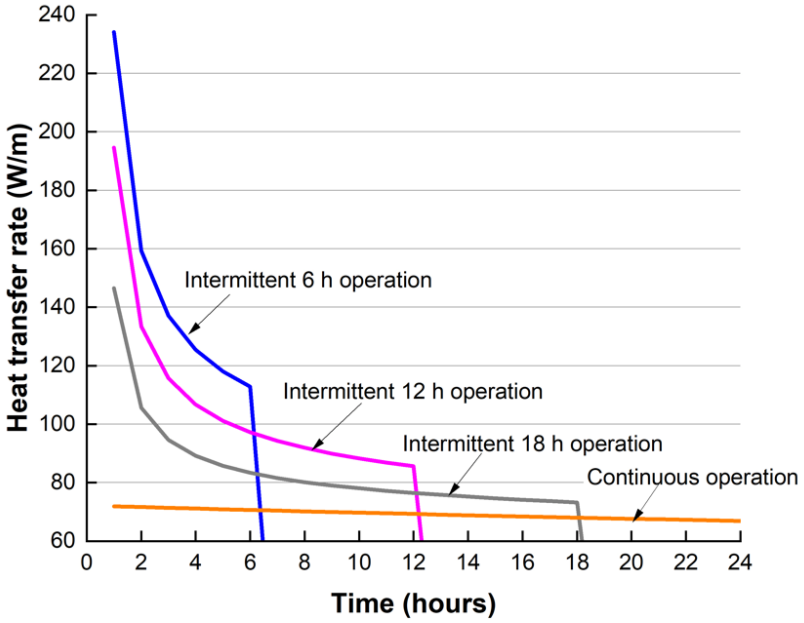


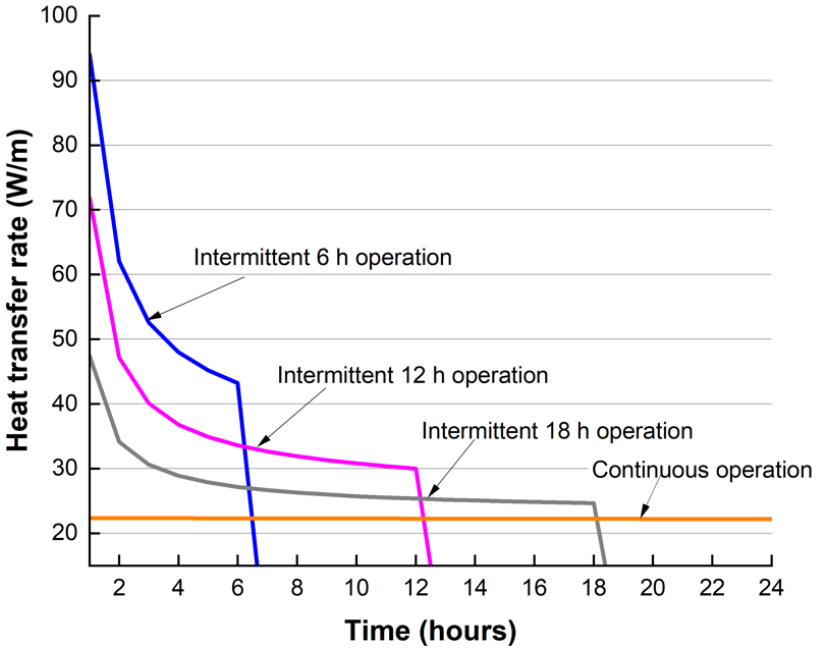
Figure 5.6 Heat transfer rate at selected date for continuous operation and intermittent operation.



(a) The second day



(b) The fourth day



(c) The middle of the fourth month (15th December)

Figure 5.7 Heat transfer rate of intermittent and continuous operation on selected day.

There is a gradual rise in the temperatures of the slinky-loop ground heat exchanger and the soil during the off period. This is because heat is released

from the soil that is surrounding the slinky-loop ground heat exchanger. However, the temperature of the heat exchanger may not be able to fully recover to the soil temperature from the previous day during the off period. The capacity of the slinky-loop ground heat exchanger to transfer heat would consequently decline on a daily basis as a result of this. Table 5.3 summarizes the daily average heat exchange rate on the selected date of each month for discontinuous 6 h, 12 h, 18 h and 24 h continuous operations in heating mode. On day 45 (15/10), the daily mean heat transfer rate of continuous operation is 40.2 W/m, and that of the intermittent 18 h operation, 12 h operation, and 6 h operation modes are 49.9 W/m, 66.2 W/m, and 99.0 W/m, respectively. On day 137 (15/01), the daily mean heat transfer rate of continuous operation is 19.3 W/m, and that of the intermittent 18 h operation, 12 h operation, and 6 h operation modes are 24.0W/m, 32.4 W/m, and 49.1 W/m, respectively. The reason for that is when the daily operation time becomes shorter, the restoration period of each day prolongs accordingly, and thus the heat transfer rate per unit length decreases slower.

Fig. 5.8 illustrates the difference of daily average heat transfer rate between intermittent operation and continuous operation. On day 15 (15/09), the daily mean heat transfer rate for the intermittent operation of 6-h running time is up to 136.1% higher than that for continuous operation, and that of intermittent 12-h operation and 18-h operation is 61.3% and 23.5%. The largest difference is on day 106 (15/12), the difference between intermittent operation and continuous operation increases to 158.2% for intermittent 6-h operation, 68.9% (intermittent 12-h operation) and 25.0% (intermittent 18-h operation).

Table 5.3 Daily average heat transfer rate on selected date.

Daily average heat Exchange rate (W/m)								
Date	01/09	15/09	15/10	15/11	15/12	15/01	15/02	15/03
Intermittent 6 h	182.1	122.6	99.0	76.8	57.5	49.1	46.8	52.3
Intermittent 12 h	153.3	83.8	66.2	50.7	37.6	32.4	31.1	35.0
Intermittent 18 h	138.1	64.1	49.9	37.9	27.8	24.0	23.1	26.3
Continuous	128.7	51.9	40.2	30.4	22.3	19.3	18.6	21.3

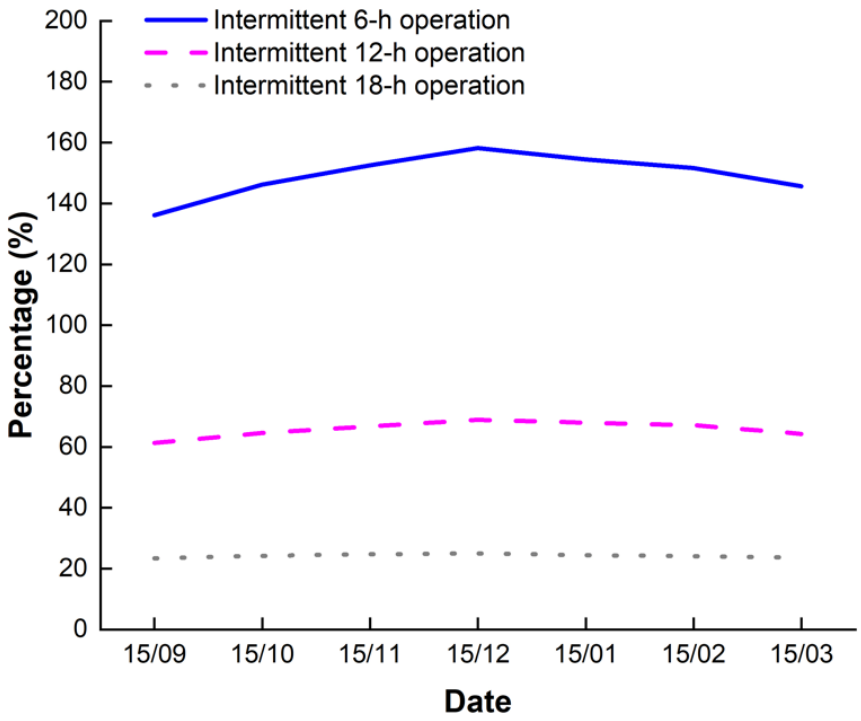


Figure 5.8 The difference of daily mean heat transfer rate between continuous operation and intermittent operation on selected date.

In terms of energy transfer, however, continuous operation would provide a larger amount of daily heat extraction than intermittent operation. It can be observed from Fig. 5.9 that the daily heat extraction amount for continuous operation is at least 35.4%, 15.5%, and 6.3% higher than intermittent 6-h

operation, 12-h operation, and 18-h operation.

It is found that the daily average and minimal heat extraction rate for intermittent operation were much higher than for continuous operation, while the daily heat extraction amount of continuous operation was the highest. As discussed earlier, the heat exchange rate of different operation modes was high at the beginning of operation and gradually declined due to the effect of heat loss in the ground along with operating time. When the system operates with a small run-stop ratio, the effect of soil heat recovery is better. It can be expected to show higher performance with the intermittent operation method without increasing the length of the GHE or using an auxiliary heat source.

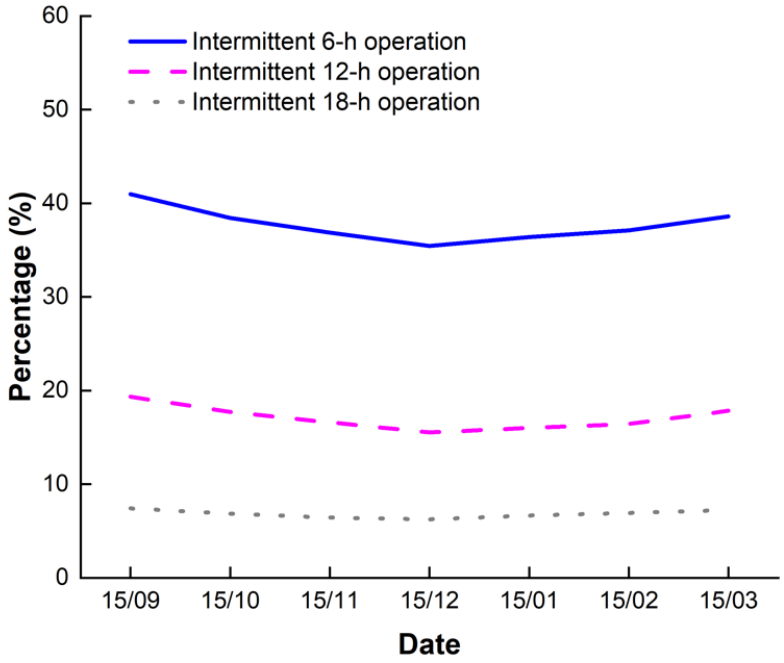


Figure 5.9 The difference of daily heat extraction amount between continuous operation and intermittent operation on selected date.

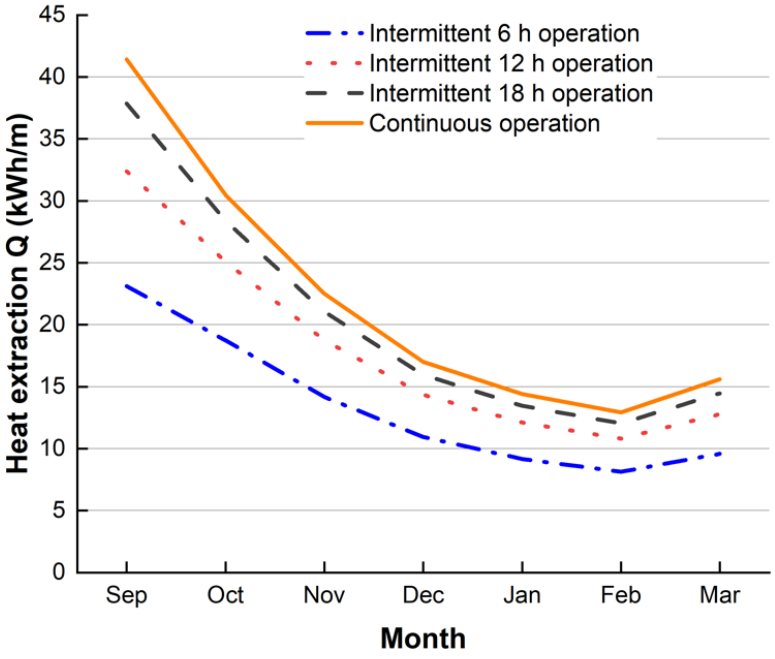


Figure 5.10 Variation of monthly heat extraction at different operation mode.

Fig. 5.10 shows the monthly heat extraction variation with time at different operation modes. The results suggested that when the system simulated in continuous operation, the monthly heat extraction amount decreases rapidly from 41.4 kWh/m in September to 12.9 kWh/m in February and increases slightly afterwards. The reduction of monthly heat extraction for discontinuous 18 h (37.9-12.0 kWh/m), discontinuous 12 h (32.4-10.8 kWh/m) and discontinuous 6 h (23.1-8.1 kWh/m) is on average 9.1%, 24.2%, and 47.4%, respectively, lower than the continuous operation. The variation of heat extraction with time and operation mode can be explained by the corresponding variation in ground thermal recovery in combination with heat transfer through the slinky-loop ground heat exchanger. Table 5.4 reflects the variation of the overall heat extraction and average heat transfer rates over 7 months under various operation modes. Taking the continuous operation as an example, the total heat extraction amount is the biggest because of the continuous 5112 hours

operation. As the daily operation time increased, the heat extraction amount of the slinky-loop heat exchanger with 6-hour-on (heating), 12-hour-on (heating), and 18-hour-on (heating) was 39.2%, 18.2%, and 7.2%, respectively, less than continuous operation. However, the average heat transfer rate (the ratio between the total heat extraction and operation hours) is the lowest when compared to intermittent operation. From the table, it can be seen that when the intermittence time becomes longer, the average heat exchange rate increases. For example, the HTR of the slinky-loop ground heat exchanger which uses the intermittent 12-hour-on (heating) operation method was higher by up to 64% that of the continuous operation method.

Table 5.4 Overall heat extraction and heat transfer rates under various modes.

Daily operation hours (h)	Total operation hours (h)	Total heat extraction (kWh/m)	Average heat transfer rate (W/m)
6	1278	93.88	73.46
12	2556	126.31	49.42
18	3834	143.23	37.36
24	5112	154.36	30.20

5.3.2 Intermittent 12 h operation with different loop pitch

Table 5.5 Boundary condition of CFD simulation.

Installation depth	1.2 m
Soil type	Loamy soil

Operation mode	Intermittent 12 h operation
The initial soil temperature	Varying temperature with the depth
Pipe temperature	1℃
Topsoil boundary condition	Monthly changed air temperature and wind speed
Climate data	Coventry
Loop pitch	0.25 m, 0.5 m, 1.0 m, and 2.0 m

To study the influence of slinky-loop pitch, a total of four different loop pitches were investigated for the purpose of this study. The loop pitches included spacings of 0.25 m, 0.5 m, 1.0 m, and 2.0 m. These four cases were surrounded by loamy soil and had the same initial varying temperature profile, as shown in Table 5.5. The performance of these slinky-loop ground heat exchanger were evaluated under intermittent heating operation (12 hours on and 12 hours off) without considering multiple trench loop thermal interactions for a seven-month heating season.

The variation of the monthly heat extraction per meter length of the soil occupied by slinky-loop ground heat exchangers at different loop pitches are shown in Fig. 5.11. The first thing to be observed from the figures is that the variation of monthly heat extraction amount presents a similar pattern. Each of the four cases started off with a relatively high amount of heat extraction. For instance, the heat extraction amount of September for the slinky-loop ground heat exchanger with a 0.25 m loop pitch was 49.77 kWh/m, 45.42 kWh/m for 0.5 m, 38.56 kWh/m for 1.0 m, and 31.42 kWh/m for 2.0 m. As the heating continued, the heat extraction reduced gradually. By the time the heating period reached February,

the heat extraction amount was nearly minimal: 10.10 kWh/m for the loop pitch of 0.25 m, 9.38 kWh/m for 0.5 m, 8.20 kWh/m for 1.0 m and 6.99 kWh/m for 2.0 m.

The monthly heat extraction amount in March for Case 1 was 8.31 kWh/m for a 2-m loop pitch; for Case 2 it was 9.77 kWh/m for a 1-m loop pitch; for Case 3 it was 11.26 kWh/m for a 1-m loop pitch; and for Case 4 it was 12.19 kWh/m for a 0.25-m loop pitch. It can be seen that the monthly heat extraction for Case 1 decreased by 67.11% from September to December, 68.45% for Case 2, 69.70% for Case 3, and 70.43% for Case 4. This is because that the heat exchanger with a shorter loop pitch will result in more thermal interference between the overlapping loop pipe in the same trench. The soil temperature will drop to a low value more quickly because of the heat loss in the soil. Thus, the reduction of heat transfer rate is more significant in a shorter loop pitch in the same period.

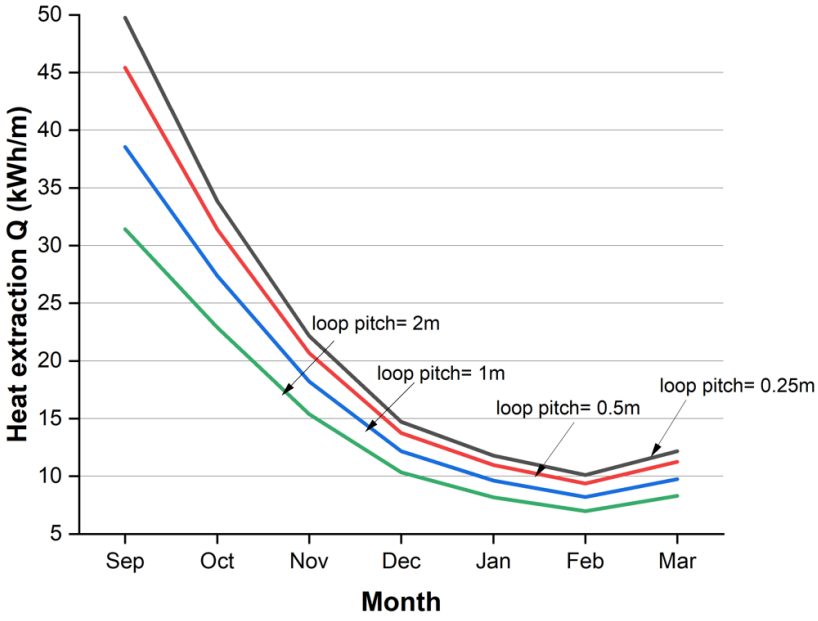


Figure 5.11 Variations in monthly heat extraction amount of slinky-loop ground heat exchangers (loop pitch= 0.25 m, loop pitch= 0.5 m, loop pitch= 1 m and loop pitch= 2 m).

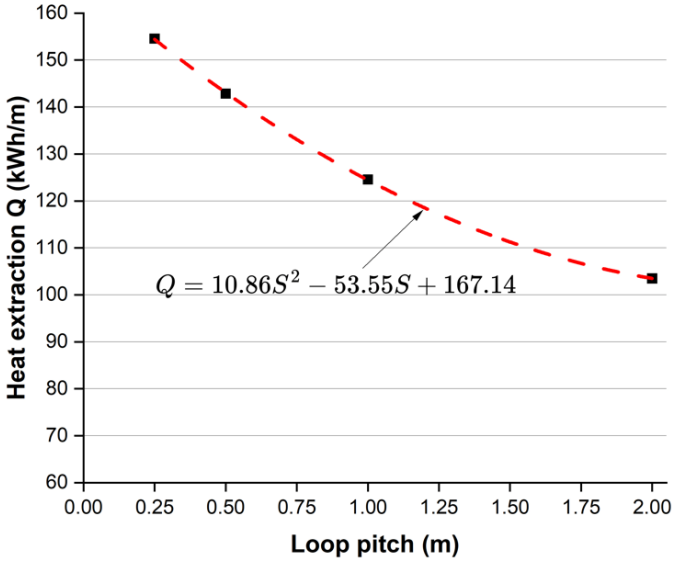


Figure 5.12 Regression line for total heat extraction amount of slinky-loop ground heat exchangers over seven months and varying loop pitch.

Fig. 5.12 shows a comparison between the thermal performance in terms of total heat extraction amount. It is obvious that the system with a loop pitch of 0.25 m had the highest heat extraction among these three configurations. As the loop pitch increased, the thermal performance of the slinky-loop ground heat exchanger with 0.5m loop pitch, 1.0m loop pitch, and 2.0m loop pitch was 7.6%, 19.4% and 33.0%, respectively, less than 0.25m loop pitch. It can be seen that a quadratic polynomial correlation can be obtained between the total heat extraction amount and loop pitch:

$$Q = 10.86S^2 - 53.55S + 167.14\ (R - Square = 0.9995) \quad (5.1)$$

Where Q is the heat extraction of the heating season without considering multiple trench loop thermal interactions (kWh/m) and S is the spacing of the loop pitch (m).

It can be seen from Fig. 5.12 that this quadratic polynomial correlation matches well with the simulated results. Hence, it could be used to accurately estimate

the thermal performance of other various loop pitches under intermittent 12-hour operation mode.

It can be concluded that a smaller loop pitch increases the contact surface to the surrounding soil in the same length trench, which would provide better thermal performance, and require less excavation work to install the system compared to the larger loop pitch configurations. However, if the loop pitch is less than the loop diameter of 1 m, this configuration would cause more significant thermal interference when considering the adjacent parallel slinky-loop ground heat exchanger pipe, especially in a shorter spacing distance between adjacent trenches. The soil temperature near the heat exchanger will drop to a low constant value in a short period of time and have a negative effect on the thermal performance of the ground heat pump system.

Although, the results indicate that a smaller loop pitch would provide a better thermal performance compared to the larger loop pitch configurations. As the slinky-loop ground heat exchangers with loop pitches less than 1 m are constructed by overlapping the pipework, the amount of pipes will lead to a significant increase in the initial material cost. Hence, the loop pitch of 1 m is suggested for a good balance between a high heat transfer rate and low potential thermal interference between adjacent trenches.

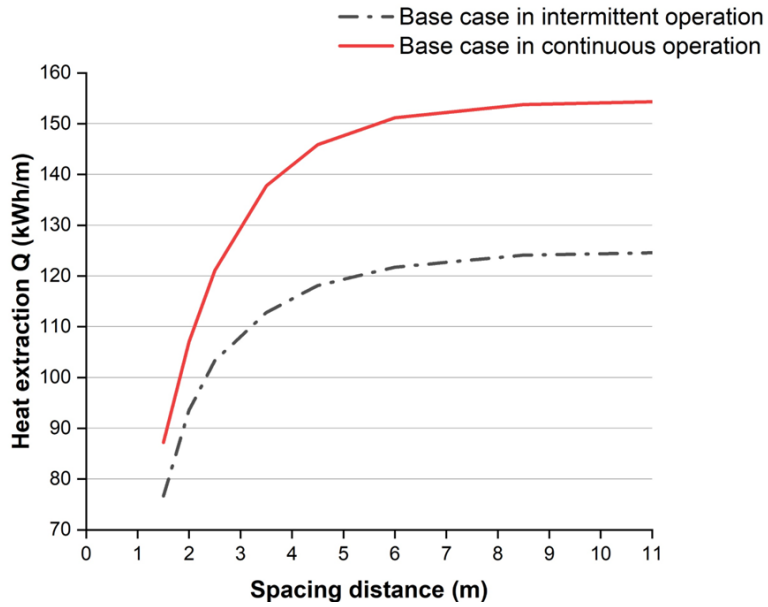
5.3.3 The effect of intermittent operation on the interference of different slinky-loop ground heat exchangers

Table 5.6 Boundary condition of CFD simulation.

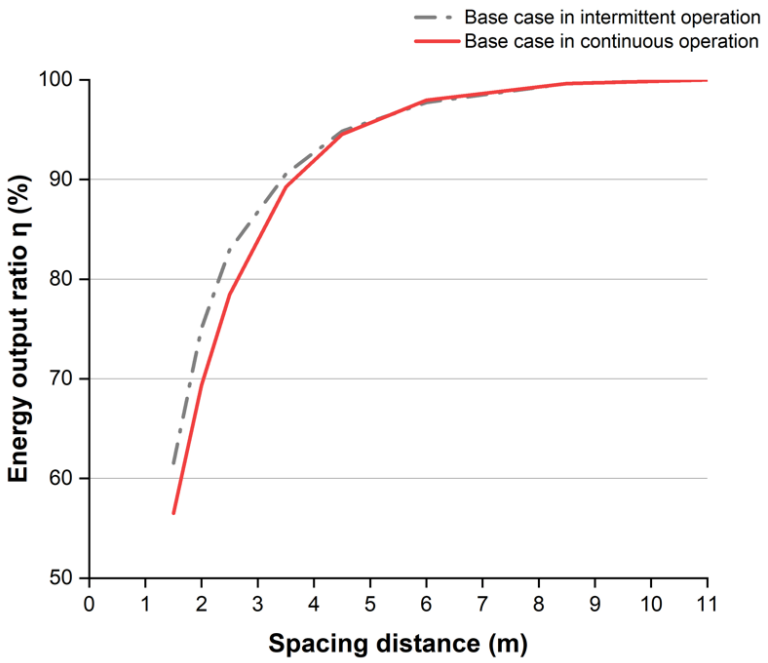
Installation depth	1.2 m
Soil type	Loamy soil

Operation mode	Intermittent 12 h operation Continuous operation
The initial soil temperature	Varying temperature with the depth
Pipe temperature	1℃
Topsoil boundary condition	Monthly changed air temperature and wind speed
Climate data	Coventry
Loop pitch	1.0 m

Table 5.6 shows the boundary condition for the simulations. One is continuous running for the entire heating season, while the other is intermittent operation with 12-hour-on (heating operation) and 12-hour-off (heat recovering). Fig. 5.13 shows the heat extraction under different space distances for two operation modes. It can be observed that for continuous operation, heat transfer increased with spacing distance by 43%, from 87 kWh/m at 1.5m distance to 154 kWh/m at 11m distance but for intermittent operation, the increase was about 38% (from 76 kWh/m to 124 kWh/m). It also shows that total heat extraction in the intermittent operation mode was lower because of the shorter total operating time than that for continuous operation for a seven months heating season. Although the heat transfer time of continuous mode was twice than that of intermittent mode, the difference of heat extraction amount between the two modes was less than 25%. This is because heat extraction amount is limited by the thermal capacity of the surrounding soil.



(a)



(b)

Figure 5.13 Variations in heat extraction by slinky-loop ground heat exchangers (in continuous and intermittent operation).

As discussed earlier, heat transfer between adjacent parallel pipes interfered with each other, resulting in a reduction in overall thermal performance. As

demonstrated in Fig. 5.13(b), the performance of the slinky-loop ground heat exchanger is highly affected by the separation distance under 4m. As the distance increased, the energy output increased to 95%, 98%, and 99% of full capacity (single loop without thermal interference) when the distance between GHE loops was 4.5m, 6m, and 8.5m, respectively.

It also indicates that energy output ratio with continuous operation increased by 38% from a spacing distance of 1.5m to 4.5m, while the increase with the intermittent operation mode was 33%. This is because the thermal interference for a short distance in continuous operation would be greater than that in intermittent operation as results of heat depletion in the ground with operating time. The off period in the intermittent operation reduced the impact caused by heat depletion. It would enable the ground to partially recover its thermal condition before the next cycle begins, improving thermal performance for the subsequent heating cycle. When the separation distance between trenches was larger than 4.5m, the two operation modes would have almost the same trend in the correlation between spacing distance and energy output.

For intermittent operation, when the separation distance is not more than 5 m, a simplified quadratic equation can be obtained between energy output ratio and spacing distance:

$$\eta = -3.61L^2 + 32.49L + 22.73 \; (R - Square = 0.9841) \qquad (5.2)$$

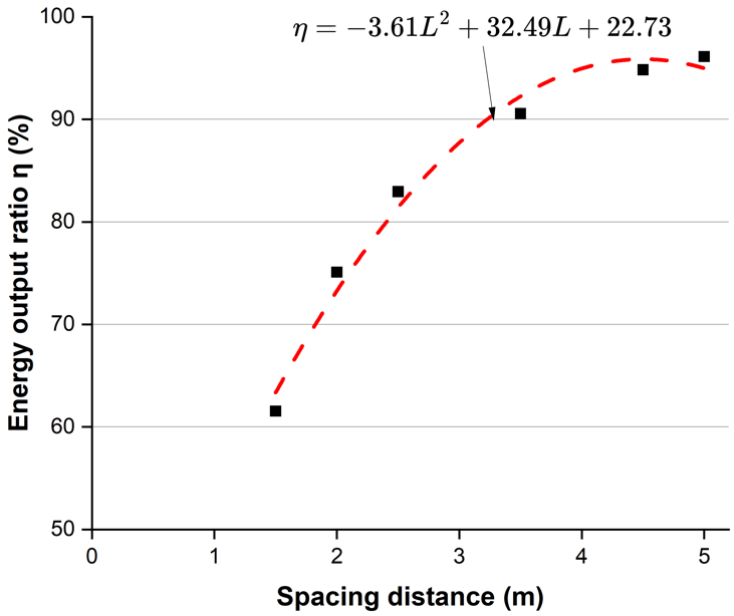


Figure 5.14 The regression line with quadratic polynomial under intermittent 12-h operation mode.

As shown in Fig. 5.14, the quadratic polynomial regression lines fit the variation of energy output ratio for different spacing distances in intermittent operation. It is found that the quadratic equation can be used to further simplify the prediction about the influence of different spacing distances between adjacent trenches under intermittent operation mode.

5.3.4 Ground thermal recovery within one-year operation

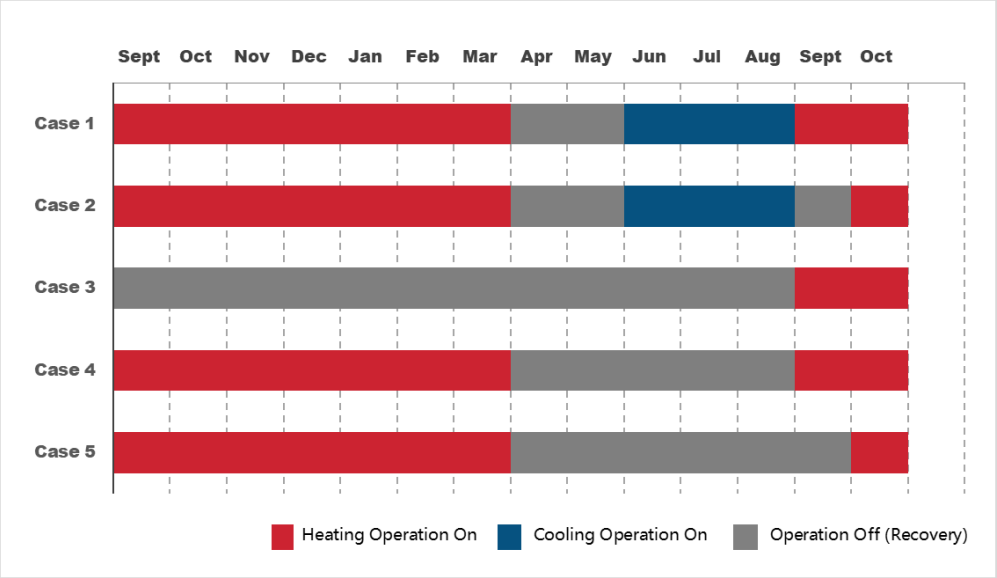


Figure 5.15 Annual operation method according to base case condition.

The heating-season operation of the ground heat exchanger affects long-term temperature changes in the ground, causing the average ground temperature to gradually rise or fall over time to such an extent. One advantage of the slinky-loop ground heat exchanger over the vertical borehole heat exchanger is that the heat in soil extracted during heating seasons could be recharged naturally with solar and ambient heat during the warm seasons.

Table 5.7 Boundary condition of CFD simulation.

Installation depth	1.2 m
Soil type	Loamy soil
Operation mode	Intermittent 12 h operation
The initial soil temperature	Varying temperature with the depth
Pipe temperature	1℃

Topsoil boundary condition	Monthly changed air temperature and wind speed
Climate data	Coventry
Loop pitch	1.0 m

In this section, the base case with a loop pitch of 1m installed in 1.2m depth in loamy soil operating in different operation modes during the whole year was analyzed. Table 5.7 presents the boundary conditions. The operation modes were applied from September of the first year to october of the second year, including a thirteen months period. For achieving combined heating and cooling in winter and summer, this proposed system has five main operational modes corresponding to different seasons, as shown in Fig. 5.15. Case 1 is the operation for the HGSHP system under double-season conditions, with the heat extraction period of 7 months, the first recovery period of 2 months, the heat injection period of 3 months. Case 2 is the operation for HGSHP system under double-season conditions, with the heat extraction period of 7 months, the first recovery period of 2 months, the heat injection period of 3 months, and the second recovery period of 1 month. Case 3 is the operation for HGSHP system under single-season conditions for the first year operation. Case 4 is the operation for HGSHP system under single-season conditions, with the heat extraction period of 7 months and the natural recovery of 5 months. Case 5 is the operation for HGSHP system under single-season conditions, with the heat extraction period of 7 months and the natural recovery of 6 months. The pipe temperature was fixed at 1 °C for operation in heating mode and 30°C for operation in cooling mode [85]. The GHE loops were operated in intermittent operation for 12 hours

per day in heating mode during the winter and cooling mode during the summer.

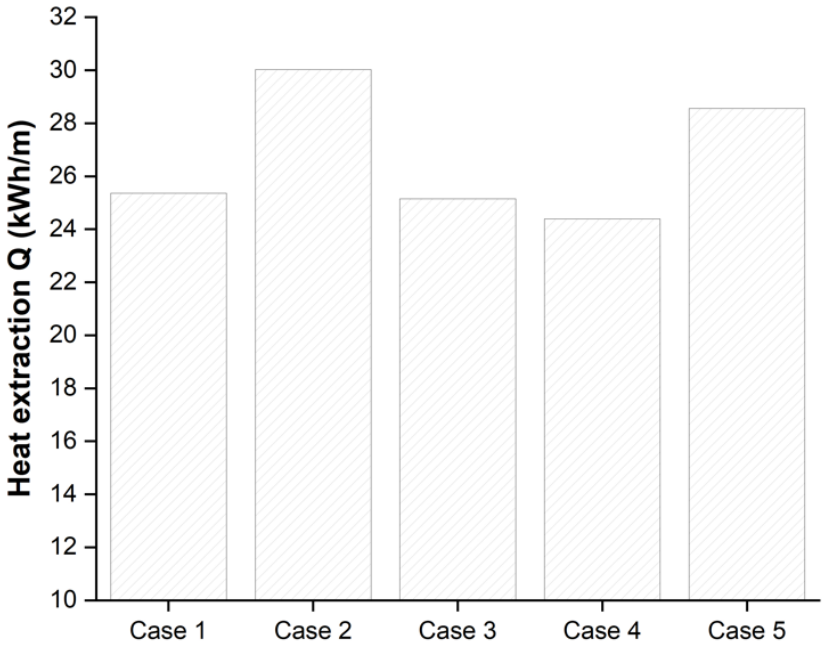


Figure 5.16 Comparision in heat extraction of the Ocotober in the second year for different operation mode.

It can be seen from Fig. 5.16 that Case 2 had the highest heat extraction among these three configurations. The thermal performance of the slinky-loop heat exchanger for Case 1, Case 3, Case 4 and Case 5 was 84.47%, 83.77%, 81.22%, and 95.12%, respectively, compared to Case 2. Case 4, and Case 5 are the heating operations under single-season conditions; the heat extraction amount in October is 24.38 kWh/m for Case 4, and 28.56 kWh/m for Case 5, respectively. After the heating operation in the first year, the natural recovery time is 5 months for Case 4 and 6 months for Case 5. From the perspective of long-term operation, under the single heating condition, due to the Case 5 takes no heat from the soil in September, the soil heat balance can be basically maintained by the soil recovery ability in the non-heating months. The results indicate that the thermal performance of the slinky-loop ground heat exchanger is also influenced by the

start date of operation. The heat extraction rate for operation with a later start date is lower due to the fact that decreasing soil temperature with increasing time during the heating season, but the heat extraction amount is higher at the same heating time because of depletion of heat from the soil during the preceding period.

Without the first year heat extraction from soil, the heat extraction amount in October for Case 3 is 25.15 kWh, which is slightly more than the value of Case 4. This indicates that 5-month natural recovery time after seven-month heat extraction will not be able to fully recover to the same soil thermal condition as non-heating operation. This will result in a minor reduction in the heat extraction capacity of HGHE over the following year, as well as a weakening of the thermal influence on the surrounding soil. This phenomena will progressively lessen over a longer recovery time, and finally appear to be relatively balanced. For double season operation, the heat extraction amount of Case 2 in October is 30.02 kWh/m. The heat extraction amount for Case 1 is 25.36 kWh/m, which is 0.8% more than the heat extraction of Case 3. This is because Case 1 and Case 2 are under cooling operation mode from June to August, and the heat exchangers discharge heat to the surrounding soil in the summer, which further increases the soil temperature and solve the problem of soil heat imbalance. In addition, under the double cooling and heating conditions, the thermal balance of soil can ensure its long-term stable operation. However, considering the system cooling operation time, the thermal recovery characteristics of the soil will have an important impact on the system operating stability.

The comparison of soil temperature in October at the center of heat exchanger between the double cooling and heating conditions and the single heating

condition is shown in Fig. 5.17. There are significant differences in the soil temperature from 1.2 m depth to 5 m depth between Case 1 and Case 4. The maximum temperature difference is 0.39℃ at 3.2 m depth below the top soil surface. And the soil temperature difference between Case 2 and Case 5 at 3.2 m below the soil surface was approximately 0.48°C. It can be attributed to this factor that the soil temperature after the cooling operation becomes higher compared to the single-season operating mode, resulting in the observed difference between Case 1 and Case 4 as well as Case 2 and Case 5. The soil temperature is higher for operations with a later start date. For example, the soil temperature at a depth of 3.1 m for Case 1 is 9.8°C and 10.5°C for Case 2. At the same depth, the soil temperature of Case 5 is 0.55°C higher than that of Case 4. This is due to the fact that the heat from the surrounding soil have already been extracted a lot by the heat exchanger during the preceding month of operation. It is also found that the soil temperature of Case 5 is higher than that of Case 1 with a maximua difference of 0.17°C at a depth of 2.8 m. This indicates that the effect of the first month operation is more significant than the summer operation.

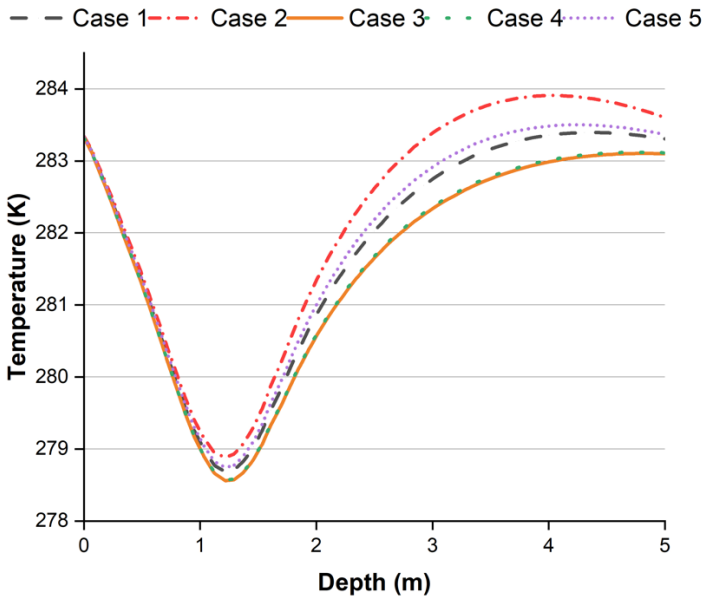
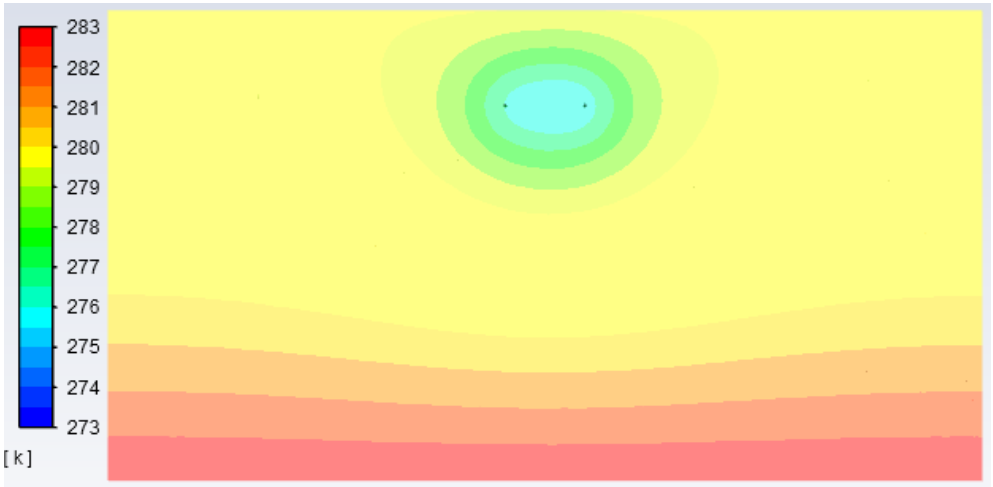


Figure 5.17 Variations in ground temperature at the end of October (the second year) at the center of heat exchanger for different operation mode (top soil surface temperature = 10.6℃).

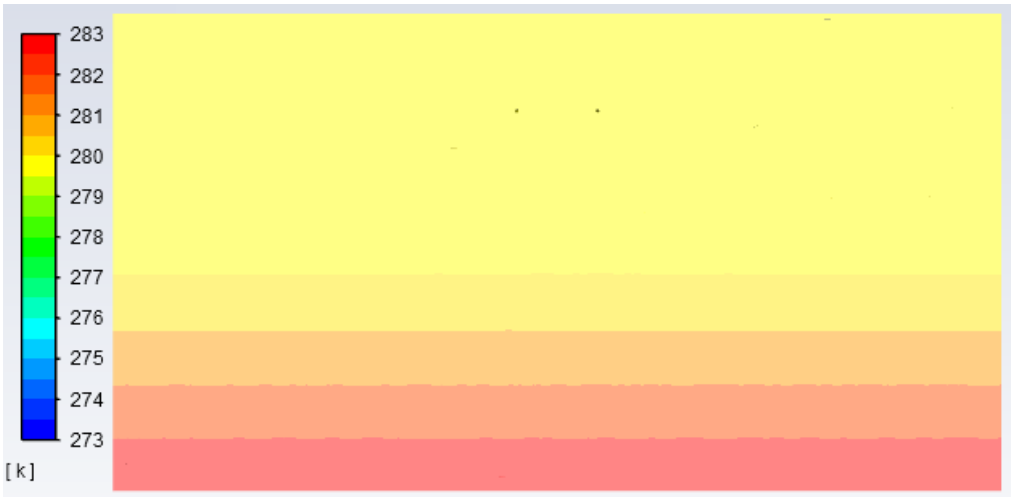
Fig. 5.18-20 show that after a 7-month intermittent 12-h operation between September and March, the temperature of the soil near the pipe surface (pipe temperature) increases with time during the following recovery period when the system is switched off. At the end of March, the heat exchanger was surrounded by a low temperature region within 4℃, and the soil temperature in the same position without first year operation was uniform and around 7 ℃, as shown in Figs. 5.18(a) and (b). It can be seen from Fig. 5.19(a) that the temperature of soil near the slinky-loop ground heat exchanger pipe increased rapidly after the first recovery month. It closely follows the temperature variation of undisturbed soil, as shown in Fig. 5.19(b). This is beacause that the soil in the shallow depth was heated by the ambient air temperature of April. As illustrated in Figs. 5.20(a) and (b), the difference of soil temperature distribution decreases further at the end of

the second month (May). The pipe temperature can be recovered to around 10℃, which is close to the soil temperature in the same position without first year operation.

To further investigate the recovery process of soil temperature after the 7-month intermittent heating operation, Fig. 5.21 illustrates the vertical soil temperature distribution at the centre of the slinky loop from the ground surface to 5 m below the surface, comparing the soil temperature in the same position without the first year operation. At the end of April, there are significant differences in the soil temperature from 1.2 m depth to 5 m depth between the two simulation results. The maximum temperature variation is 0.54℃ at 2.6 m depth below the top soil surface. And the soil temperature difference between heating operation and without heating operation at 1.2 m below the soil surface was approximately 0.35°C. It can be observed that this difference in the soil temperature decreased from 0.13°C to 0.06°C (at 1.2 m depth) , 0.22°C to 0.11°C (at 2.6 m depth), for May and June. By the end of July, these two predicted soil temperature lines exhibit a high degree of overlap.

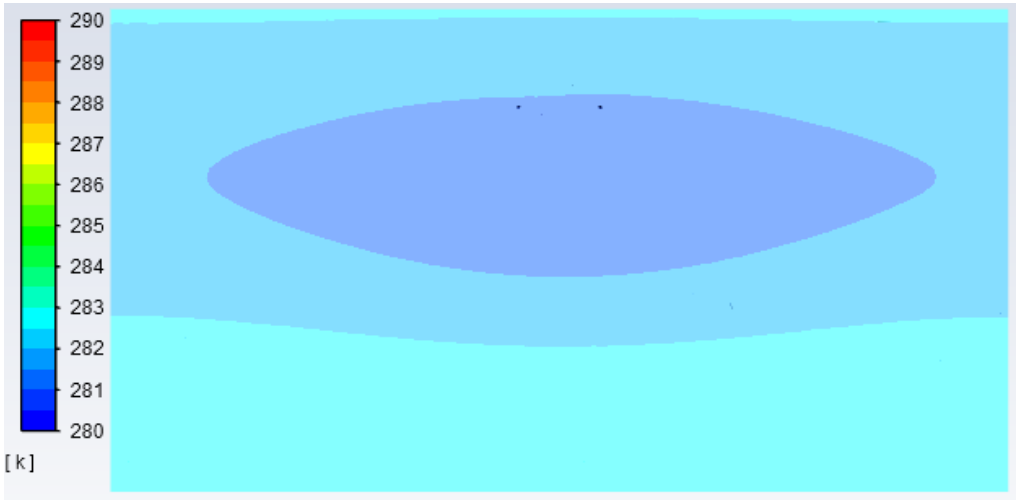


(a) Soil temperature after heating operation

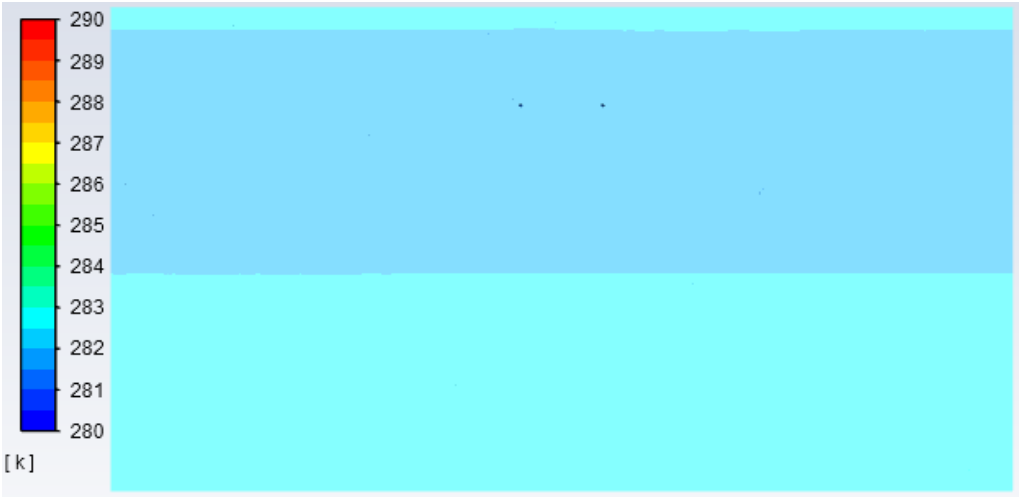


(b) Soil temperature without heating operation

Figure 5.18 Isotherm generated for the effect of heating operation at the end of March in vertical section view.

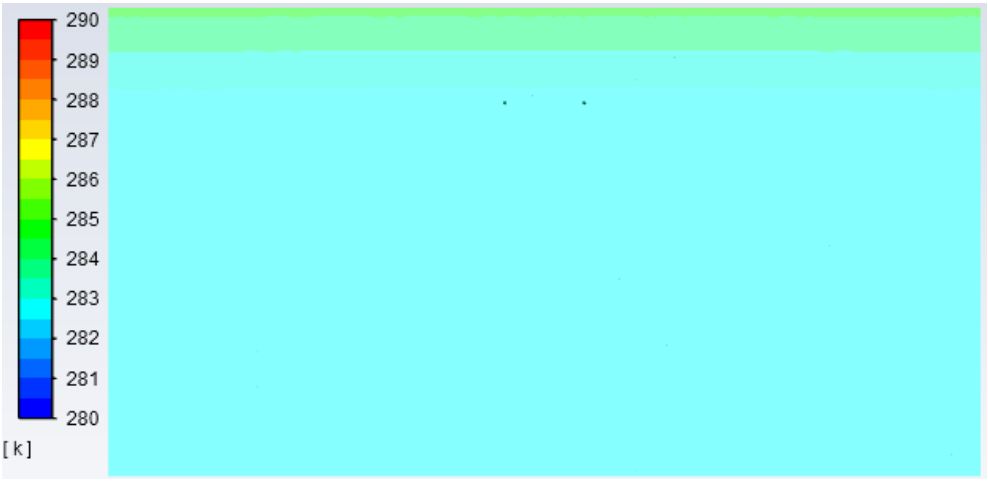


(a) Soil temperature after heating operation

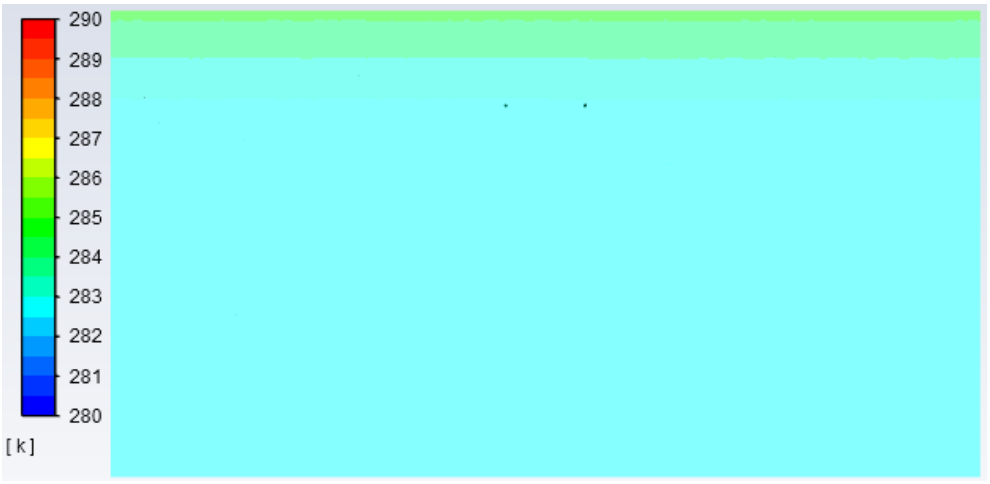


(b) Soil temperature without heating operation

Figure 5.19 Isotherm generated for the effect of heating operation at the end of first recovery month (April) in vertical section view.



(a) Soil temperature after heating operation



(b) Soil temperature without heating operation

Figure 5.20 Isotherm generated for the effect of heating operation at the end of second recovery month (May) in vertical section view.

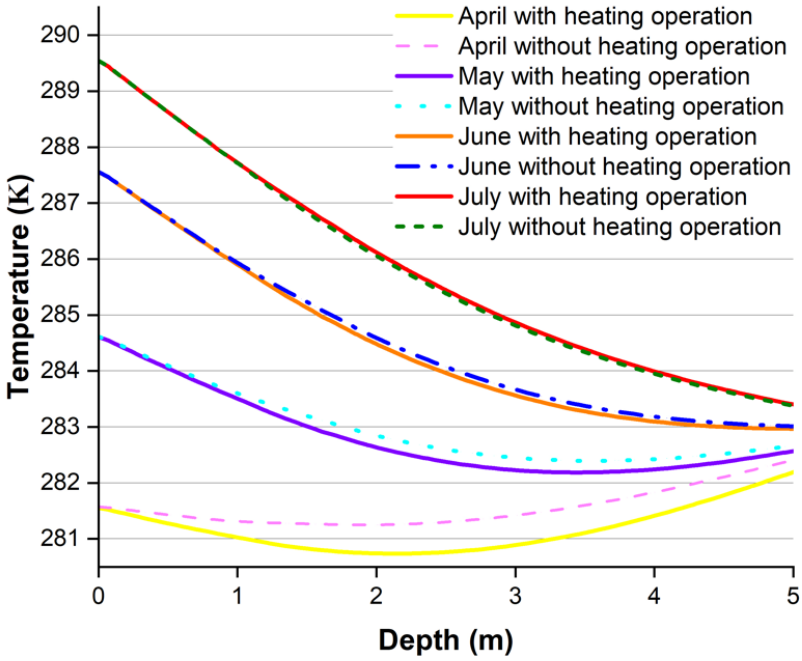


Figure 5.21 Effect of heating operation on the predicted variation of soil temperature from April to July in recovery peroid.

In order to study the temperature variations of soil with different operation

modes, the soil (i.e., at the center of the heat exchanger loop, buried depth ranging from 0 m to 5 m) temperature was obtained. The comparison of soil temperature at the end of August (the initial soil condition of the second heating season) in the center of heat exchanger between the double cooling and heating condition and the single heating condition is shown in Fig. 5.22. It can be observed that the soil temperature was raised a lot after a three-month cooling operation, and the heat was concentrated around the heat exchanger. The soil temperature with summer operation increased from 16.7℃ at top surface to 23.1℃ at a depth of 1.2m and then reduced to 11.5℃ at a depth of 5m. The difference of soil temperature between Case 3 and the cooling operation is 8.5℃ at a depth of 1.2m. This is because that the temperature of working fluid is 30℃, which was not only beneficial for the soil thermal recovery, but also siginificantly enhanced the soil temperature within 5 m depth. The soil temperature of single heating season and Case 3 are slightly higher than the initial soil temperature in the first heating season. This is because that the initial soil temperature is obtained from empirical Eq. (3.6) which was calculated by the annual data of ambient temperature. The soil temperature of Case 3 and the single season operation mode is almost the same. This means that the five months thermal recovey can nearly mitigate the impact of the first year heat extraction. The off-time period alleviated heat loss in the ground around the heat exchanger and contributed to recovering the heat exchange rate. Therefore, the thermal performance of the second year operation is almost the same as the first year.

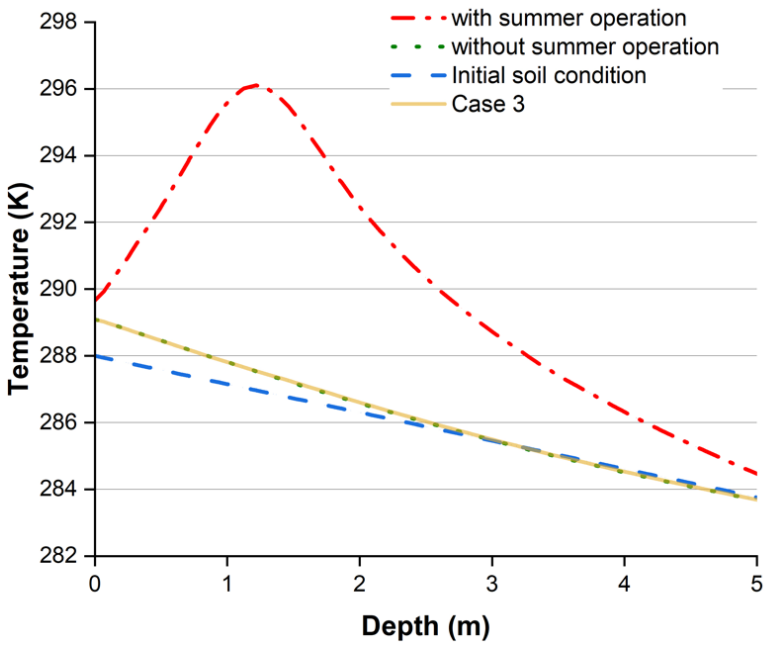


Figure 5.22 Variations in ground temperature at the end of August at the center of heat exchanger for different operation mode.

5.4 Conclusions

This chapter proposes the intermittent operation method that considers the recovery of soil temperature as an alternative to minimize the soil thermal imbalance caused by the slinky-loop ground heat exchanger system. The effects of the intermittent operation method on the slinky-loop ground heat exchanger system performance, loop pitch, and annual operation mode were analysed using a numerical model.

The discontinuous operation was operated intermittently, 18 h operation, 12 h operation and 6 h operation a day, which allowed the soil to recover its temperatures after the system was off, and for continuous operation, where heat was continuously extracted from the surrounding soil during the heating period until the soil temperature reached steady. Although continuous operation has a

higher total heat extraction amount, the intermittent operation method showed a higher average heat transfer rate of the slinky-loop ground heat exchanger than the continuous operation method. The daily average heat transfer rate increases with the decrease in daily switch-on operation time. According to the building heating demand in a real-life situation, intermittent operation is suggested for better heat transfer performance.

The results of the simulation indicate that reducing loop pitch of the slinky-loop heat exchanger would increase the contact surface to the surrounding soil in the same length of trench, which would improve the overall thermal performance, and require less excavation work to install the system compared to the larger loop pitch configurations. When the loop pitch was reduced to a quarter of the loop diameter, this would increase 24% in total heat extraction compared to a loop pitch of 1m. The obtained quadratic polynomial correlation could be used to predict the thermal performance of other various loop pitches under intermittent 12-h operation mode.

The results also revealed that intermittent 12-h operation would reduce the effect of heat depletion and thermal interference from adjacent parallel pipes.

Heat extraction of slinky-loop ground heat exchanger can be transferred from topsoil surface boundary conditions, such as warm air temperature during the recovery period, and thus the reduction of soil temperature near the GHE due to seven-month heating operation can be relieved. The soil temperature near the slinky-loop ground heat exchanger can be fully recovered in July. Among the five annual operations, the thermal performance for the next heating season is the best when the cooling operation is added, and heating operation starts later from October. This operation mode results in the highest heat extraction amount

in October.

Chapter 6: Analysis of heat demands-varying on-off period operation and installation sites for slinky-loop ground heat exchanger models

6.1 Introduction

Numerous research have performed numerical model to predict the short-term thermal performance of GHE. This is helpful for obtaining optimal design and economic feasibility before GSHP system installation. There is still a lack of precision in predicting the thermal performance of slinky-loop ground heat exchanger considering heating degree day (HDD) for the whole heating season. Heating degree day (HDD) is a commonly used as temperature index for the requirement of energy for space heating in order to maintain comfortable indoor temperatures [131]. There are several ways to determine the HDD: from long-term hourly temperature records, mean daily temperatures, daily maximum and minimum temperatures, to mean monthly temperatures and their standard deviations [132].

This work presents a novel intermittent operating strategy that takes into account the degree-day method as a potential solution for accurately predicting the daily operation hours and studying the effects of the intermittent operation method in real-life situation. The daily operating time for the simulations depends on the heating degree-day hours of a given city. The effect of installation sites has been analysed based on the intermittent 12 h operation mode.

6.2 Description of heating hours

6.2.1 Heating degree day heating hours

The heating degree day base temperature ought to correspond to the outdoor temperature in such a way that, for a given indoor air temperature, the outside heat transfer resulting from conduction through the building envelope and exchange of indoor and outdoor air (via leakage and controlled ventilation) precisely offsets the internal heat gains caused by solar heat gain (primarily radiation entering the building through windows) and people, lighting, and equipment. In such circumstances, the specified internal air temperature will be maintained in without the use of heating system, meaning the consumption of zero energy for heating. The heating system would be required to operate only when the outdoor temperature decreases below the base temperature. This base temperature is variable and may be defined according to the standards that are applicable in different countries, and the UK Carbon Trust recommends 15.5 °C; this means that any temperature below this will require heating [133].

To compare the demands-varying on-off based operation on the heating degree day method and the intermittent operation of 12-hour-on (heating), the total operation time is 2556 hours for both of them. Table 6.1 shows the daily operation hours calculation through the heating degree day method. The monthly operation time is determined based on the percentage of heating degree day from September to March. Thus, the daily average operation hours can be obtained. However, the time step size was set to be one hour; the daily operation hours need to be rounded off. It should be noted that total operation hours should still be 2556 hours. From September 1st to September 17th, the daily operation hour

is set as 3 hours while the rest of September is 4 hours.

Table 6.1 Daily operation hours calculation through heating degree day method.

Month	Days	HDD	HDD % for Sept-Mar	hr, 50% on (2556 hours)	hr/day	hr/day
Sep	30	82.7	4.74	121.14	4.04	3 or 4
Oct	31	165.3	9.47	242.14	7.81	8
Nov	30	214.6	12.30	314.35	10.48	10
Dec	31	328.6	18.83	481.35	15.53	16
Jan	31	387.4	22.20	567.48	18.31	18
Feb	28	297.4	17.04	435.64	15.56	16
Mar	31	268.9	15.41	393.90	12.71	13

Table 6.2 Predicted daily and monthly operation hours through heating degree day method.

Month	Sept	Oct	Nov	Dec	Jan	Feb	Mar	Total
Daily operation hours	3/4	8	10	16	18	16	13	
Monthly operation hours	103	248	300	496	558	464	403	2556

6.2.2 Domestic house heating hours

Domestic house heating energy use was based on gas consumption data from the energy company, including cooking and hot water as well as central heating. To compare the demands-varying on-off operation based on a domestic house energy consumption, and the intermittent operation based on the heating degree day method, the total operation time of the heating season is 2556 hours for both of them. Table 6.3 displays the calculation of daily operation through the real heating energy use. The monthly operation time is determined based on the percentage of energy consumption from September to March. Therefore, the daily average operation hours can be obtained. However, the time step size was set to be one hour; the daily operation hours need to be rounded off. To achieve total operation hours of 2556 hours, from the 1st to 17th of December, the daily operation hour is set as 17 hours, while rest of the 14 days of December is 18 hours.

Table 6.3 Daily operation hours calculation through energy consumption.

Month	Days	Energy (kWh)	Energy % for Sept-Mar	hr, 50% on (2556 hours)	hr/day	hr/day
Sep	30	358.4	1.98	50.72	1.69	2
Oct	31	1550.4	8.59	219.44	7.08	7
Nov	30	2632.6	14.58	372.62	12.42	12
Dec	31	3799.6	21.04	537.79	17.35	17/18
Jan	31	3927.9	21.75	555.94	17.93	18
Feb	28	3153.9	17.46	446.39	15.94	16
Mar	31	2636.1	14.60	373.10	12.04	12

Table 6.4 Predicted daily and monthly operation hours through energy consumption.

Month	Sept	Oct	Nov	Dec	Jan	Feb	Mar	Total
Daily operation hours	2	7	12	17/18	18	16	12	
Monthly operation hours	60	217	360	541	558	464	372	2556

6.2.3 Three typical meteorological condition

According to the climatic conditions of the UK, the cities of Edinburgh (North UK, latitude 55.953), Coventry (Midlands, latitude 52.412), and Reading (South UK, latitude 51.455) are studied for the investigation of local ambient air temperature, wind speed and soil properties. Busby [130] calculated soil thermal diffusivity values based on soil temperature data from 65 United Kingdom Meteorological Office weather stations. These are located throughout the UK, including different soil types, and occupying the depth range of a horizontal loop ground collector. Table 6.5 shows the soil properties of these three cities from Busby's published data.

Table 6.5 Soil properties from three locations.

Soil type	Location	Density (kg/m^3)	Specific heat	Thermal conductivity	Diffusivity ($10^{-6}m^2/$

			(kJ/kgK)	(W/mK)	$s)$
Clay	Edinburgh	1320	1.139	1.08	0.7175
Loamy	Coventry	1470	1.039	1.5	0.9842
Loamy and Clay	Reading	1520	1.014	1.34	0.8700

The monthly average temperature in three cities as shown in Table 6.6 were used in the simulation. The monthly average wind speed in three cities as shown in Table 6.7 were used in the simulation [127].

Table 6.6 Monthly average ambient temperature for three cities.

Temperature (℃)	Coventry	Edinburgh	Reading
September	13.83	12.1	14.6
October	10.63	9.1	11.4
November	7.33	5.8	7.5
December	4.75	3.6	5.2
January	4.5	3.3	4.6
February	4.67	3.4	4.7
March	6.13	4.7	6.4

Table 6.7 Monthly average wind speed for three cities.

Wind speed (m/s)	Coventry	Edinburgh	Reading
September	4.68	5.42	4.78

October	5.08	5.78	5.14
November	5.20	6.08	5.28
December	5.52	6.44	5.56
January	5.78	6.97	5.86
February	5.60	6.58	5.61
March	5.31	6.28	5.36

6.3 Results and Discussion

The effect of different daily operation hours and installation sites are discussed. The simulation results are presented as the amount of heat transfer per meter length of trench for a given period (in kWh/m).

6.3.1 Comparison for heating degree day heating hours and real house heating hours

Table 6.8 Boundary condition of CFD simulation.

Installation depth	1.2 m
Soil type	Loamy soil
Operation mode	Intermittent operation
The initial soil temperature	Varying temperature with the depth
Pipe temperature	1℃
Topsoil boundary condition	Monthly changed air temperature and wind speed
Climate data	Coventry
Loop pitch	1.0 m

In this chapter, a residential house heating operation was analyzed. Two daily operation hours were applied from the heating degree day calculation result and the real residential house energy bill during a seven month period. The total operation time is 2556 hours for both operation modes. As described previously, the same boundary conditions were applied with Coventry monthly average air temperature, wind speed, and local loamy soil properties. The results were obtained by assuming the initial varying soil temperature. The slinky-loop ground heat exchanger temperature was fixed at 1 °C with a loop diameter of 1 m and a loop pitch of 1 m buried at 1.2 m depth without considering the thermal interference from the adjacent trenches. Table 6.8 shows the boundary conditions. Table 6.9 summarizes the heat extraction amount, daily operation hours, and monthly operation hours. The monthly heat extraction proportion for both operation modes were compared, as shown in Fig. 6.1. It can be seen that the biggest difference between the two operation modes is in September. The heat extraction proportion of September is 14.5% for HDD operation and 10.7% for domestic house operation. The reason is that the heating degree day estimated 103 hours for heating demand, whereas the real domestic house operation only took 60 hours for heating. Since the heat transfer rate is very high at the first month, the difference between operation hours caused a siginificant difference in heat extraction amount compared to other months. The heat extraction amount in October based on the heating degree day method is 21.93 kWh/m and 21.38 kWh/m for domestic house operation mode. In November, the heat extraction for heating degree day mode decreased to 17.7 kWh/m and 19.78 kWh/m for domestic house operation mode. The performance of the slinky-loop ground heat exchanger descends gradually due to the heat loss in the surrounding

soil with operating time. The monthly heat extraction of both operarion modes is getting very close after December. This difference reduction can be explained by Fig. 6.2, which illustrates the vertical soil temperature distribution at the centre of the slinky loop from the ground surface to 5 m below the surface. At the end of September, the soil temperature varies significantly between the two operation modes at depths ranging from 1.2 to 5 m. And the soil temperature difference between heating degree day method and domestic house operation at 1.2 m below soil surface was approximately 1.19°C, which reduced to around 0.26°C and 0.09 °C at a distance of 3 m and 4m below soil surface in vertical direction, respectively. It can be observed that this difference in the soil temperature decreased from 0.32 °C to 0.30°C (at 1.2 m depth), 0.17°C to 0.03°C (at 3 m depth), at the end of October and November. By the end of December, these two predicted soil temperature lines are nearly overlapped. This means that the predicted daily operation hours from the two modes has a negligible impact on the soil temperature after three months of operation. It is noticed that the predicted total heat extraction amount for the heating degree day method is 110.42 kWh/m and 108.19 kWh/m for the domestic house operation mode. The difference between total heat extraction amounts is minimal. It indicates that the heating degree day method can be used to predict the real operation time and thermal performance of the slinky-loop ground heat exchanger system.

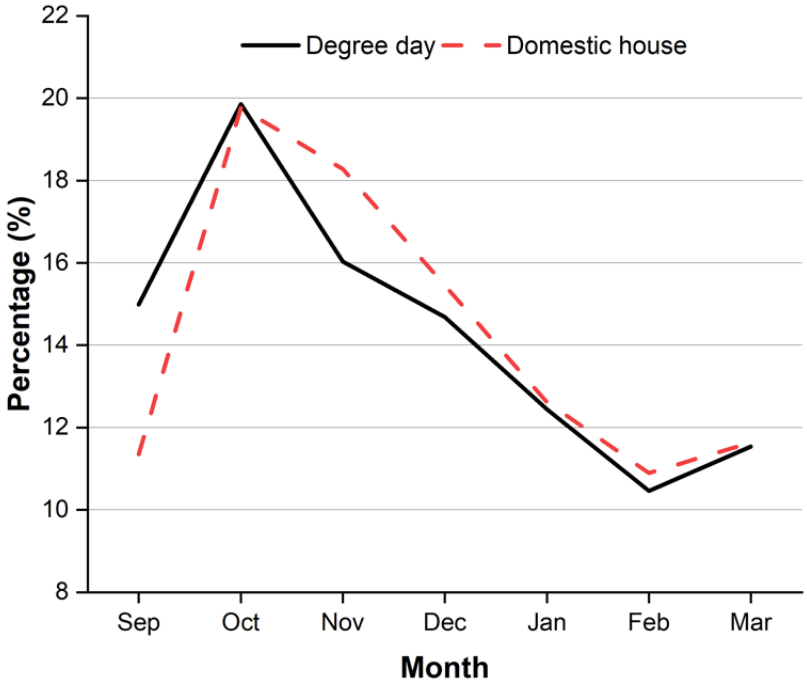


Figure 6.1 Monthly heat extraction proportion of the heating season based on heating degree day method and real house operation mode.

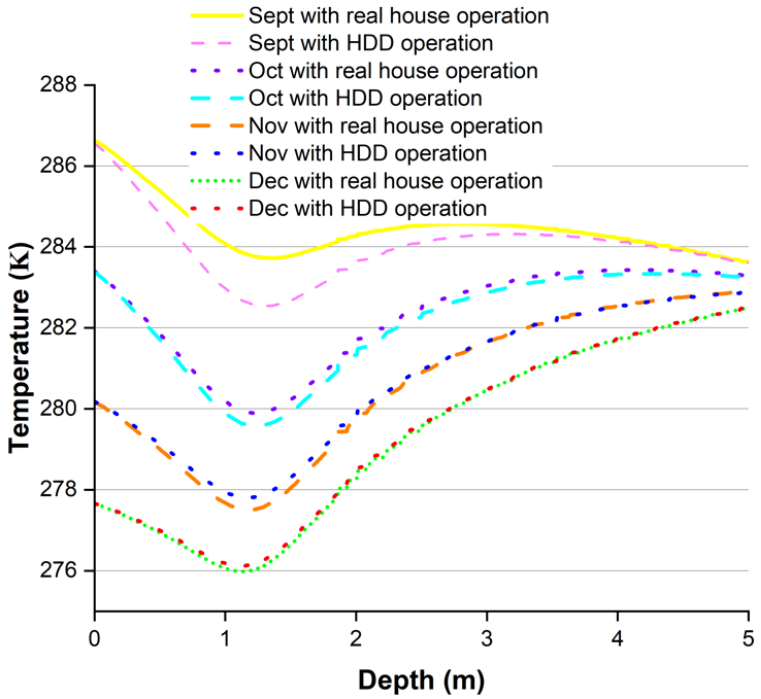


Figure 6.2 Effect of HDD and real house operation modes on the predicted variation of soil temperature at the end of first four months.

Table 6.9 Monthly heating time and heat extraction by two operation modes.

	Month	Sept	Oct	Nov	Dec	Jan	Feb	Mar	Total
Degree Day	Daily hours	3/4	8	10	16	18	16	13	
	Monthly hours	103	248	300	496	558	464	403	2556
	Heat extraction (kWh)	16.5	21.9	17.7	16.2	13.7	11.5	12.7	110.4
Domestic house	Daily hours	2	7	12	17/18	18	16	12	
	Monthly hours	60	217	360	541	558	464	372	2556
	Heat extraction (kWh)	12.3	21.4	19.8	16.7	13.6	11.8	12.6	108.2

6.3.2 Comparison for heating degree day operation and intermittent 12 h operation modes

Table 6.10 Boundary condition of CFD simulation.

Installation depth	1.2 m
Soil type	Loamy soil
Operation mode	Intermittent operation
The initial soil temperature	Varying temperature with the depth
Pipe temperature	1℃
Topsoil boundary condition	Monthly changed air temperature and wind speed
Climate data	Coventry
Loop pitch	1.0 m

As described previously, Case 1 has been created as demands-varying on-off

based operation on the heating degree day method, and Case 3 is the intermittent operation of 12-hour-on (heating). Case 2 has been performed to further investigate the effect of daily operation hours; the simulation from September to November is the same as heating degree day operation, and then switched to intermittent 12-hour-on operation mode from December. Fig. 6.3 shows the simulation results of heat transfer amount through the slinky-loop ground heat exchanger at the depth of 1.2m in loamy soil, with three different daily operation time for the base case. The boundary conditions are shown in Table 6.10.

The first thing to be observed from the figures is that the heat extraction amount from December to March presents a similar pattern. The biggest difference between heating degree day operation (Case 1) and intermittent 12 h operation (Case 3) is the first month. As shown in Table 6.11, the calculated heating degree day hours for September, for instance, were 3 or 4 heating hours per day instead of the constant value of 12-hour-on operation, and the resulting discrepancy in daily operation hours would have a significant impact on the heat transfer amount in the first heating months. The different heat extraction amount for the first month also have an impact on the soil temperature at the end of September. The difference decreased to 14.5% and 6% at the end of the second and third month, respectively, and became negligible at the end of the heating season. The total heat extraction amount of the intermittent 12-hour-on operation exhibits a difference of 12.6% when compared to the heating degree day operation in the same period with the same total operation hours. As shown in Table 6.12, the heat extraction from December to March for Case 2 is 14.77, 12.21, 10.85, and 12.81 kWh/m, respectively. And the heat extraction from December to March for Case 3 is 14.35, 12.11, 10.81, and 12.79 kWh/m, respectively, which are

almost the same as in Case 2. This suggests that the variation in daily operating hours during the initial three months has a minimal effect on heat extraction during the subsequent four months of operation.

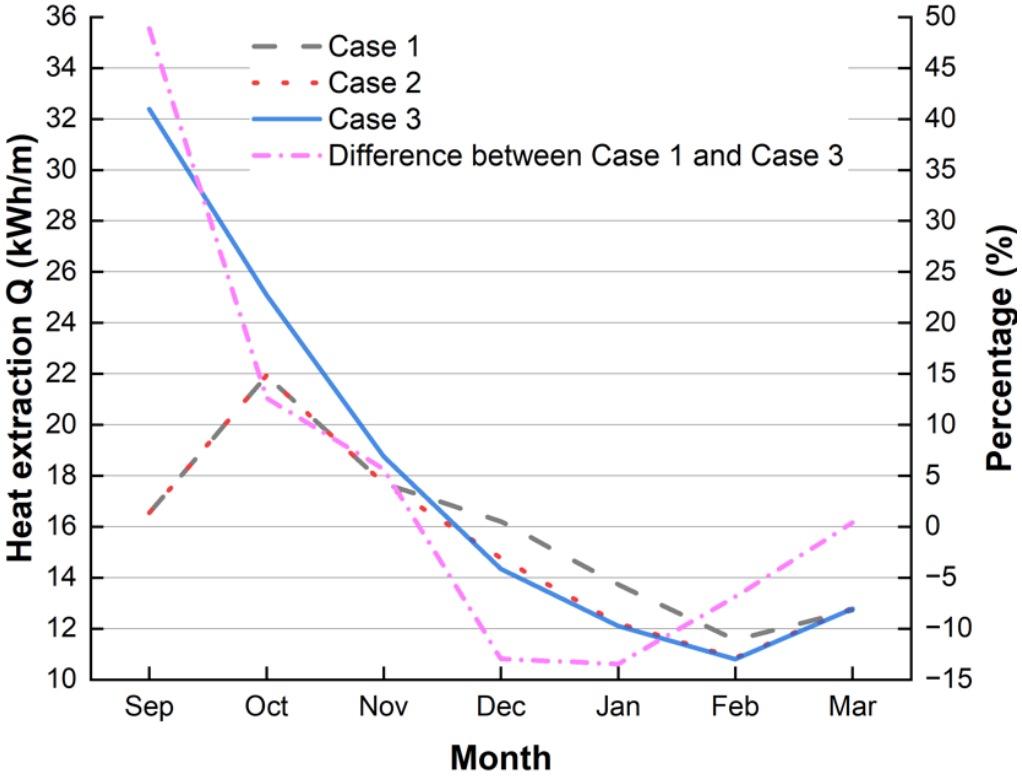


Figure 6.3 Monthly heat extraction in three operation modes.

Table 6.11 Daily heating time in three operation modes.

(hrs)	Sept	Oct	Nov	Dec	Jan	Feb	Mar	Total
Case 1	3/4	8	10	16	18	16	13	2556
Case 2	3/4	8	10	12	12	12	12	2115
Case 3	12	12	12	12	12	12	12	2556

Table 6.12 Monthly heat extraction in three operation modes.

(kWh/m)	Sept	Oct	Nov	Dec	Jan	Feb	Mar	Total

Case 1	16.55	21.93	17.70	16.21	13.74	11.55	12.74	110.4
Case 2	16.55	21.93	17.70	14.77	12.21	10.85	12.81	106.8
Case 3	32.39	25.10	18.76	14.35	12.11	10.81	12.79	126.3

6.3.3 Comparison for three locations

Table 6.13 Boundary condition of CFD simulation.

Installation depth	1.2 m
Soil type	Loamy soil
Operation mode	Intermittent 12 h operation
The initial soil temperature	Varying temperature with the depth
Pipe temperature	1℃
Topsoil boundary condition	Monthly changed air temperature and wind speed
Climate data	Edinburgh, Coventry, and Reading
Loop pitch	1.0 m

The external environment consists of a set of atmospheric conditions that interact with soil at the ground surface. The cities of Edinburgh, Coventry, and Reading are selected to assess the impact of the installation location external environment and the local soil properties. The boundary conditions are presented in Table 6.13. The system had been simulated with a pipe surface temperature of 1℃ for 12- hour-on (heating) and 12-hour-off (recovery period) operation, which allowed the soil to recover its temperatures after the system off. The heat exchanger is installed at 1.2 m depth without considering the thermal

interference from the adjacent trench. The loop diameter and loop pitch were 1m. The average monthly temperature and wind speed of these three cities are illustrated in Tables 6.6 and 6.7. The variation characteristic of the monthly average ambient temperature are similar for different cities. Fig. 6.4 shows the monthly total heat extraction per unit length of the trench for three installation locations using the same soil type with time is again similar for different external environmental conditions. It can be seen that in the first month of the heating season, the monthly heat extraction was 30.3 kWh/m for a slinky-loop ground heat exchanger installed at Edinburgh, 31.7 kWh/m for that at Coventry and 32.4 kWh/m at Reading. The relative high heat extraction is due to the relatively high and varying ground soil temperature around the heat exchanger in all situations. After three months of intermittent operation, the monthly heat exchanger extraction significantly decreases to 11.9 kWh/m for a slinky-loop ground heat exchanger installed in Edinburgh, 13.6 kWh/m for that in Coventry, and 14.3 kWh/m in Reading, due to the significant reduction in the surrounding soil temperature as well as the monthly ambient temperature. The stored heat in the surrounding soil has been extracted by the heat exchanger. In February, heat extraction decreased further to 8.7 kWh/m after running the slinky-loop ground heat exchanger system for 1836 hours at the ambient temperature of Edinburgh, around 10.1 and10.3 kWh/m at ambient temperature of Coventry, and Reading, respectively. It is found that there is no significant difference of the heat extraction when running the slinky-loop ground heat exchanger between 1836 hours and 2184 hours in Coventry and Reading, because the ambient air temperature of these two cities is getting close in January and February. However, the ambient air temperature gradually increases in March, which warms up the

top soil temperature. The monthly heat exchanger extraction increases to 10.4 kWh/m for a slinky-loop ground heat exchanger installed at Edinburgh, 12.1 kWh/m for that at Coventry, and 12.5 kWh/m at Reading.

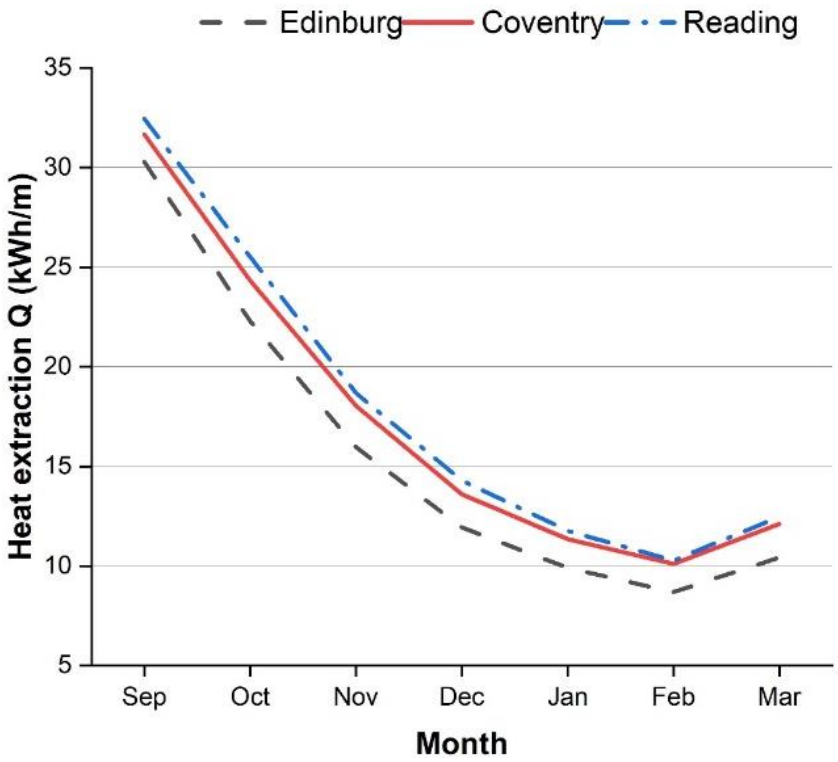


Figure 6.4 The monthly heat extraction per unit length of the trench for three installation locations using the same soil type (loamy).

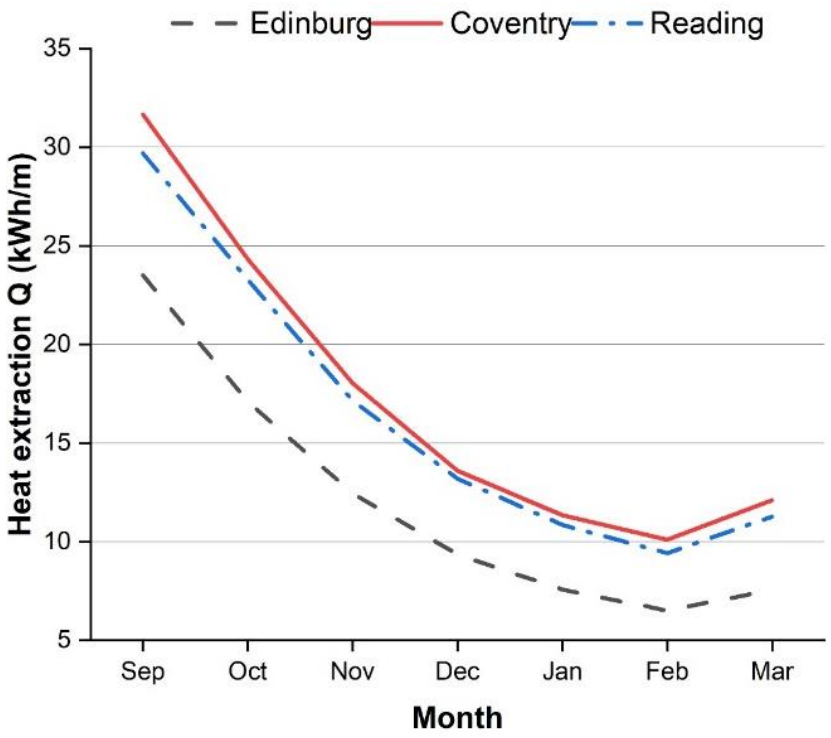


Figure 6.5 The monthly heat extraction per unit length of the trench for three installation locations using the local soil type.

The soil thermal properties are important parameters to take into account when designing a slinky-loop ground heat exchanger system. To investigate the real operation thermal performance of a ground heat exchanger in different areas, further simulation is performed using the corresponding soil types from Edinburgh, Coventry, and Reading. The soil thermal properties for three cities, as shown in Table 6.5, were used in the simulation based on the data recommended for the determination of thermal properties for horizontal ground collector loops [130]. Fig. 6.5 illustrates the predicted monthly total extraction per unit length of the trench for three installation locations using various local soil types. The soil thermal conductivity in Coventry is highest, and the soil in Edinburgh has the lowest thermal conductivity. At the first month operation, the monthly heat extraction was 23.5 kWh/m for a slinky-loop ground heat

exchanger installed at Edinburgh, 31.7 kWh/m for that at Coventry and 29.7 kWh/m at Reading. The slinky-loop ground heat exchanger installed in soil with a higher thermal conductivity had a higher heat transfer amount, despite the fact that the average monthly ambient temperature of Reading is higher than in Coventry. After intermittent operation running the slinky-loop ground heat exchanger for 5 months, the monthly heat extraction significantly decreases to 6.5 kWh/m for a slinky heat exchanger installed at Edinburgh, 10.1 kWh/m for that at Coventry and 9.4 kWh/m at Reading. It was evident from the figure that the most influencing parameter on the thermal performance is the thermal conductivity of the soil surrounding the slinky-loop ground heat exchanger considering three different local ambient air temperatures and wind speeds.

6.4 Conclusions

This chapter proposes the heat demands-varying on-off operation mode that considers the heating degree day method and real house monthly energy consumption as the basis to predict the different daily operation hours during the heating season. The monthly heat extraction amount was compared to the intermittent 12-h operation with the same total operation time of 2556 hours. The effects of the installation sites were analysed with the intermittent 12-h operation modes.

It was found that the predicted total heat extraction amount of the heating degree day method was observed to be close to the value of the real house operation mode. The discrepancy between the two modes of heat transfer amount is 2%. This demonstrates that the heating degree day prediction approach could be utilised to evaluate the thermal performance of a slinky-loop ground heat

exchanger system in a real-life situation.

After the first month of operation, the difference between the amount of heat extracted using the heating degree day method and the amount extracted using the intermittent 12-hour operation method is less than 15%. The operation mode with different daily operating hours during the initial three months has little effect on monthly heat extraction during the next four months.

The cities of Edinburgh, Coventry, and Reading are selected to assess the impact of the installation location external environment and the soil properties. Although the three typical cities have different local weather conditions, the soil type has a greater effect on thermal performance compared to the weather conditions in the UK.

Chapter 7: Design and application consideration of slinky-loop ground heat exchanger system for a building case

This chapter demonstrates the design considerations of the HGSHP system with slinky-loop ground heat exchanger, which include the building heating demand, estimated heat transfer rate, selection of heat pump, etc. In the final part of this chapter, the economic analysis, energy savings, and environmental savings are implemented.

7.1 Design consideration

Fig. 7.1 is a schematic figure illustrating the use of the proposed HGSHP system, which is buried 1.2 m below the ground surface. For indoor heating distribution system combined with the ground source heat pump unit, and the slinky-loop ground heat exchanger will be used to extract heat from the surrounding soil.

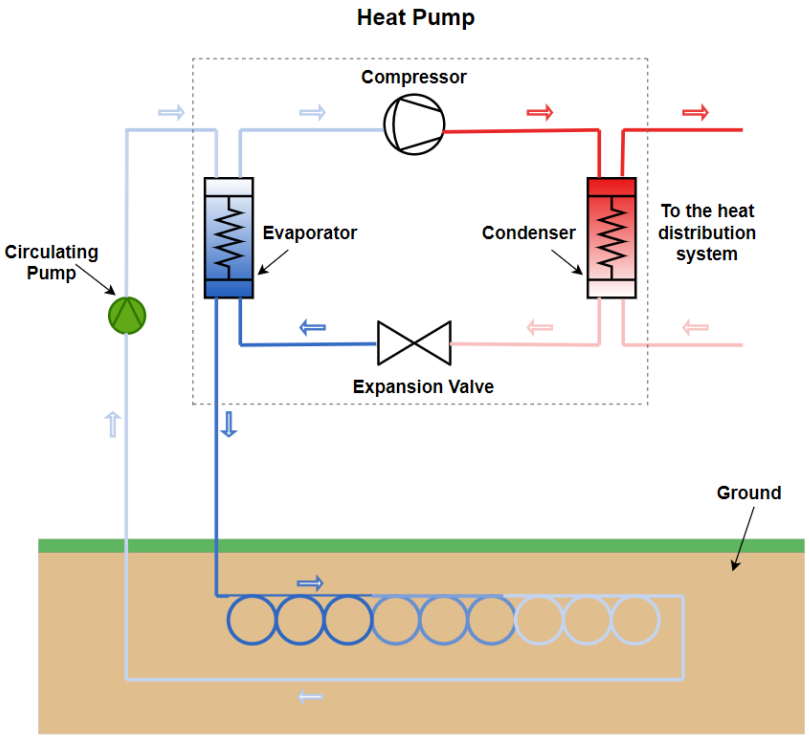


Figure 7.1 Proposed horizontal ground-source heat pump system.

Based on the results from the previous simulations, the following framework may be considered in the slinky-loop ground heat exchanger system:

The building heating load.

The space heating requirement is the most important parameter affecting the design and size of the slinky-loop ground heat exchanger system. While the heating demand of a building is influenced by its location, house design, window area, insulation level, and other factors. A precise assessment of the heating load is essential for selecting the proper size of the slinky-loop ground heat exchanger. For most building structures, heat loss is caused by the infiltration of heated air, radiation, natural and mechanical ventilation and also through conduction convection. As a result, the heating load of a building should be assessed not only for the heat loss through building envelopes, but also for the casual heat gain and solar radiation through the windows. To be more specific, there are two

main parts for the building heat loss during the heating season: one is heat loss through the building fabric, and the other one is heat loss through ventilation. Further details of properly sizing the heating system for buildings were provided by the CIBSE.

Soil temperature.

The findings of the numerical modelling indicate that increasing the ground temperature will increase the thermal capacity of the soil and thus enhance the entire system performance. An estimated ground temperature variation with depth throughout the year was determined using Eq. (3.6), as mentioned in Chapter 3.3.3.

System working fluid.

A list of some common working fluids and their advantages and disadvantages can be found in Appendix A. The choice of the working fluid for the ground source heat pump system is considered as a crucial factor in efficiently utilizing the low-grade energy from the slinky-loop ground heat exchanger installed at shallow depth to meet the heating demand. The operation temperature of the working fluid within the HGSHP system is regulated to remain above 0℃ in order to mitigate the production of ice below its freezing point. Therefore, the freezing point of the working fluid should be no less than 5℃ lower than the average temperature of the heat pump, which is defined as the mean temperature between the inlet and outlet. In order to mitigate the risk of freezing when the temperature is below -4℃, it is customary to incorporate an antifreeze solution within the heat pump system to reduce the freezing point below -10℃. An optimal antifreeze solution should possess desirable characteristics such as greater thermal conductivity, lower viscosity and corrosivity, and more

importantly to be environmentally friendly. Additionally, it is critical to account for any potential alteration in the characteristics of water/antifreeze mixtures as the temperature of the loop decreases. For example, at temperatures below -10°C, glycols (propylene glycol in particular) become significantly more viscous and require more pumping power, which reduces the overall efficacy of the system. Significantly less energy will be transferred if the flow stops being turbulent.

Soil thermal properties.

As shown in the simulation results, one of the most important considerations in affecting the slinky-loop ground heat exchanger system is the soil thermal properties. The heat extraction rate of the slinky-loop ground heat exchanger can be increased with a greater thermal capacity. The main factors influencing the thermal behaviour of soil are its composition, moisture content, vegetation, and climate. It is recommended that the thermal characteristics of soil should be determined based on local situations. The soil thermal properties from 65 United Kingdom Meteorological Office weather stations can be found in Appendix B.

The ground heat exchanger configuration and layout

The simulation results suggest that increasing the spacing distance between the parallel pipes in adjacent trenches will reduce the thermal interference. It is suggested that the centre-to-centre trench separation distance should be between 5-6m to achieve good thermal performance while making use of the available land. To maximize the heat transfer of the slinky-loop ground heat exchanger, loop diameter and loop pitch of 1 m are most commonly used in commercial installations. This is also to ensure that the surface areas of slinky-loop ground heat exchanger are fully contacted with the surrounding soil.

Ground heat exchanger pipe material

A buried pipe in the trench and connected to the building is the typical means of extracting heat energy. Plastic pipes exhibit good corrosion resistance and satisfactory thermal resistance. In addition, the plastic pipe can serve as an effective insulation material to mitigate the heat loss at the junction of the heat pump and the pipeline. HDPE is recommended due to its superior strength, flexibility, and anticipated extended lifetime of more than 50 years. However, it has been advised that the installation of underground piping should be conducted to avoid any joints.

System operation strategies.

The intermittent operation varying with heating demand was recommended for the slinky-loop ground heat exchanger system according to the simulation results from the effect of continuous and intermittent operation. This will enable the system to meet the required heating load during the winter heating season as well as facilitate the recovery of soil temperature from the heat loss during switch-off period. Through such system operation strategy, a better heat transfer rate for the system can be achieved.

7.2 Annual space heating demand

For this research, a semi-detached house with three bedrooms and a total floor space of $85m^2$ was chosen as the representative case study. This selection was made in order to evaluate the design considerations of slinky-loop ground heat exchanger . The retrofit project has already been carried out in this case study building structure, and it is a typical design of the standard post-war masonry house with the outlook shown in Fig. 7.2. It was constructed by a 1948 solid masonry wall adding EPS (Expanded Polystyrene) insulation and the U-value of

0.2 W/m^2K. The U-values for EPS insulation roof and Vacuum insulating glass windows are 0.2 W/m^2K and 0.5 W/m^2K, respectively. In addition, the attic floor has a U-value of 0.9 W/m^2K by combining with rock wool, while the ground floor is made of concrete with a U-value of 0.85 W/m^2K. Under the pressure differential of 50 Pa, the airtightness of the main building and loft are set to be 2.69 ACH and 4.18 ACH, respectively. The 30-year average data of the weather conditions for Nottingham including temperature, wind speed and solar radiation were collected from WeatherOnline [134]. The lowest recorded temperature is -2.0 ℃. January and February are the months with the maximum wind speed of 17.7 m/s during the high-intensity wind energy times. Fig. 7.3 depicts the floor plan layout. The case study building 3D model in IES software is shown in Fig. 7.4.



Figure 7.2 Outlook of the case study building.

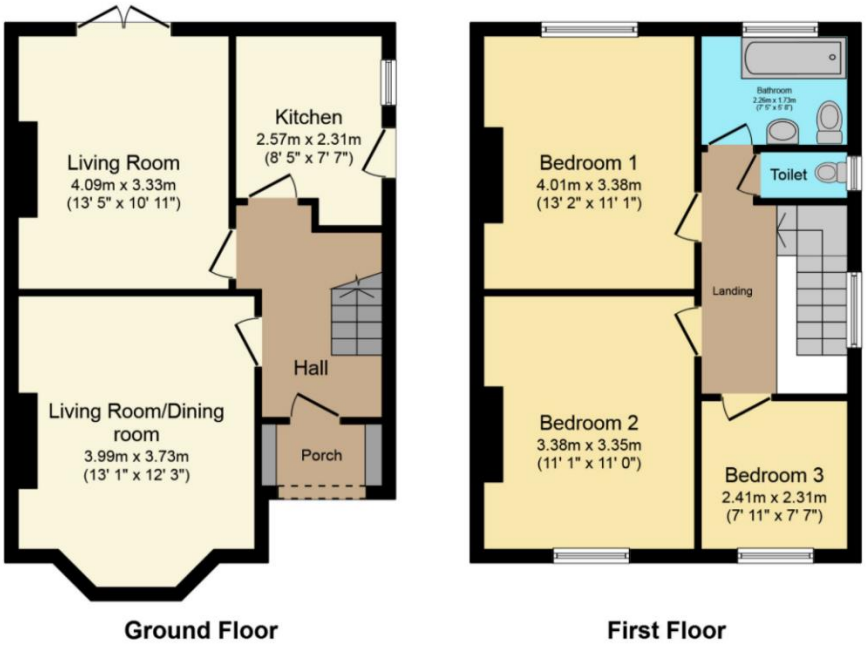


Figure 7.3 Floor plan layout of the semidetached house.



Figure 7.4 Case study 3D model geometric wireframe view.

According to simulation results from IES VE software, the total fabric heat loss is 3714 kWh, and the total ventilation heat loss is 4572 kWh. The heating demand of the two-floor semi-detached house are 3281 kWh for the whole heating season. In this study, the peaking hourly heating load is 6 kW on the coldest day, as shown in Fig. 7.5.

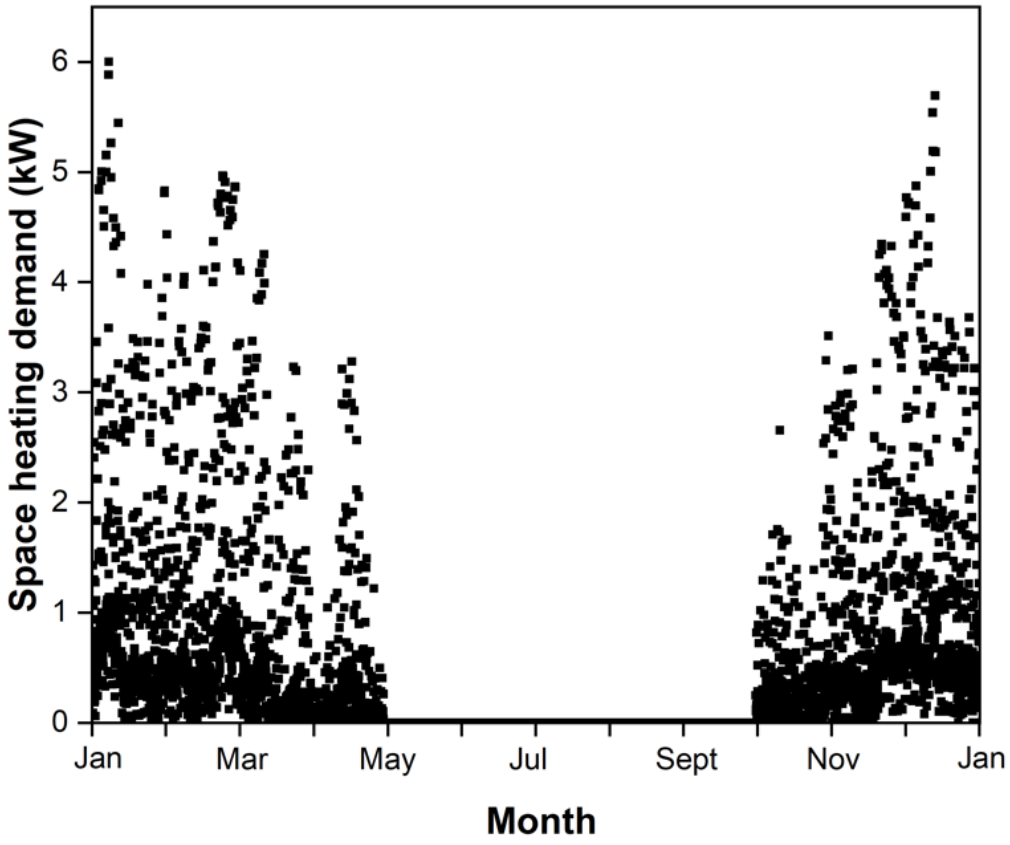


Figure 7.5 Annual space heating demand.

7.3 Required length of slinky-loop ground heat exchanger

The specifications of the heat pump are listed in Table 7.1. The COP for 6 kW Kensa Evo Ground Source Heat Pump is 3.84 at 35℃ thermal output, and the seasonal mean COP was 3.78. The SCOP of the heat pump product represents the seasonal heating performance without considering water circulating pumps for slinky-loop ground heat exchanger pipes. Because pump size and electricity use vary significantly from installation to installation, it is important to calculate the required length for the slinky-loop ground heat exchanger when sizing the water circulating pump.

Table 7.1 Specifications of heat pump.

Components	Specification
Heat pump	Manufacture: Kensa Heat Pump, UK
	Model: S6-P0K
	Nominal kW rating: 6 kW (two compressor)
	COP at B0/W35: 3.84 SCOP at 35 °C: 3.78

The trench length for the slinky-loop ground heat exchanger is L_{slinky}. The trench length for connecting straight pipe is L_C. The spacing distance L between two adjacent trenches is 6 m. It should be noted that this chapter is only for the simple economic analysis for HGSHP system, thus the number of trenches in this work is assumed to be two, as shown in Fig. 7.6. For practical use, it will consider the multiple trenches for different available land space.

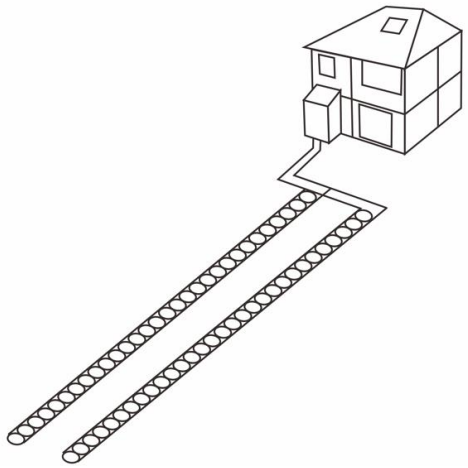


Figure 7.6 Schematics of installation layout for slinky-loop ground heat exchanger system.

The required length of a slinky-loop ground heat exchanger system for domestic space heating is based on the simulation results from the previous chapter. According to the simulation results, the average heat extraction rate per meter length of trench in the coldest day is 33 W for the system in 12-h-on intermittent operation with loamy soil (thermal conductivity of 1.5 W/mK).

Heat pump power output:

$$Q_{heat\ pump=}\frac{Q_{heating}}{COP} \tag{7.1}$$

Heat extraction from ground heat exchanger:

$$Q_{GHE=}Q_{heating} - Q_{heat\ pump} \tag{7.2}$$

$$L_{slinky} = \frac{Q_{GHE}}{q} = \frac{Q_{heating} - \frac{Q_{heating}}{COP}}{q} \tag{7.3}$$

$$L_{trench} = L_{slinky} + L_C \tag{7.4}$$

Where L_{trench} is the require length of trench, L_{slinky} is the required trench length for slinky-loop heat exchanger, $Q_{heating}$ is the heating load in the coldest hour, q is the average heat extraction rate per meter length of trench in the coldest day and L_C is trench length of connecting straight pipe part (approximately 10 m).

As shown in Fig. 7.6, the ground pipe length includes the length of inlet straight pipe in slinky-loop ground heat exchanger trench L_{slinky}, the length of outlet straight pipe in slinky-loop ground heat exchanger trench L_{slinky}, the length of total slinky loop $3.14 \cdot L_{slinky}$, the length of inlet connecting pipe L_C and outlet connecting pipe L_C.

$$L_{pipe} = 5.14 \cdot L_{slinky} + 2 \cdot L_C \tag{7.5}$$

The calculated total length of trench is 144 m, and the HDPE pipe length is 709 m.

7.4 Calculation for circulating pump

In heating mode, the input power for the ground heat exchanger pump to circulate ethylene glycol should be considered due to the long heat exchanger pipe. Therefore, the energy is consumed by both heat pump and water circulating pumps. The pump power is determined by the following equations [135]:

$$TDH = EH + FH + PH \tag{7.6}$$

Where TDH is the total dynamic head, EH is the elevation head, FH is the friction head loss, and PH is the pressure head.

The elevation head is determined by the difference in elevation that liquid will travel, while the friction head loss can be calculated based on the Hazen-William equation [136]:

$$FH = \frac{10.67 \cdot L_{Index} \cdot {V_S}^{1.852}}{C^{1.852} \cdot D^{4.87}} \tag{7.7}$$

Where V_S is the volumetric flow rate in slinky loop heat exchangers, C is the roughness coefficient, L_{Index} is the length of the Index circuit, and D is the diameter of heat exchanger pipes.

The pressure head is determined by the following equations [137]:

$$PH = \frac{\Delta P}{\rho g} \tag{7.8}$$

Where ΔP pressure loss of the fluid, ρ is the density, and g is gravity.

The pressure loss of the fluid can be determined by the Darcy-Weisbach equation [138]:

$$\Delta P = \lambda \frac{L_{Index}}{D} \cdot \frac{\rho v^2}{2} \tag{7.9}$$

Where v is the fluid velocity and λ is the friction factor.

For straight heat exchanger, λ can be determined by:

$$\lambda = 0.3164Re^{-0.25} \qquad (Re = 3 \times 10^3 \sim 10^5) \tag{7.10}$$

Where Re is the Reynold number.

For slinky-coil heat exchanger, λ can be determined by [139]:

$$\lambda = 8.5Re^{-0.63} \qquad (Re < 6200) \tag{7.11}$$

Therefore, the total dynamic head is 7.4 m, the volumetric flow rate in slinky loop pipe is 1.38 m^3/h, and the total volumetric flow rate is 2.76 m^3/h

The total power input for the water pump can be determined as follows:

$$W_{pump} = \frac{V \cdot TDH \cdot \rho g}{\eta_{pump}} \tag{7.12}$$

Where V is the total volumetric flow rate.

Water circulating pumps and their specifications are listed in Table 7.2. The calculated power input for a slinky-loop ground heat exchanger is 101 W.

Table 7.2 Specifications of water pump.

Components	Specification
Water circulating pump (To horizontal GHE)	Manufacture: Grundfos, UK
	Model: CRI 5-2 A-P-A-E-HQQE
	Power: 0.37 kW
	$\eta_{pump} = 56.5\%$ (V= 2.76 m^3/h, TDH = 7.4 m)

7.5 Coefficient of Performance

The performance of HGSHP systems is largely depending on the required

heating demand and the power consumption of a compressor. However, the performance of the HGSHP system may be overestimated due to neglecting of power input for operating water circulating pumps in the source side of heat pump. In this work, by assuming the power input in heat pump is completely transferred to heat, the evaluation of system performance is conducted considering heat processing in the overall system operation. Hence, the power input is calculated by summing these two parts.

The heating performance is represented by the coefficient can then be formulated as:

$$COP = \frac{Q_b}{Q_{hp} + Q_{cp}} \tag{7.13}$$

$$Q_{hp} = \frac{Q_b}{SCOP} \tag{7.14}$$

Where, Q_b is the total heating demand of the building, while Q_{hp} and Q_{cp} are the energy consumed by heat pump and slinky-loop ground heat exchanger circulating water pump, respectively.

The total heating demand Q_b is 3281 kWh, the HGSHP system thermal output is 6 kW. Thus, the total operation time is around 547 hours, and the energy consumption of circular pump Q_{cp} is 55 kWh. The SCOP of the Kensa heat pump S6-P0K is 3.78, Q_{hp} is 868 kWh.

Therefore, the COP for the horizontal ground source heat pump system with loamy soil is 3.55.

As mentioned in Chapter 4.3.2 and 6.3.3, soil thermal properties have a significant impact on the heat extraction amount. The simulation of intermittent 12-h-on operation with sandy soil (higher thermal conductivity of 2.79 W/mK) has been conducted using the same boundary condition. It was found that the

average heat extraction rate per meter length of trench in the coldest day is 57 W. The calculation method for trench length is the same as mentioned in Chapter 7.3, the calculated length for the installation trench is 88 m and for the pipe is 421 m. Hence, the total dynamic head is 5.36 m, and the total volumetric flow rate is 2.76 m^3/h. According to the manufacturer's product technical information, the circulating pump efficiency is 58.6% (V= 2.76 m^3/h, H= 5.36 m). The calculated power input for a circulating water pump to slinky-loop ground heat exchanger is 72 W. The COP for the horizontal ground source heat pump system with sandy soil is 3.62.

7.6 Energy and environmental saving

Table 7.3 presents the energy consumption and CO_2 emission levels of the three different heating systems, as part of a comparative economic study. The carbon factor of gas and electricity can be seen in Appendix F [140, 141].

Table 7.3 Comparison of energy consumption and CO_2 emission of various heating systems.

Heating system	Capital cost (£)	COP	Energy Consumed (kWh)	Annual CO_2 emission (kg)
HGSHP (loamy)	6551	3.55	924	193
HGSHP (sandy)	4598	3.62	906	189
Electric heater	2499	1	3281	686

Gas-fired heater	2275	0.89	3687	675

Fig. 7.7 illustrates the energy consumption and first-year carbon dioxide (CO_2) emissions associated with the operation of three heating systems: the HGSHP system, the electric heater, and the gas-fired condensing boiler. The data presented in the figure refers to a one-year period. Based on official government data [142], it is evident that residential heating constitutes around 14% of the United Kingdom's carbon emissions, so posing a significant challenge to the government's goal of achieving carbon neutrality by the year 2050. The emissions mostly attributed to gas boilers need the exploration of low-carbon alternatives, so HGSHP systems are expected to serve as feasible substitutes. Consequently, gas boilers have already been the focus of significant legislation, including a prohibition on the installation of gas boilers in any property that is newly constructed after the year 2035 [143]. In regard to the reduction of CO_2 emissions, the HGSHP (loamy) heating system demonstrates superior performance compared to both the gas-fired condensing boiler and electric heater systems. The reduction in CO_2 emissions amounts were more than 250% and 255%, respectively. For the HGSHP system with sandy soil, the annual CO_2 emissions are 18 kg less than those in loamy soil in the first year of operation. The National Grid ESO has predicted the carbon factor of electricity will be reduced, and the decrease rate is about 4.4% [144]. Given an assumed operational lifespan of 20 years for the HGSHP (loamy) heating system, it has the potential to mitigate carbon dioxide (CO_2) emissions by about 11.3 tones and 5.7 tones for gas boiler and electric boiler, respectively, as shown in Fig. 7.8.

This estimation is based on the CO_2 emission factors of 0.183 kg/kWh for gas and 0.209 kg/kWh for electricity in the first year [140, 141].

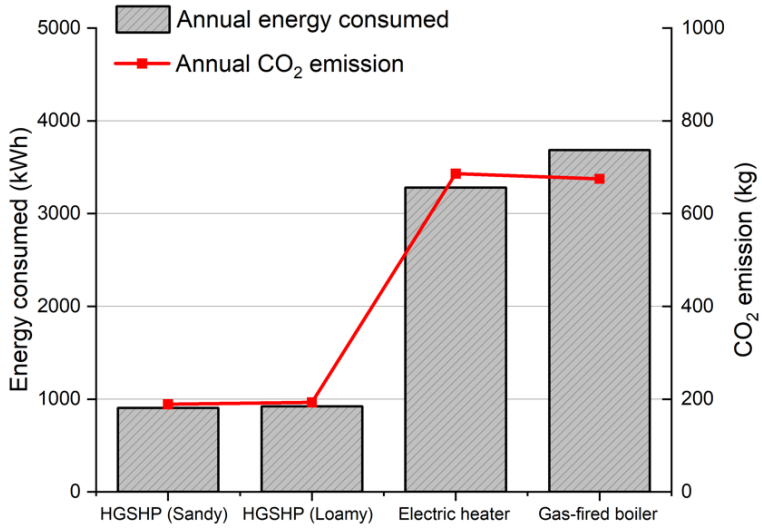


Figure 7.7 Comparison of annual energy consumed and CO_2 emission of different heating system.

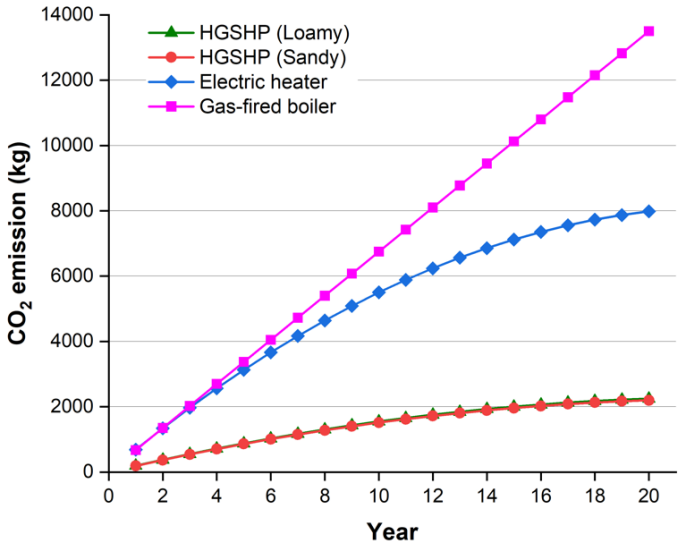


Figure 7.8 Comparison of accumulated CO_2 emission of different heating systems.

7.7 Economic considerations

The installation fees associated with HGSHP systems are much greater in comparison to other systems such as air source heat pump (ASHP) systems. While HGSHP are known for their reliable energy efficiency, the significant capital investment required for their implementation remains an important concern in applications. The heating load of a building, the local electricity price, the government subsidy, the amount of energy used by the water pump and heat pump, and the system installation costs are all crucial information to have when estimating the economical behavior of a HGSHP system. The payback period is commonly used as a method for evaluating the economic aspect of a horizontal ground source heat pump system. This study conducts an economic analysis of a HGSHP system for space heating. The cost effectiveness of the HGSHP system is evaluated by employing the net present value method (NPV) and discounted payback period (DPP). A comparison is made between the HGSHP system, electric heating and gas-fired condensing heating systems. Table 7.4 presents a comparison of the capital costs, consisting of material, labor and government grant. The detailed capital cost for HGSHP with sandy soil can be found in Appendix C.

Table 7.4 Initial investment of horizontal ground source heat pump system and conventional heating system.

Heating system	Item and its description	Price (£)
HGSHP	Kensa Shoebox heat pump	5970
	Flowmeters ＆circulating pump	1757

	Working fluid	1695
	Pipe work	1595
	Buffer tank	499
	Excavation ＆installation work	1584
	MCS heat loss ＆ umbrella scheme	951
	Government grant Boiler Upgrade Scheme (BUS)	-7500
		6551
Electric heater	Fusion comet 6kW electric boiler	1199
	Flue, filter, etc.	300
	Installation fees	1000
		2499
Gas-fired condensing heater	Worcester Bosch gas boiler	975
	Flue, filter, etc.	300
	Installation fees	1000
		2275

In order to assess the economic performance of the proposed HGSHP system, time-equivalent economic evaluation has been further conducted. To compare the cost of different heating operation methods under different timing and magnitude of costs, the present value cost (PVC) has been used as a method of valuing future costs in present's terms. The PVC can be referred to the current worth of a future stream of costs, discounted at a specific interest rate, which

can be expresses as:

$$PVC = \frac{R_n}{\left(1 + {R_d}/{100}\right)^n} \tag{7.15}$$

Where, R_n is the estimated net cash flow in the year n, and R_d is the real discount rate.

The real discount rate R_d can be determined by using Eq. (7.16) [145]:

$$R_d = \frac{R_m - R_i}{1 + R_i} \tag{7.16}$$

Where, R_m is the market interest rate and R_i is the inflation rate. The values of R_m, R_i as well as the energy increasing rate for UK are presented in Table 7.5 below.

Electricity prices have possibly become 2.2 times higher since 2012. Hence, discounted payback period was predicted with growing electricity prices. The calculation process for gas and electricity increase rate can be found in Appendix D [146]. The price of gas and electricity in the first year are based on two-year averages taken from the Government' Energy Price Guarantee from 2021 to 2023, which can be found in Appendix E [147].

Table 7.5 Economic indicators and energy price increase rate.

Market interest rate R_m (%)	Inflation rate R_i (%)	Electricity price increase rate (%)	Natural gas increase rate (%)	Real discount rate R_d (%)
5.25 [148]	4.6 [149]	7.73	12.32	0.62

To further analyse the profitability of the investment in the GSHP system, the net present value (NPV) has been calculated based on the present value of cash

inflows and outflows over a period, which can be defined as:

$$NPV = \sum_{n=0}^{i-1} \frac{R_n}{\left(1 + {R_d}/{100}\right)^n} \tag{7.17}$$

Where, i is the analysis period of year, n is the current year and $n = 0$ represents the base year.

7.8 Discounted payback period

In this study, the total system cost, including the initial capital cost and accumulated 20 years' savings of the concerned HGSHP system, is used as the performance indicator. In payback analysis, DPP is described as a payback period variation and modification that accounts for time value and utilises discounted cash flows when determining the payback period with the unit of years. The payback period is the time required for a system's entire accumulated savings or benefits to cover the investment costs. Because the time value of money must be taken into account in payback calculations, all costs need to be discounted to determine the discounted payback period. Payback occurs when the overall accumulated present value (PV) savings exceed the total PV costs of an alternative retrofit technology. The discounted payback period is simply the amount of time that has passed between when the savings begin to accumulate and when payback occurs. Based on the findings of the study (see Table 7.3), the annual operating costs of the HGSHP (loamy soil) heating system for individual residences have been found to be approximately 71.8% lower than those of the electric heater system. This percentage would rise to 72.4% when the GHE surrounding soil is sandy soil. However, when considering the annual operation cost, the difference between HGSHP heating system and the gas-fired

condensing boiler is small. Given that the cost of electricity per kilowatt-hour (kWh) is 3.6 times higher than that of gas, annual operational expenses for heating with a gas-fired condensing boiler amount to £295, whereas for heating with an HGSHP (loamy soil), the cost reaches £268. Fig. 7.9 illustrates that the discounted payback period for the horizontal ground source heat pump is approximately 7 years when compared to the electric heater heating system. When the HGSHP system is installed in sandy soil (thermal conductivity =2.79 W/mK), the discounted payback period for the horizontal ground source heat pump can be reduced to 4.5 years compared to the electric heater heating system, as shown in Fig. 7.10. This is because that the required trench length for the HGSHP system in sandy soil is less than that in loamy soil due to the higher average heat transfer rate. The shorter trench can save the initial investment. Also, it causes less energy to be consumed by the fluid circulating pump, and increases the value of COP. It can be concluded that the HGSHP system installed in soil types with higher thermal conductivity can achieve a shorter discounted payback period.

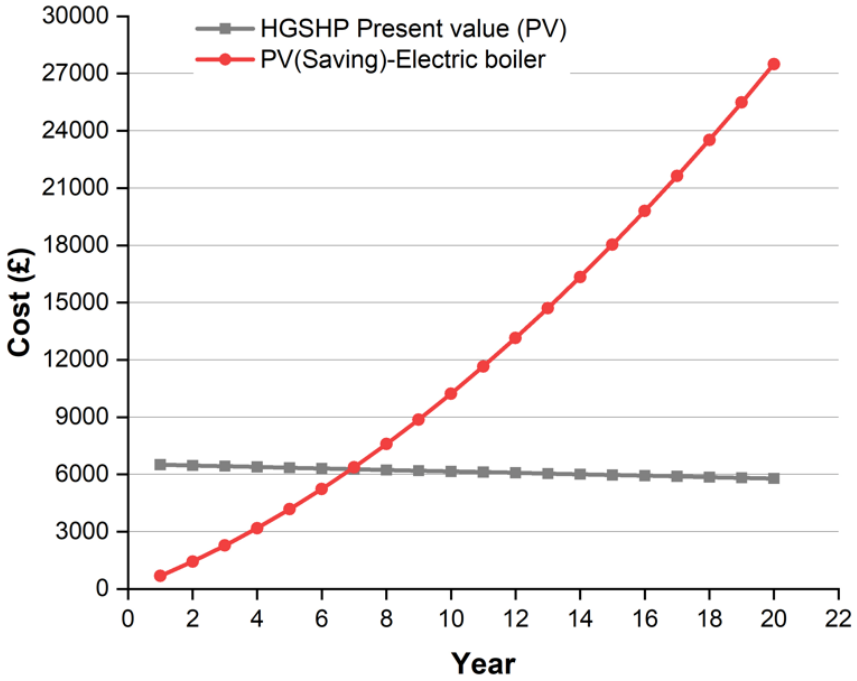


Figure 7.9 Breaking point for the discounted payback period of HGSHP & electric heating system in loamy soil.

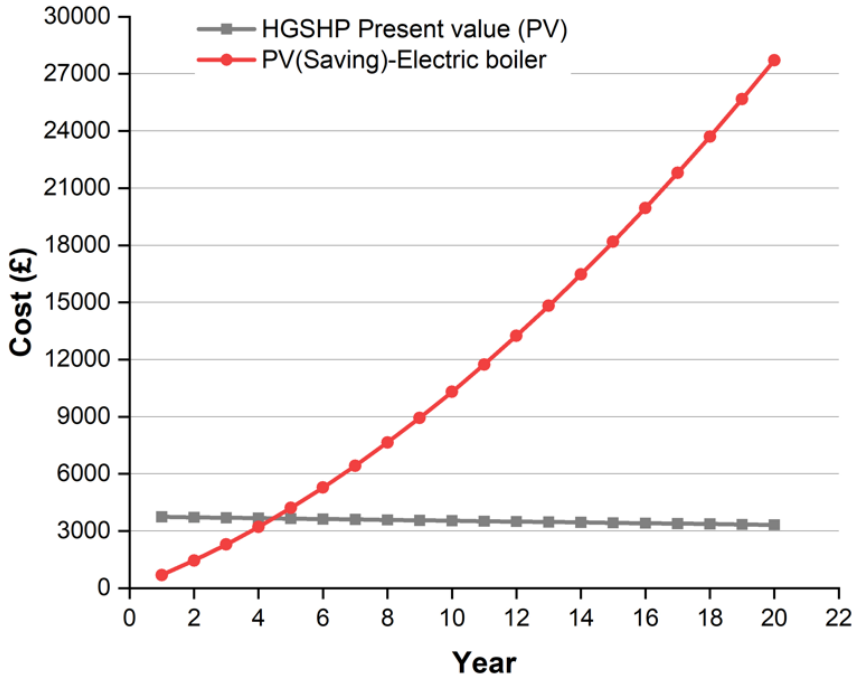


Figure 7.10 Breaking point for the discounted payback period of HGSHP & electric heating system installed in sandy soil with higher thermal conductivity.

7.9 Comparison for different heat pump system

Heat pumps play a significant role in the transformation to an electrical power-based energy system in the future. The primary obstacle to integrating heat pumps is the initial investment and operational cost, which is affected by COP. This study compares the air source heat pump (ASHP) and borehole ground source heat pump (BGSHP), and HGSHP system in terms of their economic and environmental benefits. Since the COP of ASHP and BGSHP are determined by the operation condition, installation site, heat pump efficiency and other factors, the values of COP in previous publications cannot be referred to in this comparison study. COP is highly dependent on the temperature difference between the heat source and heat sink[150]. The temperature of the heat source is the main factor that determines COP for various heat pump systems. The actual heat pump COP of ASHP and BGSHP are estimated through the ideal COP of the three different heat pump system. The average soil temperature at the depth of 1.2 m can be obtained from Eq. (3.6), the daily average temperature in heating season is shown in Fig. 7.11. The average soil temperature at a depth of 1.2 m during the heating season is 9.3℃. In the heating season, the average deep soil temperature with a borehole heat exchanger is 10℃[32]. The average air temperature throughout the heating season is 7.4℃, as indicated in Table 3.2. At maximum theoretical efficiency,

$$COP_{ideal} = \frac{T_H}{T_H - T_C} \tag{7.18}$$

where $T_H$and T_C are the thermodynamic temperatures of the hot and cold heat reservoirs, respectively.

As seen in Eq. (7.18) [150], the $\mathrm{COP_{ideal}}$ is determined by the ratio of the

entropic mean temperature of the heat sink, T_H, relative to the difference between the entropic mean temperatures of the heat sink and heat source T_C. The calculated COP_{ideal} of three heat pump systems are shown in Table 7.6. In Section 7.5, the calculated COP for HGSHP is 3.55. Thus, the actual COP values for BGSHP and ASHP are calculated according to the ratio of the actual COP, relative to the COP_{ideal}. The calculated actual COP for BGSHP and ASHP are 3.65 and 3.31, respectively.

Table 7.6 Estimated COP for BGSHP and ASHP system.

Heating system	T_H (℃)	T_C (℃)	$\mathrm{COP_{ideal}}$	COP
HGSHP	35	9.3	11.98	3.55
BGSHP	35	10	12.32	3.65
ASHP	35	7.4	11.15	3.31

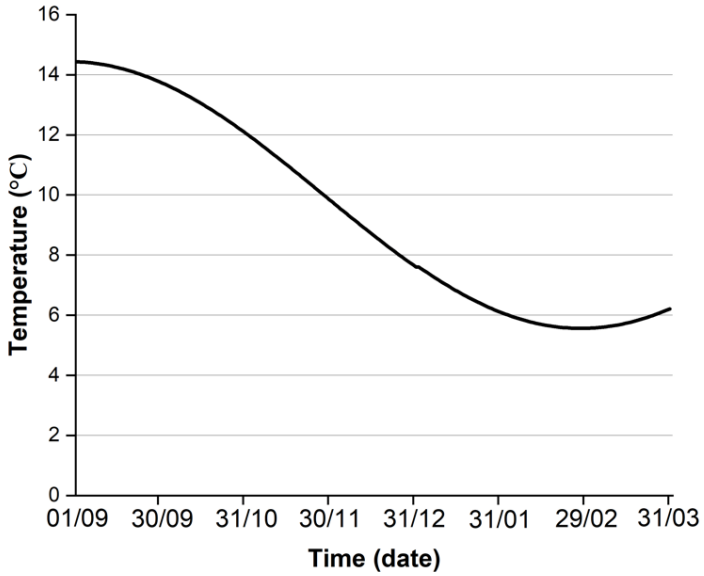


Figure 7.11 The daily average soil temperature at a depth of 1.2 m from Sept 1st to Mar 31st.

Table 7.7 presents the annual energy consumption and CO_2 emission levels of the three different heat pump systems, as part of a comparative economic and environmental study. Using the same method mentioned in chapter 7.6 and 7.7. The discounted payback period of BGSHP and ASHP systems are obtained. Given a 20-year operational lifespan for the heat pump heating system, the accumulated CO_2 emissions are 2.25 tones, 2.19 tones, and 2.41 tones for HGSHP, BGSHP, and ASHP, respectively, as shown in Fig. 7.12. This estimation is calculated using the CO_2 emission parameters of 0.209 kg/kWh for electricity in the initial year. The reason for BGSHP having the lowest carbon emission is its superior coefficient of performance (COP) compared to the other two heat pump systems.

Table 7.7 Comparison of energy consumption and CO_2 emission of various heat pump systems

Heating system	Capital cost (£)	COP	Energy Consumed (kWh)	Annual CO_2 emission (kg)
HGSHP	6551	3.55	924	193
BGSHP	13557	3.65	899	188
ASHP	3281	3.31	991	207

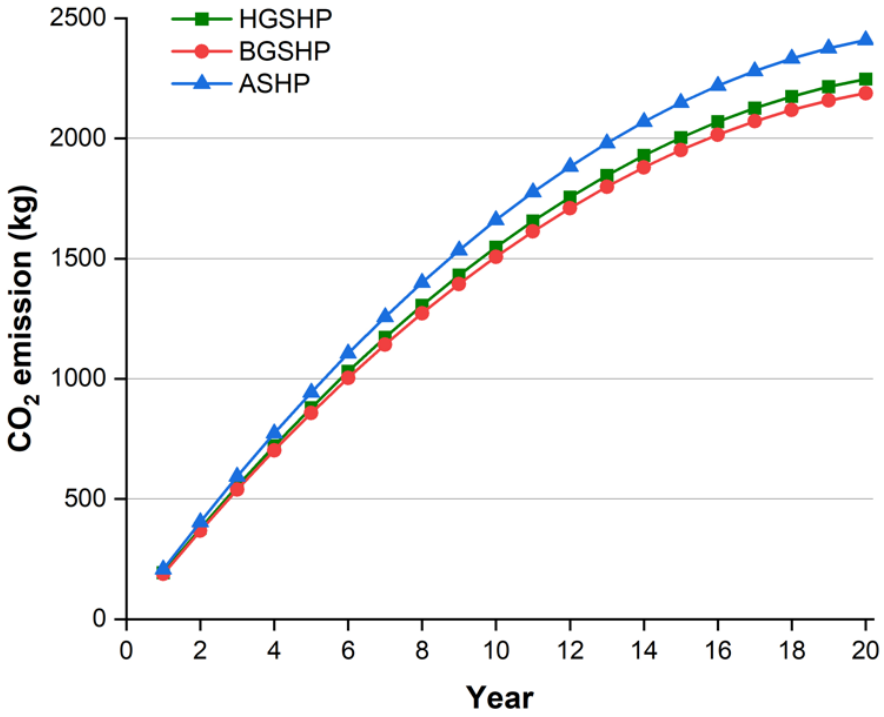


Figure 7.12 Comparison of accumulated CO_2 emission of HGSHP, BGSHP, and ASHP heating systems.

Table 7.8 Initial investment of borehole ground source heat pump system and air source heat pump system.

Heating system	Item and its description	Price (£)
BGSHP	Kensa Shoebox heat pump	5970
	Flowmeters ＆circulating pump	1757
	Working fluid, Pipe work＆ Buffer tank	2379
	Drilling ＆installation work (two boreholes)	10000

	MCS heat loss & umbrella scheme	951
	Government grant Boiler Upgrade Scheme (BUS)	-7500
	13557	
ASHP	Mitsubishi 6kW R32 1Ph Mono ASHP UQ & 150L Pre-Plumbed Std Cylinder	5830
	installation work	4000
	MCS heat loss & umbrella scheme	951
	Government grant Boiler Upgrade Scheme (BUS)	-7500
	3281	

Table 7.8 displays a comparison of the initial investments and government grant for BGSHP and ASHP systems. Figure 7.13 shows that the borehole ground source heat pump has a discounted payback period of roughly 11 years when compared to an electric heater heating system. Based on the ground condition of the site, the temperature at 100 m below ground level is likely to remain consistent throughout the year, which ensures that the performance of borehole collectors remains consistent and unaffected. This type of system is perfect for areas where the available land is limited, such as in urban areas, a location that experiences extreme weather conditions, or on sloping terrain. Despite BGSHP has been proven as highly efficient, high initial cost

discourages homeowners and small-medium enterprises to opt for such systems [17]. The HGSHP system is recommended in rural residential areas because of the large amount of outdoor space required. And it provides a cost-effective alternative that can potentially promoting the use of these systems over the world. The discounted payback period for the ASHP can be reduced from 7 years to 4.2 years compared to the HGSHP system with slinky-loop ground heat exchanger, as shown in Fig. 7.14. This is because air source heat pumps are often cheaper than GSHP heating systems, as the installation costs are limited to the unit itself. And a slinky-loop ground heat exchanger system requires additional expenses for the necessary groundwork and ground arrays. The actual COP estimated in this part was based on the heating season average air temperature. However, the COP of air source heat pumps fluctuates depending on the months and time of day. During winter, buildings have a particular challenge as the air, which serves as a source of heat for heating, reaches its lowest temperature. As a result, the building heating system will require more electricity to operate effectively. Therefore, air source heating has the potential to result in higher long-term costs for end-users.

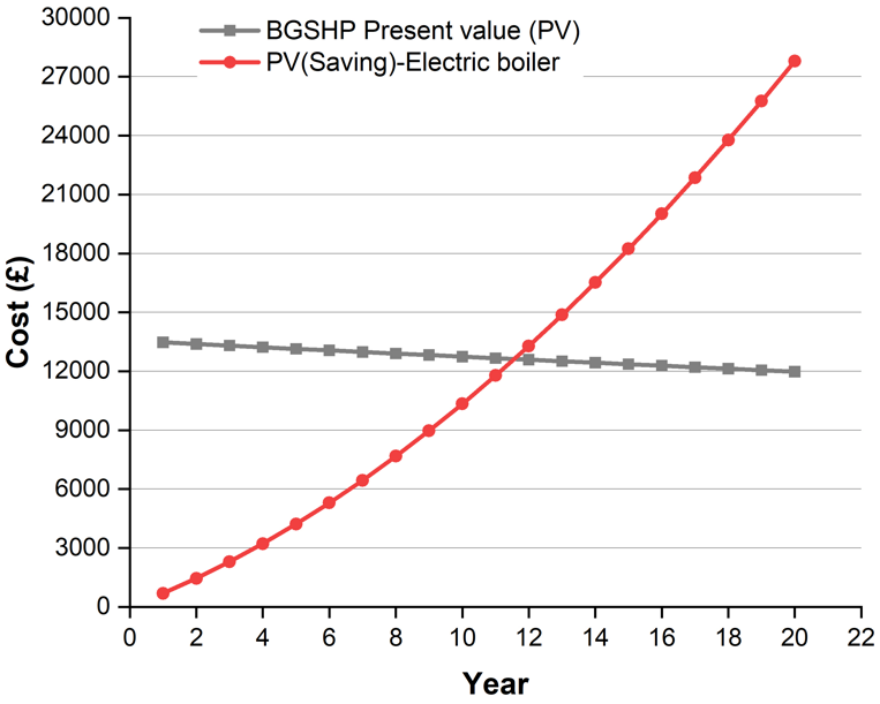


Figure 7.13 Breaking point for the discounted payback period of BGSHP & electric heating system.

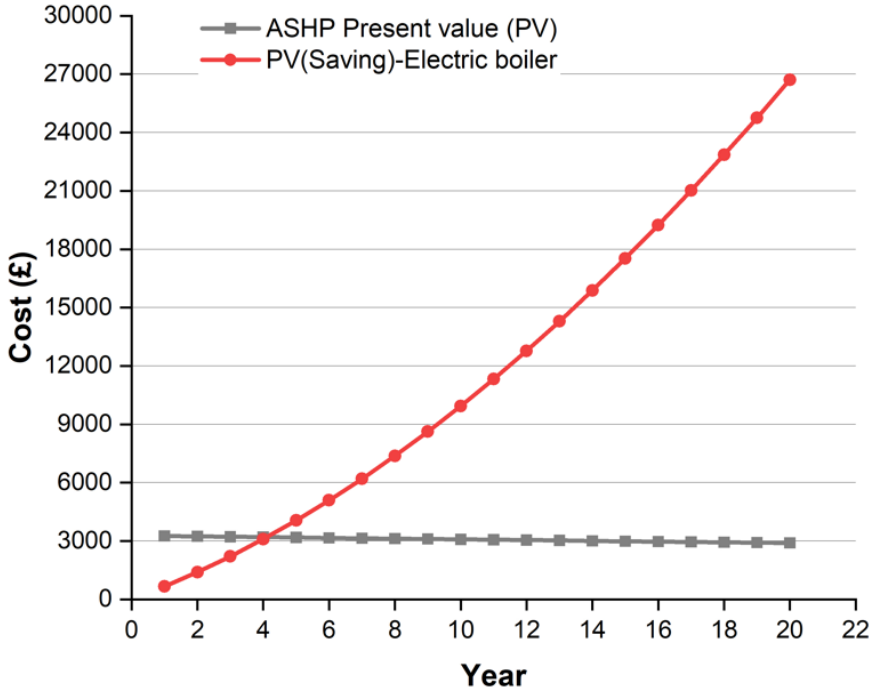


Figure 7.14 Breaking point for the discounted payback period of ASHP & electric heating system.

Chapter 8: Conclusion and future work

8.1 Main conclusion

This study has dealt with the investigation of the performance of slinky-loop ground heat exchanger system. Firstly, the numerical methodology for the dynamic thermal simulation of slinky-loop ground heat exchanger has been proposed. Then, a three-dimension numerical model is created and validated with the published experimental results, which were discussed in Chapter 3. It has evaluated the thermal performance under different boundary conditions, initial soil temperatures and pipe temperature. Chapter 4 has investigated the thermal interference from adjacent trenches and has also studied the effect of soil properties and installation depth. Chapter 5 has studied the intermittent operation mode through various daily operation hours. The effect of loop pitch, thermal interference from parallel pipe, and annual operation mode on slinky-loop ground heat exchanger thermal performance based on intermittent 12-hours-on operation were analyzed. Chapter 6 considered the heating degree day operation as a novel method for accurate prediction about the daily operation hours and compared the intermittent operation method in a real-life situation. The effect of installation sites has been analysed. Finally, the economic analyses of the HGSHP system and factors of system design considerations were discussed in Chapter 7.

From this research, the following conclusions can be derived:

- The monthly changed air temperature and wind speed of Coventry were compared to the average heating season boundary condition. The difference in total heat extraction between these two boundary conditions was about

10%. For topsoil boundary conditions, monthly air temperature and wind speed changes are suggested for better prediction about heat transfer rate and heat extraction amount.

- The initial soil temperature also has an impact on performance. With two types of initial soil temperature - uniform and varied with depth - the thermal performance of a slinky-loop ground heat exchanger was estimated. The difference in predicted heat transfer through a 1.2 m deep heat exchanger in loamy soil using a constant temperature profile versus that with varying temperatures is up to 16% in the first month, then drops to 6% and 2% in the second and third months. Slinky-loop ground heat exchanger installed at shallower depths might have a significantly bigger heat transfer difference during the initial month due to the greater temperature disparity between the constant value and the varying profile.
- The heat extraction rate was shown to increase with decreasing temperatures of the slinky-loop ground heat exchanger pipe. The linear equation can be utilised for estimating the energy extraction of various fluid/ heat exchanger pipe temperatures.
- The effect of trench spacing was analysed for distances from 1.5 to 11 m. Heat transfer between parallel pipes would interfere with each other, resulting in a reduction in overall thermal performance in short distances. Correlations have been obtained from the simulation results to estimate the thermal performance of different spacing distances. It is suggested that the centre-to-centre trench separation distance should be between 5-6m to achieve good thermal performance while making use of the available land.
- The heat transfer amount through a heat exchanger is affected by the depth

of the installation. The estimated total heat extraction for a heating season would decrease as the installation depth increased. This is due to the fact that the topsoil in summer was heated by solar radiation and warm air in the early part of the heating season, while rising air and soil temperatures in the later part of the heating season resulted in higher temperatures in the shallower soil. However, if heating begins later, such as in December, when the topsoil is cooler, the total heat extraction increases with installation depth. The modelling results also showed that the effect of trench separation will increase with installation depth. However, installation depth has less influence than trench separations on the thermal performance.

- The simulation findings revealed that increasing soil thermal conductivity would significantly improve overall performance over a seven-month heat extraction for a heat exchanger, with 297% and 123% higher in sandy and loam soil, respectively, than clayey soil. Furthermore, soil with a higher thermal conductivity will exacerbate the phenomena of thermal interference between parallel pipes separated by a shorter distance.
- Continuous operation requires continually extracting heat from the surrounding soil during the heating period, whereas intermittent operation considers soil temperature recovery as an alternative to minimizing the soil thermal imbalance generated by the slinky-loop ground heat exchanger system. Despite having a higher overall heat extraction amount, the intermittent operation method demonstrated a higher average heat transfer rate of the GHE than the continuous operating method. The daily average heat transfer rate increases as the daily switch-on operation time decreases. Correlations have been obtained to estimate the thermal performance of

different daily operation hours. Intermittent operation is suggested for enhanced heat transfer performance based on the actual building heating demand.

- The simulation results show that reducing the loop pitch of a slinky-loop ground heat exchanger increases the contact surface to the surrounding soil in the same length of trench, improving overall thermal performance and requiring less excavation work to install the system than larger loop pitch configurations. When the loop pitch was lowered to a fourth of the loop diameter, overall heat extraction increased by 24% per meter length of trench when compared to a loop pitch of 1m. The derived quadratic polynomial correlation might be utilised for predicting the thermal performance of different loop pitches in intermittent 12-h operation mode.
- The findings indicated that implementing a 12-hour intermittent operation strategy would mitigate the impact of heat depletion and thermal interference from neighbouring parallel piping.
- The reduction of soil temperature near the slinky-loop ground heat exchanger due to seven-month heating operation can be fully recovered at the fourth month after the heating season. When the cooling operation is included, the thermal performance for the second heating season improves, and the start date for the second heating season also has an impact on the thermal performance.
- The heat demands-varying on-off operation mode predicts the variable daily operation hours during the heating season by using the heating degree day method and the house monthly energy consumption as the basis. The difference between the two modes is only 2%. This proves that the heating

degree day prediction method can assess the thermal performance of a household slinky-loop ground heat exchanger system in a real-life situation. The difference between the heat extraction amount using the heating degree day method and the intermittent 12-hour-on operation mode is less than 15% after the first month of operation. The operation mode with different daily operating hours during the initial three months has little effect on monthly heat extraction during the next four months.

- The cities of Edinburgh, Coventry, and Reading were selected to evaluate the impact of the installation site's external environment and soil properties. The thermal conductivity of the soil surrounding the heat exchanger pipe was found to be the most influential factor on thermal performance.
- The economic study shows that the slinky-loop ground heat exchanger system installed with loamy and sandy soil would be able to save about 71.8% and 72.4% in operating costs compared to electric boiler heating systems, respectively. The required length of pipe in sandy soil is 40.6% less than that in loamy soil. The initial investment for the system in sandy soil is 29.8% lower than that in loamy soil. This HGSHP (loamy) system would be able to decrease CO2 emissions by about 71.4% and 71.9% compared to gas and electricity heating systems, respectively. The predicted discounted payback period is 7 years for the HGSHP (loamy) system, and 4.5 years for the HGSHP (sandy) compared to the electricity heating system, respectively. This study also concluded the comparison between the ASHP, BGSHP, and HGSHP system in terms of their economic and environmental benefits.

8.2 Recommendation for future work

The project studied the thermal behaviour of slinky-loop ground heat exchanger installed in shallow depth. More investigation is recommended in the following fields:

First, a more accurate assessment of the ground heat exchanger's performance can be achieved with the inclusion of accurate field meteorological conditions and soil thermal parameters in the numerical modelling. Accurate representation of these factors can significantly enhance the accuracy of predicted results. The methodology described in this study is founded upon a pure heat conduction process, wherein the ground is represented as a homogenous and isotropic medium. The proposed methodology does not consider several factors such as multi-layered ground, solar radiation, cloud cover, precipitation, infiltration, vegetation height, groundwater movement, or heat gains from anthropogenic activities. Therefore, the development of design tools that are able to assess the influence of the aforementioned aspects in situations in which slinky-loop ground heat exchanger systems may be strongly influenced represents a potential field for improvement. Because these parameters are not always known in advance, determining how to estimate their influence is another essential step in the process of calculating the size of the slinky-loop ground heat exchanger trench.

The GHE side of the GSHP system (i.e., the slinky-loop ground heat exchanger) was the primary focus of this study. The development of dynamic control optimisation approaches for the entire GSHP system, including the load distribution side, would be advantageous. The annual performance of GSHP can be assessed by establishing a coupled model that combines the building heating

and cooling model with the slinky-loop ground heat exchanger model. This model can analyse different design conditions under three building load scenarios (balanced, heating dominant, or cooling dominant). Under the assumption that the building heating/cooling demand is completely supplied by the HGSHP system, the variation in ground temperature can be used as an indicator to compare long-term performance. This method could be used to investigate the system's behaviour in real-operation conditions.

In addition, seasonal load imbalance is also an important consideration in the design and operation of HGSHP systems with slinky-loop ground heat exchanger. However, the exploration of prospective methods to effectively alleviate the seasonal load imbalance issue was not the emphasis of this study. Future research on the development of practical methods to address seasonal load imbalance in the slinky-loop ground heat exchanger will be beneficial.

There are certain combined solar thermal and GSHP systems that function in conjunction with other systems, such as solar panels and cooling towers. These systems have the potential to address the temperature imbalance that exists beneath the ground surface and supply additional energy in operation. In addition, hybrid GSHP systems have the potential to assist in the enhancement of a system's COP as well as the reduction of its CO2 emissions. Hybrid ground source heat pump systems that have been properly inspected may achieve greater levels of energy efficiency and improve economic advantages.

Reference list

[1] I. E. Agency, *Global Energy Review: CO2 Emissions in 2021*: IEA, 2021. [Online]. Available: www.iea.org

[2] D. f. E. S. a. N. Zero. "Energy Security Bill factsheet: Low-carbon heat scheme." https://www.gov.uk/government/publications/energy-security-bill-factsheets/energy-security-bill-factsheet-low-carbon-heat-scheme (accessed.

[3] C. F. Calvillo, A. Katris, O. Alabi, J. Stewart, L. Zhou, and K. Turner, "Technology pathways, efficiency gains and price implications of decarbonising residential heat in the UK," *Energy Strategy Reviews,* vol. 48, p. 101113, 2023/07/01/ 2023, doi: https://doi.org/10.1016/j.esr.2023.101113.

[4] Office for National Statistics. "Cost of living insights: Energy." https://www.ons.gov.uk/economy/inflationandpriceindices/articles/costoflivinginsights/energy (accessed 04 May, 2023).

[5] R. M. Singh, A. K. Sani, and T. Amis, "15 - An overview of ground-source heat pump technology," in *Managing Global Warming*, T. M. Letcher Ed.: Academic Press, 2019, pp. 455-485.

[6] Z. Qi, Q. Gao, Y. Liu, Y. Y. Yan, and J. D. Spitler, "Status and development of hybrid energy systems from hybrid ground source heat pump in China and other countries," *Renewable and Sustainable Energy Reviews,* vol. 29, pp. 37-51, 2014/01/01/ 2014, doi: https://doi.org/10.1016/j.rser.2013.08.059.

[7] European Heat Pump Association. "The European Heat Pump Outlook 2021: 2 million heat pumps within reach." https://www.ehpa.org/2022/06/12/ehpa_news/the-european-heat-pump-outlook-2021-2-million-heat-pumps-within-reach/ (accessed 10 May, 2023).

[8] Climate Change Committee. "Reducing UK emissions – 2019 Progress Report to Parliament." https://www.theccc.org.uk/publication/reducing-uk-emissions-2019-progress-report-to-parliament/ (accessed 10 May, 2023).

[9] Jonathan Massam and Tom Wellingham. "The heat pump market is only just warming up." https://www.pwc.co.uk/industries/real-estate-and-infrastructure/real-assets/heat-pump-market-only-just-warming-up.html (accessed 10 May, 2023).

[10] GOV.UK. "Boiler Upgrade Scheme." https://www.find-government-grants.service.gov.uk/grants/boiler-upgrade-scheme (accessed 28 April, 2023).

[11] Department for Business Energy & Industrial Strategy and The Rt Hon Kwasi Kwarteng MP. "Plans unveiled to decarbonise UK power system by 2035." https://www.gov.uk/government/news/plans-unveiled-to-decarbonise-uk-power-system-by-2035 (accessed 12 May, 2023).

[12] House of Commons Committee. "Decarbonising heat in homes." https://publications.parliament.uk/pa/cm5802/cmselect/cmbeis/1038/report.html (accessed 13 May, 2023).

[13] L. Hu, Z. H. Rizvi, L. Tobber, and F. Wuttke, "Thermal performance of three horizontal ground heat exchanger systems: comparison of linear-loop, spiral-coil and slinky-coil arrangements," (in English), *Frontiers in Energy Research,* Original Research vol. 11, 2023-October-13 2023, doi: 10.3389/fenrg.2023.1188506.

[14] S. J. Rees, "5 - Horizontal and compact ground heat exchangers," in *Advances in Ground-Source Heat Pump Systems*, S. J. Rees Ed.: Woodhead Publishing, 2016, pp. 117-156.

[15] Z. Xiong, D. E. Fisher, and J. D. Spitler, "Development and validation of a Slinky™

ground heat exchanger model," *Applied Energy,* vol. 141, pp. 57-69, 2015/03/01/ 2015, doi: https://doi.org/10.1016/j.apenergy.2014.11.058.

[16] Y. Al-Ameen, A. Ianakiev, and R. Evans, "Recycling construction and industrial landfill waste material for backfill in horizontal ground heat exchanger systems," *Energy,* vol. 151, pp. 556-568, 2018/05/15/ 2018, doi: https://doi.org/10.1016/j.energy.2018.03.095.

[17] S. Selamat, A. Miyara, and K. Kariya, "Numerical study of horizontal ground heat exchangers for design optimization," *Renewable Energy,* vol. 95, pp. 561-573, 09/01 2016, doi: 10.1016/j.renene.2016.04.042.

[18] R. Sangi and D. Müller, "Dynamic modelling and simulation of a slinky-coil horizontal ground heat exchanger using Modelica," *Journal of Building Engineering,* vol. 16, pp. 159-168, 2018/03/01/ 2018, doi: https://doi.org/10.1016/j.jobe.2018.01.005.

[19] F. Tang and H. Nowamooz, "Outlet temperatures of a slinky-type Horizontal Ground Heat Exchanger with the atmosphere-soil interaction," *Renewable Energy,* vol. 146, pp. 705-718, 2020/02/01/ 2020, doi: https://doi.org/10.1016/j.renene.2019.07.029.

[20] L. Pu, L. Xu, D. Qi, and Y. Li, "Structure optimization for horizontal ground heat exchanger," *Applied Thermal Engineering,* vol. 136, pp. 131-140, 2018/05/25/ 2018, doi: https://doi.org/10.1016/j.applthermaleng.2018.02.101.

[21] R. R. Dasare and S. K. Saha, "Numerical study of horizontal ground heat exchanger for high energy demand applications," *Applied Thermal Engineering,* vol. 85, pp. 252-263, 2015/06/25/ 2015, doi: https://doi.org/10.1016/j.applthermaleng.2015.04.014.

[22] C. S. A. Chong, G. Gan, A. Verhoef, R. G. Garcia, and P. L. Vidale, "Simulation of thermal performance of horizontal slinky-loop heat exchangers for ground source heat pumps," *Applied Energy,* vol. 104, pp. 603-610, 2013/04/01/ 2013, doi: https://doi.org/10.1016/j.apenergy.2012.11.069.

[23] Y. Wu, G. Gan, A. Verhoef, P. L. Vidale, and R. G. Gonzalez, "Experimental measurement and numerical simulation of horizontal-coupled slinky ground source heat exchangers," *Applied Thermal Engineering,* vol. 30, no. 16, pp. 2574-2583, 2010/11/01/ 2010, doi: https://doi.org/10.1016/j.applthermaleng.2010.07.008.

[24] Y. Wu, G. Gan, R. Gonzalez, A. Verhoef, and P. L. Vidale, "Prediction of the thermal performance of horizontal-coupled ground-source heat exchangers," *International Journal of Low-Carbon Technologies,* vol. 6, 11/03 2011, doi: 10.1093/ijlct/ctr013.

[25] P.-O. Fontaine, D. Marcotte, P. Pasquier, and D. Thibodeau, "Modeling of horizontal geoexchange systems for building heating and permafrost stabilization," *Geothermics,* vol. 40, no. 3, pp. 211-220, 2011/09/01/ 2011, doi: https://doi.org/10.1016/j.geothermics.2011.07.002.

[26] Y. Zhou, B. Asal, N. Makasis, and G. Narsilio, "Ground-Source Heat Pump Systems: The Effects of Variable Trench Separations and Pipe Configurations in Horizontal Ground Heat Exchangers," (in English), *Energies,* vol. 14, no. 13, p. 3919, 2021 2021, doi: https://doi.org/10.3390/en14133919.

[27] Y. Yuan, X. Cao, J. Wang, and L. Sun, "Thermal interaction of multiple ground heat exchangers under different intermittent ratio and separation distance," *Applied Thermal Engineering,* vol. 108, pp. 277-286, 2016/09/05/ 2016, doi: https://doi.org/10.1016/j.applthermaleng.2016.07.120.

[28] Z. Hu, M. Zhu, W. He, X. Meng, C. Yang, and Z. Xu, "Experimental study and performance evaluation of a ground heat exchanger with different

intermittent ratios and soil thermal properties," *Geothermics,* vol. 102, p. 102402, 2022/06/01/ 2022, doi: https://doi.org/10.1016/j.geothermics.2022.102402.

[29] M. H. Jahangir, M. Ghazvini, F. Pourfayaz, and M. H. Ahmadi, "A numerical study into effects of intermittent pump operation on thermal storage in unsaturated porous media," *Applied Thermal Engineering,* vol. 138, pp. 110-121, 2018/06/25/ 2018, doi: https://doi.org/10.1016/j.applthermaleng.2018.04.023.

[30] Jalaluddin and A. Miyara, "Thermal performance investigation of several types of vertical ground heat exchangers with different operation mode," *Applied Thermal Engineering,* vol. 33-34, pp. 167-174, 2012/02/01/ 2012, doi: https://doi.org/10.1016/j.applthermaleng.2011.09.030.

[31] S. Selamat, A. Miyara, and K. Kariya, "Analysis of Short Time Period of Operation of Horizontal Ground Heat Exchangers," *Resources,* vol. 4, pp. 507-523, 07/13 2015, doi: 10.3390/resources4030507.

[32] G. Gan, "Dynamic thermal performance of horizontal ground source heat pumps – The impact of coupled heat and moisture transfer," *Energy,* vol. 152, pp. 877-887, 2018/06/01/ 2018, doi: https://doi.org/10.1016/j.energy.2018.04.008.

[33] G. Gan, "Dynamic thermal modelling of horizontal ground-source heat pumps," *International Journal of Low-Carbon Technologies,* vol. 8, pp. 95-105, 05/07 2013, doi: 10.1093/ijlct/ctt012.

[34] W. Choi, R. Ooka, and Y. Nam, "Impact of long-term operation of ground-source heat pump on subsurface thermal state in urban areas," *Sustainable Cities and Society,* vol. 38, pp. 429-439, 2018/04/01/ 2018, doi: https://doi.org/10.1016/j.scs.2017.12.036.

[35] Y. Cui, J. Zhu, and F. Meng, "Techno-economic evaluation of multiple energy piles for a ground-coupled heat pump system," *Energy Conversion and Management,* vol. 178, pp. 200-216, 2018/12/15/ 2018, doi: https://doi.org/10.1016/j.enconman.2018.10.042.

[36] M. E. Suryatriyastuti, H. Mroueh, and S. Burlon, "Understanding the temperature-induced mechanical behaviour of energy pile foundations," *Renewable and Sustainable Energy Reviews,* vol. 16, no. 5, pp. 3344-3354, 2012/06/01/ 2012, doi: https://doi.org/10.1016/j.rser.2012.02.062.

[37] P. Bayer, G. Attard, P. Blum, and K. Menberg, "The geothermal potential of cities," *Renewable and Sustainable Energy Reviews,* vol. 106, pp. 17-30, 2019/05/01/ 2019, doi: https://doi.org/10.1016/j.rser.2019.02.019.

[38] D. Banks, "The Design of Groundwater-Based Open-Loop Systems," in *An Introduction to Thermogeology: Ground Source Heating and Cooling*, 2012, pp. 202-247.

[39] E. Energy. "Ground source heat pumps use sustainable energy." https://www.earthtestenergy.com/domestic-ground-source-heat.html (accessed.

[40] Ó. R. Eidesgaard, N. H. Schovsbo, L. O. Boldreel, and J. Ólavsdóttir, "Shallow geothermal energy system in fractured basalt: A case study from Kollafjørður, Faroe Islands, NE-Atlantic Ocean," *Geothermics,* vol. 82, pp. 296-314, 2019/11/01/ 2019, doi: https://doi.org/10.1016/j.geothermics.2019.07.005.

[41] C. E. UK. https://climateemergency.org.uk/ground-source-heat-pumps/ (accessed.

[42] G. A. Florides, P. Christodoulides, and P. Pouloupatis, "Single and double U-tube ground heat exchangers in multiple-layer substrates," *Applied Energy,* vol.

102, pp. 364-373, 2013/02/01/ 2013, doi: https://doi.org/10.1016/j.apenergy.2012.07.035.

[43] H. Zeng, N. Diao, and Z. Fang, "Heat transfer analysis of boreholes in vertical ground heat exchangers," *International Journal of Heat and Mass Transfer,* vol. 46, no. 23, pp. 4467-4481, 2003/11/01/ 2003, doi: https://doi.org/10.1016/S0017-9310(03)00270-9.

[44] L. D. Haiwen Shu, Rongron Hua, "Analysis of Selection of Single or Double U-bend Pipes in a Ground Source " *Renewable Energy Resources and a Greener Future Vol.VIII-11-2,* 2006. [Online]. Available: http://oaktrust.library.tamu.edu/bitstream/handle/1969.1/5466/ESL-IC-06-11-305.pdf?sequence=4.

[45] B. B. Sanner, "SHALLOW GEOTHERMAL ENERGY," 2001.

[46] H. Javadi, S. S. Mousavi Ajarostaghi, M. A. Rosen, and M. Pourfallah, "Performance of ground heat exchangers: A comprehensive review of recent advances," *Energy,* vol. 178, pp. 207-233, 2019/07/01/ 2019, doi: https://doi.org/10.1016/j.energy.2019.04.094.

[47] T. You, B. Wang, W. Wu, W. Shi, and X. Li, "Performance analysis of hybrid ground-coupled heat pump system with multi-functions," *Energy Conversion and Management,* vol. 92, pp. 47-59, 2015/03/01/ 2015, doi: https://doi.org/10.1016/j.enconman.2014.12.036.

[48] M. Alberdi-Pagola, S. E. Poulsen, R. L. Jensen, and S. Madsen, "Thermal design method for multiple precast energy piles," *Geothermics,* vol. 78, pp. 201-210, 2019/03/01/ 2019, doi: https://doi.org/10.1016/j.geothermics.2018.12.007.

[49] J. Lund, B. Sanner, L. Rybach, R. Curtis, and G. Hellström, "Geothermal (ground source) heat pumps—A world overview," *Geo-Heat Center Quart Bull,* vol. 25, 01/01 2004.

[50] CEC. California's Customer Energy Centre. www.consumerenergycenter.orgSacramento: California Energy Commission (accessed.

[51] J. Raymond, M. Malo, D. Tanguay, S. E. Grasby, and F. Bakhteyar, "Direct Utilization of Geothermal Energy from Coast to Coast: a Review of Current Applications and Research in Canada," 2015.

[52] J. W. Lund and T. L. Boyd, "Direct utilization of geothermal energy 2015 worldwide review," *Geothermics,* vol. 60, pp. 66-93, 2016/03/01/ 2016, doi: https://doi.org/10.1016/j.geothermics.2015.11.004.

[53] M. Aydin, A. Sisman, A. Gültekin, and B. Dehghan B, *An Experimental Performance Comparison between Different Shallow Ground Heat Exchangers*. 2015.

[54] S. Javed, P. Fahlén, and J. Claesson, *VERTICAL GROUND HEAT EXCHANGERS: A REVIEW OF HEAT FLOW MODELS*. 2009.

[55] H. Yang, P. Cui, and Z. Fang, "Vertical-borehole ground-coupled heat pumps: A review of models and systems," *Applied Energy,* vol. 87, no. 1, pp. 16-27, 2010/01/01/ 2010, doi: https://doi.org/10.1016/j.apenergy.2009.04.038.

[56] I. Sarbu and C. Sebarchievici, "Chapter 4 - Types of Compressors and Heat Pumps," in *Ground-Source Heat Pumps*, I. Sarbu and C. Sebarchievici Eds.: Academic Press, 2016, pp. 47-70.

[57] P. Mogensen, "Fluid to duct wall heat transfer in duct system heat storage," *Document - Swedish Council for Building Research,* pp. 652-657, 01/01 1983.

[58] J. D. Spitler and S. E. A. Gehlin, "Thermal response testing for ground source heat pump systems—An historical review," *Renewable and Sustainable Energy Reviews,* vol. 50, pp. 1125-1137, 2015/10/01/ 2015, doi:

https://doi.org/10.1016/j.rser.2015.05.061.
[59] Z. Fang, N. Diao, and P. Cui, "Discontinuous operation of geothermal heat exchangers," *Tsinghua Science and Technology,* vol. 7, pp. 194-197, 01/01 2002.
[60] D. P. Hart and R. Couvillion, "Earth-coupled heat transfer: offers engineers and other practitioners of applied physics the information to solve heat transfer problems as they apply to earth-coupling," *(No Title),* 1986.
[61] H. S. Carslaw and J. C. Jaeger, *Conduction of Heat in Solids*. Clarendon Press, 1959.
[62] L. R. Ingersoll, O. J. Zobel, and A. C. Ingersoll, "Heat Conduction with Engineering, Geological, and Other Applications," *Physics Today,* vol. 8, no. 3, pp. 17-17, 1955, doi: 10.1063/1.3061951.
[63] M. A. Bernier, "Ground-coupled heat pump system simulation," *ASHRAE Transactions,* vol. 107, pp. 605-616, 01/01 2001.
[64] P. Eskilson and J. Claesson, "SIMULATION MODEL FOR THERMALLY INTERACTING HEAT EXTRACTION BOREHOLES," *Numerical Heat Transfer,* vol. 13, no. 2, pp. 149-165, 1988/03/01 1988, doi: 10.1080/10407788808913609.
[65] J. D. Spitler and M. Bernier, "2 - Vertical borehole ground heat exchanger design methods," in *Advances in Ground-Source Heat Pump Systems*, S. J. Rees Ed.: Woodhead Publishing, 2016, pp. 29-61.
[66] H. Zeng, N. Diao, and Z. Fang, "A finite line-source model for boreholes in geothermal heat exchangers," *Heat Transfer—Asian Research,* vol. 31, pp. 558-567, 11/01 2002, doi: 10.1002/htj.10057.
[67] Y. Man, H. Yang, N. Diao, P. Cui, L. Lu, and Z. Fang, "Development of spiral heat source model for novel pile ground heat exchangers," *HVAC&R Research,* vol. 17, no. 6, pp. 1075-1088, 2011/12/01 2011, doi: 10.1080/10789669.2011.610281.
[68] S. Park, S.-R. Lee, H. Park, S. Yoon, and J. Chung, "Characteristics of an analytical solution for a spiral coil type ground heat exchanger," *Computers and Geotechnics,* vol. 49, pp. 18-24, 2013/04/01/ 2013, doi: https://doi.org/10.1016/j.compgeo.2012.11.006.
[69] Y. Man, H. Yang, N. Diao, J. Liu, and Z. Fang, "A new model and analytical solutions for borehole and pile ground heat exchangers," *International Journal of Heat and Mass Transfer,* vol. 53, no. 13, pp. 2593-2601, 2010/06/01/ 2010, doi: https://doi.org/10.1016/j.ijheatmasstransfer.2010.03.001.
[70] P. Cui, X. Li, Y. Man, and Z. Fang, "Heat transfer analysis of pile geothermal heat exchangers with spiral coils," *Applied Energy,* vol. 88, no. 11, pp. 4113-4119, 2011/11/01/ 2011, doi: https://doi.org/10.1016/j.apenergy.2011.03.045.
[71] H. Park, S.-R. Lee, S. Yoon, H. Shin, and D.-S. Lee, "Case study of heat transfer behavior of helical ground heat exchanger," *Energy and Buildings,* vol. 53, pp. 137-144, 2012/10/01/ 2012, doi: https://doi.org/10.1016/j.enbuild.2012.06.019.
[72] D. Wang, L. Lu, and P. Cui, "A new analytical solution for horizontal geothermal heat exchangers with vertical spiral coils," *International Journal of Heat and Mass Transfer,* vol. 100, pp. 111-120, 2016/09/01/ 2016, doi: https://doi.org/10.1016/j.ijheatmasstransfer.2016.04.001.
[73] D. Wang, L. Lu, and P. Cui, "A novel composite-medium solution for pile geothermal heat exchangers with spiral coils," *International Journal of Heat and Mass Transfer,* vol. 93, pp. 760-769, 2016/02/01/ 2016, doi: https://doi.org/10.1016/j.ijheatmasstransfer.2015.10.055.
[74] J.-S. Jeon, S.-R. Lee, and M.-J. Kim, "A modified mathematical model for spiral coil-type horizontal ground heat exchangers," *Energy,* vol. 152, pp. 732-743,

2018/06/01/ 2018, doi: https://doi.org/10.1016/j.energy.2018.04.007.
[75] S. Mukerji, W. Murphy, and K. Tagavi, "Steady-State Heat Transfer Analysis of Arbitrarily Coiled Buried Pipes," *Journal of Thermophysics and Heat Transfer - J THERMOPHYS HEAT TRANSFER,* vol. 11, pp. 182-188, 04/01 1997, doi: 10.2514/2.6250.
[76] H. Li, K. Nagano, and Y. Lai, "A new model and solutions for a spiral heat exchanger and its experimental validation," *International Journal of Heat and Mass Transfer,* vol. 55, no. 15, pp. 4404-4414, 2012/07/01/ 2012, doi: https://doi.org/10.1016/j.ijheatmasstransfer.2012.03.084.
[77] H. Li, K. Nagano, and Y. Lai, "Heat transfer of a horizontal spiral heat exchanger under groundwater advection," *International Journal of Heat and Mass Transfer,* vol. 55, no. 23, pp. 6819-6831, 2012/11/01/ 2012, doi: https://doi.org/10.1016/j.ijheatmasstransfer.2012.06.089.
[78] H. Fujii, K. Nishi, Y. Komaniwa, and N. Chou, "Numerical modeling of slinky-coil horizontal ground heat exchangers," *Geothermics,* vol. 41, pp. 55-62, 2012/01/01/ 2012, doi: https://doi.org/10.1016/j.geothermics.2011.09.002.
[79] S. K. Soni, M. Pandey, and V. N. Bartaria, "Ground coupled heat exchangers: A review and applications," *Renewable and Sustainable Energy Reviews,* vol. 47, pp. 83-92, 2015/07/01/ 2015, doi: https://doi.org/10.1016/j.rser.2015.03.014.
[80] B. Li, Z. Han, C. Bai, and H. Hu, "The influence of soil thermal properties on the operation performance on ground source heat pump system," *Renewable Energy,* vol. 141, pp. 903-913, 2019/10/01/ 2019, doi: https://doi.org/10.1016/j.renene.2019.04.069.
[81] Z. Liu, W. Xu, C. Qian, X. Chen, and G. Jin, "Investigation on the feasibility and performance of ground source heat pump (GSHP) in three cities in cold climate zone, China," *Renewable Energy,* vol. 84, pp. 89-96, 2015/12/01/ 2015, doi: https://doi.org/10.1016/j.renene.2015.06.019.
[82] Y. Man, H. Yang, J. D. Spitler, and Z. Fang, "Feasibility study on novel hybrid ground coupled heat pump system with nocturnal cooling radiator for cooling load dominated buildings," *Applied Energy,* vol. 88, no. 11, pp. 4160-4171, 2011/11/01/ 2011, doi: https://doi.org/10.1016/j.apenergy.2011.04.035.
[83] S. Bae and Y. Nam, "Economic and environmental analysis of ground source heat pump system according to operation methods," *Geothermics,* vol. 101, p. 102373, 2022/05/01/ 2022, doi: https://doi.org/10.1016/j.geothermics.2022.102373.
[84] Jalaluddin, A. Miyara, K. Tsubaki, S. Inoue, and K. Yoshida, "Experimental study of several types of ground heat exchanger using a steel pile foundation," *Renewable Energy,* vol. 36, no. 2, pp. 764-771, 2011/02/01/ 2011, doi: https://doi.org/10.1016/j.renene.2010.08.011.
[85] A. B. Platts, D. A. Cameron, and J. A. Ward, "Validation of a model for two horizontal ground coupled heat exchangers based on field testing," *Energy and Buildings,* vol. 138, pp. 11-25, 2017/03/01/ 2017, doi: https://doi.org/10.1016/j.enbuild.2016.12.007.
[86] H. Esen, M. Inalli, and M. Esen, "Numerical and experimental analysis of a horizontal ground-coupled heat pump system," *Building and Environment,* vol. 42, no. 3, pp. 1126-1134, 2007/03/01/ 2007, doi: https://doi.org/10.1016/j.buildenv.2005.11.027.
[87] H. Demir, A. Koyun, and G. Temir, "Heat transfer of horizontal parallel pipe ground heat exchanger and experimental verification," *Applied Thermal Engineering,* vol. 29, no. 2, pp. 224-233, 2009/02/01/ 2009, doi: https://doi.org/10.1016/j.applthermaleng.2008.02.027.

[88] V. R. Tarnawski, W. H. Leong, T. Momose, and Y. Hamada, "Analysis of ground source heat pumps with horizontal ground heat exchangers for northern Japan," *Renewable Energy,* vol. 34, no. 1, pp. 127-134, 2009/01/01/ 2009, doi: https://doi.org/10.1016/j.renene.2008.03.026.

[89] A. Rezaei B, E. M. Kolahdouz, G. F. Dargush, and A. S. Weber, "Ground source heat pump pipe performance with Tire Derived Aggregate," *International Journal of Heat and Mass Transfer,* vol. 55, no. 11, pp. 2844-2853, 2012/05/01/ 2012, doi: https://doi.org/10.1016/j.ijheatmasstransfer.2012.02.004.

[90] G. Gan, "A numerical methodology for comprehensive assessment of the dynamic thermal performance of horizontal ground heat exchangers," *Thermal Science and Engineering Progress,* vol. 11, pp. 365-379, 2019/06/01/ 2019, doi: https://doi.org/10.1016/j.tsep.2019.04.013.

[91] K. Kupiec, B. Larwa, and M. Gwadera, "Heat transfer in horizontal ground heat exchangers," *Applied Thermal Engineering,* vol. 75, pp. 270-276, 2015/01/22/ 2015, doi: https://doi.org/10.1016/j.applthermaleng.2014.10.003.

[92] A. Benazza, E. Blanco, M. Aichouba, J. L. Río, and S. Laouedj, "Numerical Investigation of Horizontal Ground Coupled Heat Exchanger," *Energy Procedia,* vol. 6, pp. 29-35, 2011/01/01/ 2011, doi: https://doi.org/10.1016/j.egypro.2011.05.004.

[93] G.-H. Go, S.-R. Lee, N. N.V, and S. Yoon, "A new performance evaluation algorithm for horizontal GCHPs (ground coupled heat pump systems) that considers rainfall infiltration," *Energy,* vol. 83, pp. 766-777, 2015/04/01/ 2015, doi: https://doi.org/10.1016/j.energy.2015.02.086.

[94] G.-H. Go, S.-R. Lee, S. Yoon, and M.-J. Kim, "Optimum design of horizontal ground-coupled heat pump systems using spiral-coil-loop heat exchangers," *Applied Energy,* vol. 162, pp. 330-345, 2016/01/15/ 2016, doi: https://doi.org/10.1016/j.apenergy.2015.10.113.

[95] B. Dehghan B, "Experimental and computational investigation of the spiral ground heat exchangers for ground source heat pump applications," *Applied Thermal Engineering,* vol. 121, pp. 908-921, 2017/07/05/ 2017, doi: https://doi.org/10.1016/j.applthermaleng.2017.05.002.

[96] M.-J. Kim, S.-R. Lee, S. Yoon, and J.-S. Jeon, "An applicable design method for horizontal spiral-coil-type ground heat exchangers," *Geothermics,* vol. 72, pp. 338-347, 2018/03/01/ 2018, doi: https://doi.org/10.1016/j.geothermics.2017.12.010.

[97] C. Li, J. Mao, H. Zhang, Z. Xing, Y. Li, and J. Zhou, "Numerical simulation of horizontal spiral-coil ground source heat pump system: Sensitivity analysis and operation characteristics," *Applied Thermal Engineering,* vol. 110, pp. 424-435, 2017/01/05/ 2017, doi: https://doi.org/10.1016/j.applthermaleng.2016.08.134.

[98] P. M. Congedo, G. Colangelo, and G. Starace, "CFD simulations of horizontal ground heat exchangers: A comparison among different configurations," *Applied Thermal Engineering,* vol. 33-34, pp. 24-32, 2012/02/01/ 2012, doi: https://doi.org/10.1016/j.applthermaleng.2011.09.005.

[99] H. Fujii, Y. Komaniwa, R. Itoi, T. Noguchi, T. Nomoto, and H. Kosukegawa, "Field Test of Slinky-coil Type Horizontal Ground Heat Exchangers," *Journal of the Geothermal Research Society of Japan,* pp. 219-228, 10/25 2010, doi: 10.11367/grsj.32.219.

[100] H. Fujii, S. Yamasaki, T. Maehara, T. Ishikami, and N. Chou, "Numerical simulation and sensitivity study of double-layer Slinky-coil horizontal ground heat exchangers," *Geothermics,* vol. 47, pp. 61-68, 2013/07/01/ 2013, doi:

https://doi.org/10.1016/j.geothermics.2013.02.006.
[101] B. Asgari, M. Habibi, and A. Hakkaki-Fard, "Assessment and comparison of different arrangements of horizontal ground heat exchangers for high energy required applications," *Applied Thermal Engineering,* vol. 167, p. 114770, 2020/02/25/ 2020, doi: https://doi.org/10.1016/j.applthermaleng.2019.114770.
[102] M.-J. Kim, S.-R. Lee, S. Yoon, and G.-H. Go, "Thermal performance evaluation and parametric study of a horizontal ground heat exchanger," *Geothermics,* vol. 60, pp. 134-143, 2016/03/01/ 2016, doi: https://doi.org/10.1016/j.geothermics.2015.12.009.
[103] C. Zhang, W. Yang, J. Yang, S. Wu, and Y. Chen, "Experimental Investigations and Numerical Simulation of Thermal Performance of a Horizontal Slinky-Coil Ground Heat Exchanger," *Sustainability*, vol. 9, no. 8, doi: 10.3390/su9081362.
[104] J. Lin, H. Nowamooz, S. Braymand, P. Wolff, and C. Fond, "Impact of soil moisture on the long-term energy performance of an earth-air heat exchanger system," *Renewable Energy,* vol. 147, pp. 2676-2687, 2020/03/01/ 2020, doi: https://doi.org/10.1016/j.renene.2018.06.106.
[105] S. Yoon, S.-R. Lee, and G.-H. Go, "Evaluation of thermal efficiency in different types of horizontal ground heat exchangers," *Energy and Buildings,* vol. 105, pp. 100-105, 2015/10/15/ 2015, doi: https://doi.org/10.1016/j.enbuild.2015.07.054.
[106] C. Han, K. M. Ellett, S. Naylor, and X. Yu, "Influence of local geological data on the performance of horizontal ground-coupled heat pump system integrated with building thermal loads," *Renewable Energy,* vol. 113, pp. 1046-1055, 2017/12/01/ 2017, doi: https://doi.org/10.1016/j.renene.2017.06.025.
[107] A. A. DiCarlo, C. E. Videchak, and R. A. Caldwell, "Optimization of spatially distributed soil conductivities for horizontal ground heat exchangers," *Applied Thermal Engineering,* vol. 167, p. 114793, 2020/02/25/ 2020, doi: https://doi.org/10.1016/j.applthermaleng.2019.114793.
[108] M. Li and A. C. K. Lai, "Review of analytical models for heat transfer by vertical ground heat exchangers (GHEs): A perspective of time and space scales," *Applied Energy,* vol. 151, pp. 178-191, 2015/08/01/ 2015, doi: https://doi.org/10.1016/j.apenergy.2015.04.070.
[109] P. Cui, H. Yang, and Z. Fang, "Numerical analysis and experimental validation of heat transfer in ground heat exchangers in alternative operation modes," *Energy and Buildings,* vol. 40, no. 6, pp. 1060-1066, 2008/01/01/ 2008, doi: https://doi.org/10.1016/j.enbuild.2007.10.005.
[110] M. M. Aslam Bhutta, N. Hayat, M. H. Bashir, A. R. Khan, K. N. Ahmad, and S. Khan, "CFD applications in various heat exchangers design: A review," *Applied Thermal Engineering,* vol. 32, pp. 1-12, 2012/01/01/ 2012, doi: https://doi.org/10.1016/j.applthermaleng.2011.09.001.
[111] D. Adamovsky, P. Neuberger, and R. Adamovsky, "Changes in energy and temperature in the ground mass with horizontal heat exchangers—The energy source for heat pumps," *Energy and Buildings,* vol. 92, pp. 107-115, 2015/04/01/ 2015, doi: https://doi.org/10.1016/j.enbuild.2015.01.052.
[112] M. Ali, K. Kariya, and A. Miyara, "Performance Analysis of Slinky Horizontal Ground Heat Exchangers for a Ground Source Heat Pump System," *Resources,* vol. 6, p. 56, 10/13 2017, doi: 10.3390/resources6040056.
[113] W. Yang, R. Xu, F. Wang, and S. Chen, "Experimental and numerical investigations on the thermal performance of a horizontal spiral-coil ground heat exchanger," *Renewable Energy,* vol. 147, pp. 979-995, 2020/03/01/ 2020,

doi: https://doi.org/10.1016/j.renene.2019.09.030.
[114] A. Kapıcıoğlu and H. Esen, "Experimental investigation on using Al2O3/ethylene glycol-water nano-fluid in different types of horizontal ground heat exchangers," *Applied Thermal Engineering,* vol. 165, p. 114559, 2020/01/25/ 2020, doi: https://doi.org/10.1016/j.applthermaleng.2019.114559.
[115] R. Du, D. Jiang, Y. Wang, and K. Wei Shah, "An experimental investigation of CuO/water nanofluid heat transfer in geothermal heat exchanger," *Energy and Buildings,* vol. 227, p. 110402, 2020/11/15/ 2020, doi: https://doi.org/10.1016/j.enbuild.2020.110402.
[116] D. A. d. V. J.R. Philip, "Moisture movement in porous materials under temperature gradients," *Transactions, American Geophysical Union,* pp. pp. 222-231, 1957. [Online]. Available: https://agupubs.onlinelibrary.wiley.com/doi/pdf/10.1029/TR038i002p00222.
[117] Ansys. "Ansys Fluent Fluid Simulation Software." https://www.ansys.com/products/fluids/ansys-fluent (accessed 10 March, 2023).
[118] MiquelM. "What Type of Pipe Is Used for Geothermal Heating?" Architreecture. https://architreecture.com/what-type-of-pipe-is-used-for-geothermal-heating/?utm_content=cmp-true (accessed.
[119] "Fluid Properties Calculator." http://www.mhtl.uwaterloo.ca/old/onlinetools/airprop/airprop.html (accessed.
[120] R. Brown, B. S. Research, and I. Association, *Heat Pumps: A Guidance Document for Designers*. BSRIA, 2009.
[121] "The geothermal association of Ireland. Newsletter 16," 2010. [Online]. Available: <http://geothermalassociation.ie/GAI%20NL%2016%20%20July%202010.pdf>
[122] "Geothermal heat pumps: installation guide," 2009. [Online]. Available: <http://www.global-greenhouse-warming.com>
[123] "GEOMAX Geothermal HVAC Systems. Eagle mountain, geothermal loop field products and accessories," 2010. [Online]. Available: <http://www.eagle-mt.com>.
[124] H. T, "Geothermal slinky loop construction." [Online]. Available: <http://ezinearticles.com/?Geothermal-Slinky-Loop-Construction&id=4104098>.
[125] G. Gan, "Dynamic thermal simulation of horizontal ground heat exchangers for renewable heating and ventilation of buildings," *Renewable Energy,* vol. 103, pp. 361-371, 2017/04/01/ 2017, doi: https://doi.org/10.1016/j.renene.2016.11.052.
[126] D. Hillel, "Soil Physics," in *Encyclopedia of Physical Science and Technology (Third Edition)*, R. A. Meyers Ed. New York: Academic Press, 2003, pp. 77-97.
[127] Weather Spark. "2022 Weather History in Coventry." https://weatherspark.com/h/y/41841/2022/Historical-Weather-during-2022-in-Coventry-United-Kingdom#Figures-Temperature (accessed 10 March, 2023).
[128] R. Garcia Gonzalez, A. Verhoef, P. L. Vidale, B. Main, G. Gan, and Y. Wu, "Interactions between the physical soil environment and a horizontal ground coupled heat pump, for a domestic site in the UK," *Renewable Energy,* vol. 44, pp. 141-153, 2012/08/01/ 2012, doi: https://doi.org/10.1016/j.renene.2012.01.080.
[129] R. H. S. Winterton, "Where did the Dittus and Boelter equation come from?,"

International Journal of Heat and Mass Transfer, vol. 41, no. 4, pp. 809-810, 1998/02/01/ 1998, doi: https://doi.org/10.1016/S0017-9310(97)00177-4.

[130] J. P. Busby, "Determination of Thermal Properties for Horizontal Ground Collector Loops," 2015.

[131] D. H. W. Li, L. Yang, and J. C. Lam, "Impact of climate change on energy use in the built environment in different climate zones – A review," *Energy,* vol. 42, no. 1, pp. 103-112, 2012/06/01/ 2012, doi: https://doi.org/10.1016/j.energy.2012.03.044.

[132] M. De Rosa, V. Bianco, F. Scarpa, and L. A. Tagliafico, "Historical trends and current state of heating and cooling degree days in Italy," *Energy Conversion and Management,* vol. 90, pp. 323-335, 2015/01/15/ 2015, doi: https://doi.org/10.1016/j.enconman.2014.11.022.

[133] L. D. D. Harvey, "Using modified multiple heating-degree-day (HDD) and cooling-degree-day (CDD) indices to estimate building heating and cooling loads," *Energy and Buildings,* vol. 229, p. 110475, 2020/12/15/ 2020, doi: https://doi.org/10.1016/j.enbuild.2020.110475.

[134] WeatherOnline. "Nottingham/watnall (117m)." https://www.weatheronline.co.uk/weather/maps/city?LANG=en&CEL=C&SI=mph&MAPS=over&CONT=ukuk&LAND=MID&REGION=0003&WMO=03354&UP=0&R=0&LEVEL=150&NOREGION=0#google_vignette (accessed.

[135] P. a. Systems. "Total Head for the Pump & System." https://www.pumpsandsystems.com/total-head-pump-system (accessed.

[136] G. Moser, S. G. Paal, D. Jlelaty, and I. F. C. Smith, "An electrical network for evaluating monitoring strategies intended for hydraulic pressurized networks," *Advanced Engineering Informatics,* vol. 30, no. 4, pp. 672-686, 2016/10/01/ 2016, doi: https://doi.org/10.1016/j.aei.2016.09.003.

[137] G. Dagan, A. Fiori, and I. Janković, "Transport in Porous Media," in *Encyclopedia of Ecology*, S. E. Jørgensen and B. D. Fath Eds. Oxford: Academic Press, 2008, pp. 3576-3582.

[138] E. Marušić-Paloka and I. Pažanin, "Effects of boundary roughness and inertia on the fluid flow through a corrugated pipe and the formula for the Darcy–Weisbach friction coefficient," *International Journal of Engineering Science,* vol. 152, p. 103293, 2020/07/01/ 2020, doi: https://doi.org/10.1016/j.ijengsci.2020.103293.

[139] H. Kosukegawa, H. Fujii, and M. Ono, "Experimental Study on the Pressure Loss of Slinky-coil Type Ground Heat Exchanger ," *Journal of the Geothermal Research Society of Japan,* vol. 39, no. 2, pp. 93-99, 2017 2017, doi: 10.11367/grsj.39.93.

[140] "Britain's Electricity Explained: 2020-2022." https://www.nationalgrideso.com/electricity-explained/electricity-and-me/great-britains-monthly-electricity-stats (accessed.

[141] (2022). *Greenhouse gas reporting: conversion factors 2021*. [Online] Available: https://www.gov.uk/government/publications/greenhouse-gas-reporting-conversion-factors-2021

[142] *Provisional UK greenhouse gas emissions national statistics 2022*. [Online] Available: https://www.gov.uk/government/statistics/provisional-uk-greenhouse-gas-emissions-national-statistics-2022

[143] (2021). *Plan to drive down the cost of clean heat*. [Online] Available: https://www.gov.uk/government/news/plan-to-drive-down-the-cost-of-clean-heat

[144] N. G. ESO. "Future Energy Scenarios (FES)."

https://www.nationalgrideso.com/future-energy/future-energy-scenarios-fes (accessed.

[145] Y. Wang, K. Qu, X. Chen, G. Gan, and S. Riffat, "An innovative retrofit Motivation-Objective-Criteria (MOC) approach integrating homeowners' engagement to unlocking low-energy retrofit in residential buildings," *Energy and Buildings,* vol. 259, p. 111834, 2022/03/15/ 2022, doi: https://doi.org/10.1016/j.enbuild.2022.111834.

[146] (2023). *Quarterly Energy Prices*. [Online] Available: https://assets.publishing.service.gov.uk/government/uploads/system/uploads/attachment_data/file/1166257/quarterly-energy-prices-june-2023.pdf

[147] (2023). *Energy Price Guarantee*. [Online] Available: https://www.gov.uk/government/publications/energy-bills-support/energy-bills-support-factsheet-8-september-2022

[148] (2023). *Interest Rates and Monetary Policy*. [Online] Available: https://commonslibrary.parliament.uk/research-briefings/sn02802/#:~:text=global%20supply%20chains.-,UK%20(Bank%20of%20England),2023%20where%20rates%20were%20increased

[149] (2023). *Rising cost of living in the UK*. [Online] Available: https://commonslibrary.parliament.uk/research-briefings/cbp-9428/#:~:text=The%20average%20forecast%20among%20economists,continue%20to%20fall%20in%202024.

[150] J. K. Jensen, T. Ommen, and L. Reinholdt, "Heat pump COP, part 2: generalized COP estimation of heat pump processes," 2018.

[151] R. H. D. Rawlings and J. R. Sykulski, "Ground source heat pumps: A technology review," *Building Services Engineering Research and Technology,* vol. 20, no. 3, pp. 119-129, 1999, doi: 10.1177/014362449902000304.

Appendix

Appendix A. Common antifreeze solution [151]

Antifreeze solution	Pros	Cons
Ethylene glycol aqueous solution	• Non-corrosive • Low volatility • Low flammability	• Toxic • Short lifespan • High viscosity at low temperature
Ethanol aqueous solution	• Low volatility • Low cost	• Flammable • Toxic • Low conductivity
Methanol aqueous solution	• Low corrosive • Low cost • Good conductor	• Flammable • Volatile • Toxic
Propylene glycol aqueous solution	• Non-corrosive • Low volatility • Low flammability • Low toxicity	• High viscosity • High cost

Appendix B. Determination of Thermal Properties for Horizontal Ground Collector Loops [130]

Table B-1 Derived thermal diffusivities and estimated parameters based on soil texture

Abbreviated station name	Depth range (cm)	Thermal diffusivity ($\times 10^{-6} m^2 s^{-1}$)	Soil texture	Bulk density ($g \cdot cm^{-3}$)	Particle density ($g \cdot cm^{-3}$)	Porosity	Volumetric moisture content	Specific heat ($J \cdot kg^{-1} K^{-1}$)	Thermal conductivity ($W \cdot m^{-1} K^{-1}$)
Mylnefield	50-100	0.4002	S_NL	1.52	2.62	0.42	0.08	1014	0.62
Edinburgh	30-50	0.7175	C_S	1.32	2.36	0.44	0.1	1139	1.08
Wellesbourne	50-100	1.7971	NL	1.54	2.66	0.42	0.08	1008	2.79
Reading	50-100	0.8700	S_SXL	1.52	2.62	0.42	0.08	1014	1.34
Coventry	30-100	0.9842	L_S	1.47	2.45	0.4	0.08	1039	1.50

Table B-2 Description of the soil texture classes

Soil texture	Description
C_S	CLAY, SAND, SANDY LOAMS, BUT GENERALLY LESS THAN 40% SILT)
L_S	LOAM TO SAND
NL	SANDY, CLAYEY AND SILTY LOAMS (MINIMUM 20%SAND)
S_NL	SAND TO SANDY, CLAYEY AND SILTY LOAMS
S_SXL	SANDY TO SANDY- LOAM AND SANDY CLAY LOAM

Appendix C. Initial investment for HGSHP with sandy soil

Heating system	Item and its description	Price (£)
HGSHP	Kensa Evo heat pump	5970
	Flowmeters ＆circulating pump	1757
	Working fluid	1006
	Pipe work	947
	Buffer tank	499
	Excavation ＆installation work	968
	MCS heat loss ＆ umbrella scheme	951
	Government grant Boiler Upgrade Scheme (BUS)	-7500
		4598

Appendix D. Determining the energy increase rate [146]

Year	Current price Gas Index 2010=100	Current price Electricity Index 2010=100
2012	122.56	113.32
2013	131.93	121.77
2014	138.13	128.43
2015	131.93	128.04
2016	124.14	127.78
2017	122.69	136.36
2018	127.44	148.14
2019	126.78	158.90
2020	114.12	159.15
2021	114.38	169.65
2022	217.28	252.88
increase rate (%)	7.73	12.32

Appendix E. Average price cap/guarantee unit rates for typical household usage (direct debit) [147]

Average price	Electricity (per kWh)	Gas (per kWh)
1 Oct 2021 - 31 Mar2022	£0.21	£0.04
1 Apr 2022 - 30 Sep 2022	£0.28	£0.07
1 Oct 2022 - 30 Mar 2023	£0.34	£0.10
1 Apr 2023 - 30 Jun 2023	£0.33	£0.10
1 Jul 2023 - 30 Sep 2023	£0.30	£0.08
Average price in two years	£0.29	£0.08

Appendix F. Carbon intensity for natural gas and electricity [140, 141]

Year	Gas carbon factor (kg/kWh)	Electricity carbon factor (kg/kWh)
2020	0.184	0.181
2021	0.183	0.265
2022	0.183	0.182
Average	0.183	0.209